LONG-TERM IMPACTS OF UTERINE INFECTION ON FERTILITY IN DAIRY COWS

By

MACKENZIE JOY DICKSON

A DISSERTATION PRESENTED TO THE GRADUATE SCHOOL
OF THE UNIVERSITY OF FLORIDA IN PARTIAL FULFILLMENT
OF THE REQUIREMENTS FOR THE DEGREE OF
DOCTOR OF PHILOSOPHY

UNIVERSITY OF FLORIDA

2021

To my parents who taught me to pursue my dreams, believe in myself, and never quit

ACKNOWLEDGMENTS

Thank you to my advisor, Dr. John Bromfield, for taking me on as a student and being an excellent mentor. I never thought I would live in Florida, but I wanted to study uterine infection and dairy cows, so I came to Gainesville. I am grateful he always pushed me to think critically, look at the data, and make my own conclusions. I will miss our weekly meetings to discuss science but will always remember and likely find myself saying “but what’s the question?” in regard to hypotheses, interpreting data, and writing. I would also like to thank my committee members, Dr. Pete Hansen, Dr. José Santos, Dr. John Driver, and Dr. Rafael Bisinotto, for their time, expertise, and advice given for expeirments, analysis, and general thinking. I am also grateful for the Animal Molecular and Cellular Biology Program and their financial support.

A big thank you to all my lab mates, past and present, especially Jason Rizo, Rachel Piersanti, Paula Molinari, and Rosabel Ramírez-Hernández, who made the lab feel like a family. Thank you to other graduate students, specifically Eliab Estrada-Cortés, Lautaro Rostoll Cangiano, Liz Palmer, Laura Jensen, and Ali Husnain, for all the time we spent discussing science or drinking beer or both at the same time. I am sure I have forgotten someone, so thank you to all my friends near and far, who are too numerous to name, for their support through the ups and downs of graduate school.

Finally, thank you to my dad, Jim, and my brother, Nolan, for their support, visiting me in Florida, and always listening when I talk about my research. Thank you to my mom, Val, for teaching me anything is possible and who would be so proud of me for completing a PhD. I wish she were here to help me celebrate. Last but not least, a huge thank you to my partner, Ben Hale. Despite living in different states the past four years, his support and confidence in me is immeasurable.

TABLE OF CONTENTS

page

LIST OF TABLES

LIST OF FIGURES

Figure page

LIST OF ABBREVIATIONS

ACTB	Beta actin
AMH	Anti-Müllerian hormone
AMP	Adenosine monophosphate
BHI	Bacto brain heart infusion broth
BoHV-4	Bovine gammaherpesvirus 4
BSA	Bovine serum albumin
Bu2cAMP	Dibutyryl cyclic AMP
cDNA	Complementary DNA
CEBPβ	CCAAT/enhancer-binding protein beta
CFU	Colony forming units
ChIP	Chromatin immunoprecipitation
CXCL8	C-X-C Motif Chemokine Ligand 8
CYP17A1	Cytochrome P450 Family 17 Subfamily A Member 1
CYP19A1	Aromatase
DPBS	Dulbecco’s phosphate buffered saline
E_2	17β-Estradiol
ELISA	Enzyme-linked immunosorbent assay
ERK	Extracellular signal-related kinase
ESR1	Estrogen receptor 1
FCS	Fetal calf serum
FDR	False discovery rate
FSH	Follicle stimulating hormone
FSHR	Follicle stimulating hormone receptor
GAPDH	Glyceraldehyde 3-phosphate dehydrogenase

GnRH	Gonadotropin-releasing hormone
hCG	Human chorionic gonadotropin
HDAC	Histone deacetylase
HEPES	4-(2-hydroxyethyl)-1-piperazineethanesulfonic acid
HSD17B1	17β-hydroxysteroid dehydrogenase type 1
HSP70	Heat shock protein 70
IFNT	Interferon tau
IGF1	Insulin-like growth factor 1
IL	Interleukin
i.m.	Intramuscular
ISG	Interferon-stimulated gene
IVC	In vitro culture
ITS	Insulin-transferrin-selenium
IVF	In vitro fertilization
LB	Luria-Bertani broth
LH	Luteinizing hormone
LHCGR	Luteinzing hormone receptor
LPS	Lipopolysaccharide
MIQE	Minimum information for publication of quantitative real-time PCR experiments
NCBI	National Center for Biotechnology Information
NFκB	Nuclear factor kappa B
P_4	Progesterone
PAMP	Pathogen-associated molecular pattern
PBS	Phosphate buffered saline

PG	Prostaglandin
PGN	Peptidoglycan
PMN	Polymorphonuclear
PTPRC	Protein tyrosine phosphatase receptor type C
RPL19	60S ribosomal protein L19
RT-PCR	Real-time polymerase chain reaction
SAS	Statisical analysis system
siRNA	Small-interfering RNA
SPSS	Statisical package for the social sciences
STAR	Steroidogenic acute regulatory protein
TBS	Tris buffered saline
TLR	Toll-like receptor
TNF	Tumour necrosis factor

Abstract of Dissertation Presented to the Graduate School
of the University of Florida in Partial Fulfillment of the
Requirements for the Degree of Doctor of Philosophy

LONG-TERM IMPACTS OF UTERINE INFECTION ON FERTILITY IN DAIRY COWS

By

Mackenzie Joy Dickson

May 2021

Chair: John J. Bromfield
Major: Animal Molecular and Cellular Biology

In cows, uterine disease is associated with infertility after disease resolution. Cows with uterine disease have reduced estradiol secretion, decreased conception rates, and increased pregnancy loss. The mechanisms responsible for this persistent infertility are unknown. The bacterial component, lipopolysaccharide (LPS), accumulates in the follicular fluid of cows with uterine disease, potentially altering the follicular environment in which oocytes develop. In vitro, LPS decreases oocyte competence and reduces *CYP19A1* expression and estradiol production in granulosa cells. Embryo transfer does not restore fertility in cows after uterine disease, suggesting uterine disease impacts the endometrium.

I hypothesized that induced uterine disease reduces the developmental competence of oocytes and alters the endometrial signature of pregnancy. Furthermore, I hypothesized that CCAAT/Enhancer-binding protein (CEBPβ), which regulates *CYP19A1* expression, mediates LPS-induced downregulation of *CYP19A1* expression and estradiol production in granulosa cells.

Cows received an intrauterine infusion of pathogenic bacteria or vehicle to induce uterine disease. Subsequently, oocytes were collected and subjected to in vitro

fertilization and embryo culture. Bacterial infusion resulted in reduced embryo development compared to vehicle infused controls.

RNA sequencing was performed on endometrial tissue on day 16 after insemination in cows that received an intrauterine bacterial infusion. The endometrial signature of pregnancy in cows following bacterial infusion was compared to the endometrial signature of pregnancy previously reported in healthy cows. Compared to healthy cows, the endometrial signature of pregnancy in cows following bacterial infusion showed a dysregulation of pathways related to inflammation and immune function, including IL-7, TLR, and iNOS signaling.

Lastly, I demonstrated that LPS reduces estradiol secretion in bovine granulosa cells from small/medium and large follicles. Interestingly the data suggests that LPS mediated changes to *CYP19A1* expression and CEBPβ nuclear localization in granulosa cells is dependent on follicle size.

In summary, intrauterine bacterial infusion reduces oocyte competence and results in a unique endometrial transcriptome of cows that fail to become pregnant, while granulosa cells exposed to LPS alter CEBPβ signaling and reduce estradiol secretion. Collectively, these studies illuminate potential mechanisms in the ovary and endometrium for the persistent infertility observed in dairy cows after the resolution of uterine disease.

CHAPTER 1
LITERATURE REVIEW

Infertility has often been cited as the predominant reason for culling cows (Norman et al., 2009). Many factors can contribute to infertility, including reproductive disorders (dystocia, retained placenta, uterine infections), non-reproductive diseases (mastitis, lameness, ketosis, respiratory diseases), large losses of body condition and high milk yield (Loeffler et al., 1999; Opsomer et al., 2000; Santos et al., 2010). The high producing dairy cow has been selected over many years for traits such as milk production and inadvertent negative selection for fertility traits has occurred simultaneously (Dematawewa and Berger, 1998; Lucy, 2001). Recently, pregnancy rates have begun improving, however the main driver of improved fertility is cow management, such as heat detection, while the rate of conception per insemination has not improved (Norman et al. 2017; Ribeiro, 2018). While the dairy farmer can manage and replace infertile cows, understanding the details of the biological processes and impairments that result in pregnancy failure or infertility could improve animal welfare, economics, and the overall dairy industry.

Impacts on Fertility Outside of the Reproductive Tract

Non-Uterine Diseases and Conditions Impair Fertility

Fertility decreases in cows diagnosed with one or more diseases in the postpartum period (Santos et al., 2010). Infection and inflammation of the mammary gland in cows (mastitis) is associated with reduced conception and pregnancy rates, and increased services per pregnancy (Moore et al., 1991; Barker et al., 1998; Loeffler et al., 1999; Schrick et al., 2001; Santos et al., 2004; Hertl et al., 2010). This decrease in fertility is, in part, likely due to reduced oocyte competence as exposure of oocytes to

follicular fluid or plasma of cows with mastitis decreases fertilization and embryo cleavage compared to oocytes exposed to follicular fluid or plasma from healthy cows (Asaf et al., 2014; Roth et al., 2020). Similarly, oocytes from cows with high somatic cell counts, indicative of mastitis, have a reduced competence to reach the blastocyst stage of development when fertilized and cultured in vitro compared with oocytes from cows with low somatic cell counts (Roth et al., 2013). Lameness is also negatively associated with fertility in dairy cows. Lame cows have altered ovarian function which manifests as an increased likelihood to develop ovarian cysts, longer calving to conception interval, and a higher risk of pregnancy failure compared to non-lame cows (Lucey et al., 1986; Barkema et al., 1994; Sprecher et al., 1997; Melendez et al., 2003; Hernandez et al., 2005). Digestive diseases, including diarrhea, bloat, or displaced abomasum, and respiratory problems, such as increased respiration rate and lung sounds, compromise estrous cyclicity and increase the incidence of pregnancy loss (Ribeiro et al., 2016a).

In addition to disease, many inflammatory pathologies and perturbations to metabolism are associated with altered ovarian function and decreased fertility in the dairy cow. Following parturition and at the onset of lactation, cows are often unable to consume sufficient energy to meet the metabolic demands of maintenance and milk production, causing weight loss and negative energy balance. Cows in negative energy balance following parturition or cows with large losses in body condition score are more likely to be anestrous, have prolonged calving to first service interval and are less likely to conceive compared to cows that maintained or gained weight after calving (Staples et al., 1990; Gillund et al., 2001; Carvalho et al., 2014). Further, cows in negative energy balance experience whole-body carbohydrate and lipid metabolism alterations (Vernon,

1989; Bell, 1995; Drackley, 1999). Cows compensate for negative energy balance by exporting lipids from adipose tissue, specifically non-esterified fatty acids, which are taken up by the liver and oxidized for energy or resynthesized into triacylglycerides (Drackley, 1999). Simultaneously, the pancreas decreases insulin secretion while peripheral tissues become resistant to insulin, allowing for redirection of glucose towards the mammary gland for milk synthesis (Bauman and Currie, 1980). These changes to metabolism also influence endocrine signaling and alter gonadotropin-releasing hormone (GnRH) and luteinizing hormone (LH) release, likely contributing to delayed ovarian activity, and decreased pregnancy per insemination (Beam and Butler, 1999; Carvalho et al., 2014). Elevated liver triacylglycerides and hypocalcemia after calving are associated with delayed onset of estrous cyclicity and reduced pregnancy rates in dairy cows (Butler and Smith, 1989; Jorritsma et al., 2000; Martinez et al., 2012; Ribeiro et al., 2013). Cows with elevated non-esterified fatty acids in circulation also have elevated non-esterified fatty acid concentrations in follicular fluid, potentially altering the oocyte microenvironment (Leroy et al., 2005). Indeed, lactation itself may influence embryo quality. The proportion of viable embryos is reduced in lactating cows compared to non-lactating cows (52.8% compared to 82.3%; Sartori et al., 2002). While many of the aforementioned diseases and metabolic alterations are distant from the reproductive tract, subsequent fertility can be negatively affected.

Genetic Influence on Reproduction

While reproductive traits have low heritability (< 0.10), geneticists have demonstrated a negative correlation between milk production and fertility (Hansen et al., 1983; Wall et al., 2003; VanRaden et al., 2004). Decreased reproductive efficiency has been correlated with increased milk production in high-producing dairy cows (Faust et

al., 1988; Butler, 1998; Washburn et al., 2002). Genetic selection of cows for increased milk production is associated with delayed first estrus detection (+4.5 d), and a longer interval (+8 d) to first ovulation postpartum (Hageman et al., 1991; Gong et al., 2002). Additionally, oocytes from high genetic merit cows resulted in fewer blastocysts compared to medium genetic merit cows following in vitro fertilization and embryo culture (Snijders et al., 2000). The nexus between genetic merit, physiology, such as lactation demands and nutrition, and frequency of diseases may all contribute to fertility problems in the dairy cow.

Uterine Disease in Dairy Cattle

Prevalence and Causes of Uterine Infection in Dairy Cattle

Uterine infection is common in postpartum dairy cows, occurring in up to 40% of the population (Sheldon et al., 2009). Factors including retained placenta, dystocia and twinning are associated with increased risk of uterine infection (Erb et al., 1981; Opsomer et al., 2000; Kim and Kang, 2003; Potter et al., 2010). During parturition, the female reproductive tract is exposed to the environment and up to 90% of postpartum dairy cows have bacteria in the upper reproductive tract (Elliott et al., 1968; Griffin et al., 1974; Sheldon et al., 2002). Viruses, viral DNA, or viral antibodies have been detected in uterine contents and blood from cows with uterine infection in various countries, including the United States (Parks and Kendrick, 1973; Frazier et al., 2001; Monge et al., 2006; Bilge-Dagalp et al., 2010). Specifically, bovine gammaherpesvirus 4 (BoHV-4) has been isolated from uterine infection cases in cattle. In most cases, however, pathogenic bacteria are also present (Frazier et al., 2001; Monge et al., 2006). Though BoHV-4 impacts endometrial epithelial and stromal cells signaling in vitro (Donofrio et

al., 2007), diagnosis of viral derived uterine infections during postpartum period is rare in cattle (Czaplicki and Thiry, 1998).

The majority of uterine infections in dairy cattle are bacterial in origin. Gram-negative *Escherichia coli* and Gram-positive *Trueperella pyogenes* bacteria are major pathogens associated with uterine infection in the postpartum bovine uterus (Hertl et al., 2010; Sheldon et al., 2010; Gilbert and Santos, 2016). Other pathogenic bacteria also found in the postpartum uterus include *Fusobacterium necrophorum* and *Bacteroides melaninogenicus* (Farin et al., 1989; Huszenicza et al., 1999; Sheldon et al., 2002; Williams et al., 2005). More recently, the use of technologies such as metagenomic sequencing has allowed for the characterization of bacteria involved in uterine infection that were previously unknown due to the bacteria being unculturable. The species *Bacteroides pyogenes*, *Porphyromonas levii*, and *Helcococcus ovis* have been positively associated with later uterine disease development, suggesting a shift in the uterine microbiome could precede uterine infection (Galvão et al., 2019).

Diagnosis of Uterine Diseases

Clinically, uterine diseases in dairy cattle are classified as puerperal metritis, clinical endometritis, subclinical endometritis, or pyometra (Földi et al., 2006; Sheldon et al., 2006). Uterine diseases are defined by the different symptoms they present. Puerperal metritis is the infection of the uterus within the first 21 days postpartum characterized by putrid discharge, necrotic debris in the uterus, enlarged uterus, fever and systemic symptoms such as loss of appetite and reduced milk production (Paisley et al., 1986; Lewis, 1997; Sheldon and Dobson, 2004; Földi et al., 2006; Sheldon et al., 2006). The incidence of puerperal metritis in postpartum dairy cows varies from ~20% to 40% (Markusfeld, 1987; Zwald et al., 2004; Sheldon et al., 2009). Clinical endometritis

is diagnosed after 21 days postpartum and is characterized by the absence of systemic signs of illness and the presence of purulent vaginal discharge due to localized endometrial inflammation (Paisley et al., 1986; Lewis, 1997; Bondurant, 1999; Sheldon et al., 2006). The prevalence of clinical endometritis ranges from 5% to 74% in a herd depending on the exact definition and diagnosis of disease (LeBlanc et al., 2002a; Gilbert et al., 2005). Subclinical endometritis is chronic inflammation of the endometrium and can only be diagnosed using cytology (Sheldon et al., 2006). There is not a clear definition in the literature regarding the proportion of polymorphonuclear (PMN) cells present in the uterus required for diagnosis of subclinical endometritis. Diagnosis criteria may use a minimum of 10% PMN cells, while others use 18% PMN cells between 20 to 60 days postpartum (Kasimanickam et al., 2004; Gilbert et al., 2005; Sheldon et al., 2006). Finally, pyometra is characterized by the accumulation of purulent fluid in the uterine lumen accompanied by uterine distension and the presence of an active corpus luteum (Noakes et al., 1990; Sheldon et al., 2006).

For the purposes of this literature review, puerperal metritis, pyometra, clinical and subclinical endometritis are considered uterine diseases. Cows diagnosed with uterine disease produce approximately 5% less milk per day and are 1.7 times more likely to be culled from the herd compared to healthy herd mates (LeBlanc et al., 2002a; Lima et al., 2019). The decrease in milk production could be underestimated as many farms have inconsistent disease recording and treatment programs (McCarthy and Overton, 2018). Further, many studies vary on reporting the severity of disease, parity, and length of milk yield measurement in relation to diagnosis (Rajala and Gröhn, 1998; Giuliodori et al., 2013; McCarthy and Overton, 2018). For example, if investigators

analyze milk yield from the entire lactation, cows could have experienced a decrease in production around disease diagnosis but that will not be noted if an average milk yield for the entire lactation is analyzed (Simerl et al., 1992; Rajala and Gröhn, 1998).

Not only is uterine disease a health and welfare concern for dairy cows but it has economic consequences to producers as well. The economic burden due to uterine disease includes the cost of treatment, loss of milk production, infertility issues, increased culling, and cost of replacement cows, resulting in cost of approximately $480 per cow, amounting to a total cost to the US dairy industry of between $650-$900 million annually (Sheldon et al., 2009; Lima et al., 2019).

Uterine Disease Negatively Impacts Fertility

Uterine inflammation negatively affects reproduction. The exact mechanism responsible for decreased fertility is unclear, but uterine disease is associated with alterations to the hypothalamic-pituitary-gonadal axis, uterine, and ovarian function (Figure 1-1, (Peter et al., 1989; Sheldon et al., 2002; Herath et al., 2009b)). Indeed, any sort of disease event that occurs within six weeks of calving decreases the fertilization rate and embryo development at first service compared to cows without any disease (Ribeiro et al., 2016a). Cows with abnormal vaginal discharge are more likely to have altered ovarian cycles, including shortened or prolonged luteal phases, and slower growth of the first dominant follicle (Peter and Bosu, 1987; Opsomer et al., 2000; Sheldon et al., 2002; Mateus et al., 2003; Williams et al., 2005; Kaneko and Kawakami, 2008). Cows with uterine disease have a longer calving to first service interval, longer calving to conception interval, decreased conception rate, increased pregnancy loss, and are more likely to be culled compared to cows without uterine disease (Borsberry and Dobson, 1989; LeBlanc et al., 2002a; Ribeiro et al., 2016a).

Treatment of Uterine Disease

The main objectives for finding a treatment for uterine disease include cow health and welfare, and secondly, maintaining reproductive performance. Traditionally treatments have included either antimicrobials or prostaglandins, as preventatives or in response to diagnosis. In the United States, there are currently only three approved antibiotics for treatment of uterine diseases: ceftiofur crystalline-free acid (Excede, Zoetis), ceftiofur hydrocholoride (Excenel, Zoetis), and oxytetracyclines (Liquamycin LA-200, Zoetis, or many generic brands). These antibiotics are approved for administration by injection only, and there are currently no treatments approved for intrauterine infusion. Interestingly, the self-cure rate of uterine disease can be as high as 77% (Steffan et al., 1984; Chenault et al., 2004; McLaughlin et al., 2012). Nevertheless, many studies have researched either prevention of uterine disease by vaccination or treatment near calving or curing uterine disease with therapy administered at time of diagnosis.

Interestingly, there is no difference in the cure rate between treatments with antibiotics or prostaglandins, but there is a lack of consensus as to whether treatment improves, (Sheldon and Noakes, 1998; LeBlanc et al., 2002b; Kasimanickam et al., 2005), does not improve, or worsens subsequent reproductive performance compared to untreated cows (Pepper and Dobson, 1987; Mejía and Lacau-Mengido, 2005; Galvão et al., 2009a; b; Dubuc et al., 2011; Lima et al., 2014). The results of different treatments could depend on diagnosis and definition of cure as well as disease severity and ovarian status (i.e. the presence of a corpus luteum) or the number of days post-partum (Steffan et al., 1984; Murray et al., 1990; Knutti et al., 2000; LeBlanc et al., 2002b; Chenault et al., 2004).

With increasing public concern of antimicrobial resistance and hormone usage in animals, other alternative treatments have been explored to reduce incidence or improve cure rate and reproductive performance of cows with uterine disease. Preventative treatments such as trace mineral injections or intrauterine infusion of 2% polyvinyl-pyrrolidone-iodine solution did not reduce disease incidence or improve reproductive performance (Nakao et al., 1988; Machado et al., 2014a). Intrauterine infusions of monosaccharides have resulted in conflicting results regarding cure rates and subsequent fertility (Brick et al., 2012; Machado et al., 2015; Maquivar et al., 2015). Chitosan microparticles, which have antimicrobial properties, did not improve cure rate or reproductive performance (de Oliveira et al., 2020). Finally, immune stimulators, such as intrauterine infusion of *E. coli* or lipopolysaccharide (LPS) after calving, mitigated visual signs of infection and even increased conception rates (Hussain and Daniel, 1992; Singh et al., 2000; Deori et al., 2004).

More recently, a vaccine administered prepartum, comprised of whole inactivated bacterial cells, was able to decrease the incidence of puerperal metritis but not endometritis in dairy cows (Machado et al., 2014b). Further, in cows with metritis, the vaccine improved subsequent reproductive performance compared to non-vaccinated controls (Machado et al., 2014b). A preventative therapeutic administered prior to calving and a second dose within one day of calving of a glycoprotein cytokine, recombinant bovine granulocyte colony stimulating factor bound to polyethylene glycol, reduced the incidence of acute puerperal metritis compared to controls, however the study lacked details on subsequent reproductive performance (Freick et al., 2018).

Although many experiments have been conducted to test different strategies to reduce the incidence or cure uterine disease, many studies lack a control group of untreated cows with uterine disease, thus making it challenging to draw conclusions on treatment efficacy (Pepper and Dobson, 1987; Murray et al., 1990; Sheldon and Noakes, 1998; Brooks, 2000; Drillich et al., 2005; McDougall et al., 2013; Lima et al., 2014). Due to a lack of effective treatments to cure disease and restore fertility, there is a need to further investigate uterine infections. As many of the aforementioned studies explain, there are complications and confounding variables that could contribute to the lack of insight into disease resolution. Accordingly, the use of an experimental model to induce uterine disease for research purposes is valuable (see below).

Physiology of Uterine Infection Induced Infertility in Dairy Cows

Impacts of Uterine Infection on the Hypothalamic-Pituitary Gonadal Axis

Uterine disease impacts endocrine signaling of the hypothalamic-pituitary-gonadal axis. Exposure to bacterial components (e.g. LPS) decreases GnRH and LH secretion in sheep (Battaglia et al., 1997, 1999, 2000; Williams et al., 2001). In both ovariectomized and intact cows, exposure to LPS either intravenously or intrauterine reduces LH pulsatility and secretion (Kujjo et al., 1995; Williams et al., 2008a). Cows treated with LPS had either delayed or inhibited ovulation likely due to alterations in LH secretion and signaling (Peter et al., 1989, 1990; Suzuki et al., 2001; Lavon et al., 2008). Interestingly, uterine disease does not seem to the circulating concentrations of follicular stimulating hormone (FSH) in cows (Sheldon et al., 2002).

Cellular Response to Uterine Infection in the Endometrium

Uterine disease is associated with repeat breeder cows that are repeatedly inseminated yet fail to become pregnant (Yusuf et al., 2010; Janowski et al., 2013). However, embryo transfer can partially rescue the reduced fertility seen in repeat breeder cows (Tanabe et al., 1985; Ribeiro et al., 2016a). Interestingly, embryo transfer recipients that were previously diagnosed with uterine disease had reduced pregnancy rates per embryo transfer compared to recipient cows without uterine disease, suggesting a long-term impact of uterine disease on the uterus (Estrada-Cortés et al., 2019; Edelhoff et al., 2020). Within one week of calving, cows that become subfertile have elevated endometrial gene expression of proinflammatory cytokines (*IL1A*, *IL1B*, *IL6*) compared to more fertile cows, however in the following weeks, there are no differences in cytokine gene expression between fertile and subfertile cows (Herath et al., 2009b). Repeat breeder cows have increased expression of endometrial proinflammatory cytokines similar to cows diagnosed with subclinical endometritis (Salasel et al., 2010; Janowski et al., 2013). This suggests that endometrial inflammation is associated with infertility. The addition of uterine fluid from an inflamed uterus to embryo culture medium decreases the number of trophectoderm cells in bovine blastocysts which may impact the establishment of pregnancy (Hill and Gilbert, 2008).

Both Gram-positive and Gram-negative bacteria express pathogen associated molecular patterns (PAMPs) which bind to pattern recognition receptors on host cells and elicit an inflammatory response. A major sub-family of pattern recognition receptors are the Toll-like receptors (TLR) of which ten members are known in the cow (Menzies and Ingham, 2006; Davies et al., 2008). Within the uterus, the endometrium produces

inflammatory cytokines in response to both Gram-positive *T. pyogenes* and Gram-negative *E. coli* (Amos et al., 2014). Endometrial epithelial cells express TLRs 1 to 7 and 9, while endometrial stroma cells express TLR 1 to 4, 6, 7, 9 and 10 (Herath et al., 2006; Davies et al., 2008). Cows diagnosed with endometritis at four weeks postpartum have elevated endometrial expression of proinflammatory molecules, *CXCL5*, *CXCL8*, *IL1A*, *IL1B*, and tumor necrosis factor alpha (*TNF*) compared to healthy cows (Gabler et al., 2009; Fischer et al., 2010).

Pyolysin, a cholesterol dependent cytolysin produced by Gram-positive *T. pyogenes*, invokes greater damage to stromal cells compared to epithelial or immune cells of the endometrium and is likely due to increased cholesterol content in stromal cells (Jost and Billington, 2005; Amos et al., 2014). Much of the endometrial epithelial cell layer is lost or damaged during parturition and uterine involution is not complete until up to six weeks postpartum (Sheldon, 2004). The lack of endometrial epithelial cells during this period could explain the susceptibility of the endometrium to tissue damage in cows with a uterine infection.

Prostaglandin expression in the uterus is highly regulated and varies depending on day of the estrous cycle. Lysis of the corpus luteum occurs due to prostaglandin $F_2\alpha$ secreted from endometrium. If prostaglandin secretion is dysregulated due to uterine infection, the ovarian physiology and cyclicity is altered. Research has shown that cows with uterine infection have elevated peripheral prostaglandin metabolites and altered endometrial secretion of prostaglandins (PGE2 and F2α) and leukotrienes (B4 and C4) (Del Vecchio et al., 1994; Mateus et al., 2003; Herath et al., 2009a; Barański et al., 2013), while endometrial gene expression of prostaglandin synthases are elevated

(Gabler et al., 2009; Peter et al., 2015). Exposure of endometrium to the Gram-negative cell wall component, LPS, increases production of luteolytic PGF2α from epithelial cells and luteotropic PGE2 from stromal cells (Herath et al., 2006; Davies et al., 2008). Further, the pro-inflammatory cytokine, TNFα, stimulates endometrial PGE2 secretion, specifically in stromal cells (Murakami et al., 2001). Bacteria and bacterial components from a uterine infection alter the endometrial endocrine function which influences ovarian function and could contribute to subfertility in dairy cows.

Few studies have assessed the endometrium of cows after the resolution of disease. Microarray data suggests there are alterations in the endometrium related to the immune system, cell adhesion, apoptotic signaling pathways, cell signaling, and chemotaxis in cows with clinical and subclinical endometritis 50 days postpartum (Salilew-Wondim et al., 2016). Further, cows that previously had uterine disease (< 21 days postpartum) have increased expression of proinflammatory cytokines (*IL1A*, *IL1B*, *TNF*) and elevated angiosclerosis compared to healthy cows (Heppelmann et al., 2016). Cows with an induced uterine infection, had alterations in the transcriptomes of ampulla, isthmus, intercaruncular and caruncular endometrium three months after an induced uterine infection compared to healthy cows (Horlock et al., 2020).

Molecular and Cellular Responses to Uterine Infections Within the Ovary

Within the first weeks postpartum, follicles from cows with uterine infection grow slower and produce less estradiol compared to healthy cows (Sheldon et al., 2002). The intrafollicular environment that supports the growth of the oocyte is critical for the developmental competence of the oocyte and potential embryo. The Gram-negative bacterial cell wall component, LPS, accumulates in follicular fluid of cows with uterine inflammation and is still present even weeks after uterine disease has resolved (Herath

et al., 2007; Piersanti et al., 2019a). In vitro experiments demonstrate LPS exposure to oocytes induces meiotic failure and decreases the ability of cleaved zygotes to become blastocysts (Soto et al., 2003; Bromfield and Sheldon, 2011). Recently, results of an in vivo experiment indicated oocytes collected from cows with resolved uterine infection have an altered transcriptome compared to oocytes from healthy cows (Piersanti et al., 2020).

Bovine granulosa cells express all ten TLRs (Price and Sheldon, 2013), each of which binds a conserved PAMP, including TLR4 and TLR2, that bind LPS and Gram-positive cell wall component, peptidoglycan (PGN), respectively. The global transcriptome of granulosa cells of cows is altered after the resolution of disease compared to normal cows, suggesting long-term impacts of infection on the microenvironment of the follicle (Piersanti et al., 2019a). When exposed to LPS, bovine granulosa cells respond to bacterial components with increased secretion of cytokines (IL-1β, IL-6, IL-8, and TNFα), as well as increased phosphorylation of extracellular-signal-regulated kinase (ERK1/2) and p38 (Herath et al., 2007; Williams et al., 2008b; Bromfield and Sheldon, 2011; Price et al., 2013; Yenuganti et al., 2014). Treatment of granulosa cells from small follicles (< 4 mm) with LPS increased expression of the *TLR4* complex; however, granulosa cells isolated from large follicles (> 8 mm) did not increase *TLR4* complex expression, suggesting differences in granulosa cells sensitivity to LPS dependent on follicle size (Shimizu et al., 2012). A common indicator of TLR activation is nuclear translocation of p65, a subunit of NFκB, however bovine granulosa cells appear to use the ERK/p38 pathway and do not utilize the p65 pathway (Bromfield and Sheldon, 2011; Price et al., 2013).

In agreement with the phenotype observed in cows with uterine disease in the first weeks postpartum, granulosa cells have decreased estradiol secretion in the presence of LPS (Sheldon et al., 2002; Herath et al., 2007). Additionally, gene expression of the enzyme responsible for conversion of androgens to estradiol, aromatase (*CYP19A1*), is downregulated (Herath et al., 2007; Williams et al., 2008b; Shimizu et al., 2012; Price et al., 2013; Onnureddy et al., 2015; Li et al., 2017; Yenuganti et al., 2017). However, granulosa cells do not alter gene expression of follicle-stimulating hormone receptor (*FSHR*), luteinizing hormone receptor (*LHCGR*), or estrogen receptor alpha (*ESR1*) in response to LPS (Herath et al., 2007). When theca cells are exposed to LPS, androstenedione, the precursor to estradiol synthesis, is not affected (Herath et al., 2007; Williams et al., 2008b), indicating the cause of reduced estradiol secretion is centered around aromatase function and not precursor availability.

The mechanism responsible for decreased estradiol production in response to LPS is unclear. In buffalo granulosa cells, experimental inhibition of histone deacetylase (HDAC) activity in conjunction with LPS treatment restored *CYP19A1* expression and improved estradiol production compared to LPS treatment alone (Mehta et al., 2015). In porcine granulosa cells, inhibition of heat-shock protein 70 (HSP70) and treatment with LPS rescued *CYP19A1* gene expression compared to LPS treatment alone (Li et al., 2017). Another report described that co-treatment of granulosa cells with insulin-like growth factor 1 (IGF1) and LPS partially attenuated production of pro-inflammatory cytokines and restored *CYP19A1* downregulation compared to LPS treatment alone (Onnureddy et al., 2015). Unfortunately, the quantification of estradiol production from cells treated with HSP70 inhibitor or IGF1 was not reported (Onnureddy et al., 2015; Li

et al., 2017). Recently, work in buffalo granulosa cells documented that LPS increases nuclear translocation of the transcription factor CCAAT/enhancer-binding protein beta (CEBPβ) and demonstrated that CEBPβ binds to the *CYP19A1* proximal promoter II, thus potentially inhibiting transcription of the *CYP19A1* (Yenuganti et al., 2017). To determine the exact mechanism by which LPS alters estradiol synthesis these results need to be replicated and further investigated.

Carryover Effect of Stressors on Oocyte Quality

Although oocytes are a finite population, bovine follicles take an estimated 120-200 days to develop from the primordial to pre-ovulatory stage (Lussier et al., 1987; Gougeon, 1996). The idea that follicular quality is determined during initial development weeks before ovulation but may not be apparent for months is known as the Britt hypothesis (Britt, 1992). There are data to indicate a carryover effect of an event that impacts fertility even after stress is resolved. Early postpartum clinical disorders such as those previously discussed can affect fertility weeks or even months later even if the animal is clinically healthy (Fonseca et al., 1983; Oltenacu et al., 1983). Additionally, corpus luteum function multiple cycles postpartum seems to be influenced by body condition at parturition (Britt, 1992). Season can impact fertility as there is a correlation with lower quality oocytes and altered steroid production from samples collected in autumn following summer heat stress compared to winter sample collection (Wolfenson et al., 1997; Rocha et al., 1998; Roth et al., 2000). Furthermore, experiments using environmental chambers demonstrated oocytes from cows after exposure to heat stress, but not during heat stress, were less likely to develop to a blastocyst compared to cows kept constant at thermal neutral temperatures (Torres-Júnior et al., 2008). More

recently, there are data showing oocyte transcriptome is altered even 60 days post infection (Piersanti et al., 2020).

Production and Regulation of Estradiol, a Major Female Sex Steroid Hormone

Discovery of Estrogens, an Integral Female Reproductive Hormone

A critical component to female reproduction and fertility is the steroid hormone estrogen. There are multiple forms of estrogens, including estrone, estradiol, and estriol. The ovary and the placenta are the main sources of estradiol, which is the most potent and bioactive class of estrogen (Simpson et al., 1994). The largest concentration of estrogens in the female is found in large ovarian follicles, followed by ovarian venous blood, then peripheral blood (Channing and Coudert, 1976).

In 1923 scientists in St. Louis, Missouri identified a compound in follicular fluid from sows, today known as estrogen, that could increase uterine weight (Allen and Doisy, 1923; Allen et al., 1924). In the 1930s, experiments in rats and men demonstrated that supplementing exogenous androgens increased the urine concentration of an estrogenic compound (Steinach and Kun, 1937; Södersten et al., 2014). Another study injected radiolabeled testosterone intravenously in pregnant mares and extracted radioactive estrone from their urine, which suggested testosterone as a potential precursor to estrogen (Heard et al., 1955). By the 1950s, it was understood that the ovary produced the majority of estrogens in females, but which specific cells were responsible for estrogen production were unknown.

Ovarian Folliculogenesis

An ovarian follicle contains the female gamete, the oocyte, surrounded by somatic granulosa cells. Female mammals are born with a finite number of oocytes (Zuckerman, 1951). In many animals, including humans and bovine, ovarian follicles are

formed in utero, while other animals, such as feline or rodents, follicles are formed shortly after birth (Mauleon, 1969; Monniaux et al., 1997). The ovary contains thousands of primordial follicles which contain an oocyte surrounded by squamous granulosa cells (Hirschfield, 1991). Once activated, the follicle will undergo growth and development to become a primary follicle. A primary follicle is characterized by an increase in size of the oocyte, initial formation of the zona pellucida, and cuboidal granulosa cells (Hirschfield, 1991). The next development stage, a secondary stage follicle, is characterized by multiple layers of granulosa cells surrounding the oocyte and a layer of theca cells outside of the granulosa cells (Hirschfield, 1991). When the follicle reaches the secondary stage, it is sensitive to gonadotropin regulation and the granulosa cells express FSHR and begin steroidogenesis (Hirschfield, 1991). Follicular stimulating hormone receptor is a G-protein coupled receptor that activates a signaling cascade mediated by adenylate cyclase, cyclic AMP, and protein kinase A (Miller and Auchus, 2011). Mechanisms such as granulosa cell proliferation and steroidogenesis are regulated by FSH. A tertiary or antral follicle is characterized by the formation of the antrum, a fluid-filled space within the granulosa cell population. The antrum contains follicular fluid, which likely arises from filtered blood (Shalgi et al., 1973; Rodgers and Irving-Rodgers, 2010). Additionally, in antral follicles, granulosa cells differentiate into mural granulosa cells which surround the basement membrane, and cumulus granulosa cells which surround the oocyte. The final follicular developmental stage is known as dominant, Graafian, or pre-ovulatory, and is awaiting cues to ovulate (Hirschfield, 1991). Although initially there are thousands of follicles in the ovary, most will undergo atresia

at some point during development and never ovulate (Baker, 1963; Erickson, 1966; Hirschfield, 1991; Gougeon, 1996).

Two-cell Theory of Ovarian Steroidogenesis

The two-cell theory regarding ovarian steroidogenesis involves the collaboration between granulosa and theca cells within the follicle to produce estrogens from cholesterol. The seminal paper for the two-cell estrogen production theory was published in 1959 (Falck, 1959). Rats were ovariectomized and the ovary dissected to isolate various cells, including interstitial, granulosa, theca, corpus luteal tissue, and pieces of the follicle wall containing multiple cell types. A portion of vaginal tissue was also isolated and used as an indicator of estrogen production via cornification of the vaginal epithelium. A series of auto-transplants were undertaken, with various ovarian cells along with vaginal tissue transplanted in the left eye and vaginal tissue alone to the right eye of rats. Cornification of the vaginal epithelium was observed when follicle wall tissue containing granulosa and theca interna cells isolated from rats was transplanted to the eye indicating synthesis of bioactive estrogen. Individually isolating granulosa and theca cells then recombining them and transplanting together also allowed for estrogen production, however when either granulosa or theca cells were transplanted alone, no estrogen was produced as indicated by a lack of vaginal epithelium cornification (Falck, 1959).

Following this seminal study, other scientists worked to understand the capabilities of individual theca and granulosa cells as both are required to produce estrogen. Initial studies utilized cell culture systems with radio-labeled precursors, such as androgens or progestins, and found conflicting results. Human studies reported theca cells producing more estrogen than granulosa cells (Ryan and Petro, 1966), while

animal studies found granulosa cells were more efficient than theca cells at producing estrogen (Ryan and Short, 1965; Bjersing and Carstensen, 1967; Lacroix et al., 1974). However, when granulosa and theca cells were cultured together, they produced more estrogen than when either were cultured individually (Ryan et al., 1968; Lacroix et al., 1974; Makris and Ryan, 1975). Androgens are the precursor to estrogens and similar studies conducted with isolated cell types found theca cells are more efficient at synthesizing androgens compared to granulosa cells (Bjersing and Carstensen, 1967; Ryan et al., 1968; Lacroix et al., 1974; Makris and Ryan, 1975).

Research next focused on the function of these cell types based on the size of the follicle from which they were isolated. Granulosa and theca cells were isolated from medium (100-300 μm) and large (500+ μm) hamster follicles and cultured either individually or recombined with cells from either the same or different sized follicles. Estradiol production was the greatest when granulosa and theca cells were both isolated from large follicles, indicating that the larger the follicle, the more estradiol production (Makris and Ryan, 1975).

Regulation of Steroidogenesis

After concluding the specific roles of each cell type, the next logical question was what regulates androgen and estrogen production in theca and granulosa cells? An experiment in cells collected from proestrus rat follicles and cultured with FSH alone, LH alone, or in combination revealed that the addition of LH, but not FSH, to the medium further elevated the androgen production in theca cells (Fortune and Armstrong, 1977). Testosterone production in theca cells could also be increased with the addition of dibutyl cyclic adenosine monophosphate (Bu2cAMP), or PGF2α, and PGE2 (Erickson and Ryan, 1976). There are reports of granulosa cells producing negligible amounts of

androgens, however theca cells produce the vast majority of androgens which can be augmented with LH stimulation or additional progesterone (Bjersing and Carstensen, 1964; Liu and Hsueh, 1986).

Isolated granulosa cells produce little to no estradiol without additions of androgen precursor or hormone stimulation to the culture medium (Dorrington et al., 1975; Erickson and Ryan, 1975). Granulosa cells do produce copious amounts of estrone and estradiol in response to the presence of androgens; however, there is a maximal amount of androstenedione that can be added to culture medium before granulosa cells reduce estrogen production, implying a possible substrate inhibition loop (Erickson and Hsueh, 1978). In the presence of androgens, the addition of FSH or Bu2cAMP further elevates estradiol production in granulosa cells (Dorrington et al., 1975; Erickson and Ryan, 1975; Moon et al., 1975; Wang et al., 1982). Follicle stimulating hormone stimulates adenylate cyclase and cyclic AMP production in a cell signaling cascade critical for estradiol production in granulosa cells (Kolena and Channing, 1972; Adashi et al., 1990). Unlike theca cells, the addition of LH or prostaglandins to granulosa cell cultures does not augment estradiol production (Dorrington et al., 1975; Erickson and Ryan, 1975; Moon et al., 1975).

In estrogen biosynthesis, progestins are the precursors to androgens. Both theca and granulosa cells can produce progesterone (Bjersing and Carstensen, 1967; Ryan et al., 1968; Lacroix et al., 1974; Makris and Ryan, 1975; Liu and Hsueh, 1986). The addition of FSH and LH to culture medium can increase progesterone production by granulosa cells but does not alter progesterone production by theca cells (Bjersing and

Carstensen, 1967; Ryan et al., 1968; Lacroix et al., 1974; Makris and Ryan, 1975; Liu and Hsueh, 1986).

The two-cell theory can be summarized as granulosa cells provide progesterone to theca cells as a precursor for androgen production, which in turn serve as the precursor for estrogen production in granulosa cells (Fortune, 1986).

Aromatase: The Critical Enzyme for Estradiol Synthesis

The key enzyme mediating estradiol synthesis, aromatase, was originally purified from microsomes in human term placenta (Pasanen and Pelkonen, 1981). Aromatase is a 55 kD monooxygenase and one enzyme in a large family of cytochrome pigment (P) 450 enzymes named due to the spectral peak measured at 450 nm (Pasanen and Pelkonen, 1981; Mendelson et al., 1985; Kellis and Vickery, 1987). Many cytochrome P450 enzymes play a role in detoxification as well as steroidogenesis and can be found in many tissues including adipocytes (Grodin et al., 1973), placenta (Ryan, 1959), fetal hepatocytes (Siiteri, 1982), brain (Naftolin et al., 1975; Roselli et al., 1985), testicular Sertoli and Leydig cells (Valladares and Payne, 1979; Tsai-Morris et al., 1985), and ovarian granulosa cells (McNatty et al., 1976). Aromatase is responsible for the aromatization process to convert androgens to estrogens, which occurs in three steps; two initial hydroxylation's of the methyl group at C19 followed by an oxidation step, culminating in multiple molecular rearrangements allowing for C19 elimination and reduction of A-ring keto group to a hydroxyl group and A ring aromatization (Yoshimoto and Guengerich, 2014). The gene that encodes for aromatase is *CYP19A1* and there are tissue-specific variations in the promoter location that regulates *CYP19A1* expression as well as tissue-specific transcription factors (Means et al., 1991; Santen et al., 2009). While the placenta and fetal liver utilize promoters upstream of exons I.1 and

I.2, ovarian granulosa cells utilize a promoter upstream of exon II (Means et al., 1991). Aromatase expression and activity is stimulated by IGF1 (Adashi et al., 1985; Steinkampf et al., 1988), FSH (Dorrington and Armstrong, 1975; Steinkampf et al., 1987), adenylate cyclase, and cyclic AMP (Wang et al., 1982; Steinkampf et al., 1987). The bovine *CYP19A1* gene, while not as homologous as primates to humans, is more similar to the human gene compared to rodents (Simpson et al., 1994).

Transcription Factor CCAAT/ Enhancer Binding Protein Beta

One transcription factor hypothesized to regulate *CYP19A1* expression is CCAAT/enhancer binding protein beta (CEBPβ). The transcription factor CEBPβ is one of six members of a family with a highly conserved basic leucine zipper domain at the C-terminus which is involved in dimerization and DNA binding (Ramji and Foka, 2002). The gene encoding CEBPβ (*CEBPB*) contains only one exon, but the mRNA can produce at least three translational products due to various initiation codons (Descombes and Schibler, 1991; Ossipow et al., 1993). Many cellular functions, including proliferation, differentiation, metabolic regulation, and immune response are regulated by CEBPβ (Huber et al., 2012). Interestingly, CEBPβ plays a role in follicle development, ovulation, and corpus luteum formation (Sterneck et al., 1997; Fan et al., 2011). One study demonstrated that CEBPβ can bind to the *CYP19A1* proximal promotor II in buffalo granulosa cells (Yenuganti et al., 2017). Interleukins (IL) 1 and 6, as well as LPS can induce CEBPβ to bind DNA and regulate gene transcription (Akira et al., 1990; Poli, 1998; Udofa et al., 2013).

Alterations in estrogen production can cause many complications in reproduction as well as general health. Estrogens are critical for bone growth, metabolism, and reproduction and deficiencies or excessive estrogen production can cause decreased

bone density, altered insulin signaling, and infertility (Stocco, 2012). In dairy cows, uterine infections impede estradiol production, although the exact mechanism is still unknown (Sheldon et al., 2002).

Induced Uterine Infection Models

There are many potentially confounding factors when studying spontaneous uterine infections in the dairy cow such as peripartum diseases and lactation. The ability to use a model where uterine infection can be induced provides an opportunity to understand the mechanism behind infection-induced infertility in the absence of other confounding factors.

The uterine infection model is not a new concept. Previous studies have created models to induce uterine inflammation and study the impact on fertility as early as the 1950s. The first experiments collected purulent uterine exudate from diseased cows and infused it into the uterus of healthy cows and caused altered luteal phases, shorter estrous cycles, and induced pyometra (Rowson and Lamming, 1953; Gallagher and Ball, 1980). Other studies have repeated the intrauterine infusion model using various bacteria (*E. coli*, *T. pyogenes*, *F. necrophorum*) isolated from purulent uterine exudate to induce local uterine inflammation, as determined by influx of PMN cells, and altered prostaglandin signaling and ovarian function (Gallagher and Ball, 1980; Farin et al., 1989; Regassa et al., 2002; Kaneko and Kawakami, 2008; Lima et al., 2015). Some experiments infused only bacteria-free filtrate, bacteria components, such as LPS, or cytokines, such as TNFα and found impacts on prostaglandin signaling and ovarian function as well (Hussain and Daniel, 1992; Williams et al., 2008b). A key component to inducing uterine infection is disrupting the uterine epithelium, as infusion of bacterial components into heifers with intact uterine mucosa does not alter ovarian or endocrine

events (Miller et al., 2007). This disruption to uterine mucosa, mimics the physical aspects of the uterine environment, as the uterine epithelium is damaged or absent following parturition.

Another component critical to inducing a uterine infection is the endocrine environment. Early experiments identified that for establishment of an infection, there must be elevated progesterone, as elevated estrogen clears potential infection (Rowson and Lamming, 1953; Farin et al., 1989). The endocrine status influences immune cell dynamics, which allows for infection establishment or clearance. Despite there being no difference in circulating peripheral leukocytes prior to infection, the influx of leukocyte to the endometrium and clearance of bacteria from the uterine lumen is much more rapid at estrus or in ovariectomized females compared to females in the luteal phase of the cycle (Broome et al., 1960; Hawk et al., 1960). These differences in leukocytic response between follicular and luteal phases were apparent in virgin heifers induced with uterine infection (Hawk et al., 1964). The impact of estradiol and progesterone on the inflammatory response was solidified when ovariectomized rabbits were treated with exogenous estradiol or progesterone and found similar results (Hawk et al., 1960). More recently, these critical aspects have been combined into one model in heifers where exogenous progesterone is given in order to mimic the luteal phase, the endometrium is scarified to damage the mucosal layer, and the combination of endometrial pathogenic *E. coli* and *T. pyogenes* isolated from metritic cows is infused into the uterus of heifers to induce uterine infection similar to clinical endometritis (Piersanti et al., 2019b).

Objectives for this Program of Study

Though there are many associations with uterine infections and infertility, the underlying mechanisms responsible for infertility are elusive. The overall objective of the

studies reported in this dissertation is to ascertain the mechanisms responsible for infection-induced infertility apparent after the resolution of uterine disease in dairy cattle. Using an experimental model of induced uterine infection, the impact of uterine infection on oocyte competence and endometrial transcriptome was analyzed. Following infection, oocyte competence over time was assessed using oocyte pick-up, in vitro fertilization and embryo culture methods (chapter 2). The long-term impact of uterine infection on the ability to establish pregnancy was characterized using RNA sequencing of intercaruncular endometrial tissues (chapter 3). Lastly, disentangling the cellular mechanism of altered estradiol production in the presence of the bacterial component, LPS, was investigated using granulosa cell cultures (chapter 4). With a better understanding of the molecular impact of uterine disease on various part of the reproductive tract, future research can work to develop therapeutics to improve fertility following uterine disease.

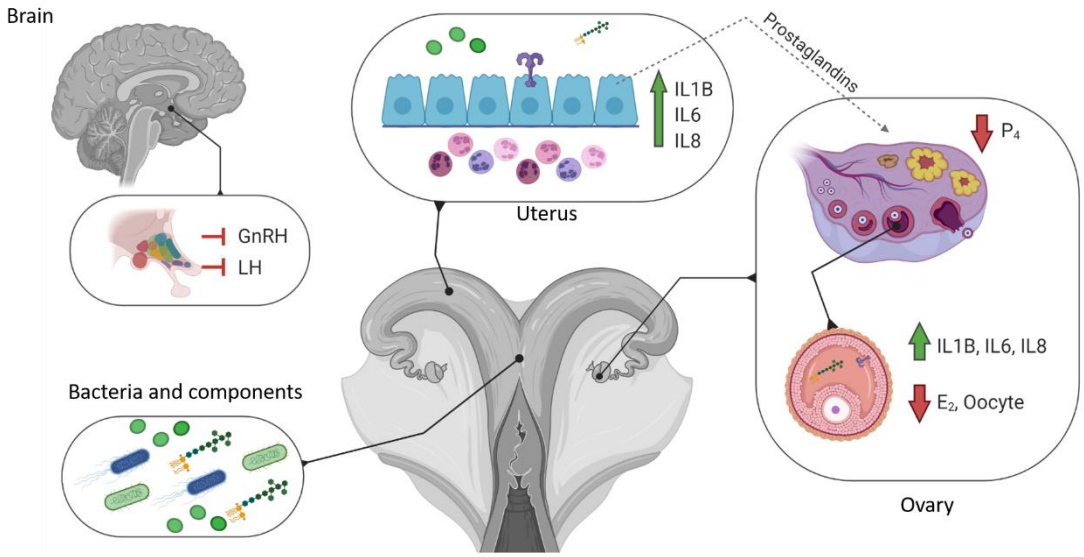

Figure 1-1. Impact of uterine infection on female reproduction. Bacteria and bacterial components, such as *E. coli* and lipopolysaccharide (LPS) or *T. pyogenes* and pyolysin, alter gonadotrophin releasing hormone (GnRH) and luteinizing hormone (LH) pulsatility from the hypothalamus and pituitary; increase cytokine production including interleukins (IL1B, IL6, IL8), and alter prostaglandin secretion in the endometrium; impact follicular growth and luteal lifespan in the ovary and increase cytokine production, alter steroid production (estradiol, E_2; progesterone, P_4) of granulosa cells, and decrease oocyte competence.

CHAPTER 2
EXPERIMENTALLY INDUCED ENDOMETRITIS IMPAIRS THE DEVELOPMENTAL CAPACITY OF BOVINE OOCYTES [1]

Abstract of Chapter 2

Uterine infection is associated with infertility in women and dairy cows, even after the resolution of infection. However, the mechanisms causing this persistent infertility are unclear. Here, we hypothesized that induced endometritis in non-lactating dairy cows would reduce the developmental competence of oocytes. Non-lactating Holstein cows received an intrauterine infusion of endometrial pathogenic bacteria (*Escherichia coli* and *Trueperella pyogenes*; n = 12) or vehicle control (n = 11) on day 2 of the estrous cycle. Bacterial infusion increased expression of endometrial inflammatory mediators, and a mucopurulent discharge in the vagina confirmed the establishment of endometritis. Oocytes were collected by transvaginal ultrasound guided ovum pick-up on day 2, 24, 45, and 66 following infusion, and subjected to in vitro fertilization and embryo culture. Bacterial infusion resulted in fewer cleaved oocytes developing to morulae compared to vehicle-infused controls (30.7% versus 45.0%), with the greatest effect observed in oocytes collected on day 24. Development to morula was inversely correlated with endometrial expression of *IL6* on day 6. The expression of genes associated with embryo quality did not differ significantly between morulae from bacteria-infused and control cows. Artificial insemination 130 days after intrauterine

[1] Reprinted with permission from Dickson, M.J., R.L. Piersanti, R. Ramirez-Hernandez, E.B. de Oliveira, J.V. Bishop, T.R. Hansen, Z. Ma, K.C.C. Jeong, J.E.P. Santos, M.I. Sheldon, J. Block, and J.J. Bromfield. 2020. Experimentally induced endometritis impairs the developmental capacity of bovine oocytes. Biol. Reprod. 103:508–520. doi:10.1093/biolre/ioaa129.

infusion resulted in normal, filamentous embryos that produced interferon-tau 16 days after conception in both infusion groups. This model of experimentally induced uterine infection successfully resulted in endometritis and a reduction in the proportion of oocytes that developed to morulae following in vitro fertilization. In conclusion, endometritis reduced the capacity of oocytes to develop to morulae.

Introduction

Uterine infections of women and dairy cows are associated with reduced fertility (Sheldon et al., 2009; Tsevat et al., 2017), yet the mechanisms responsible for persistent infertility are unclear. An estimated 3.6 million cases of Gonorrhea or Chlamydia infections occur in women annually in the United States (Centers for Disease Control and Prevention, 2018), of which 10% cause pelvic inflammatory disease (Kreisel et al., 2017). Bacterial infections of the reproductive tract and pelvic inflammatory disease both result in uterine inflammation (Deb et al., 2004; Tsevat et al., 2017). Each case of pelvic inflammatory disease costs approximately $3,000 and results in high rates of hospitalization (Owusu-Edusei et al., 2013). Similarly, bacterial infection of the postpartum uterus is ubiquitous in dairy cows, with up to 40% of cows developing a clinical uterine disease (Dohmen et al., 2000; Sheldon et al., 2009). Cows diagnosed with postpartum uterine disease are less likely to become pregnant and are more likely to abort (Ribeiro et al., 2016a). Uterine disease in cows costs approximately $900 million annually in the United States due to treatment cost, loss of milk production, infertility, increased culling, and cost of replacement cows (Sheldon et al., 2009; Lima et al., 2019).

Although infections occur in the uterus, ovarian signaling and function are altered in cattle with active uterine infection. Cows with uterine disease have slower follicle

growth, impaired ovulation, and delayed and irregular ovarian cyclicity (Opsomer et al., 2000; Sheldon et al., 2002; Ribeiro et al., 2013). Interestingly, infertility in cows is evident even after resolution of disease, as many cows remain unable to conceive (Borsberry and Dobson, 1989; LeBlanc et al., 2002a; Santos et al., 2010).

The Gram-negative bacteria, *Escherichia coli*, and Gram-positive bacteria, *Trueperella pyogenes*, are common pathogens that cause clinical endometritis in dairy cows (Sheldon et al., 2019). Outer membrane components of Gram-negative bacteria, including lipopolysaccharide (LPS), are detectable in follicular fluid, and follicular fluid LPS concentrations are correlated with the severity of uterine inflammation (Herath et al., 2007; Piersanti et al., 2019a). Granulosa cells produce an inflammatory response to LPS and other bacterial components in vitro, and uterine infection changes the transcriptome of granulosa cells long after the clearance of infection (Bromfield and Sheldon, 2011; Piersanti et al., 2019a). Oocytes cultured in the presence of bacterial components have an increased frequency of meiotic failure (Bromfield and Sheldon, 2011) and a decreased capacity to develop to the blastocyst (Soto et al., 2003). Oocytes are a finite resource in the ovary and require in excess of 100 days to develop from the primordial follicle until ovulation (Zuckerman, 1951; Britt et al., 2018), this allows for the intriguing possibility that oocytes could be affected during uterine infection and bear prolonged perturbations that could compromise their quality and affect fertility long after the resolution of infection.

Lactation, negative energy balance (when the metabolic energy required for maintenance and lactation exceeds the energy available from the diet), uterine environment, and common postpartum diseases can influence fertility of the postpartum

dairy cow. To disentangle the effects of uterine infection on oocyte quality from other postpartum factors, we experimentally induced endometritis in non-lactating dairy cows, and collected oocytes to assess their capacity to develop to morulae following in vitro fertilization and embryo culture. We hypothesized that induced endometritis in non-lactating dairy cows would reduce the competence of oocytes to develop into embryos following in vitro fertilization and embryo culture. We aimed to establish infection in non-lactating cows using pathogenic bacteria, determine the impact of uterine infection on oocyte quality and subsequent embryo development, and assess the ability of cows to conceive following artificial insemination.

Materials and Methods

The University of Florida Institutional Animal Care and Use Committee approved all animal procedures (protocol number 201508884). The experiment was conducted from February to August 2018 at the University of Florida Dairy Research Unit.

Experimental Protocol and Establishment of Uterine Infection

Establishment of endometritis followed the protocol of Piersanti et al. (Piersanti et al., 2019b), with minor modifications (Fig. 2-1). Twenty-three 2-year-old first lactation Holstein cows were enrolled in the study. Cows were free of clinical disease following parturition (including uterine disease) prior to enrollment. At least 38 days prior to the beginning of the study cows were vaccinated against bovine viral diarrhea, infectious bovine rhinotracheitis, parainfluenza, bovine respiratory syncytial virus, and multiple serovars of Leptospira (Bovi-Shield Gold FP 5 VL5 HB; Zoetis, Parsippany, NJ) and dewormed using moxidectrin (Cydectin; Bayer HealthCare, LLC, Animal Health Division, Shawnee Mission, KS). Lactation was ended within 67 days of calving and at least 45 days prior to the initiation of the study by a final milking and intramammary treatment

with ceftiofur hydrochloride (Spectramast, Zoetis, Parsippany, NJ) followed by a teat sealant (Orbeseal, Zoetis). No cows developed mastitis during the study period. Cows were maintained on pasture and fed a total mixed ration daily with free access to water. Cows were blocked by days postpartum and divided into two cohorts consisting of two infusion groups (vehicle or bacteria intrauterine infusion, see below). Random assignment to either treatment group was performed for each block by random number generation in Microsoft Excel.

Estrous cycles of cows were synchronized (Fig.2-1) using 100 µg GnRH (gonadorelin diacetate tetrahydrate; Ovacyst, Bayer) i.m. followed by 25 mg prostaglandin (PG) $F_{2\alpha}$ (dinoprost tromethamine; Prostamate, Bayer) i.m. 7 days later, followed by GnRH after 3 days and 10 days, $PGF_{2\alpha}$ 7 days later and another, final GnRH injection 56 h following $PGF_{2\alpha}$ to stimulate ovulation (Souza et al., 2008). Progesterone (200 mg) in corn oil (Sigma-Aldrich, St. Louis, MO) was administered i.m. to cows daily starting on the final day of GnRH administration and continued for 7 days. On the day of intrauterine infusion (experimental day 0) cows received an epidural anesthetic of 60 mg lidocaine hydrochloride 2% (Aspen Veterinary Resources, Greely, CO) injected into the intercoccygeal intervertebral space. External genitalia were cleaned with 1% virkon solution (DuPont, Wilmington, DE), followed by 1% chlorohexidine solution (Aspen Veterinary Resources), and 70% ethanol. A sheathed Neilson catheter (450 mm; Supplies for Farmers, Lincolnshire, UK) was introduced transvaginally into the reproductive tract and guided into the uterine body via rectal palpation. Once in the uterine body, the sheath was retracted to expose the catheter port, which was rotated three times against the endometrial lining to debride the

endometrium prior to intrauterine infusion. Bacteria-infused cows (*n* = 12) received 10 mL of Luria-Bertani (LB) broth containing 5.05×10^7 CFU/mL *E. coli* MS499 and 10 mL of LB containing 3.65×10^7 CFU/mL of *T. pyogenes* MS249*,* followed by 10 mL of LB to flush the catheter. Vehicle-infused cows (*n* = 11) received an intrauterine infusion of 30 mL of LB broth.

Propagation of Pathogenic *E. coli* and *T. pyogenes* for Intrauterine Infusion

Bacterial cultures were prepared as previously described by Piersanti et al. (Piersanti et al., 2019b). Briefly, *E. coli* MS499 was cultured from frozen glycerol stocks on LB agar (Goldstone et al., 2014a). The day before intrauterine infusion, a single bacterial colony was picked from the plate and inoculated into LB broth containing 1% tryptone, 0.5% yeast extract and 1% sodium chloride. The culture was incubated overnight at 37ºC with shaking at 200 rpm. In parallel, *T. pyogenes* MS249 was grown from frozen glycerol stocks on Trypticase Soy Blood agar at 37ºC for 48 h (Goldstone et al., 2014b). The day prior to intrauterine infusion, a single bacterial colony was selected and inoculated into Bacto Brain Heart Infusion broth (BHI; Fisher Scientific, Pittsburgh, PA) supplemented with 5% fetal bovine serum (Fisher Scientific) and cultured overnight at 37ºC with shaking at 200 rpm. Bacterial growth was monitored by measuring optical density at 600 nm. A final preparation of 5.05×10^7 CFU/mL *E. coli* or 3.65×10^7 CFU/mL of *T. pyogenes* MS249 were diluted in sterile LB broth and loaded into 10 mL syringes for infusion. To measure the final concentrations of bacterial cells infused, ten-fold serial diluted bacterial cultures were plated on agar and grown at 37ºC to count CFU. Sterile LB broth for flushing catheters and vehicle infusions was loaded into 10 mL syringes. Infusions were transported to the farm on ice.

Evaluation of Uterine Infection

Rectal temperature was measured (AG-102 thermometer, AG-Medix, Mukwonago, WI) between 7 AM and 9 AM on day -2, 1, 3, 5, and 10. Vaginal mucus samples were collected and examined using a clean, gloved hand on day -2, 3, 5, 10, 14, 20, 28, 49, and 70. Briefly, the vulva was cleaned with 70% alcohol and dried with paper towels. Mucus was collected by introducing a clean, gloved hand into the vagina and retrieving any contents from the lateral, dorsal and ventral vaginal walls. Mucus was graded on a scale of 0 to 4 according to Sheldon et al., (2009) where grade 0 was no mucus or clear/translucent mucus; grade 1 was mucus containing flecks of white or off-white pus; grade 2 was mucus containing ≤ 50% white or off-white mucopurulent material; grade 3 was mucus containing > 50% purulent material; and grade 4 was mucus containing > 50% purulent material and dark brown blood.

Endometrial cytobrush samples were collected on day 6, 28, 49 or 50, and 69 or 70 (Fig. 2-1). Briefly, external genitalia were cleaned with 1% chlorohexidine solution followed by 70% ethanol. Guided by rectal palpation, the cytobrush tool (Medscand Medical, Cooper Surgical, Trumball, CT) contained within a metal sheath and covered in a plastic chemise was introduced into the vagina and passed through the cervix. The plastic chemise was retracted over the tool exposing the brush to the endometrium. The brush was rotated three times to collect endometrial cells before being retracted into the metal sheath and removed from the cow. The cytobrush was smeared on a clean, glass slide for cytology and then the brush was snap frozen in liquid nitrogen and stored at -80ºC until used for real time RT-PCR. For cytology, slides were air dried and stained with Rapid Chrome Kwik-Diff (Thermo Fisher Scientific, Waltham, MA) to assess the proportion of polymorphonuclear cells present. A total of 200 cells were counted at both

10x and 40x magnification on a Nikon Optiphot microscope (Nikon Instruments, Melville, NY) and the proportion of polymorphonuclear cells was determined.

Blood was collected via coccygeal venipuncture on days -2, 5, and 145 into evacuated tubes containing lithium heparin (Becton Dickson, Franklin Lakes, NJ) for plasma collection or Z serum clot activator (Griener Bio-One, Monroe, NC) for serum collection, and centrifuged for 10 min at 2,400 × *g* at room temperature, aliquoted and stored at -20ºC. Plasma haptoglobin (Life Diagnostics, Inc., West Chester, PA) and serum progesterone (DRG International, Springfield Township, NJ) were quantified using commercially available ELISAs according to the manufacturer's instructions. The haptoglobin and progesterone intra-assay coefficient of variation was 4.2% and 2.9%, and the limit of detection was 3.91 ng/mL and 0.3 ng/mL, respectively. Serum anti-Müllerian hormone (AMH) was quantified by a commercial laboratory (Ansh Labs, Webster, TX). The intra-assay coefficient of variation was 1.5% for high (1721 pg/mL), 2.8% for medium (687 pg/mL) and 0.4% for low (336 pg/mL) concentration bovine serum AMH controls. The inter-assay coefficient of variation was 9.3%, 7.4% and 5.7% for high, medium and low concentration controls, respectively. The limit of detection for AMH was 22 pg/mL.

Follicle Aspiration for Oocyte Pick-up and Follicle Ablation

To assess the impact of endometritis on oocytes over time, transvaginal ultrasound-guided oocyte pick-up was performed on experimental days 2, 24, 45, and 66 (Fig. 2-1). Between each oocyte pick-up procedure, dominant follicle ablation was performed 4 days prior to oocyte pick-up to maximize the number of oocytes collected and facilitate estrous synchronization. In brief, cows were restrained and received epidural anesthetic in the intercoccygeal intervertebral space using 3 mg xylazine

(AnaSed; Akorn, Lake Forest, IL) and 60 mg of lidocaine hydrochloride 2%. External genitalia were cleaned with 1% chlorhexidine solution followed by 70% ethanol. The vagina was rinsed three times by lavage, first using 100 mL of 0.5% chlorhexidine solution and then twice with 100 mL sterile 0.9% saline. The oocyte pick-up instrument, including a 7.5 MHz convex ultrasound probe (Choice Medical, South Pasadena, FL) covered in a disposable chemise, was introduced into the vagina using sterile lubricant. The ovary was visualized by ultrasound (Aloka SSD-500, Hitachi Healthcare Americas, Twinsburg, OH) and an 18-gauge needle and vacuum were employed for dominant follicle (> 8 mm) ablation or follicle (< 8 mm) aspiration for oocyte pick-up. Follicular aspirates from dominant follicle (> 8 mm) ablation were discarded. Follicle aspirates (< 8 mm) were collected into ovum pick-up medium (IVF Bioscience, Falmouth, UK) and subsequently filtered and rinsed using an embryo flush filter (Watanabe Tecnologia Aplicada, Brazil). Oocytes were isolated and washed in three drops of 39°C HEPES-buffered oocyte maturation medium (IVF Bioscience) and matured in glass vials containing HEPES buffered maturation medium at 38.5ºC for 24 ± 3 h. All procedures for oocyte maturation, fertilization, and embryo culture were performed keeping oocytes and subsequent embryos from each cow at each time point as an individual group.

In Vitro Fertilization and Embryo Culture

Following oocyte maturation, groups of 1 to 12 oocytes were transferred to 100 µL drops of BO-IVF media overlaid with light mineral oil (IVF Bioscience). Oocytes were fertilized with sperm from the sire Monument 014HO04784 (Select Sires, Plain City, OH) to yield a final concentration of 2×10^6 sperm/mL and placed in a humidified incubator at 38.8ºC with 6% O_2, 6% CO_2 and balanced N_2. After 22 ± 2 h of fertilization, oocytes were rinsed in oocyte wash medium (IVF Bioscience) and cumulus cells were

removed by mechanical pipetting (CooperSurgical, Trumbull, CT). Subsequently, oocytes were moved to 100 µL drops of BO-IVC embryo culture medium (IVF Bioscience) overlaid with light mineral oil. Embryos were cultured in groups of 1 to 12 at 38.8ºC in a humidified environment of 6% O_2 and 6% CO_2 and balanced N_2. Embryos were assessed for cleavage 3.5 days after fertilization, and development to morula 6 days after fertilization. Six days after fertilization after fertilization, morulae from each individual cow were washed three times in DPBS containing 0.2% polyvinylpyrrolidone, the zona pellucida removed in Tyrode's acid solution (Sigma-Aldrich), and washed three times in DPBS before snap freezing in liquid nitrogen and storage at -80ºC. Embryo development was halted at the morula stage, prior to differentiation to inner cell mass and trophectoderm, in order to analyze a homogenous cell population.

Fixed-time Artificial Insemination

Beginning at experimental day 110, estrous cycles of cows were synchronized for fixed-time artificial insemination (Fig 2-1). The synchronization protocol was initiated using $PGF_{2\alpha}$ followed by injection of GnRH 48 h later, and another GnRH injection 6 days later, two subsequent $PGF_{2\alpha}$ injections 24 h apart, one week after the previous GnRH injection, and a final GnRH injection 12 h before insemination. On experiment day 130, all cows were inseminated with 500 µL of semen from the sire Passat 7HO12659 (Select Sires). Sixteen days following insemination, cows were euthanized on experimental day 146 (details below) to recover embryos and collect reproductive tissues.

Postmortem Tissue Collection

Cows were euthanized by captive bolt and exsanguination 146 days after intrauterine infusion (16 days following insemination; Fig. 2-1). Reproductive tracts were

collected, placed on ice, and processed within 1 h of slaughter. Excess tissue was trimmed, and the reproductive tract (cervix, uterus, oviduct, and ovaries) was weighed. The uterine horn ipsilateral to the side of ovulation was identified by the corpus luteum in the ovary. The ovaries and oviducts were removed for further processing. The uterus was clamped with hemostats near the utero-tubal junction and at the uterine bifurcation. The ipsilateral horn was flushed with 20 mL of 0.9% saline to collect uterine fluid and potential embryos. An additional three uterine flushes were performed to maximize the potential of recovering an embryo. The first uterine flush was examined for the presence of an embryo prior to centrifugation for 10 min at 1,000 × *g* to remove debris, snap-frozen in liquid nitrogen and stored at -80°C. Embryo morphology was recorded prior to sampling the distal portion of trophectoderm using clean 20 gauge needles. Trophectoderm samples were washed twice in PBS, snap-frozen in liquid nitrogen and stored at -80°C.

Interferon Tau Quantification in Uterine Fluid

Interferon tau (IFNT) content of uterine fluid was quantified by ELISA (Bishop JV and Hansen TR, unpublished in collaboration with a Biopharma Company). Briefly, glycosylated recombinant bovine IFNT was purified from cultures of human HEK cells that were transformed with bovine IFNT cDNA (bTP509) and used to generate polyclonal antibodies in goats (#51; 3.5 μg/mL) and in rabbits (#5670; 9.6 μg/mL). These antibodies were used as capture and biotinylated detection antibodies, respectively, in a sandwich ELISA. The ELISA had a detection range of 7.8 to 500 pg/mL and limit of detection of 61 pg/mL. The intra-assay coefficient of variation was 0 to 1.4% for high (500 pg/mL), 0 to 3.9% for medium (100 pg/mL) and 0.9 to 2.2% for low

(20 pg/mL) concentration recombinant bovine IFNT controls. The inter-assay coefficient of variation was 1.1%, 1.6% and 1.8% for high, medium and low concentration controls, respectively. The ELISA specifically detects IFNT and does not cross-react with IFNω, IFNα/β or IFNγ. Samples were assayed undiluted or at dilutions in steer serum of 1:10, 1:100, 1:1,000, 1:5,000 or 1:10,000 to detect IFNT in the linear range of the assay. Operators were blind to the treatment of samples being assayed. Samples below the limit of detection were assigned a concentration of 61 pg/mL for statistical analysis.

RNA Extraction and Real-Time RT-PCR

Total RNA was extracted from cytobrush and trophectoderm samples using the Trizol method (Life Technologies, Carlsbad, CA). Total RNA was extracted from morula that were pooled from a single cow at each time point using the RNeasy micro kit according to the manufacturer's instructions (Qiagen, Hilden, Germany). Reverse transcription was performed using the Verso cDNA synthesis kit (Thermo Fisher Scientific). Morula cDNA underwent additional selective pre-amplification using SsoAdvanced PreAmp Supermix (Bio-Rad, Hercules, CA) prior to real time RT-PCR.

Primers were designed using the NCBI database (Table 2-1). Amplification efficiency for each primer pair was evaluated and met MIQE guidelines of $r^2 > 0.98$ and efficiency of 90% to 110% (Bustin et al., 2009). Real time RT-PCR was performed in duplicate using a two-step PCR protocol for cytobrush samples and a three-step protocol for morula and trophectoderm. Each 20 µL reaction consisted of 500 nM of each forward and reverse primer and iTaq Universal SYBR green master mix (Bio-Rad) and cDNA. A Bio-Rad CFX Connect light cycler (Bio-Rad) was employed with an initial denaturation step at 95°C for 30 sec followed by 40 cycles at 95°C for 5 sec, specific

annealing temperature (Table 2-1) for 10 sec and final extension at 60°C for 30 sec. A no template negative control was used in place of cDNA to determine non-specific amplification for each primer pair. Relative expression for genes of interest were calculated using the $2^{-\Delta Ct}$ method relative to selected housekeeping genes (*GAPDH* for endometrial cytobrush data; geometric mean of *GAPDH*, *RPL19*, and *SDHA* for morula data; and geometric mean of *ACTB* and *GAPDH* for trophectoderm data). Reference gene expression was stable across experimental treatments ($P > 0.05$).

Statistical Aanalysis

Rectal temperature, haptoglobin, polymorphonuclear cell number, progesterone, AMH, gene expression, and IFNT were analyzed using SPSS v25 (IBM Corporation, Armonk, NY). Data were analyzed with a generalized linear mixed model with repeated measures (if applicable) and autoregressive covariance structure. The fixed effects of treatment, day, and the interaction were analyzed using pairwise comparisons. Analysis of treatment combined all days and only analyzed an effect of bacterial infusion, while analysis of day combined treatments and only assessed effect of each day regardless of treatment. Rectal temperature and haptoglobin each had a pre-infusion data point (day -2) which was used as a covariate. Gene expression and haptoglobin data were log transformed for normality. Vaginal mucus grade, oocyte cleavage and morula development data were analyzed using logistic regression with Poisson and binomial distribution, respectively, with the GLIMMIX procedure in SAS (SAS Institute, Cary, NC). Cow within treatment was considered a random effect, and fixed effects of treatment, day, and the interaction were analyzed. Carcass weight, uterine weight, corpus luteum diameter, and number of embryos collected at slaughter were analyzed using the two-

tailed t-test function in GraphPad Prism 7.04 (GraphPad Software, La Jolla, CA). Statistical significance was set at $P \leq 0.05$.

Results

Establishment of Uterine Infection

Intrauterine infusion of bacteria induced clinical endometritis, as determined by an increased vaginal mucus grade compared to vehicle infusion ($P \leq 0.05$; Fig. 2-2A). Although the proportion of cows with polymorphonuclear cells present in uterine cytology samples on day 6 was not different between treatments, polymorphonuclear cells were detected in 5 of 12 bacteria-infused cows, and only 1 of 11 vehicle-infused cows ($P > 0.05$; Fig. 2-2B). Bacteria-infused cows did not have elevated rectal temperatures compared to vehicle-infused cows, and no cows exhibited fever (> 39.5ºC, $P > 0.05$; Fig 2-2C). Circulating haptoglobin concentrations on day 5 were not significantly increased by bacteria infusion compared to vehicle infusion ($P > 0.05$; Fig. 2-2D) but the four highest concentrations were all in the bacteria-infusion group. Together these data show that clinical endometritis was induced by bacteria infusion without causing systemic disease.

Endometrial inflammation was evaluated using samples collected on days 6, 28, 49 and 70 (Fig. 2-3). Expression of endometrial *CXCL8*, *IL1B*, *IL6*, *PTGS2*, and *TNF* were increased ($P \leq 0.05$; Fig. 2-3B-D, F, G) on day 6 in bacteria-infused cows compared to vehicle-infused controls. Expression of endometrial *IL1B* and *PTGS2* remained increased on day 28 in bacteria-infused cows compared to vehicle-infused controls ($P \leq 0.05$; Fig. 2-3C, F). Expression of endometrial *TNF* was increased in bacteria-infused cows compared to vehicle controls overall ($P \leq 0.05$; Fig. 2-3H), while *AKR1C4*, *CXCL8*, *IL1B*, *IL6*, *PTGES*, *PTGS2*, *PTPRC* and *TNF* expression were

affected by day relative to infusion ($P \leq 0.05$; Fig. 2-3A-H), and *CXCL8*, *IL6*, and *PTGS2* expression were affected by the interaction between treatment and day relative to infusion ($P \leq 0.05$; Fig. 2-3B, D, F). The expression of *CXCL8*, *IL1B*, *IL6*, *PTGES*, and *TNF*, was different on day 6 compared with days 28, 49, and 70, while *PTGES*, *PTGS2*, *PTPRC* and *TNF* expression was different on day 28 compared to days 49 and 70. The expression of *PTGS2* was different on day 6 compared to day 28, while expression of *AKR1C4* was different on days 6 and 28 compared to day 70. Finally, the expression of *PTPRC* was different on day 6 compared to day 49 and 70, while expression of *IL1B* on day 70 was different compared to days 28 and 49. These findings provide further evidence of endometritis in the bacteria-infused cows.

Developmental Competence of Oocytes Following In Vitro Fertilization

Oocytes were collected from cows by aspiration of follicles (< 8 mm) on days 2, 24, 45 and 66. There was no impact of intrauterine infusion on the total number of oocytes collected (vehicle, n = 438 vs. bacteria, n = 493; $P > 0.05$). There was variability in the number of oocytes (range 1 to 26) collected from each cow at any given time point, with an average of 10.7 ± 1.0 oocytes collected from vehicle-infused cows and 10.7 ± 0.9 oocytes collected from bacteria-infused cows at each time point (Fig. A-1). Following IVF, the overall cleavage rate of oocytes on day 3.5 post fertilization was 62.9 ± 2.2% (Fig. 2-4A), and there was no difference in oocyte cleavage rate between treatment groups (bacteria: 63.5 ± 3.3%, vehicle: 62.3 ± 3.0%, respectively, $P > 0.05$). However, the day of oocyte collection affected ($P \leq 0.05$) the rate of oocyte cleavage, resulting in an increased rate of oocyte cleavage in the bacteria-infused group compared to vehicle infusion on day 2 (68.7 ± 8.4% and 53.1 ± 4.6%, respectively; $P \leq 0.05$). The overall proportion of oocytes to develop to morulae was 24.3 ± 1.7% (Fig. 2-

4B), whereas the overall proportion of cleaved oocytes to develop to morulae was 37.5 ± 2.4% (Fig. 2-4C). The proportion of oocytes that developed to morulae was not affected by bacterial infusion, day of oocyte collection, or the interaction between the two (Fig. 2-4B). However, oocytes collected from bacteria-infused cows on day 24 had a reduced capacity to develop to morulae compared to those collected from vehicle-infused cows (15.5 ± 3.8% and 35.4 ± 4.0%, respectively; $P \leq 0.05$). Bacteria infusion reduced the overall proportion of cleaved oocytes to develop to morulae compared to vehicle-infusion (30.7 ± 3.0% and 45.0 ± 1.1%, respectively, $P \leq 0.05$; Fig 2-4C). Specifically, bacteria infusion reduced the proportion of cleaved oocytes to develop to morulae day 24 compared to vehicle infusion (21.4 ± 5.0% and 45.6 ± 4.4%, respectively; $P \leq 0.05$).

Markers of embryo quality were assessed by real time RT-PCR using pooled morulae derived from a single cow at a single time point (Fig. 2-5). Genes related to stress response (*HSPA1A*), growth factor signaling, and metabolism (*IGF2R*, *SLC2A1*), apoptosis (*BAX*, *BCL2)*, and DNA methylation (*DNMT3A*) were analyzed. Bacterial infusion did not significantly alter the expression of any genes related to embryo quality ($P > 0.05$; Fig. 2-5A-F). The expression of *HSPA1A* increased 112% in morulae developed from bacteria-infused cows compared to vehicle-infused cows ($P = 0.08$; Fig. 2-5D). Day of oocyte collection affected expression of *BAX* and *DNMT3A* ($P \leq 0.05$; Fig. 2-5A, C). The expression of *BAX* on days 2 and 24 was different from days 45 and 66. *DNMT3A* expression was different on day 45 compared to days 24 and 66.

The association between morula development of cleaved embryos and endometrial expression of inflammatory mediators on day 6 was evaluated for all cows

(Fig. 2-6). There was a negative association between endometrial expression of *IL6* and the capacity of cleaved oocytes to develop to morulae ($P \leq 0.05$, $r^2 = 0.05$; Fig. 2-6C). There was no association between endometrial expression of *CXCL8*, *IL1B*, *PTGES*, *PTGS2*, or *TNF* with the capacity of cleaved oocytes to develop to morulae ($P > 0.05$; Fig. 2-6A-B, D-F).

Effect of Intrauterine Infusion on In Vivo Embryo Development

Cows were inseminated on day 130, following estrous synchronization (Fig. 2-1). Sixteen days post-insemination, cows were euthanized, and uterine contents were collected by uterine flushing. Hot hanging carcass weights for vehicle and bacteria-infused cows were not different (363.9 ± 6.6 kg versus 368.9 ± 8.0 kg respectively; $P > 0.05$), and total reproductive tract weights were not different between treatments (vehicle, 466 ± 16 g vs. bacteria, 449 ± 17 g; $P > 0.05$). A corpus luteum was present in all cows at euthanasia indicating a positive response to synchronization (corpus luteum diameter was 22.6 ± 0.8 mm and 22.5 ± 0.5 mm in vehicle and bacteria-infused cows respectively, $P > 0.05$). A total of 12 filamentous embryos (vehicle = 6 of 11, bacteria = 6 of 12) were recovered 16 days following insemination (Fig. 2-7A). It was not possible to measure the length of each conceptus due to fragmentation. Interferon-tau was measured in all uterine fluid samples and was detected in 17 of 23 samples (vehicle = 8 of 11, bacteria = 9 of 12). Uterine fluid IFNT concentrations ranged from 0.086 to 6,858 ng/mL and was not different between bacteria-infused cows and vehicle-infused cows ($P > 0.05$, Fig. 2-7B). There was no effect of infusion on serum progesterone on day 15 post-insemination ($P > 0.05$; Fig. 2-7C), 1 day prior to euthanasia. There was no significant effect of infusion on the serum AMH concentration from -2 to 145 days ($P >$

0.05; Fig. 2-7D). There was no effect of infusion on trophectoderm expression of *CDKN1C*, *IFNT2*, or *PPARG* in day 16 embryos ($P > 0.05$; Fig. 2-8).

Discussion

Infertility persists after resolution of uterine infections (Sheldon et al., 2009; Santos et al., 2010; Tsevat et al., 2017). Women and cows previously diagnosed with uterine infection have lower conception rates compared to healthy counterparts (Borsberry and Dobson, 1989; Tsevat et al., 2017). However, the culprit behind uterine infection associated infertility remains elusive. Uterine infection alters the uterine environment and ovarian function (Sheldon et al., 2002; Herath et al., 2009a). In order to determine the impact of uterine infection on the oocyte, the present study tested the hypothesis that endometritis reduces the capacity of the oocyte to develop to an embryo independent of a perturbed uterine environment. Our experiment successfully induced endometritis in non-lactating cows, and we found a reduction in the capacity of oocytes to develop to the morula stage during in vitro fertilization and culture. These findings demonstrate that uterine infection leaves a long-term impact on oocytes, even after clearance of infection.

The oocyte has been shown to have a greater influence on future blastocyst development when compared to culture conditions or the contribution of sperm (Rizos et al., 2002). We successfully collected oocytes from all cows and there was no impact of uterine infection on the number of oocytes recovered or the fertilization rate; however, there was variability in the number of oocytes collected from each cow, but this was corrected for when assessing developmental competence using our statistical approach. Overall, fewer cleaved putative zygotes developed to morulae when oocytes were collected from bacteria-infused cows. Thus, even though cleavage rates were

elevated in oocytes collected from cows 2 days after bacterial infusion, the relative ability to continue development to morulae was reduced compared to vehicle-infused cows. The largest reduction in developmental competence was observed when oocytes were collected 24 days following bacterial infusion, after endometrial inflammation was resolved. Bovine follicular development takes between 120 and 200 days, with approximately 42 days between antrum formation and ovulation (Lussier et al., 1987). All oocytes collected for in vitro fertilization and embryo culture were collected at the small antral follicle stage (< 8 mm), 4 days after dominant follicle ablation, and approximately 20 days prior to potential ovulation. Thus, the timeline of follicular development indicates that small antral follicles aspirated from day 24 onwards would have likely been at the secondary stage of follicle development at the time of intrauterine infusion. Oocytes collected on day 24 were likely in the process of antrum formation at the time of uterine infusion. Oocytes collected on day 45 or 66 would have been earlier secondary stage follicles at the time of uterine infusion. While embryo development was numerically reduced on days 45 and 66, the enhanced reduction of developmental competence on day 24 suggests that specific stages of follicles are more susceptible to damage by uterine infection. Recovery from infertility following endometritis may simply require an extended period to clear negatively affected oocytes/follicles. However, spontaneous metritis causes altered transcription in granulosa cells of dominant follicles 63 days postpartum (Piersanti et al., 2019a), and thus may require a longer period to recover oocyte health. The induction of bacterial uterine infection in isolation from other postpartum complications used here potentially underestimates the detrimental impact of spontaneous uterine infection on the oocyte.

In parallel, these studies established endometritis in healthy non-lactating cows. It is unclear if infertility in cows is mediated solely by uterine infection or if the confounding demands of lactation and other postpartum diseases also impact oocyte quality. We have previously established an experimental disease model comparable to clinical endometritis in virgin Holstein heifers by intrauterine infusion of pathogenic *E. coli* and *T. pyogenes* isolated from cows with active metritis (Goldstone et al., 2014a; b; Piersanti et al., 2019b). In this model, cattle do not exhibit a systemic response to uterine infection, lacking pyrexia, but do display purulent vaginal discharge (Piersanti et al., 2019b). In this experiment, increased endometrial inflammation, characterized by increased expression of pro-inflammatory genes, occurred within one week of bacterial infusion and was resolved within four weeks. In addition, bacteria-infused cows had elevated vaginal mucus grade compared to vehicle-infused cows. Previous studies have demonstrated that other, non-reproductive diseases are detrimental to dairy cow fertility. Mastitis alters endocrine function and ovarian cyclicity, in addition to increasing the time to conception (Moore et al., 1991; Santos et al., 2004). Oocytes collected from dairy cows with mastitis are less likely to develop to a blastocyst compared to oocytes isolated from healthy cows (Roth et al., 2013). Whereas lame cows have increased occurrence of ovarian cysts and a decreased ability to conceive compared to non-lame cows (Melendez et al., 2003). In general, cows diagnosed with one disease in the postpartum period, regardless if it is classified as uterine or non-uterine, have a reduced likelihood to conceive and an increased incidence of abortion (Santos et al., 2010; Ribeiro et al., 2016a).

The mechanisms by which uterine infection reduces developmental competence of oocytes is unclear. Transfer of a healthy embryo into a cow with previous uterine infection does not resolve the negative impact of disease on fertility (Ribeiro et al., 2016a), suggesting that the uterus is in part responsible for infection associated infertility. Herein, the inverse association between the degree of endometrial inflammation on day 6 of infection with reduced embryo development, may be associated with inflammatory signals from the uterus that alter oocyte developmental competence either directly, or by altering endocrine signaling to the ovary (Herath et al., 2006). In vitro, bacterial LPS stimulates expression of inflammatory mediators by granulosa cells via the Toll-like receptor 4 pathway (Bromfield and Sheldon, 2011). Whereas bacterial LPS accumulates in the follicular fluid of cows with uterine infection and alters the follicular environment up to 63 days postpartum (Piersanti et al., 2019a). Similarly, exposure of oocytes to LPS during in vitro maturation reduces meiotic competence, increases reactive oxygen and apoptosis, and alters DNA methylation patterns of oocytes (Bromfield and Sheldon, 2011; Zhao et al., 2017). It is unclear if cell wall components of Gram-positive bacteria are present in follicular fluid of cows with uterine disease or if these components effect oocyte competence. In parallel, uterine infection in these experiments may also disrupt hypothalamic-pituitary axis signaling, reducing GnRH and LH secretion which could negatively impact the growth and development of small follicles (Haziak et al., 2014), however hormonal signaling was not evaluated in the present study.

Embryo quality in those oocytes that could develop to morulae, as well as the ability of the cows to conceive following insemination was examined. We selected a

specific subset of genes to analyze known to be indicators of embryo quality (Sagirkaya et al., 2006). Embryo development was halted at the morula stage in order to sample a homogeneous cell population instead of blastocyst embryos where treatment could affect the allocation of trophectoderm and inner cell mass cells, possibly confounding gene expression. Genes were chosen based on their function, including metabolism, measured by glucose transporter (*GLUT1*); stress, measured by heat-shock protein 70 (*HSPA1A*); apoptosis, measured by *BAX* and *BCL2*; DNA methylation, measured by *DNMT3A*; and growth factor signaling, measured by insulin like growth factor 2 receptor (*IGF2R*). In morulae derived from bacteria-infused cows, *HSPA1A* expression was elevated. Environmental stressors, such as heat stress can increase *HSPA1A* gene expression in bovine embryos, even prior to embryonic genome activation implying altered expression is driven by maternal mRNA present in the oocyte (Edwards et al., 1997). Additionally, loss of function in the maternally inherited *IGF2R* gene results in developmental abnormalities, including large offspring syndrome (Barlow et al., 1991; Young et al., 2001). Conversely, increased IGF-2 signaling increases embryo development in vitro (DeChiara et al., 1990; Gicquel and Le Bouc, 2006). It is important to note that embryo quality was assessed using a targeted approach with in vitro produced embryos, thus, we cannot exclude the possibility that other factors important in embryo progression are altered as a result of uterine infection, or that the uterine environment may aid in the recovery of perturbed embryos.

Finally, the effect of prior uterine infection on the health of embryos conceived by insemination was assessed. All recovered embryos on day 16 of pregnancy were filamentous. Our sample size here is small in terms of number of inseminations and

therefore, there is insufficient statistical power to make conclusions regarding the impact of experimental uterine infection on conception rate. Of embryos recovered, we did not observe an effect of infusion on trophectoderm expression of cell cycle regulation (*CDKN1C*), peroxisome proliferator-activated receptor gamma (*PPARG*), or interferon tau (*IFNT2*). The lack of difference in gene expression in recovered embryos is not surprising as these genes are critical to embryogenesis (Thatcher et al., 1989; Zhang et al., 1997; Ribeiro et al., 2016b); however, our results may be biased as we could only test embryos recovered at flushing which may exclude embryos that failed to develop earlier. Maternal recognition of pregnancy in the cow is driven by trophectoderm secretion of IFNT starting as early as the blastocyst (Thatcher et al., 1989; Hernandez-Ledezma et al., 1992). Here, the number of uterine flush samples with detectable IFNT was greater than the number of cows where an embryo was collected, suggesting that several embryos were not recovered due to technical error, or that embryo development failed prior to collection on day 16. Regardless of the discrepancy, the rate at which embryo recovery and IFNT detection differed was similar between treatments based on the number of cows used here. Previous studies have demonstrated that uterine disease reduces IFNT concentration in uterine fluid (Ribeiro et al., 2016a), whereas we did not find any observable effect of bacterial infusion on IFNT concentration in uterine fluid on day 16 of pregnancy. It is important to note however that the method of IFNT quantification and variation of values reported are not consistent between experiments in the literature. Previous studies have used antiviral assays (Ribeiro et al., 2016a), RNA sequencing (Mamo et al., 2012), or the same ELISA used here (Tríbulo et al., 2019). It is also unclear as to the minimum concentration of IFNT required for maternal

recognition of pregnancy in the cow (Hansen et al., 2017), or the best day or days to test for pregnancy status based on IFNT. However, it is believed that reduced IFNT secretion reflects poorer embryo quality and reduces pregnancy success.

In conclusion, intrauterine infusion of pathogenic bacteria to induce endometritis in dairy cows reduces the capacity of oocytes to develop to morulae. These novel findings demonstrate that uterine infection has a detrimental impact on the oocyte weeks after the occurrence of infection. These data aid in our understanding of the mechanisms of uterine infection associated infertility in dairy cows, and potentially women with reproductive tract infection or pelvic inflammatory disease. Future studies are required to determine the specific mechanism by which uterine disease diminishes oocyte quality.

Acknowledgments of Chapter 2

The authors would like to thank Tod Pritchard, Miguel Torrado Vazquez, and the staff of the University of Florida Dairy Research Unit.

Table 2-1. Primer sequences and annealing conditions used for real time RT-PCR.

Gene Symbol	Primer Sequence	Annealing Temp. (ºC)	Accession number
ACTB	5’ – TTGGCCTTAGGGTTCAGGG	60	NM_173979.3
	3’ – CAGAAGCACTCGTACGTGGG		
AKR1C4	5’ – TGCAACCAGGTGGAATGTCA	60	NM_181027.2
	3’ – ACCCATTCTTTTAGTCGTTGGGA		
BAX	5’ – CAGGGTGGTTGGGACGG	60	NM_173894.1
	3’ – CTTCCAGATGGTGAGCGAGG		
BCL2	5’ – GAGTTCGGAGGGGTCATGTG	60	NM_001166486.1
	3’ – ACAAAGGCGTCCCAGCC		
CDKN1C	5’ – GCCTCTCATCTCCGACTTCT	60	NM_001077903.2
	3’ – CCCAGGAACCTCGTTCGAC		
CXCL8	5’ – GCAGGTATTTGTGAAGAGAGCTG	60	NM_173925.2
	3’ – CACAGAACATGAGGCACTGAA		
DNMT3A	5’ – CCATGTACCGCAAGGCTATCTA	60	XM_024998.68.1
	3’ – CCTGTCATGGCACATTGGAA		
GAPDH	5’ – AGGTCGGAGTGAACGGATTC	60	NM_001034034.2
	3’ – ATGGCGACGATGTCCACTTT		
HSPA1A	5’ – GACAAGTGCCAGGAGGTGATTT	60	NM_203322.3
	3’ – CAGTCTGCTGATGATGGGGTTA		
IFNT2	5’ – TCCATGAGATGCTCCAGCAGT	60	NM_001015511.4
	3’ – TGTTGGAGCCCAGTGCAGA		
IGF2R	5’ – CAGGTCTTGCAACTGGTGTATGA	60	NM_174352.2
	3’ – TTGTCCAGGGAGATCAGCATG		

Table 2-1. Continued

Gene Symbol	Primer Sequence	Annealing Temp. (ºC)	Accession number
IL1B	5’ – CTTCATTGCCCAGGTTTCTG	60	NM_174093.1
	3’ – CAGGTGTTGGATGCAGCTCT		
IL6	5’ – ATGACTTCTGCTTTCCCTACCC	60	NM_173923.2
	3’ – GCTGCTTTCACACTCATCATTC		
PPARG	5’ – ATTATTCTCAGTGGAGACCGCC	60	NM_181024.2
	3’ – CAAGGCTTGCAGCAGATTGT		
PTGES	5’ – GCTGCGGAAGAAGGCTTTTG	60	NM_174443.2
	3’ – AAAGCCCAGGAACAGGAAGG		
PTGS2	5’ – CGTGAAAGGCTGTCCCTTTA	62	NM_001105323.1
	3’ – ATCTAGTCCAGAGTGGGAAGAG		
PTPRC	5’ – CTCGATGTTAAGCGAGAGGAAT	56	NM_001206523.1
	3’ – TCTTCATCTTCCACGCAGTCTA		
RPL19	5’ – ATGCCAACTCCCGCCAGCAGAT	60	NM_001040516.2
	3’ – TGTTTTTCCGGCATCGAGCCCG		
SDHA	5’ – GGAACACTGACCTGGTGGAG	60	NM_174178.2
	3’ – GGAACACTGACCTGGTGGAG		
SLC2A1	5’ – AGCGTCATCTTCATCCCAGC	60	NM_174602.2
	3’ – AGCTTCTTCAGCACGCTCTT		
TNF	5’ – CACATACCCTGCCACAAGGC	62	NM_173966.3
	3’ – CTGGGGACTGCTCTTCCCTCT		

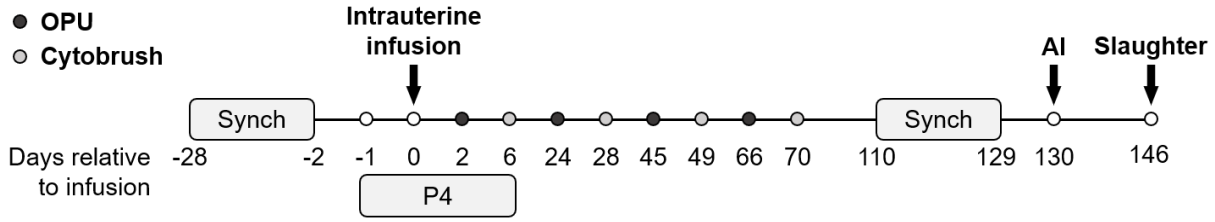

Figure 2-1. Timeline of major experimental events. Estrous cycles were synchronized with gonadotrophin releasing hormone and prostaglandin F2α prior to intrauterine infusion of either Luria-Bertani broth vehicle medium (Vehicle; n = 11) or pathogenic E. coli and T. pyogenes in Luria-Bertani broth (Bacteria; n = 12) on experimental day 0. Major events include oocyte pick-up (OPU, ●), endometrial cytobrush (●) sampling, artificial insemination (AI), progesterone (P4) administration, and slaughter. Timeline is not drawn to scale.

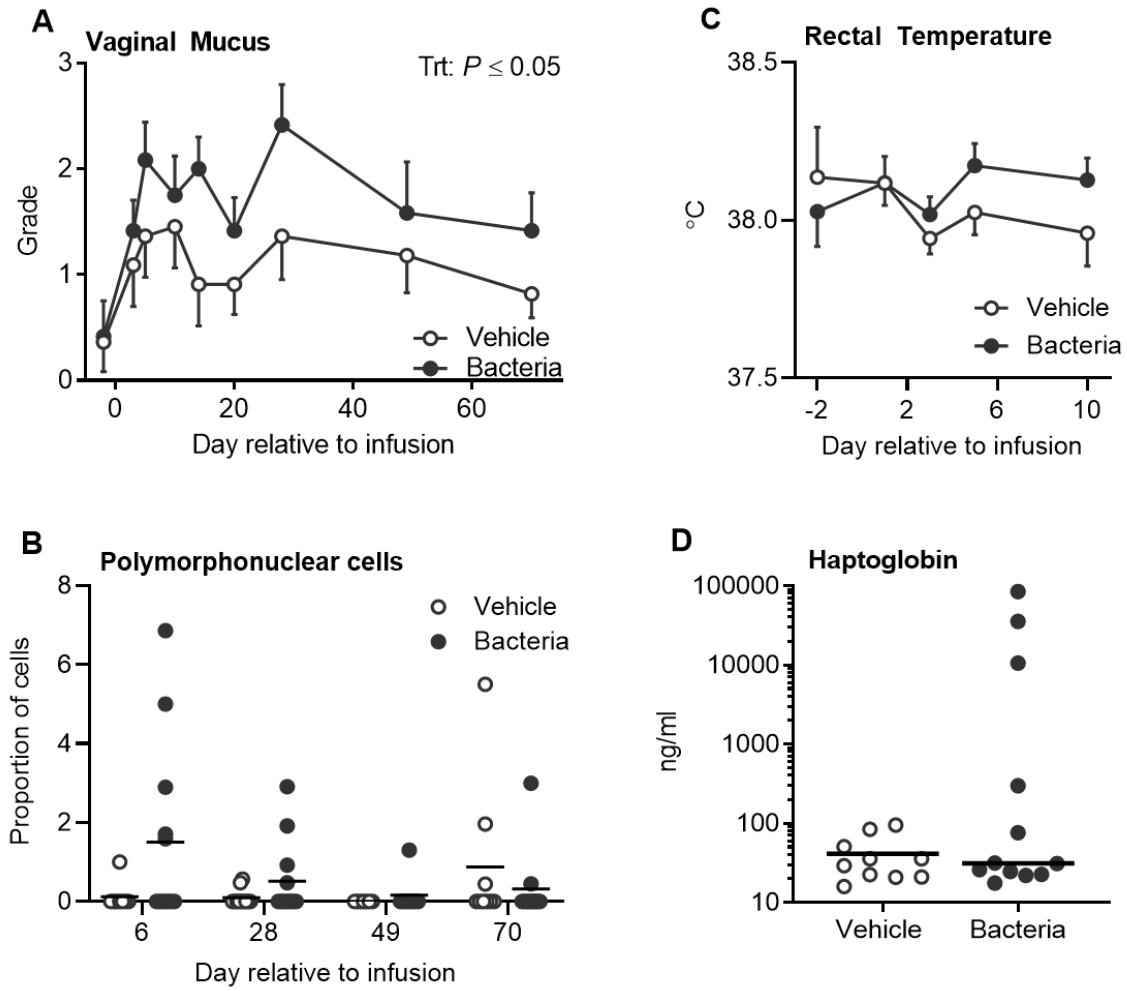

Figure 2-2. Establishment and quantification of uterine disease. Vaginal mucus (A) was collected and graded on a scale of 0 to 4 based on presence of mucopurulent discharge. Data are the mean grade ± SEM. The proportion of polymorphonuclear cells in cytological samples (B) was assessed in a total of 200 cells per cow. Each dot represents a cow and the solid line represents the mean. Rectal temperatures (C) are displayed as mean ± SEM. Plasma haptoglobin (D) was evaluated on day 5 relative to infusion, and each dot represents an individual cow and the solid line represents the mean.

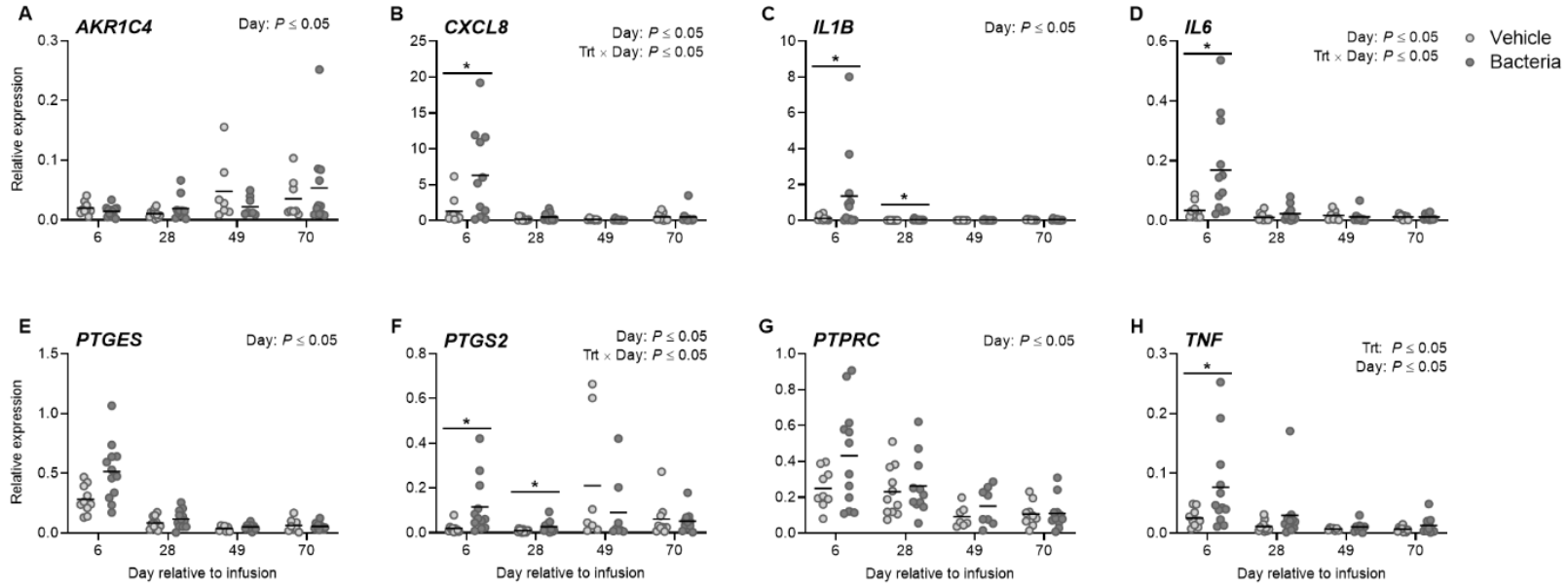

Figure 2-3. Endometrial expression of inflammatory mediators following intrauterine infusion. Expression of *AKR1C4* (A), *CXCL8* (B), *IL1B* (C), *IL6* (D), *PTGES* (E), *PTGS2* (F), *PTPRC* (G), and *TNF* (H) in cytobrush samples were evaluated by real time RT-PCR. Data are presented as expression relative to *GAPDH*. Each dot represents a single cow and the solid line indicates the mean. Comparisons between treatments at a given day are indicated by * when $P \leq 0.05$.

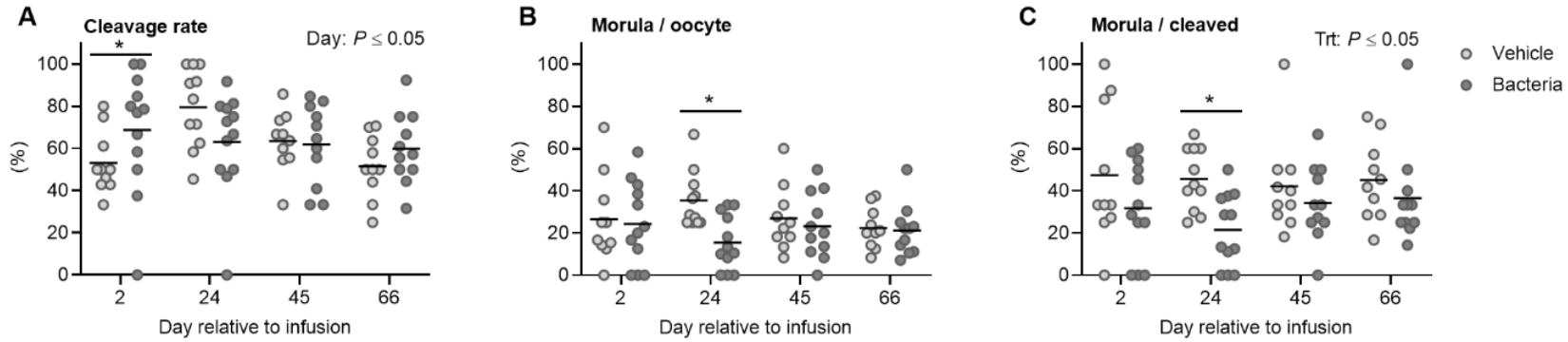

Figure 2-4. Effect of intrauterine infusion on developmental capacity of oocytes following in vitro fertilization and embryo culture. Oocytes were collected via ultrasound guided transvaginal oocyte pick-up on day 2, 24, 45 and 66 relative to infusion of either Luria-Bertani broth vehicle medium (Vehicle; n =11) or pathogenic *E. coli* and *T. pyogenes* in Luria-Bertani broth (Bacteria; n = 12) and subjected to in vitro fertilization and embryo culture. Pooled oocytes from each cow were maintained as an individual replicate throughout fertilization and culture. Each dot represents an individual cow, and the solid line represents the mean of the treatment. The proportion of oocytes that cleaved 3.5 days post-insemination (A), the proportion of oocytes to develop to morulae 6 days post-insemination (B) and the proportion of cleaved oocytes to develop to morulae 6 days post-insemination (C) are shown. Comparisons between treatments on a specific day are indicated by * when $P \leq 0.05$.

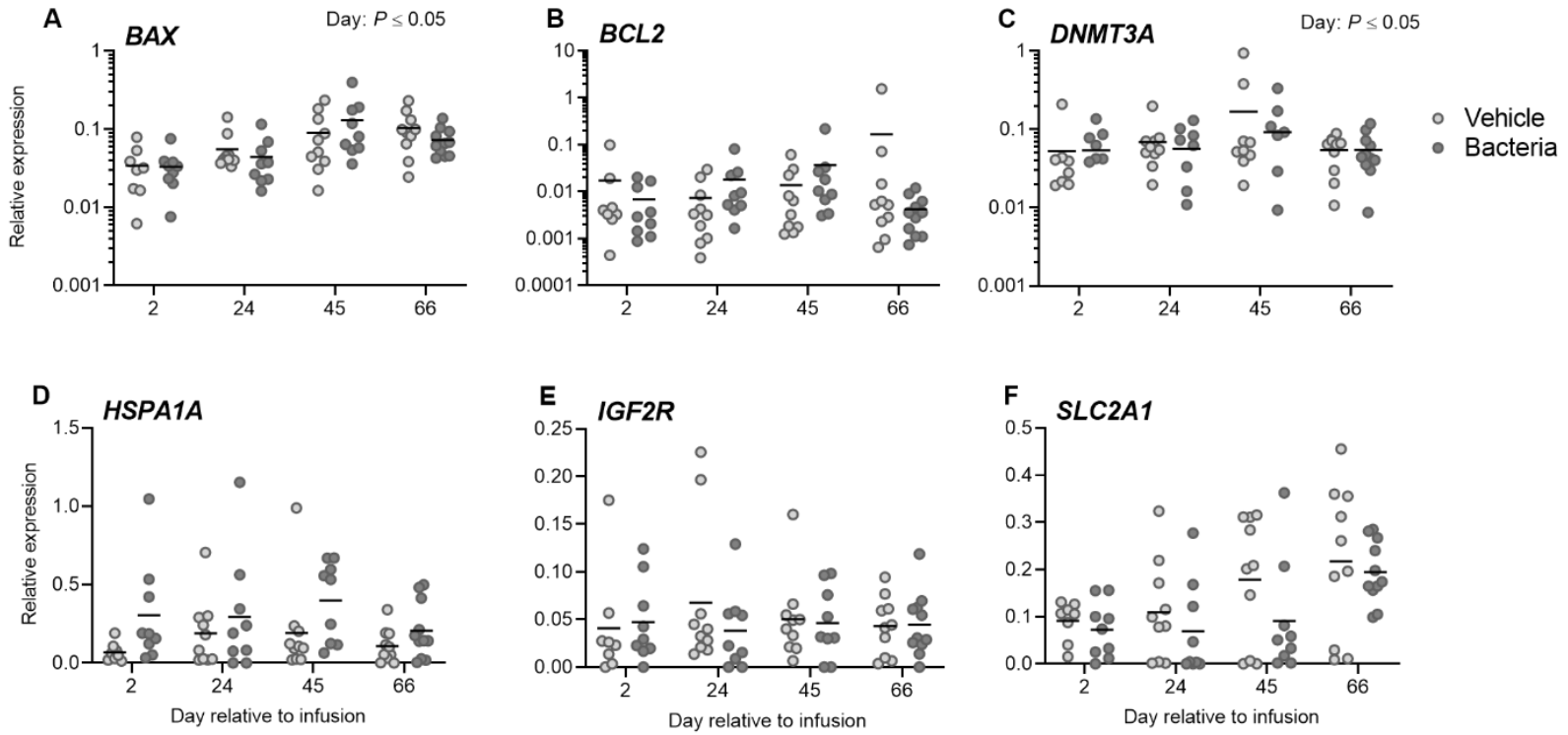

Figure 2-5. Effect of intrauterine infusion on gene expression of IVF derived morula stage embryos. Morula stage embryos derived by oocyte pick-up, in vitro fertilization and embryo culture from cows receiving intrauterine infusion of either Luria-Bertani broth vehicle medium (vehicle; n =11) or pathogenic *E. coli* and *T. pyogenes* in Luria-Bertani broth (bacteria; n = 12) were probed for gene expression of *BAX* (A), *BCL2* (B), *DNMT3A* (C), *HSPA1A* (D), *IGF2R* (E) and *SLC2A1* (F) by real time RT-PCR. Data are presented as expression relative to the geometric mean of the housekeeping genes *GAPDH*, *SDHA* and *RLP19*. Each dot represents the average expression for an individual cow, and the solid line represents the mean of the treatment.

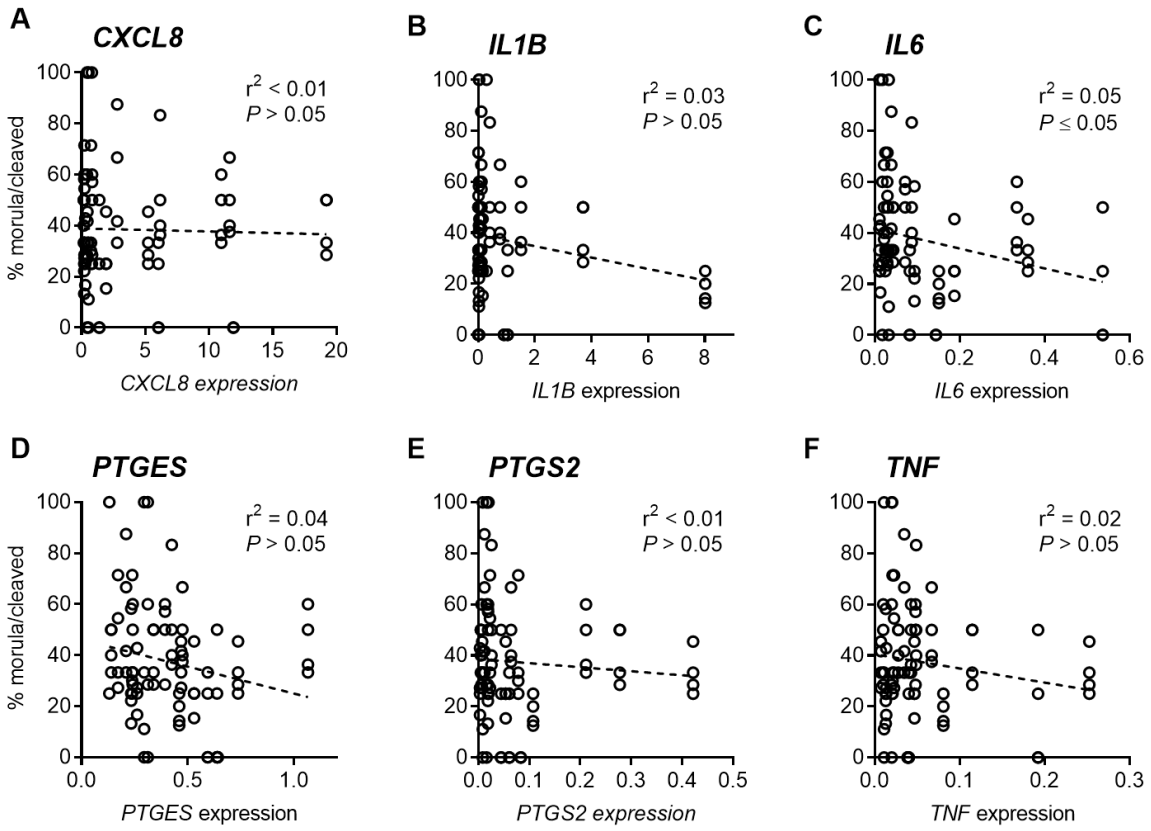

Figure 2-6. Association between morula development and endometrial inflammation. Endometrial expression of *CXCL8* (A), *IL1B* (B), *IL6* (C), *PTGES* (D), *PTGS2* (E), and *TNF* (F) was determined by real time RT-PCR on day 6 relative to infusion. Linear correlation was performed using the total proportion of cleaved oocytes to develop to morulae from all cows.

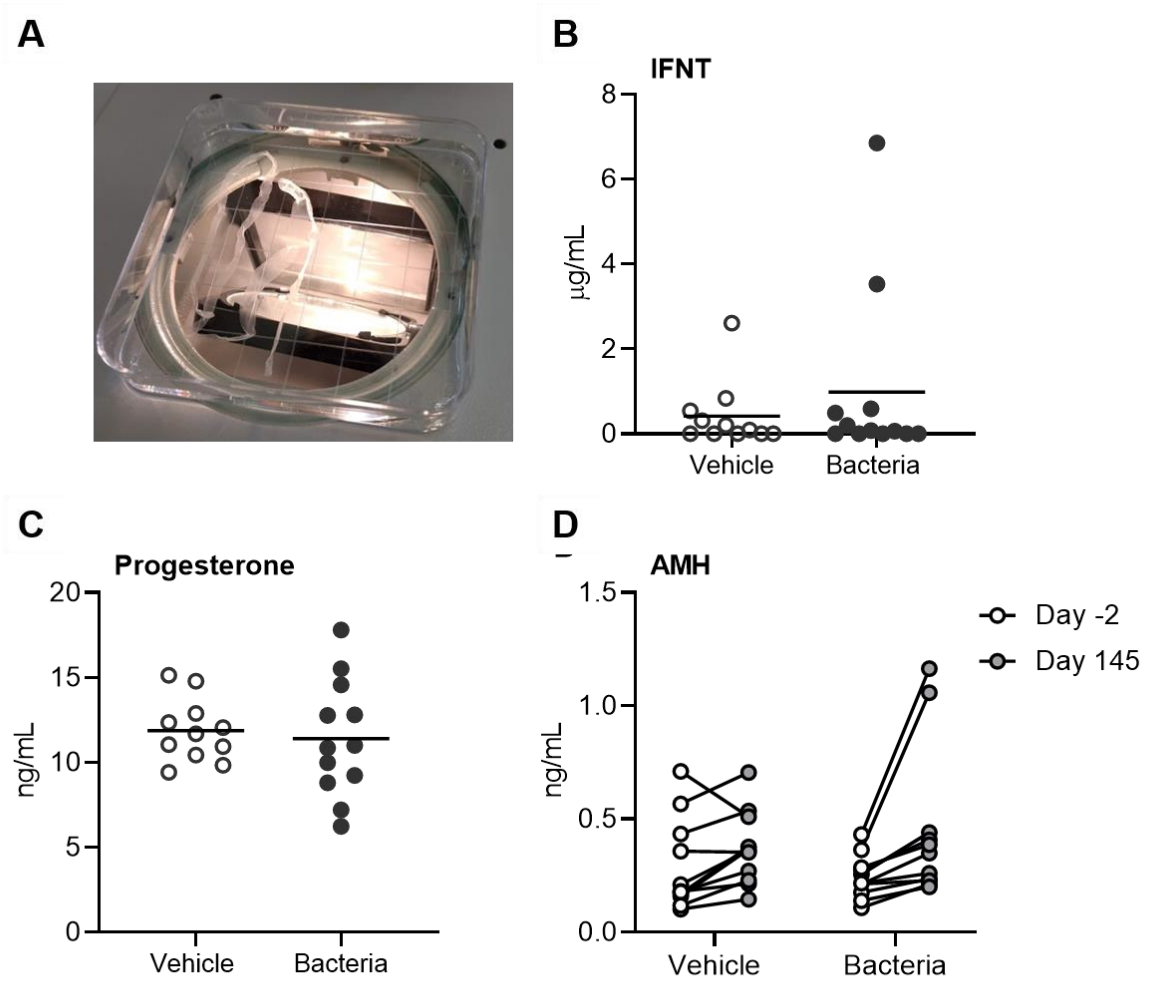

Figure 2-7. Effect of intrauterine infusion on embryo recovery, interferon-tau concentration, serum progesterone, and anti-Müllerian hormone. Cows were synchronized and inseminated on day 130 post infusion of either Luria-Bertani broth vehicle medium (vehicle; n =11) or pathogenic *E. coli* and *T. pyogenes* in Luria-Bertani broth (bacteria; n = 12). Uterine content was collected ex vivo, 16 days post-insemination. All recovered embryos were filamentous in morphology (A). Interferon tau (IFNT) concentration (B) was quantified in uterine fluid by ELISA. Serum progesterone (C) was quantified 15 days after insemination. Each dot represents a cow and the solid line is the mean. Anti-Müllerian hormone (D) was quantified on day -2 prior to intrauterine infusion and day 145 after infusion. Each dot represents a cow.

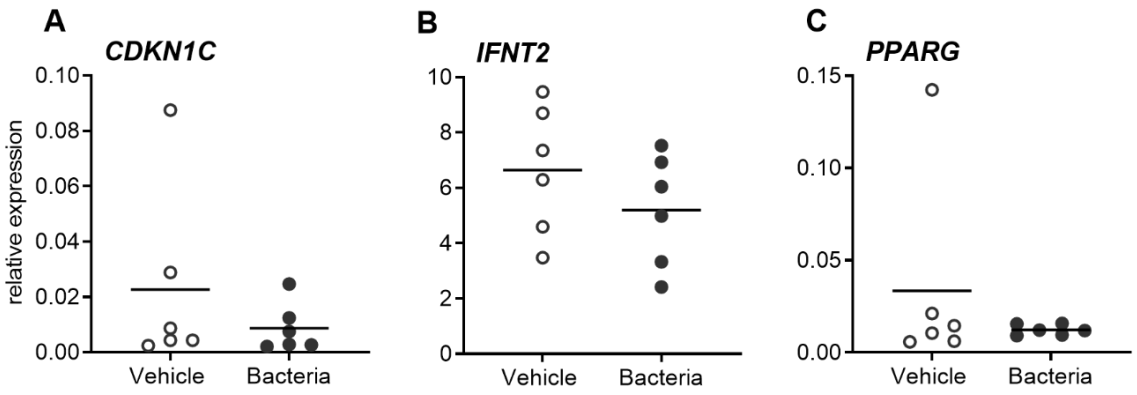

Figure 2-8. Effect of intrauterine infusion on gene expression of trophectoderm from in vivo derived embryos. Cows were synchronized and inseminated on day 130 post infusion of either Luria-Bertani broth vehicle medium (Vehicle; n =11) or pathogenic *E. coli* and *T. pyogenes* in Luria-Bertani broth (Bacteria; n = 12). Total RNA was isolated from trophectoderm of day 16 in vivo derived embryos and expression of *CDKN1C* (A), *IFNT2* (B) and *PPARG* (C) was evaluated by real time RT-PCR. Data displayed are expression relative to the geometric mean of the housekeeping genes *ACTB* and *GAPDH*. Each dot represents an embryo and the solid line depicts the mean.

CHAPTER 3
INTRAUTERINE INFUSION OF BACTERIA ALTERS THE ENDOMETRIAL TRANSCRIPTOME OF COWS IN RESPONSE TO PREGNANCY

Abstract of Chapter 3

Uterine disease occurs in up to 40% of dairy cows and negatively impacts fertility after the resolution of disease. To better understand the endometrial mechanisms by which uterine disease decreases fertility, cows were inseminated 130 days after intrauterine infusion of pathogenic *E. coli* and *T. pyogenes*. Pregnancy status was confirmed 16 days after insemination and endometrial tissue was subjected to RNA sequencing. We hypothesized that intrauterine infusion of pathogenic bacteria alters the endometrial signature of pregnancy compared to healthy cows. A total of 171 differentially expressed genes were identified in the endometrium of non-pregnant cows compared to pregnant cows after infusion with bacteria. Furthermore, we compared our results with previous studies describing the endometrial signature of pregnancy in healthy cows. Our analysis revealed 28 differentially expressed genes, 5 altered canonical pathways, and 5 predicted upstream regulators uniquely regulated by pregnancy in the endometrium of cows after infusion with bacteria compared to the healthy cows. Unique genes and pathways regulated by pregnancy status in cows after infusion with bacteria included *TRANK1*, iNOS signaling, TLR signaling and IL-7 signaling pathways that were not altered by pregnancy in healthy cows. We speculate that intrauterine infusion with pathogenic bacteria results in dysregulation of pathways that effect pregnancy establishment and may play a role in the decreased fertility observed in cows after uterine disease. In conclusion, intrauterine infusion with bacteria results in a unique endometrial environment of cows that fail to become pregnant after insemination. Understanding the mechanisms responsible for decreased fertility in cows

with uterine disease will increase our knowledge of endometrial changes required for successful pregnancy and improve fertility in dairy cows.

Introduction

An estimated 90% of dairy cows have bacteria present in the uterus shortly after calving (Elliott et al., 1968; Griffin et al., 1974; Sheldon et al., 2002) and up to 40% of postpartum cows will develop metritis or clinical endometritis (Sheldon et al., 2009). Even after the resolution of uterine disease, cow fertility and profitability are diminished. Cows with uterine disease are less likely to become pregnant, have a greater incidence of pregnancy loss, and are more likely to be culled compared to cows that did not develop uterine disease (LeBlanc et al., 2002a; Ribeiro et al., 2016a). Reduced fertility of these cows is apparent after disease resolution, suggesting that tissues of the reproductive tract are perturbed by uterine disease (Carvalho et al., 2019). The mechanisms responsible for reduced fertility in cows after uterine disease have yet to be determined, but likely involve changes to the uterus, ovary and hypothalamic-pituitary axis.

Cows with uterine infection have increased expression of pro-inflammatory cytokines and prostaglandins in the endometrium during disease compared to healthy cows (Gabler et al., 2009; Fischer et al., 2010; Peter et al., 2015). Additionally, ovarian function is altered in cows with uterine disease, evidenced by slower growth of follicles and extended luteal life (Opsomer et al., 2000; Sheldon et al., 2002). Intrauterine infusion of pathogenic bacteria reduces the ability of oocytes to develop to morula stage embryos after in vitro fertilization and culture, suggesting the oocyte competence is diminished during and after infection (Chapter 2). Interestingly, the transfer of embryos derived from healthy donors to recipients that previously had uterine disease did not

resolve inflammation associated pregnancy loss, suggesting the endometrium plays a pivotal role in the reduced fertility observed in cows with a previous uterine disease (Ribeiro et al., 2016a; Estrada-Cortés et al., 2019; Edelhoff et al., 2020). In fact, persistent changes to the transcriptome of granulosa cells, endometrium and oviduct tissues are altered in cows 3 months after uterine infection, suggesting uterine infection imparts a long-term impact on reproductive tissues and may be responsible for altered fertility of cows after resolution of uterine disease (Piersanti et al., 2019a; Horlock et al., 2020).

The endometrium supports the developing conceptus prior to implantation and is likely an important factor in determining the success of pregnancy. The transcriptome of the bovine endometrium changes throughout the estrous cycle (Bauersachs et al., 2005; Mitko et al., 2008), during lactation or negative energy balance (Wathes et al., 2009; Cerri et al., 2012; Bauersachs et al., 2017), and in response to the presence of an embryo (Forde et al., 2011, 2012; Bauersachs et al., 2012). While little is known about the effects of uterine infection on the endometrial response to pregnancy, three robust studies have described the bovine endometrial transcriptome of healthy, pregnant animals at the time of maternal recognition of pregnancy compared to healthy animals at the same stage of the estrous cycle (Bauersachs et al., 2012; Cerri et al., 2012; Forde et al., 2012). These three studies identified pregnancy mediated genes in the endometrium and describe pathways regulated by pregnancy, including interferon-tau (IFNT) signaling. However, these studies identified endometrial genes and pathways regulated by pregnancy, and do not identify genes associated with pregnancy failure in cattle. Moreover, the endometrial transcriptome during pregnancy recognition has not

been evaluated in cows after uterine infection that fail to become pregnant. We hypothesized that intrauterine infusion of pathogenic bacteria perturbs the expression of pregnancy regulated genes of the endometrium, specifically we believe that intrauterine infusion of pathogenic bacteria alters the endometrial transcriptome of cows that fail to become pregnant following artificial insemination. To investigate our hypothesis, we performed intrauterine infusion of pathogenic bacteria into non-lactating cows followed by timed-artificial insemination 130 days later. Sixteen days after insemination, pregnancy status was evaluated, and endometrial transcriptome analysis was performed comparing pregnant and non-pregnant animals. Finally, we compared the pregnancy related endometrial transcriptome of cows after infusion of bacteria to the pregnancy related transcriptome previously reported using healthy, cycling cows.

Materials and Methods

The University of Florida Institutional Animal Care and Use Committee approved all animal procedures (protocol number 201508884). The experiment was conducted from February to August 2018 at the University of Florida Dairy Research Unit. The studies described here used cows previously reported in chapter 2.

Experimental Design and Intrauterine Infusion

The study used 23 two-year old primiparous non-lactating Holstein cows. The study design, treatments, and sample collection have previously been reported in detail (Chapter 2). Briefly, estrous cycles of healthy cows were synchronized using GnRH (gonadorelin diacetate tetrahydrate; Ovacyst, Bayer Healthcare LLC, Whippany Hanover, NJ) and prostaglandin (PG) $F_{2\alpha}$ (dinoprost tromethamine; Prostamate, Bayer Healthcare LLC) in a modified Ovsynch protocol (Souza et al., 2008). Progesterone (200 mg) in corn oil (Sigma-Aldrich, St. Louis, MO) was administered i.m. to cows daily

starting on the final day of estrous synchronization and continued for 7 days. On the day of intrauterine infusion (experimental day 0; two days after completion of estrous synchronization), cows received an epidural anesthetic of 60 mg lidocaine hydrochloride 2% (Aspen Veterinary Resources, Greely, CO) injected into the intercoccygeal intervertebral space. External genitalia were cleaned with 1% virkon solution (DuPont, Wilmington, DE), followed by 1% chlorohexidine solution (Aspen Veterinary Resources) and 70% ethanol. A sheathed Neilson catheter (450 mm; Supplies for Farmers, Lincolnshire, UK) was introduced transvaginally into the reproductive tract and guided into the uterine body via rectal palpation. Once in the uterine body, the sheath was retracted to expose the catheter port, which was rotated three times against the endometrial lining to debride the endometrium prior to intrauterine infusion of treatment. Cows received either 5.05×10^7 CFU/mL *Escherichia coli* MS499 and 3.65×10^7 CFU/mL of *Trueperella pyogenes* MS249 in a total of 30 mL of Luria-Bertani (LB) broth or 30 mL of LB broth alone as vehicle.

Propagation of Pathogenic *E. Coli* and *T. Pyogenes* for Intrauterine Infusion

Bacteria were cultured as previously described (Chapter 2). Briefly, *E. coli* MS499 was cultured from frozen glycerol stocks on LB agar (Goldstone et al., 2014a) and *T. pyogenes* MS249 was grown from frozen glycerol stocks on Trypticase Soy Blood agar at 37ºC for 48 h (Goldstone et al., 2014b). The day before intrauterine infusion, a single colony of *E. coli* MS499 was selected and inoculated into LB broth containing 1% tryptone, 0.5% yeast extract and 1% sodium chloride, and a single colony of *T. pyogenes* MS249 was inoculated into Bacto Brain Heart Infusion broth (Fisher Scientific, Pittsburgh, PA) supplemented with 5% fetal bovine serum (Fisher Scientific). Bacteria were cultured overnight at 37ºC with shaking at 200 rpm and

bacterial growth was monitored by measuring optical density at 600 nm. A final preparation of 5.05×10^7 CFU/mL *E. coli* MS499 or 3.65×10^7 CFU/mL of *T. pyogenes* MS249 were diluted in sterile LB broth and loaded into 10 mL syringes for infusion. To measure the final concentrations of bacteria that were infused, ten-fold serial dilutions of bacterial cultures were plated on agar and grown at 37ºC to count CFU. Sterile LB broth for flushing catheters and vehicle treatment was loaded into 10 mL syringes. Syringes were transported to the farm on ice for immediate application.

Fixed-Time Artificial Insemination and Sample Collection

On experimental day 110, estrous cycles of cows were synchronized for fixed-time artificial insemination using $PGF_{2\alpha}$ followed by injection of GnRH 48 h later, followed by GnRH 6 days later and, two subsequent $PGF_{2\alpha}$ injections 24 h apart one week after the previous GnRH injection, and a final GnRH injection 12 h before insemination. On experimental day 130, all cows were artificially inseminated with 500 µL of commercial semen from sire Passat 7HO12659 (Select Sires, Plain City, OH). One day prior to slaughter, on experimental day 145, serum was collected by coccygeal venipuncture into evacuated tubes containing Z serum clot activator (Greiner Bio one, Monroe, NC) and centrifuged for 10 min at 2,400 × *g* at room temperature, aliquoted and stored at -20ºC. All cows were slaughtered on experimental day 146, sixteen days after insemination. Reproductive tracts were collected, placed on ice, and processed within one hour of collection. The corpus luteum was identified and maximal cross section diameter was measured using calipers. Using hemostats, the uterus was clamped at the uterine bifurcation and the horn ipsilateral to the corpus luteum was flushed with 20 mL of sterile PBS to recover uterine contents. Following recovery of any conceptus, uterine fluid was centrifuged for 10 min at 1,000 × *g* to remove cellular

debris, and supernatant was snap frozen in liquid nitrogen and stored at -80°C. Two additional uterine flushes were performed to maximize the recovery of any conceptus. The uterine horn ipsilateral to the corpus luteum was opened and intercaruncular endometrium was dissected with sterile forceps and scissors, snap frozen in liquid nitrogen and stored at -80°C.

Quantification of Peripheral Progesterone and Interferon Tau in Uterine Fluid

Serum progesterone was quantified using a commercially available ELISA according to manufacturer's instructions (DRG International, Springfield Township, NJ) as previously reported (Dickson et al., 2020). The intra-assay coefficient of variation was 2.9% and the limit of detection was 0.3 ng/mL. Interferon tau content of uterine fluid was quantified by ELISA as previously reported (Dickson et al., 2020). Briefly, glycosylated recombinant bovine IFNT was purified from cultures of human HEK cells that were transformed with bovine IFNT cDNA (bTP509) and used to generate polyclonal antibodies in goats (#51; 3.5 μg/mL) and rabbits (#5670; 9.6 μg/mL). These antibodies were used as capture and biotinylated detection antibodies, respectively, in a sandwich ELISA. The ELISA had a detection range of 7.8 to 500 pg/mL and limit of detection of 61 pg/mL. The intra-assay coefficient of variation was 0 to 1.4% for high (500 pg/mL), 0 to 3.9% for medium (100 pg/mL) and 0.9 to 2.2% for low (20 pg/mL) concentration recombinant bovine IFNT controls. The inter-assay coefficient of variation was 1.1%, 1.6% and 1.8% for high, medium and low concentration controls, respectively. The ELISA specifically detects IFNT and does not cross-react with IFNω, IFNα/β or IFNγ. Samples were assayed undiluted or diluted in steer serum of 1:10, 1:100, 1:1,000, 1:5,000 or 1:10,000.

RNA Extraction and cDNA Library Preparation

Intercaruncular endometrial tissue was thawed and immersed in 350 µL RLT buffer (Qiagen, Hilden, Germany) and homogenized using 2.8 mm ceramic beads (Qiagen) in a bead beater tissue homogenizer (Precellys 24; Bertin Technologies SAS, Montigny-le-Bretonneux, France). Samples were processed using two cycles of 45 s each at 6500 rpm with a 30 s interval between cycles. After homogenization, endometrial RNA was purified using the RNeasy mini kit and on-column DNase digestion according to the manufacturer's instructions (Qiagen). Total RNA was quantified, and RNA quality was assessed using an Agilent 2100 Bioanalyzer (Agilent Technologies, Santa Clara, CA). Only samples with a total RNA 28S:18S ratio > 0.5 and RNA integrity number ≥ 6.8 were used for library construction. Library preparation was conducted by Novogene Inc. (Sacramento, CA) using NEBNext Ultra II RNA Library Prep Kit for Illumina (New England BioLabs Inc., Ipswich, MA). Barcoded libraries were assessed using Qubit 2.0 (ThermoFisher, Invitrogen, Grand Island, NY), Agilent 2100 Bioanalzyer (Agilent Technologies), and quantified with qPCR. Individual libraries were pooled at equal molar concentrations and sequencing was performed using the Illumina NovaSeq 6000 platform producing paired-end 150 base pair reads and Q30 >80%.

Read Mapping and Differential Gene Expression Analysis

Original data files from high-throughput sequencing were transformed into sequenced raw reads by CASAVA base recognition and stored in FASTQ format files. Reads were filtered to remove adaptors, reads with more than 10% uncertain nucleotides, and reads with more than 50% low quality reads. After data filtering, paired-end clean reads of each sample were aligned to the latest bovine reference genome (ARS-UCD1.2) using HISAT2 v2.1 and quantification was performed using

FeatureCounts v1.5.0. Differential expression analysis between pregnant and non-pregnant cows was performed using the DESeq2 R package v2_1.6.3. The resulting *P* values were adjusted using the Benjamini and Hochberg's approach for controlling the False Discovery Rate (FDR). Genes with an FDR ≤ 0.05 were considered to be differentially expressed between pregnant and non-pregnant cows.

Pathway Analysis of Differentially Expressed Genes

Ingenuity Pathway Analysis (Qiagen) was used to identify canonical pathways, gene networks, and upstream regulators of differentially expressed genes affected by pregnancy (Krämer et al., 2014). Differentially expressed genes with an FDR ≤ 0.05 were used for analysis. Canonical pathways with a $-\log_{10} P \geq 1.3$ with corresponding z-scores to predict activation ($z \geq 2$) or inactivation ($z \leq -2$) were identified. A network score of $z \geq 2$ gives 99% confidence the network was not identified by chance. Gene networks were identified by assessing the number of differentially expressed genes in each network. Predicted upstream regulators of differentially expressed genes were limited to genes, RNAs, and protein, and predicted diseases and functions, were identified by z-scores ≥ 2 or ≤ -2 and were considered significant predictors of activation or inhibition of differentially expressed genes, respectively.

Real Time RT-PCR

Reverse transcription was performed using the Verso cDNA synthesis kit (Thermo Fisher Scientific, Waltham, MA). All primers were designed using the National Center for Biotechnology Information (NCBI) database (Table A-8). Amplification efficiency for each primer pair was evaluated and met MIQE guidelines of $r^2 > 0.98$ and efficiency of 90% to 110% (Bustin et al., 2009). Real time RT-PCR was performed in duplicate 20 µL reactions including forward and reverse primer, iTaq Universal SYBR

green master mix (Bio-Rad, Hercules, CA) and 2 to 40 ng cDNA. A Bio-Rad CFX Connect light cycler (Bio-Rad) was employed with an initial denaturation step at 95°C for 30 sec followed by 40 cycles of a two-step protocol using 95°C for 5 s and annealing and extension at 60°C for 30 s. The primer set for *OXTR* required a three-step protocol using 63°C as annealing temperature for 5 s and extension at 60°C for 30 s. A no template control was used to determine non-specific amplification for each primer pair. Relative expression for each gene was calculated using the $2^{-\Delta Ct}$ method relative to the geometric mean of the selected housekeeping genes (*ACTB*, *GAPDH*, *RPL19*). Housekeeping gene expression was stable across treatments and pregnancy status ($P > 0.05$).

Endometrial Transcriptome Data Sets from Comparison Papers

Results of the experiments presented here were compared to the data of other transcriptome analyses describing differences between pregnant and cycling animals. Data from other studies analyzed bovine endometrial tissue from day 15 (Bauersachs et al., 2012), day 16 (Forde et al., 2012), or day 17 (Cerri et al., 2012) of pregnancy compared to the corresponding day of the estrous cycle in cows that were not bred. Briefly, all studies synchronized estrous cycles of animals and inseminated a portion of cows with semen, with the remaining cows not bred (Cerri et al., 2012; Forde et al., 2012) or inseminated with sperm-free supernatant (Bauersachs et al., 2012). All studies only considered cows as pregnant when a conceptus was recovered. Gene lists were obtained from published supplemental tables and gene identities verified. Gene expression data from Bauersachs et al., and Cerri et al., were obtained from microarray (Affymetrix) and published supplemental tables included NCBI gene identification numbers. Sequencing data from Forde et al., were identified with Ensembl transcript

identification numbers and were converted to NCBI gene identification numbers using Ensembl biomart with database Ensembl Genes 100 and the bovine genome ARS-UCD1.2 (Yates et al., 2020). Any Ensembl transcript identification that was not automatically detected and converted, was manually identified using UniProt accession numbers, or RefSeq mRNA accession numbers provided in supplemental table from the original publication. NCBI gene identification numbers from all datasets were verified using bioDBnet (Mudunuri et al., 2009). Only confirmed gene identification numbers that were current and identified a single gene were used for downstream analysis. Genes were considered differentially expressed and used for comparisons if they had an FDR ≤ 0.05 and had $\log_2$ fold-change ≥ 1.5 or ≤ -1.5 (Tables A-9 to A-11).

Each data set was analyzed independently using Ingenuity Pathway Analysis (Qiagen) to identify canonical pathways, gene networks, and predicted upstream regulators of defined differentially expressed genes. The same threshold values described above were applied to these datasets, with canonical pathways significant if $-\log_{10} P \geq 1.3$ and upstream regulators if z-scores ≥ 2 or ≤ -2.

Statistical and Data Analyses

The experimental unit was the cow and, unless otherwise stated, data were analyzed with tow main factors to investigate the effects of treatment (infusion of vehicle vs. infusion of bacteria), pregnancy status (non-pregnant vs pregnant), and the interaction between treatment and pregnancy. Oocyte number, morulae number, morulae development rate, concentration of peripheral progesterone, corpus luteum diameter, and IFNT data were analyzed with general linear model with effects of treatment, pregnancy status, and the interaction between treatment and pregnancy status using SPSS v26 (IBM Corporation, Armonk, NY). Endometrial qPCR data were

log transformed for normality and data analyzed using a general linear model with the effects of treatment, pregnancy status, and the interaction of treatment and pregnancy status. Pairwise comparisons were used to analyze the interaction term. Data for all transcripts were used for principal component analysis using ClustVis (Metsalu and Vilo, 2015). Genes that were differentially expressed in non-pregnant compared to pregnant cows were selected using an FDR ≤ 0.05 and are reported as $\log_2$ fold-change. A heat map was generated for differentially expressed genes with Heatmapper (Babicki et al., 2016) using Pearson distance measurement method and complete linkage clustering. GraphPad Prism v8.4 was utilized for linear regression analysis comparing RNA sequencing data with qPCR results.

Results

Effect of Intrauterine Infusion and Classification of Pregnancy Status

Detailed results for all cows are previously reported (Chapter 2). No cows had clinical signs (vaginal discharge, uterine pus, fever) of uterine disease at the time of insemination (d 130) or slaughter (d 146). There was no effect of intrauterine infusion on corpus luteum diameter, circulating concentration of progesterone, or uterine fluid IFNT concentration on d 146 post infusion ($P > 0.05$; Table 3-1). A total of 12 filamentous conceptuses (vehicle = 6 of 11, bacteria = 6 of 12) were recovered 16 days following insemination. Interferon tau was detected in 17 of 23 uterine fluid samples (vehicle = 8 of 11, bacteria = 9 of 12) and ranged from 0.086 to 6858 ng/mL. Uterine fluid IFNT was at concentrations greater than 61 ng/mL in all cows from which an embryo was recovered. Using the presence of an embryo and uterine IFNT concentration to determine pregnancy status, there was no difference ($P > 0.05$) in the distribution of pregnant (Vehicle, $n = 6$; and Bacteria, $n = 7$) or non-pregnant (Vehicle, $n = 5$; and

Bacteria, *n* = 5) cows according to intrauterine infusion. Retrospective analysis of previously reported oocyte developmental competence in these cows showed no difference in the number of oocytes collected per cow or in the rate of morula development between pregnant and non-pregnant cows (Dickson et al., 2020).

Effect of Pregnancy on the Endometrial Transcriptome of Cows After Intrauterine Infusion of Pathogenic Bacteria

The quality of endometrial RNA restricted our ability to construct sequencing libraries and perform transcriptome analysis on all samples. The quality of RNA recovered from all vehicle infused cows and five bacteria infused cows was below the threshold for analysis (RNA integrity number < 6.8). As a result, all analysis described from hereon was performed only using endometrial tissue of cows after intrauterine infusion of pathogenic bacteria. The endometrial transcriptome of 4 non-pregnant and 3 pregnant cows after intrauterine infusion of pathogenic bacteria was evaluated.

After sequencing and read processing of intercaruncular endometrial tissue, 445,762,946 high quality reads were used for analysis (approximately 63.7 million reads per sample). An average of 95.7% high quality reads were aligned to the reference genome resulting in the detection of 26,092 unique transcripts in the endometrium (Table A-12). The most abundant endometrial genes identified based on total read counts are described in Table A-13. Principal component analysis using the expression of all transcripts of pregnant and non-pregnant cows explains 29% and 23.8% of the variance observed, with no distinct clustering of pregnant and non-pregnant transcriptomes (Fig. A-3). Linear regressions of RNA sequencing reads and gene expression measured by qPCR of three target genes (*CPM*, *OXTR*, and *STC2*)

revealed an $r^2 > 0.85$ suggesting a robust linear relationship between sequencing data and targeted PCR amplification (Fig. A-4).

Effect of Pregnancy on Endometrial Gene Expression After Intrauterine Infusion of Pathogenic Bacteria

After intrauterine infusion of pathogenic bacteria, a total of 171 differentially expressed genes were identified in the intercaruncular endometrium of non-pregnant cows compared to pregnant cows 16 d after insemination (FDR ≤ 0.05; Fig. 3-1A, Table A-14). Of the 171 differentially expressed genes, 140 genes were downregulated and 31 were upregulated in non-pregnant cows compared to pregnant cows. A heatmap shows the uniform expression of the 171 differentially expressed genes identified in intercaruncular endometrium of non-pregnant cows compared to pregnant cows after intrauterine infusion of pathogenic bacteria (Fig. 3-1B).

Analysis of the 171 differentially expressed genes identified 23 canonical pathways altered in the endometrium of non-pregnant cows compared to pregnant cows after intrauterine infusion of pathogenic bacteria (Fig. 3-2, Table A-15). The most significant canonical pathways identified in the endometrium of non-pregnant cows compared to pregnant cows include 1) interferon signaling; 2) activation of IRF by cytosolic pattern recognition receptors; 3) role of pattern recognition receptors in recognition of bacteria and viruses; and 4) necroptosis signaling pathway.

Using the 171 differentially expressed genes, ten gene networks were differentially regulated in the endometrium of non-pregnant cows compared to pregnant cows after intrauterine infusion of pathogenic bacteria (Table A-16). Altered gene networks in the endometrium of non-pregnant cows include 1) connective tissue disorders, immunological disease, inflammatory disease; 2) dermatological diseases

and conditions, immunological disease, organismal injury and abnormalities; and 3) antimicrobial response, infectious diseases, inflammatory response.

A total of 119 genes, RNAs, or proteins were identified as predicted upstream regulators of differentially expressed genes identified in the endometrium of non-pregnant cows compared to pregnant cows, of which 36 were activated and 83 were inhibited (Table A-17). The top five upstream regulators predicted to be activated in the endometrium of non-pregnant cows after intrauterine infusion of pathogenic bacteria include 1) MAPK1 (kinase); 2) NKX2-3 (transcription regulator); 3) IL1RN (cytokine); 4) TRIM24 (transcription regulator); and 5) PNPT1 (enzyme). The top five upstream regulators predicted to be inhibited in the endometrium of non-pregnant cows after intrauterine infusion of pathogenic bacteria include 1) IFNG (cytokine); 2) IFNA2 (cytokine); 3) PRL (cytokine); 4) IRF7 (transcription regulator); and 5) the signaling group interferon alpha.

Comparing Pregnancy Effects on the Endometrial Transcriptome of Cows After Intrauterine Infusion of Pathogenic Bacteria to Previous Studies Conducted in Healthy Cows

Three previous studies report the effect of pregnancy on the endometrial transcriptome of healthy cows at the time of maternal recognition of pregnancy (d 15, 16 and 17 post insemination). All three of the previous studies compared the transcriptome of the endometrium of healthy pregnant cows to healthy, non-pregnant cycling cows that were not subjected to artificial insemination (Bauersachs et al., 2012; Cerri et al., 2012; Forde et al., 2012). Transcriptome data from these previous studies using healthy cows were compared to the findings reported here using bacteria infused cows that failed to become pregnant, with the goal to identify genes that may play a role in pregnancy failure observed in cows with a previous uterine disease. Data from all studies were

restricted to differentially expressed genes with a stringent threshold (FDR ≤ 0.05 and log_2FC ≥ 1.5 or ≤ -1.5; Fig. 3-3A). The differentially expressed genes identified in the endometrium of cows that failed to become pregnant following intrauterine infusion of pathogenic bacteria was modified to the same stringent criteria (FDR ≤ 0.05 and log_2FC ≥ 1.5 or ≤ -1.5), restricting analysis to 90 differentially expressed genes from the original 171 differentially expressed genes (Table A-18). To summarize the previous studies using the stringent criteria of differential gene expression, a total of 67, 216 and 218 differentially expressed genes were identified in the endometrium of healthy non-pregnant cows compared to healthy pregnant cows at the corresponding day of the estrous cycle (d 15, d 16 and d 17, respectively; Fig. 3-3A). A complete list of differentially expressed genes identified in the endometrium of healthy non-pregnant cows compared to healthy pregnant cows is provided in Tables A-9 to A-11. When comparing the pregnancy associated changes to endometrial transcriptome of all four studies, a total of 24 genes were consistently downregulated in the endometrium of cows that were not pregnant, regardless of previous exposure to bacteria (Fig. 3-3B, Table A-19). A total of 12 genes were identified that were consistently downregulated in the endometrium of healthy non-pregnant cows compared to healthy pregnant cows that were not differentially expressed in the endometrium of non-pregnant cows after intrauterine infusion of pathogenic bacteria (Fig. 3-3B). Furthermore, 28 unique genes were identified in the endometrium of non-pregnant cows compared to pregnant cows following intrauterine infusion of pathogenic bacteria that were not identified in the previous studies using healthy cows (Fig. 3-3B, Table A-19). These unique differentially expressed genes identified in the endometrium of cows that failed to become pregnant

after intrauterine infusion of pathogenic bacteria may play a role in the pregnancy failure observed in cows following uterine disease. Of the 28 unique genes identified in the endometrium of non-pregnant cows after intrauterine infusion of pathogenic bacteria compared, 10 genes were upregulated, and 18 genes were downregulated. Within those 28 genes, 5 encode for non-coding RNAs, 2 are pseudo genes and 3 are uncharacterized proteins (Fig. 3-3B).

Differentially expressed genes from each study were analyzed to identify dysregulated canonical pathways and predicted upstream regulators of differentially expressed genes. Using the defined, stringent list of differentially expressed genes, only 18 canonical pathways were identified in endometrium of non-pregnant cows compared to pregnant cows following intrauterine infusion of pathogenic bacteria at d 16 (Fig. 3-4). In comparison, a total of 16, 39 and 40 canonical pathways were identified in the endometrium of healthy non-pregnant cows compared to healthy pregnant cows at d 15, d 16 and d 17 (Fig. 3-4; Table A-20). A total of 11 identified canonical pathways were conserved in the endometrium of non-pregnant cows compared to pregnant cows amongst the four studies, including 1) interferon signaling, 2) activation of IRF by cytosolic pattern recognition receptors, and 3) role of pattern recognition receptors in recognition of bacteria and viruses (Fig. 3-4). Interestingly, five canonical pathways were uniquely identified in the endometrium following intrauterine infusion of pathogenic bacteria of non-pregnant cows compared to non-pregnant cows, including iNOS signaling, Toll-like receptor signaling, and IL-7 signaling pathway (Fig. 3-4). There were no canonical pathways effected by pregnancy that were only identified in healthy cows and not in cows following intrauterine infusion of pathogenic bacteria.

Using the defined, stringent list of differentially expressed genes a total of 112 predicted upstream regulators of differentially expressed genes were identified in the endometrium following intrauterine infusion of pathogenic bacteria of non-pregnant cows compared to pregnant cows (Fig. 3-5, Table A-21). In comparison, a total of 124, 161 and 177 predicted upstream regulators were identified in the endometrium of healthy non-pregnant cows compared to healthy pregnant cows at d 15, d 16 and d 17 (Fig. 3-5, Table A-21). In total, 94 predicted upstream regulators of differentially expressed genes were identified in the endometrium of non-pregnant cows compared to pregnant cows of all four studies, including the inhibition of IFN, IL-1β, NFκB and PRL, and the activation of ACKR2, IL-1RN, and IL-10RA (Fig. 3-5, Table A-21). A total of 14 predicted upstream regulators were identified only in the endometrium of healthy non-pregnant cows compared to healthy pregnant cows (Fig. 3-5), while five unique predicted upstream regulators were identified in the endometrium following intrauterine infusion of pathogenic bacteria of non-pregnant cows compared to pregnant cows, including the activation of ISG15 and AIRE, and inhibition of DUSP1, NFKBIA, and PF4 (Fig. 3-5). Examples of gene networks of associated with predicted upstream regulators of differentially expressed genes identified in the endometrium of cows following intrauterine infusion of pathogenic bacteria are shown in Fig. A-5.

Quantification of Endometrial Target Genes Identified Using Transcriptome Analysis in Cows After Intrauterine Infusion of Vehicle or Pathogenic Bacteria

Following transcriptome analysis, qPCR was performed on endometrial tissue of all 21 cows that were subjected to intrauterine infusion of either vehicle or pathogenic bacteria. Samples described here failed to meet the quality threshold for transcriptome

analysis but could be applied to gene expression analysis using qPCR (Table 3-1, Fig. 3-6).

Expression of interferon-stimulated genes (known to be upregulated in pregnant cows), *ISG15* and *MX1* were increased in the endometrium of pregnant cows compared to non-pregnant cows, regardless of intrauterine infusion ($P \leq 0.05$; Fig. 3-6A-B). Expression of *OXTR* (known to be downregulated in pregnant cows) was decreased in the endometrium of pregnant cows compared to non-pregnant cows ($P \leq 0.05$) and was also increased after intrauterine infusion of pathogenic bacteria compared to vehicle infused cows ($P \leq 0.05$; Fig 3-6C).

Of the 28 unique genes identified in the endometrium of non-pregnant cows compared to pregnant cows after intrauterine infusion of pathogenic bacteria that were not identified in the previous studies using healthy cows (Fig. 3-3B), five genes that are not regulated by type 1 interferons (*MEF2B*, *CPM*, *STC2*, *FAM135B*, and *FLRT1*) were selected for analysis by qPCR. Expression of *MEF2B*, *CPM*, *STC2*, and *FAM135B* were unaffected by pregnancy or intrauterine infusion (Fig. 3-6D-G); however, expression of endometrial *FLRT1* was affected by pregnancy status, specifically in cows after intrauterine infusion of vehicle medium, but not after intrauterine infusion of pathogenic bacteria ($P \leq 0.05$; Fig. 3-6H).

Of the 12 genes identified that were consistently downregulated in the endometrium of healthy non-pregnant cows compared to healthy pregnant cows that were not differentially expressed in the endometrium of non-pregnant cows after intrauterine infusion of pathogenic bacteria (Fig 3-4B), three genes (*ABHD1*, *TIMD4*, and *TRANK1*) were selected for analysis by qPCR (Fig. 3-6I-K). Endometrial expression

of *ABHD1*, *TIMD4*, and *TRANK1* were affected by pregnancy status but not intrauterine infusion. Specifically, *ABHD1* expression was decreased in the endometrium of non-pregnant cows after intrauterine infusion of bacteria, but not in cows after intrauterine infusion of vehicle medium (Fig. 3-6I). Expression of *TIMD4* was decreased in the endometrium of non-pregnant cows after intrauterine infusion of either vehicle medium or pathogenic bacteria (Fig. 3-6J). In addition to being affected by pregnancy status, the expression of *TRANK1* was also affected by the interaction of intrauterine infusion and pregnancy status ($P \leq 0.05$; Fig. 3-6K). Specifically, *TRANK1* expression was lower in non-pregnant cows compared to pregnant cows after intrauterine infusion of pathogenic bacteria ($P < 0.05$), but not in cows that received an intrauterine infusion of vehicle medium. In addition, expression of *TRANK1* was higher in non-pregnant cows after intrauterine infusion of vehicle medium compared to non-pregnant cows after intrauterine infusion of pathogenic bacteria ($P < 0.05$). Endometrial expression of inflammatory mediators, *CXCL8* or *IL6*, were not affected by pregnancy status or intrauterine infusion ($P > 0.05$; Fig. 3-6L-M).

Discussion

Uterine infection occurs in up to 40% of dairy cows within weeks of calving; however, the consequences of uterine infection can have lasting impacts as cows previously diagnosed with a uterine disease are less likely to conceive compared to healthy herd mates (Ribeiro et al., 2016a). Previous studies have shown that uterine infection has negative impacts on fertility, with alterations in the transcriptomes of ampulla, isthmus, endometrium, oocytes, and granulosa cells months after the resolution of disease (Piersanti et al., 2019a, 2020; Horlock et al., 2020). A portion of infection-induced infertility can be explained by an impact on the female gametes, as

oocytes from cows with a previous uterine infection are less competent compared to oocytes from healthy cows (Dickson et al., 2020). However, the transfer of embryos from healthy donors to recipients with prior uterine disease does not resolve uterine disease associated infertility (Ribeiro et al., 2016a; Estrada-Cortés et al., 2019; Edelhoff et al., 2020). Thus, there may be long-term impacts of uterine disease on the endometrium responsible for the observed decrease in fertility.

To study uterine infection in a controlled manner, we used a model of induced uterine infection where cows received an intrauterine infusion of pathogenic bacteria or control medium (Piersanti et al., 2019b; Dickson et al., 2020). Cows that received bacteria in the uterus had elevated vaginal mucus discharge scores and endometrial inflammation compared to control cows within one week that was resolved by four weeks post infusion (Dickson et al., 2020). Four months after intrauterine infusion of treatment all cows responded to estrous synchronization and there was no difference due to bacteria infusion on circulating progesterone, the size of corpus luteum, the number of embryos recovered at d 16 post insemination, or uterine fluid interferon tau concentration (Dickson et al., 2020). To determine the endometrial effect of intrauterine infusion of pathogenic bacteria that may be responsible for uterine disease associated reduced fertility, intercaruncular endometrial tissue was subjected to RNA sequencing analysis. However, RNA quality of endometrial tissue recovered from cows infused with vehicle control medium was below a suitable standard for sequencing, as such only the endometrium of cows infused with pathogenic bacteria was subjected to sequencing according to pregnancy status on d 16 after insemination. Analysis of this subset of tissues identified differentially expressed genes and canonical pathways of the

endometrium of cows that did not become pregnant after earlier intrauterine infusion of bacteria. Furthermore, we also compared our findings of pregnancy related changes in the endometrium of cows after intrauterine infusion of bacteria to previous reports describing the effect of pregnancy on the endometrium in healthy cows that used cycling cows as the basis of comparison. Because all cows included in the current study responded to estrous synchronization, maintained oocyte developmental competence (according to in vitro fertilization data) and were inseminated, these new data can be extrapolated to suggest possible endometrial mechanisms by which intrauterine infusion of pathogenic bacteria reduces fertility.

When comparing the present data to that of previous studies, there were 24 genes and 11 pathways that were conserved and consistently downregulated in the non-pregnant endometrium (regardless of bacterial infusion), suggesting at the time of maternal recognition of pregnancy in bovine (d 15-17) there is a robust group of genes and pathways consistently expressed in response to pregnancy. In the bovine, maternal recognition of pregnancy is driven by IFNT secreted from the conceptus between days 15-17 of gestation (Bazer et al., 1997). The collective data from the analysis described here show that many of the conserved genes identified across all four studies include endometrial interferon-inducible genes (*EIF2AK2*, *IFI6*, *IFI16*, *IFI27*, *IFIH1*, *IFIT5*, *MX1*, *MX2*, *STAT1, XAF1*). Consistently downregulated pathways in the non-pregnant endometrium across all studies, included interferon signaling, activation of interferon regulatory factor, role of pattern recognition receptors in recognition of bacteria and viruses and necroptosis signaling pathway. This suggests that after intrauterine infusion of bacteria, cows that become pregnant induce the expression of the same robust

endometrial genes identified in healthy comparison studies, it may therefore be that IFNT signaling is not impaired in the endometrium of cows after infusion of bacteria.

Although pregnancy itself mediated a large number of consistent changes to the transcriptome of the endometrium, a number of differentially expressed genes, canonical pathways, and predicted upstream regulators were uniquely identified in the endometrium of non-pregnant cows after intrauterine infusion with pathogenic bacteria compared to healthy cycling cows. It is these unique genes and pathways that may provide an insight into the mechanisms by which uterine infection results in decreased fertility in cattle. Moreover, many of the unique genes, canonical pathways, and predicted upstream regulators identified in the endometrium of non-pregnant cows previously infused with pathogenic bacteria that were not differentially expressed in healthy cows were related to inflammation and immune function.

Establishment and maintenance of pregnancy requires maternal immune tolerance of the allogeneic conceptus, coordinated by a unique repertoire of immune cells including natural killer cells, macrophages, effector T cells, regulatory T cells and B cells (Miller et al., 2020). Interleukin (IL)-7 signaling is critical for development and function of T cells, specifically effector Th17 cells, and decidua natural killer cells, the most abundant lymphocytes in the decidua (Mincheva-Nilsson, 2003; Fry and Mackall, 2005). Interestingly, IL-7 signaling was identified as an altered pathway unique to the endometrium of non-pregnant cows after intrauterine infusion with pathogenic bacteria that was not identified in the endometrium of healthy non-pregnant cows. Dysregulated IL-7 influences pregnancy outcomes in women. Women with recurrent miscarriage have altered *IL7* and *IL7R* expression in the decidua compared to healthy pregnant women

(Wu et al., 2016), and obese pregnant mothers have reduced peripheral IL-7 compared to normal weight mothers (Tagoma et al., 2019). Conversely, exogenous administration of IL-7 during early pregnancy causes fetal resorption, decreased *Foxp3* gene expression in the decidua (indicative of T regulatory cells), and an increased ratio of Th17 effector to T regulatory cells compared to wild type control mice (Wu et al., 2016). Altered IL-7 signaling in the endometrium of non-pregnant cows after infusion with pathogenic bacteria may be impacting immune cell dynamics required for pregnancy by reducing maternal immune tolerance of the conceptus. The role of IL-7 in pregnancy in normal pregnancy and after uterine infection warrants further investigation.

Transcription factor, autoimmune regulator (AIRE), was a predicted activated upstream regulator uniquely identified in the endometrium of non-pregnant cows after intrauterine infusion of pathogenic bacteria compared to the endometrium of healthy non-pregnant cows. As a transcription factor AIRE works with its binding partners to target markers of inactive chromatin and induce transcription elongation. Expression of AIRE in the thymus is critical for the development of T cell competence and elimination of self-reactive T-cells that would result in autoimmune disease (Perniola, 2018). Differentially expressed genes downstream of AIRE in the endometrium of non-pregnant cows after infusion with bacteria were all downregulated (*EIF2AK2*, *IFI44*, *HERC6*, *PARP14*, *TNFSF10*), suggesting the upregulation of these genes could be important for pregnancy establishment. Contrary to our findings where AIRE is predicted to be activated in the non-pregnant endometrium, the expression of endometrial *AIRE* has been shown to be increased in highly fertile cows compared to lower fertile cows (Moran et al., 2015). Conversely, mice lacking AIRE are subfertile due to a depletion of

the ovarian follicular reserve resulting in less embryo implantations compared to wild type mice (Jasti et al., 2012; Warren et al., 2019). The role of endometrial AIRE in the mouse is debated, with local *Aire* knockdown inhibiting implantation (Soumya et al., 2016), while others suggest endometrial AIRE does not play a role in decidualization (Warren et al., 2019). The role of AIRE should be further explored in the cow to assess any potential roles in pregnancy establishment and fertility after uterine infection.

Inflammation is required for many aspects of reproduction including ovulation, implantation, and parturition. Establishment and maintenance of pregnancy requires a balance of pro- and anti-inflammatory processes that when dysregulated can be detrimental to pregnancy success (Mor et al., 2011). Nitric oxide (NO) is an immune regulator with an important role during implantation and pregnancy (Purcell et al., 1999; Kwon et al., 2004). The inducible nitric oxide synthase (iNOS) pathway, regulated by *NOS2* expression, was identified as a unique canonical pathway in the endometrium of non-pregnant cows after intrauterine infusion of pathogenic bacteria compared to non-pregnant healthy cows. Compared to healthy women, peritoneal macrophages in women with endometriosis have elevated *NOS2* expression, and NO production which can be further exacerbated after LPS stimulation (Wu et al., 1999; Osborn et al., 2002). In mice, elevated NO inhibits implantation (Barroso et al., 1998). Cows in the current study and cows diagnosed with a uterine infection are exposed to LPS from Gram-negative *E.coli* in the uterus that could potentially alter endometrial nitric oxide production and iNOS signaling, resulting in reduced fertility; however these potential mechanisms require further investigation.

Toll-like receptors (TLR) respond to pathogen-associated molecular patterns and initiate a cellular signaling cascade that culminates in an innate immune response and production of pro-inflammatory cytokines (Akira et al., 2001). The bovine endometrium expresses TLRs 1 to 7 and 9 (Herath et al., 2006; Davies et al., 2008). The data here show the expression of TLRs 2 to 10 in the endometrium of all cows after infusion of bacteria but was not affected by pregnancy status. Using the data presented here, the TLR signaling pathway was uniquely dysregulated in the endometrium of non-pregnant cows after infusion with bacteria and not altered in healthy cows. In women, activation of TLR signaling in human stroma cells of the early pregnant decidua can decrease the proportion of regulatory T cells in peripheral lymphocytes in vitro (Wu et al., 2019), further suggesting that TLR signaling plays a role in pregnancy and dysregulation is associated with pregnancy pathology (Mor et al., 2005). Interestingly, bovine endometrial epithelial cells increase production of inflammatory cytokines in response to sperm via the TLR2/TLR4 pathways (Ezz et al., 2019), which may be the reason we observed changes in cows after infusion of bacteria where all cows were inseminated, whereas data obtained from other studies using healthy cows did not inseminate healthy cycling cows (Bauersachs et al., 2012; Cerri et al., 2012; Forde et al., 2012).

Lipopolysaccharide binding-protein (LBP) is involved in both iNOS signaling and TLR signaling pathways. Expression LBP (*LOC514978*) was reduced in the endometrium of non-pregnant cows compared to the pregnant cows after the infusion of pathogenic bacteria. In women, circulating LBP has been suggested as a potential biomarker for intra-amniotic infection and preterm labor, however results vary, and LBP is currently not considered reliable for clinical use (Chen et al., 2009; Torbé et al.,

2011). Despite inconsistent results in women, associations between LBP concentrations and fertility warrants further investigation in cows.

Nuclear factor kappa B inhibitor alpha (NFKBIA), which encodes for inhibition of nuclear-factor κB alpha (IκBα), is also involved in both iNOS signaling and TLR signaling pathways, and was uniquely identified as a predicted upstream regulator in the endometrium of non-pregnant cows after infusion with bacteria. Expression of NFKBIA and phosphorylation of IκBα is reduced in the endometrium of women with endometriosis compared to healthy women and while endometriosis patients have reduced fertility, there is no supportive data for a role of endometrial NFKBIA in fertility (Ponce et al., 2009). The dysregulation of iNOS and/or TLR signaling pathways in the endometrium could be hindering pregnancy establishment of cows after infusion with pathogenic bacteria.

Appropriate angiogenesis of the endometrium is critical for establishment of pregnancy (Torry et al., 2007). A chemokine with antiangiogenic activity, platelet factor 4 (PF4) was identified as an inhibited upstream regulator of differentially expressed genes unique to the endometrium of non-pregnant cows after infusion with bacteria. Platelet factor 4 inhibits angiogenesis as well as inhibiting endothelial proliferation and migration (Bikfalvi, 2004). In women, preconception circulating PF4 concentrations are positively correlated with adverse pregnancy outcomes, including hypertensive disorders and placental abruption (Theilen et al., 2020), while women with recurrent miscarriages also have elevated circulating PF4 compared to control patients (Kotani et al., 2020). It is therefore unclear what role PF4 inhibition may play in non-pregnant cows

after infusion with bacteria but suggests that dysfunction of endometrial angiogenesis may contribute to altered fertility.

Dual-specificity phosphatase 1 (DUSP1) was identified as an inhibited upstream regulator of differentially expressed genes unique to the endometrium of non-pregnant cows after infusion with bacteria. DUSP1 is a phosphatase commonly studied in tumor biology, however little is known about its role in fertility. Although not explored in domestic animals, reduced placental DUSP1 is associated with pre-eclampsia in women (Yang et al., 2016). However, DUSP1 is known to negatively regulate mitogen-activated protein kinase (MAPK) pathway by dephosphorylating serine and threonine residues (Shah et al., 2014) and may play a role in pregnancy establishment and maintenance by dysregulating MAPK signaling important in bovine fertility (Thatcher et al., 2001; Salilew-Wondim et al., 2010).

Non-coding RNAs regulate basal and gene specific transcription, translation and in some cases protein function, while some non-coding RNAs may indeed encode proteins that have yet to be identified in the bovine. Interestingly, 18% of the unique genes (5 of 28) identified in the endometrium of non-pregnant cows after infusion with bacteria were non-coding RNAs. Our understanding of non-coding RNA function in the bovine endometrium is poor. However, endometrial expression profiles of non-coding RNAs in swine and goat have been characterized throughout the estrous cycle and peri-implantation period (Su et al., 2014; Wang et al., 2016, 2017; Liu et al., 2019). In the pig, expression of long non-coding RNAs at the time of embryo implantation were correlated with genes involved in MAPK signaling, including *DUSP4*, *DUSP10*, and *CD14* (Wang et al., 2017). In addition, LPS can induce expression of specific non-

coding RNAs in the pig, suggesting non-coding RNAs may play a role in the regulation of inflammation (Zhang et al., 2021). We did not analyze specific non-coding RNAs or their potential targets in the current study; however, the expression of non-coding RNAs and their role in inflammation and pregnancy establishment warrant further investigation in the cow.

Due to the poor quality of RNA obtained in our study from cows after infusion with vehicle medium, we chose to perform targeted PCR for select genes using tissues from all cows after infusion with vehicle medium or pathogenic bacteria, according to pregnancy status. We selected genes to analyze based on the current transcriptome analysis and further comparison to previous studies that have not been shown to be regulated by IFNT (*MEF2B*, *STC2*, *CPM*, *FLRT1*, *FAM135B*). We believed this approach would allow us to better determine genes involved in infection induced infertility, and not simply a reflection of pregnancy status. Additionally, we targeted genes (*ABHD1*, *TIMD4*, *TRANK1*) that were uniquely altered in the endometrium of non-pregnant healthy cows and not identified in cows after infusion with bacteria which may reflect genes involved in endometrial receptivity that are affected by bacteria infusion. Collectively, we hoped this approach would allow us to identify endometrial genes involved in in infection induced infertility using a larger number of samples than were used for RNA sequencing. In general, this approach did not bear fruit. For example, expression of *FLRT1* was unique to non-pregnant cows after infusion of bacteria using transcriptome data, but PCR analysis using all samples suggest that pregnancy status was the major factor regulating endometrial *FLRT1* expression. Similarly, expression of *ABHD1* and *TIMD4* which were not identified in non-pregnant

cows after bacterial infusion were found to be regulated by pregnancy status when measured by PCR in all samples regardless of intrauterine infusion, suggesting the expression of these genes is not likely involved infection related infertility. However, tetratricopeptide repeat and ankyrin repeat containing 1 (*TRANK1*), which was identified in the endometrium of healthy cows of previous studies and not in cows after infusion of bacteria, was affected by the interaction of pregnancy status and intrauterine infusion. This suggests that endometrial *TRANK1* expression may play a role in infection related infertility. The role of *TRANK1* in the endometrium is unknown; however, endometrial expression of *TRANK1* in women is upregulated in stromal cells during early decidualization compared to later decidualization or non-decidualized endometrium (Rytkönen et al., 2019). The function of TRANK1 has been best studied in the brain and is involved in the regulation of neural development and differentiation, with gene polymorphism associated with mental illness including bipolar disorder (Jiang et al., 2019; Li et al., 2020). However, female and male homozygous TRANK1 knock-out mice are reported to be fertile (International mouse phenotyping consortium: Trank1). With such little information known about TRANK1, and if it has a role in the endometrium of the cow, further investigation is required before a mechanistic link between fertility and uterine infection can be hypothesized.

The poor quality of endometrial RNA sampled from vehicle infused cows limited our ability to execute our ideal experiment of using RNAseq to analyze the healthy non-pregnant, healthy pregnant, bacteria infused non-pregnant, and bacteria pregnant cows. Additionally, the final number of samples with robust RNA quality subjected to sequencing from cows after infusion with bacteria was low. Despite this drawback, we

were able to compare our transcriptome analysis after bacterial infusion to analysis of others used to identify endometrial genes regulated by pregnancy in healthy non-pregnant cows (compared to healthy pregnant cows). However, the previous reports utilized different breeds of cows, different days of pregnancy (15, 16, 17), different transcriptome tools (microarray), and performed sequence alignment with older versions of the bovine genome; all of which could increase variation amongst the studies. Alternatively, these differences in experimental strategies could be viewed as a strength as this collective analysis identified a robust set of pregnancy associated genes that were consistently characterized amongst the four studies. In the pursuit of future studies to identify genes and mechanisms associated with infection related infertility, we should consider a large number of samples with good quality RNA, and potentially at earlier stages of pregnancy. Furthermore, we must account for the impacts of uterine infection on oocyte and embryo viability. Developmental competence of oocytes after bacterial infusion was similar between pregnant and non-pregnant cows in the current study based on in vitro fertilization and embryo culture, but perhaps future experiments should utilize embryo transfer from healthy control donors to recipients after infusion of bacteria to better separate potential effects on the germ line from those on the endometrium.

In conclusion, we identified endometrial genes in cows that failed to become pregnant after an intrauterine infusion of pathogenic bacteria. Furthermore, we compared our data with that from others using healthy cows that were never bred and identified unique genes that may be causative of uterine infection related infertility. Additionally, we identified a robust set of endometrial genes, pathways and upstream regulators associated with pregnancy, regardless of prior uterine infection. However,

further investigation into the potential mechanisms of infection related infertility is warranted, including endometrial *TRANK1* expression, and iNOS, TLR and IL-7 signaling pathways. Characterization of these pathways associated to infection related infertility may led to improvements in fertility of women and cattle that are susceptible to reproductive tract infection.

Table 3-1. Characteristics of cows after intrauterine infusion of vehicle or pathogenic bacteria.

	Vehicle		Bacteria		*P* value[a]	
	Non-Pregnant	Pregnant	Non-Pregnant	Pregnant	Trt	Preg
n	5	6	5	7		
CL diameter (mm)[b]	21.8 ± 0.7	23.3 ± 1.3	23.4 ± 0.6	21.8 ± 0.6	0.99	0.96
P4 (ng/mL) [c]	12.0 ± 0.9	11.8 ± 0.7	11.7 ± 1.4	11.2 ± 1.5	0.72	0.80
IFNT (ng/mL) [2]	0.1 ± 0.0	765.0 ± 384.8	0.0 ± 0.0	1685.8 ± 978.6	0.49	0.07
Oocyte (n) [d]	37.2 ± 10.6	42.0 ± 8.0	40.4 ± 8.1	41.6 ± 9.6	0.88	0.75
Morula (n) [d]	8.6 ± 2.2	11.0 ± 1.7	10.6 ± 2.7	8.3 ± 2.6	0.88	0.99
Morula/oocyte (%)	25.3 ± 2.2	27.9 ± 4.0	25.3 ± 4.8	16.5 ± 3.4	0.14	0.42

[a] Comparison of vehicle or bacteria intrauterine infusion (Trt) or pregnancy status (Preg).

[b] Quantified 16 days post insemination at time of conceptus collection.

[c] Circulating progesterone quantified 15 days post insemination.

[d] Sum of four rounds of oocytes collections, in vitro fertilization, and embryo cultures.

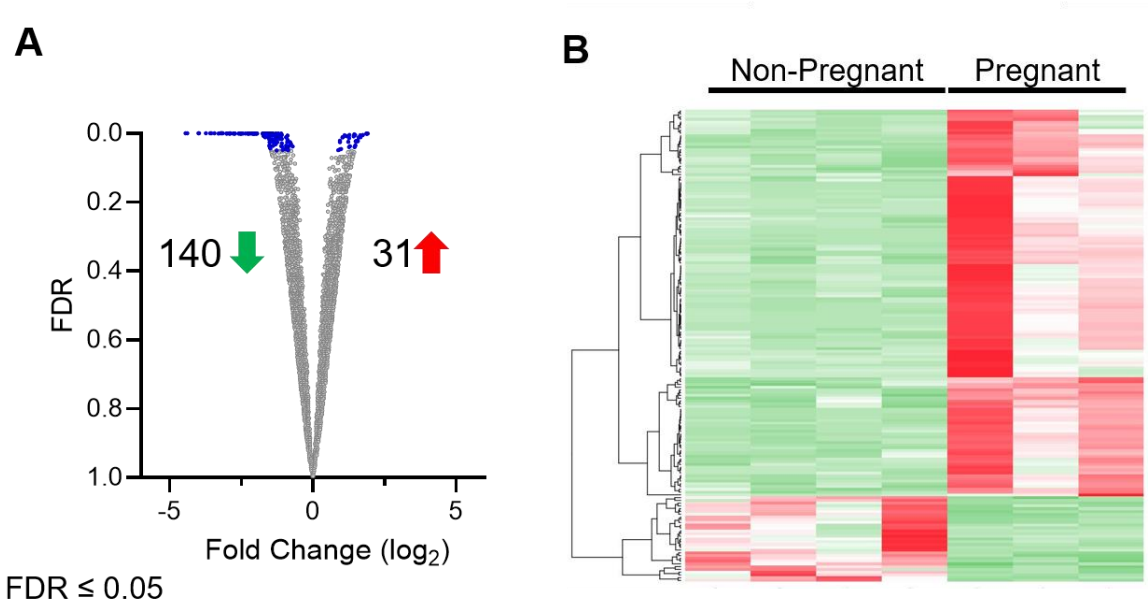

Figure 3-1. Differentially expressed endometrial genes of non-pregnant cows compared to pregnant cows after intrauterine infusion of pathogenic bacteria. Cows were inseminated 130 days after intrauterine infusion of pathogenic bacteria and endometrial tissue collected 16 days later. Based on the presence of an embryo and interferon tau cows were designated as pregnant (n = 3) or non-pregnant (n = 4). Endometrial tissue was subjected to RNA sequencing analysis. (A) Volcano plot depicting the fold change (log2) and false discovery rate (FDR) of each endometrial gene of non-pregnant cows compared to pregnant cows. Differentially expressed genes (FDR < 0.05) are colored blue. A total of 140 genes were downregulated and 31 genes were upregulated in the endometrium of non-pregnant cows compared to pregnant cows. (B) Heatmap presents hierarchal clustering of differentially expressed genes with each column representing a single cow and each row a single gene. Rows were clustered with Pearson distance measurement method and complete linkage. Gene expression intensities are shown in green (decreased) to red (increased)

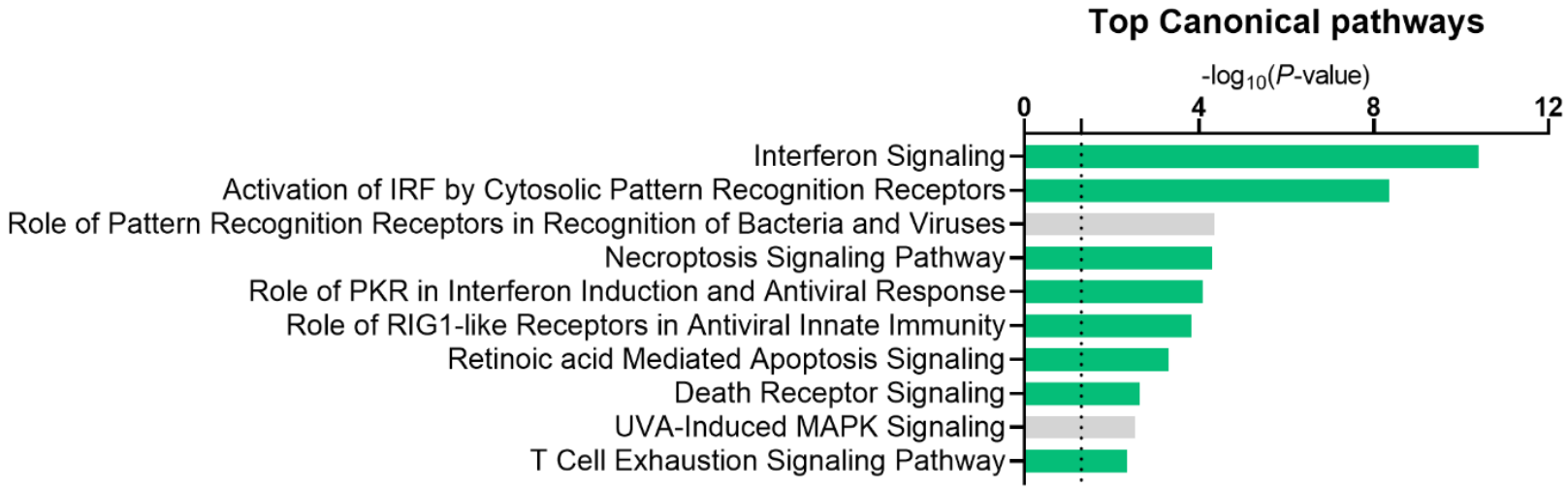

Figure 3-2. Altered canonical pathways in the endometrium of non-pregnant cows compared to pregnant cows after intrauterine infusion of pathogenic bacteria. The top 10 altered canonical pathways were identified using IPA based on 171 differentially expressed genes characterized in the endometrium of non-pregnant cows compared to pregnant cows after infusion with bacteria. Pathways were considered significant if $-\log_{10} P \geq 1.3$, depicted by the dotted line. Most pathways were predicted to be inhibited (green, z-score ≤ -2). Grey bars represent significantly affected canonical pathways where a z-score could not be calculated. A full list of altered canonical pathways can be found in Table A-15.

.

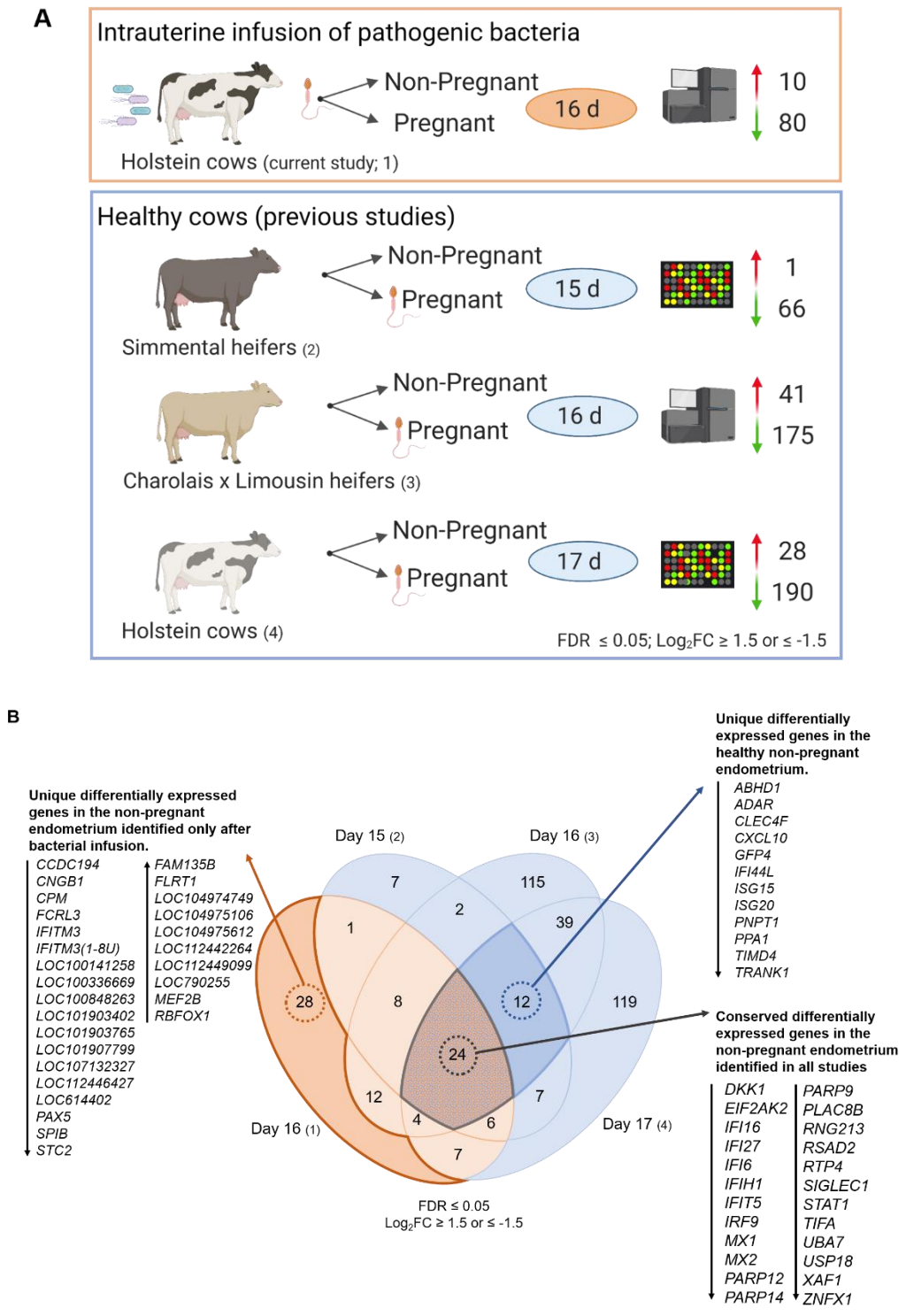

Figure 3-3. Differentially expressed genes in the endometrium of non-pregnant cows compared to pregnant cows using previously published studies. Data from previously published studies using healthy cows were used to compare with

current data from cows after infusion with bacteria. (A) Differentially expressed genes with an FDR ≤ 0.05 and $\log_2$ FC ≥ 1.5 or ≤ -1.5 from all studies were considered. Holstein cows after intrauterine infection of pathogenic bacteria were inseminated and sixteen days later classified as non-pregnant or pregnant based on the presence of a conceptus and IFNT (orange). Three previous studies were used for comparison (blue), including 1) microarray analysis of Simmental heifers either inseminated with sperm-free supernatant and classified as non-pregnant cycling or inseminated and classified as pregnant based on presence of a conceptus fifteen days later (Bauersachs et al., 2012); 2) RNA sequencing of crossbred Charolais and Limousin heifers either never inseminated and classified as non-pregnant cycling, or inseminated and classified as pregnant based on presence of a conceptus sixteen days later (Forde et al., 2012); and 3) microarray analysis of Holstein cows were either not inseminated and classified as cycling, or inseminated and classified as pregnant based on the presence of a conceptus seventeen days later (Cerri et al.,2012). Comparisons show differentially expressed genes in the non-pregnant cows compared to the pregnant cows. (B) A Venn diagram displays the overlap of differentially expressed endometrial genes in all four studies. The orange segment represents the current study in cows after infusion of bacteria, and the blue segments represent previous studies using healthy cows. Arrows depict if genes were upregulated or downregulated in the endometrium of non-pregnant cows compared to pregnant cows. A complete list of differentially expressed genes from all studies can be found in Tables A-9 to A-11 and A-18, and a list with details of genes listed in the figure can be found in Table A-19.

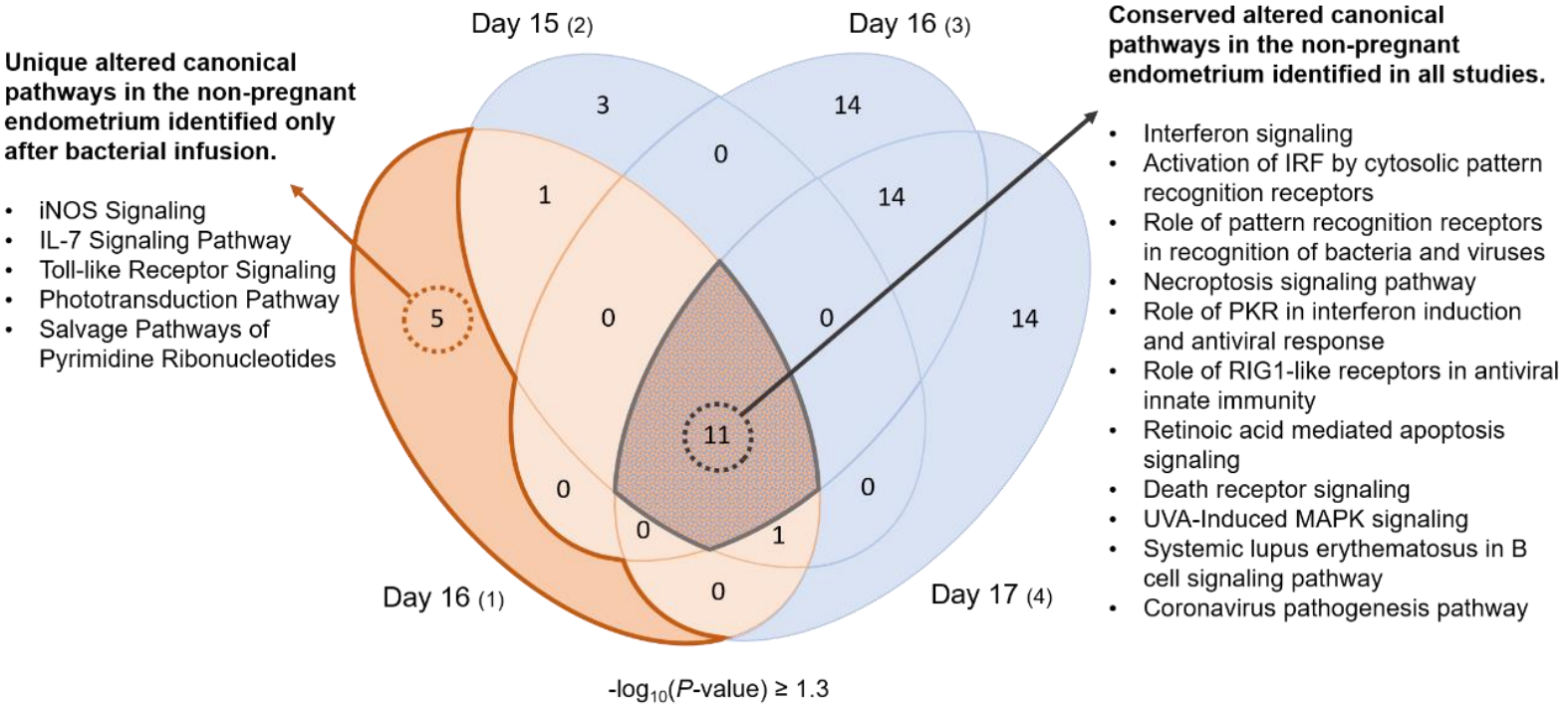

Figure 3-4. Altered canonical pathways in the endometrium of non-pregnant cows compared to pregnant cows using previously published studies. Data from previously published studies using healthy cows were used to compare with current data from cows after infusion with bacteria. Altered canonical pathways were determined using the differentially expressed genes identified in the endometrium of non-pregnant cows compared to pregnant cows. Canonical pathways were considered significant if $-\log_{10}$ (*P* value) ≥ 1.3. The orange segment represents the current study in cows after infusion of bacteria, and the blue segments represent previous studies using healthy cows. A complete list of altered canonical pathways, z-score, *P*-value and associated genes from all studies can be found in Table A-20.

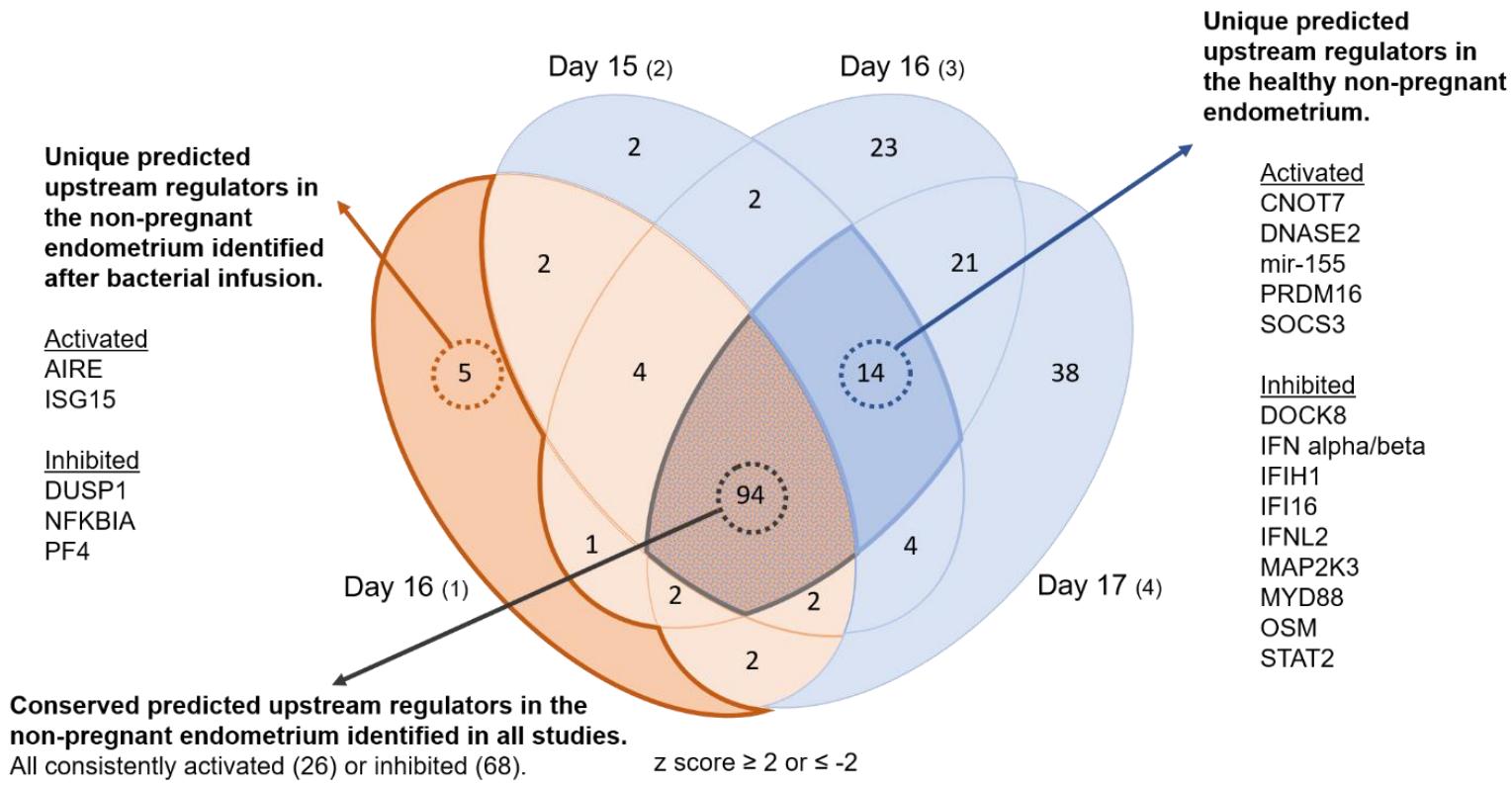

Figure 3-5. Predicted upstream regulators in the endometrium of non-pregnant cows compared to pregnant cows using previously published studies. Data from previously published studies using healthy cows were used to compare with current data from cows after infusion with bacteria. Significant predicted upstream regulators of differentially expressed endometrial genes had a z-score ≥ 2 or ≤ -2. The orange segment represents the current study in cows after infusion of bacteria, and the blue segments represent previous studies using healthy cows. A complete list of predicted upstream regulators, associated genes, activation status, z-score and *P*-value from all studies can be found in Table A-21

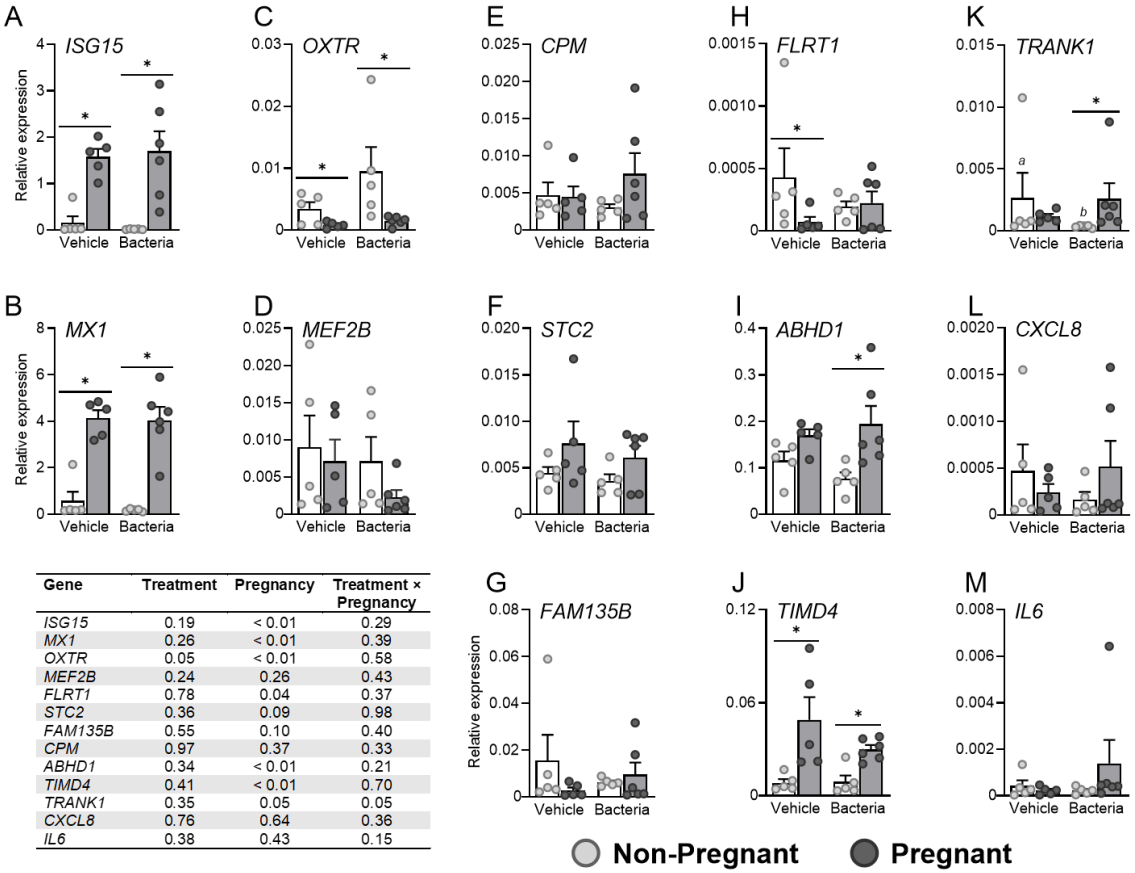

Gene	Treatment	Pregnancy	Treatment × Pregnancy
ISG15	0.19	< 0.01	0.29
MX1	0.26	< 0.01	0.39
OXTR	0.05	< 0.01	0.58
MEF2B	0.24	0.26	0.43
FLRT1	0.78	0.04	0.37
STC2	0.36	0.09	0.98
FAM135B	0.55	0.10	0.40
CPM	0.97	0.37	0.33
ABHD1	0.34	< 0.01	0.21
TIMD4	0.41	< 0.01	0.70
TRANK1	0.35	0.05	0.05
CXCL8	0.76	0.64	0.36
IL6	0.38	0.43	0.15

Figure 3-6. Effect of pregnancy status and intrauterine infusion of pathogenic bacteria on the expression of endometrial genes identified by transcriptome analysis. Cows were inseminated 130 days after intrauterine infusion of either vehicle medium or pathogenic bacteria. Endometrial tissue collected 16 days later and based on the presence of an embryo and interferon tau cows were designated as vehicle-non-pregnant (n = 5), vehicle-pregnant (n = 5), bacteria-non-pregnant (n = 5), or bacteria-pregnant (n = 6). Endometrial expression of (A) *ISG15*, (B) *MX1*, (C) *OXTR*, (D) *MEF2B*, (E) *CPM*, (F) *STC2*, (G) *FAM135B*, (H) *FLRT1*, (I) *ABHD1*, (J) *TIMD4*, (K) *TRANK1*, (L) *CXCL8*, and (M) *IL6* was evaluated by real-time RT-PCR. Data are presented as expression relative to the geometric mean of three housekeeping genes (*ACTB*, *GAPDH*, and *RPL19*). Each dot represents a cow, and the bar represents the mean ± SEM. * indicates $P \leq 0.05$ between pregnant and non-pregnant within an infusion group. Superscripts indicate $P \leq 0.05$ between treatment groups within a pregnancy status.

CHAPTER 4
LIPOPOLYSACCHARIDE ALTERS CEBPβ SIGNALING AND REDUCES ESTRADIOL PRODUCTION IN BOVINE GRANULOSA CELLS

Abstract of Chapter 4

Bacterial infection of the uterus can reduce fertility by reducing dominant follicle growth and decreasing estradiol synthesis. The bacterial component, lipopolysaccharide (LPS), accumulates in the follicular of cows with uterine infection and alters granulosa cell function. In vitro culture of granulosa cells suggests that LPS exposure decreases *CYP19A1* expression and reduces estradiol secretion; however, the mechanisms of how LPS mediates reduced *CYP19A1* expression are unknown. Interestingly, the transcription factor CCAAT/Enhancer-binding protein beta (CEBPβ) has been shown to induce the transcription of LPS regulated cytokines and bind the promoter region of *CYP19A1* in various cell types of humans, rodents, and buffalo. We hypothesized that LPS alters CEBPβ signaling that results in reduced *CYP19A1* expression and decreased estradiol secretion. We studied this potential mechanism using cultured bovine granulosa cells of small/medium and large follicles. Granulosa cells were treated with medium alone or medium containing ultrapure LPS in the presence of FSH and androstenedione. In, granulosa cells of small/medium and large follicles, LPS increased gene expression of inflammatory mediators *CXCL8* and *IL6* and decreased estradiol secretion. However, only granulosa cells of large follicles had reduced expression of *CYP19A1* after exposure of LPS, whereas protein abundance of aromatase was unaffected. Interestingly, LPS increased expression of *CEBPB* and reduced nuclear localization of CEBPβ in granulosa cells from small/medium follicles. In granulosa cells from large follicles, LPS did not alter *CEBPB* gene expression and nuclear localization of CEBPβ. These data suggest follicle size dependent effects of LPS on estradiol

secretion in bovine granulosa cells. Further evaluation of the mechanisms by which CEBPβ influences estradiol secretion in bovine granulosa cells of various follicles sizes is needed and may help to better understand estradiol synthesis and the pathophysiology of uterine infection in cows.

Introduction

Bacteria are ubiquitous in the postpartum uterus of the cow and uterine infection develops in up to 40% of cows within three weeks following calving (Sheldon et al., 2009). Disease caused by uterine infection in the cow is associated with subfertility after the resolution of disease and increases the likelihood of cows leaving the herd (LeBlanc et al., 2002a; Carvalho et al., 2019). Interestingly, the ovary is rarely a site of bacterial infection, but uterine disease causes reduced dominant follicle growth and estradiol production (Sheldon et al., 2002).

After the resolution of uterine disease, granulosa cells exhibit an altered transcriptome compared to healthy cows (Piersanti et al., 2019a; Horlock et al., 2020), suggesting a perturbed intrafollicular environment of cows following uterine infection. Bacterial components, such as lipopolysaccharide (LPS) derived from Gram-negative bacteria cell wall, accumulate in the follicular fluid of cows diagnosed with uterine disease (Herath et al., 2007; Piersanti et al., 2019a). In parallel, granulosa cells express Toll-like receptor 4 (TLR4), the receptor for LPS, which mediates an inflammatory response to bacterial LPS by increasing synthesis of interleukin (IL)-6, IL-1β, IL-8, and tumor necrosis factor alpha (TNFα) (Herath et al., 2007; Williams et al., 2008b; Bromfield and Sheldon, 2011; Shimizu et al., 2012; Price et al., 2013). Additionally, granulosa cells exposed to LPS *in vitro* secrete less estradiol (Herath et al., 2007; Williams et al., 2008b; Price et al., 2013), which is likely due to the concurrent reduction

of aromatase (*CYP19A1*) expression in granulosa cells of small follicles (< 5 mm), medium follicles (4-8 mm) and dominant follicles (> 8 mm) exposed to LPS (Herath et al., 2007; Shimizu et al., 2012; Price et al., 2013; Onnureddy et al., 2015; Li et al., 2017; Yenuganti et al., 2017). However, the molecular mechanisms by which LPS exposure decreases *CYP19A1* expression and subsequently reduces estradiol secretion remain elusive.

Estradiol production is a coordinated process involving both theca and granulosa cells (Fortune, 1986). Steroidogenic acute regulatory protein (STAR) transports cholesterol into the inner mitochondrial matrix of granulosa and theca cells which can then be converted to progesterone (Miller, 2007); however, only theca cells can convert progesterone to androstenedione, which is then utilized by granulosa cells to convert androstenedione to testosterone via 17-beta-hydroxysteroid dehydrogenase (HSD17B1). Granulosa cells can then convert testosterone to estradiol via aromatase (Yoshimoto and Guengerich, 2014). Previous work testing the effects of LPS on steroidogenesis in theca cells is inconclusive (Herath et al., 2007; Magata et al., 2014; Shimizu et al., 2016)

The transcription factor, CCAAT/Enhancer-binding protein beta (CEBPβ) has been shown to promote the transcription of LPS regulated cytokines including IL-6 and TNFα in leukocytes and is known to be modulated by LPS (Stein and Yang, 1995; Greenwel et al., 2000). In addition, CEBPβ has been shown to bind a consensus sequence in the *CYP19A1* promoter of buffalo granulosa cells (Yenuganti et al., 2017) and human endometriosis stromal cells (Yang et al., 2002), and interestingly, CEBPβ knockout results in the upregulation of *CYP19A1* expression in the mouse ovary

(Sterneck et al., 1997). However, there is no consensus if CEBPβ activity increases or decreases *CYP19A1* expression. In bovine granulosa cells, it is unknown if LPS influences the activity of CEBPβ which could then modulate *CYP19A1* expression and results in reduced estradiol secretion.

Here, we endeavored to determine the mechanism by which LPS exposure downregulates granulosa cell *CYP19A1* expression and results in reduced estradiol production in bovine granulosa cells. We hypothesized that LPS stimulates altered CEBPβ signaling to downregulate *CYP19A1* expression, resulting in decreased estradiol secretion. To achieve this objective, we employed *in vitro* culture of bovine granulosa cells from small/medium (2-8 mm) and large (> 8 mm) follicles to determine the role of CEBPβ in LPS mediated changes to *CYP19A1* expression and estradiol production.

Materials and Methods

Bovine ovaries from cattle of undetermined breeds were obtained from a local abattoir (Florida Beef, Inc., Zolfo Springs, FL) and transported to the laboratory for use within six hours of collection. Ovaries were transported at 22°C in saline containing 1% penicillin/streptomycin (Thermo Fisher Scientific; Walton, MA). Upon arrival to the laboratory, ovaries were washed three times in warm (38.5°C) saline.

Granulosa Cell Culture

Between 10 and 15 ovaries were processed together to provide each biological replicate. Cells from small/medium (2 to 8 mm) diameter follicles were collected by slicing the surface of ovaries with a scalpel blade and vigorously rinsing the ovary in collection medium (Minitube; Verona, WI). Resultant collection medium was then filtered using a sterile 100 µm cell strainer (Corning; Corning, NY) to removed cumulus oocyte

complexes and tissue debris. The remaining filtrate was then passed through a sterile 40 µm filter (Thermo Fisher Scientific) to collect granulosa cells. Granulosa cells were retained in the filter and rinsed using complete cell culture medium (Medium 199 (Gibco; Thermo Fisher Scientific), 10% fetal calf serum (FCS; Corning), 1% insulin-transferrin-sodium selenite (ITS; 10 mg/L human recombinant insulin, 5.5 mg/L human recombinant transferrin, 6.7 µg/L selenious acid; Corning), 1% penicillin/streptomycin (50 IU/mL penicillin and 50 µg/mL streptomycin; Thermo Fisher Scientific), and 1% L-glutamine (2 mM L-alanyl-L-glutamine dipeptide in 0.85% NaCl; GlutaMAX; Thermo Fisher Scientific)). The resultant cell suspension was centrifuged at 500 × *g* for 10 min. A red blood cell lysis was performed on the cell pellet by the addition 900 µL of cell culture grade H_2O (Hyclone; Chicago, IL), immediately followed by the addition of 100 µL of sterile 10x PBS. Cells were washed with DPBS without calcium or magnesium (Hyclone) by centrifugation at 500 × *g* for 10 min. The resultant cell pellet was resuspended in 1 mL of complete culture medium containing hyaluronidase (100 U/mL; Millipore Sigma; Burlington, MA) and vortexed for 10 s every 3 min for 10 min. Cells were again washed by centrifugation at 500 × *g* for 10 min in complete cell culture medium. Cell concentration was adjusted to 1.5×10^6 cells/mL and plated (TPP, Trasadingen, Switzerland) in 500 µL (24-well plates for RNA isolation and supernatant) or 2 mL (6-well plates for protein isolation) of complete cell culture medium and cultured at 38.5°C with 5% CO_2 in humidified air.

Cells from large (> 8 mm) diameter follicles were aspirated using a sterile needle and syringe into granulosa cell collection medium (Medium 199 (Gibco; Thermo Fisher Scientific), 0.5% BSA (5 g/L; Thermo Fisher Scientific), 20 mM HEPES (Hyclone), 2 mM

sodium pyruvate (Gibco), 50 ug/mL heparin (Thermo Fisher Scientific), and 1% penicillin/streptomycin (50 IU/mL penicillin and 50 µg/mL streptomycin; Thermo Fisher Scientific)). Following initial aspiration, granulosa cells were treated in the same manner as granulosa cells isolated from small/medium diameter follicles, with the exception of no treatment with hyaluronidase.

For cells from small/medium follicles, non-adherent cells were aspirated after 12 to 14 h of culture, and adherent granulosa cells were washed in warm DPBS and cultured for a further 24 h in complete culture medium. For cells from large follicles, granulosa cells were cultured undisturbed for 48 h to allow for cell adherence. Immediately prior to the application of any treatment, cells were washed in warm DPBS and treatments were applied to cells using complete medium containing phenol red-free Medium 199 (Gibco), 10% charcoal-stripped FCS (Corning), 1% ITS (10 mg/L human recombinant insulin, 5.5 mg/L human recombinant transferrin, 6.7 µg/L selenious acid), 1% penicillin/streptomycin (50 IU/mL penicillin and 50 µg/mL streptomycin), 1% L-glutamine (2 mM L-alanyl-L-glutamine dipeptide in 0.85% NaCl; GlutaMAX), 1 ng/mL follicle stimulating hormone (Folltropin-V; Vetoquinol, Lavaltrie, Canada), and 1 µM androstenedione (Thermo Fisher Scientific).

Dose-Dependent Experiments

To determine the impact of LPS concentration on estradiol production, granulosa cells from small/medium follicles were treated with control medium or with medium containing ultrapure LPS (*E. coli* 0111-B4; tlrl-3pelps, Invivogen, San Diego, CA) in sequential ten-fold increasing concentrations, from 1 to 10^4 ng/mL for 24 h, for a total of five concentrations. Granulosa cells from large follicles were treated with control medium or with medium containing ultrapure LPS at concentrations of 10^3 or 10^4 ng/mL

for 24 h. The experiment was repeated using 10 independent biological replicates (n = 10) for granulosa cells from small/medium follicles and 9-14 independent biological replicates (n = 9-14) for granulosa cells from large follicles. Following treatment, supernatants were collected and stored at -20ºC, and cells were stored in RLT lysis buffer (Qiagen, Hilden, Germany) or PhosphoSafe extraction buffer (Millipore Sigma) with protease inhibitor (Halt Protease Inhibitor Cocktail; Thermo Fisher Scientific) at -80ºC.

Excess Androstenedione Experiment

To determine the impact of androstenedione availability on granulosa cell secretion of estradiol, granulosa cells from small/medium follicles were treated with 0, 1 or 10 µM androstenedione in the presence or absence of 10^3 ng/mL ultrapure LPS for 24 h. This experiment was performed in 6 independent biological replicates (n = 6). Following treatment, supernatants were collected and stored at -20ºC, and cells were stored in RLT lysis buffer or PhosphoSafe extraction buffer with protease inhibitor at -80ºC.

Time-Course Experiments

To assess estradiol production over time, granulosa cells from small/medium follicles were exposed to either medium alone or medium containing 10^4 ng/mL of ultrapure LPS for 0.5, 2, 4, 8, or 12 h. This experiment was repeated using 6 independent biological replicates (n = 6). Following treatment, supernatants were collected and stored at -20ºC, and cells were stored in RLT lysis buffer or PhosphoSafe extraction buffer with protease inhibitor at -80ºC.

RNA Isolation and RT-PCR

Total RNA was isolated from granulosa cells using the RNeasy Mini kit (Qiagen) according to manufacturer's instructions. For verification of cell culture purity, total RNA was isolated from cells at the time of cell isolation prior to plating, at the time of initial treatment (36 or 48 h after initial plating), and 24 h after treatment (60 or 72 h after initial plating). Quality and quantity of RNA was assessed by an ultraviolet-visible spectrophotometer, Nanodrop2000 (Thermo Fisher Scientific). Reverse transcription was performed on 1 µg of RNA using the Verso cDNA synthesis kit (Thermo Fisher Scientific). Primers were designed using the NCBI database and are detailed in Table 4-1. All primers were validated to ensure they met the MIQE guidelines of $r^2 > 0.98$ and efficiency of 90% to 110% (Bustin et al., 2009), and product size was verified by agarose gel electrophoresis and melt curve analysis. Each PCR reaction consisted of 20 µL containing cDNA, iTaq Universal SYBR green master mix (Bio-Rad, Hercules, CA) and 500 nM of each sequence specific primer with exception of *CYP17A1* which included 300 nM primer. A Bio-Rad CFX Connect light cycler was employed with an initial denaturation step at 95°C for 30 s followed by 40 cycles at 95°C for 5 s followed by an annealing and extension at 60°C for 30 s for the two-step protocol. Three genes (*AMH*, *CYP17A1*, *STAR*) required a three-step protocol with an initial denaturation step at 95°C for 30 s followed by 40 cycles at 95°C for 5 s followed by a primer specific annealing temperature for 5 sec (*AMH*, 58°C; *CYP17A1*, 57°C; *STAR*, 54°C) followed by extension at 60°C for 30 sec. A no template negative control, replacing cDNA with water was included for each primer set. Relative expression for each gene of interest were calculated using the $2^{-\Delta Ct}$ method relative to the geometric mean of the reference genes (*ACTB* and *GAPDH*). Standard RT-PCR using Dream Taq Hot Start green PCR

master mix (Thermo Fisher Scientific) was performed to evaluate the presence of hematopoietic immune cells (*PTPRC*) and theca cells (*CYP17A1*) in cell preparations. A thermocycler (MultiGene OptimMax Thermal Cycler, Labnet International; Edison, NJ) was employed to perform RT-PCR using a protocol of 95°C for 2 min, then 30 cycles of 95°C for 30 s, specific annealing temperature for 30 s, and 72°C for 1 min, with a final extension step of 72°C for 10 min. Annealing temperature for *PTPRC* primers was 60°C and annealing temperature for *CYP17A1* was 57°C. Amplification products were visualized after agarose gel electrophoresis using Diamond Nucleic Acid Dye (Promega, Madison, WI) and Gel Doc EZ Gel Documentation System (Bio-Rad).

Protein Extraction and Immunoblotting

Samples were isolated in PhosphoSafe extraction buffer with protease inhibitor before quantifying protein concentration using a bicinchoninic protein assay (Thermo Fisher Scientific). Equal concentrations of protein (10 µg) were loaded into 10% precast polyacrylamide gels (Mini-Protean TGX; Bio-Rad) and subjected to electrophoresis at 100 V for 1 h. Separated proteins were then transferred to nitrocellulose membranes using wet transfer for 4 h at 45 V at 4ºC. Revert 700 total protein stain (Li-cor, Lincoln, NE) was employed to verify equal protein loading using a Li-Cor Odyssey CLx infrared imager (Li-cor). For immunoblotting, membranes were blocked overnight in 5% BSA in TBS with 0.1% Tween (TBS/T, pH 7.6) or 3% milk in TBS/T. Membranes were probed for aromatase (MCA2077S; Bio-Rad), and CEBPβ (NBP1-46179 Novus Biologicals, Littleton, CO). Primary antibodies were diluted in 5% BSA in TBS/T (aromatase) or TBST alone (CEBPβ) and incubated for 6 h at 4ºC with agitation. Membranes were washed three times with agitation for 5 min in TBS/T and incubated with an appropriate secondary antibody (Li-cor) conjugated with infrared dye 680RD or 800CW in blocking

solution for 1 h at room temperature with agitation. Membranes were washed three times for 5 min in TBS/T and visualized on a Li-Cor Odyssey CLx infrared imager. Target protein was normalized to total protein stain (Figure A-6) from the same blot using the western blot function on the Li-cor Odyssey CLx infrared imager. Antibodies are detailed in Table 4-2.

Immunocytochemistry for Nuclear Localization of CEBPβ

Chamber slides (Thermo Fisher Scientific) were used to culture granulosa cells for immunocytochemistry. Slides were preincubated with 100 uL of FCS for 30 min at room temperature prior to addition of granulosa cells. Granulosa cells were plated directly onto slides at a concentration of 2×10^5 cells/mL in complete culture medium. Before application of treatments, granulosa cells isolated from 2-8 mm diameter follicles were cultured for 24 h and granulosa cells isolated from > 8 mm diameter follicles were cultured for 48 h to allow cells to adhere. After pre-incubation in complete culture medium, granulosa cells were washed in DPBS and medium was replaced with serum-free medium overnight prior to application of treatment. Immediately prior to treatment, cells were washed in DPBS and treated with either control medium alone or 10^4 ng/mL of ultrapure LPS for 6 or 24 h. After treatment, cells were fixed in 2% paraformaldehyde for 15 min at room temperature. Cells were washed three times in DPBS and stored at 4°C. Slides were washed in PBS with 0.1% Tween (PBS/T) twice for 5 min each, and permeabilized in PBS containing 0.1% Triton-X for 10 min. Cells were then washed three times in PBS/T and incubated in blocking solution containing 1% normal goat serum and 1% BSA in PBS for 1 h at room temperature. Cells were then incubated in primary antibody (1:500 CEBPβ) overnight with agitation at 4°C before washing three times in PBS/T and incubation in secondary antibody (1:800 anti-rabbit AlexaFlour 488)

for 1 h at room temperature. Cells were washed and mounted using 50% glycerol in PBS containing 1.5 μg/ml Hoechst 33342 (Invitrogen). Slides were imaged using a Zeiss Axio Observer 7 (Zeiss, Jena, Germany) fitted with an Andor DSD2 Confocal Unit and Zyla Plus 4.2-megapixel camera using a Plan-Apochromat 40× objective lens. A minimum of 7 independent fields of view were quantified in granulosa cells of 5 replicate from small/medium follicles (n = 5) and 7 replicates from large follicles (n = 7). A no primary control was included to assess background staining. Nuclear localization of CEBPβ was quantified using ImageJ by splitting the image into individual color channels, converting to a binary image and overlaying nuclear location with CEBPβ labeling and calculating the mean fluorescence intensity of CEBPβ for each nucleus (Schneider et al., 2012).

Quantification of Estradiol Production

Estradiol concentration of cell free supernatants was evaluated using a commercially available enzyme immunoassay (DRG International, Springfield, NJ) according to the manufacturer's instructions. All samples were run in duplicate, and the limit of detection was 10.6 pg/mL. Samples were diluted if needed in standard zero buffer. The intra-assay coefficient of variation ranged from 1.49% to 5.6% depending on the experiment.

Statistical Analysis

All statistical analyses were performed using SPSS v26 (IBM Corporation, Armonk, NY). A general linear model was used to analyze estradiol, gene expression, protein abundance, and fluorescent intensity data. Gene expression data were log transformed for normality. Fixed effects depended on experiment, but replicate was always considered a random effect. For dose-dependent experiments, the fixed effect

was dose and least significant difference pairwise comparisons were analyzed between doses. For time-course experiments and immunocytochemistry, fixed effects included hour, LPS, and the interaction of hour and LPS. For the androstenedione experiment, fixed effects included androstenedione supplementation, LPS, and the interaction of androstenedione and LPS. Least significant difference pairwise comparisons were also analyzed for time-course and androstenedione experiments. Statistical significance was set at $P \leq 0.05$. Graphs were made using GraphPad Prism v9 (San Diego, CA) and depict estimated marginal means ± standard error of the mean unless otherwise stated.

Results

Lipopolysaccharide Increases Expression of Inflammatory Mediators and Decreases Estradiol Secretion in Granulosa Cells from Small/Medium Follicles

The purity of granulosa cell cultures were assessed to determine the presence of contaminating thecal (*CYP17A1*) or CD45+ hematopoietic immune cells (*PTPRC*) (Herath et al., 2007; Richards et al., 2018). Expression of *PTPRC* or *CYP17A1* was not detected in granulosa cells isolated from small/medium follicles, suggesting granulosa cell isolation yielded pure cultures. However, moderate *CYP17A1* expression was observed in granulosa cells after a total of 60 h of culture, suggesting spontaneous luteinization of cultured cells (Fig. A-7A-B).

Granulosa cells from small/medium follicles were exposed to increasing concentrations of ultrapure LPS for 24 h in the presence of 1 ng/mL FSH and 1 μM androstenedione (Fig. 4-1). Exposure of granulosa cells to 10^4 ng/mL of ultrapure LPS increased expression of both *CXCL8* and *IL6* compared to medium alone controls (Fig. 4-1A, B; $P \leq 0.05$). Granulosa cell expression of *CYP19A1* or *HSD17B1* was not affected by exposure to ultrapure LPS for 24 h (Fig. 4-1C, D). In the absence of LPS,

granulosa cells secreted 11.3 ± 2.5 ng/mL of estradiol into culture medium by 24 h. Interestingly, granulosa cell exposure to either 10^3 or 10^4 ng/mL of LPS decreased estradiol secretion compared to medium alone by 29.8% and 47.6%, respectively (Fig. 1E; $P \leq 0.05$). Exposure of granulosa cells to 10^4 ng/mL ultrapure LPS for 24 h did not affect aromatase abundance measured by western blot (Fig. 4-1F). As granulosa cells from small/medium follicles secreted less estradiol in response to LPS, but in the absence of altered *CYP19A1* and *HSD17B1*, the expression of other factors known to contribute to estradiol secretion were evaluated (Fig. 4-2). Expression of *AMH*, *ESR1*, *FSHR*, *LHGHR*, *STAR*, *HDAC1*, or *HDAC10* were all detected in granulosa cells, but were not affected by exposure to LPS for 24 h (Fig. 4-2A-G).

Because 24 h estradiol secretion was decreased after exposure of granulosa cells 10^3 ng/mL of LPS with no observable change to the expression of *CYP19A1, HSD17B1* or aromatase abundance, we evaluated gene expression in granulosa cells exposed to 10^4 ng/mL of LPS for 0.5, 2, 4, 8 and 12 h (Fig. 4-3). Exposure of granulosa cell to LPS increased expression of *CXCL8* by 0.5 h compared to medium alone and remained elevated by 12 h (Fig. 4-3A; $P \leq 0.05$). Expression of granulosa cell *IL6* was increased after 4 h of LPS exposure compared to medium alone and remained elevated by 12 h (Fig. 4-3B; $P \leq 0.05$). Expression of *CYP19A1*, *HSD17B1*, and *STAR* (Fig. 4-3C-E) were not affected by LPS exposure compared to medium alone; however, the expression of *CYP19A1* did increase over time ($P \leq 0.05$). However, LPS did not affect estradiol secretion after 12 h compared to medium alone (Fig. 4-3F). Collectively, granulosa cells of small/medium follicles responded to LPS stimulation by increasing

expression of inflammatory mediators, and reduced estradiol secretion in the absence of altered *CYP19A1* expression or aromatase abundance.

Excess Androstenedione Does Not Ameliorate LPS Mediated Reduced Estradiol Secretion in Granulosa Cells from Small/Medium Follicles

Androstenedione supplementation is required for cultured granulosa cells to synthesize estradiol. As we observed decreased estradiol secretion after exposure to LPS for 24 h with no observable change to expression of *CYP19A1, HSD17B1* or aromatase abundance, we aimed to determine if androstenedione availability contributed to LPS-mediated estradiol decreases in the presence of FSH (Fig. 4-4). In the absence of androstenedione, after 24 h, estradiol secretion of granulosa cells was 0.04 ± 0.03 and 0.08 ± 0.04 ng/mL in the absence or presence of 10^3 ng/mL of ultrapure LPS, respectively. Compared to granulosa cells cultured in the absence of androstenedione, supplementation of culture medium with 1 μM androstenedione increased 24 h estradiol secretion 7.6 ± 1.8 and 6.9 ± 1.9 ng/mL in the absence or presence of ultrapure LPS, respectively (Fig. 4-4A; $P \leq 0.05$). Interestingly, compared to cells supplemented with 1 μM androstenedione, supplementation of culture medium with 100 μM androstenedione reduced 24 h estradiol secretion to 4.6 ± 1.6 and 3.6 ± 1.4 ng/mL in the absence or presence of ultrapure LPS, respectively (Fig. 4-4A**;** $P \leq 0.05$). Regardless of androstenedione supplementation, LPS exposure had no effect on expression of granulosa cell *CYP19A1*, *HSD17B* or *STAR* expression; however, supplementation of culture medium with 1 μM androstenedione, but not 100 μM androstenedione, increased the expression of *CYP19A1* compared to cells cultured in the absence of androstenedione (Fig 4-4C; $P \leq 0.05$). Androstenedione supplementation did not affect *HSD17B1* expression (Fig. 4-4B), while supplementation

with either 1 or 100 μM androstenedione decreased granulosa cell *STAR* expression (Fig. 4-4D; $P \leq 0.05$). These data suggest that androstenedione supplementation is required for estradiol secretion, but excess supplementation does not enhance, and in fact impairs, estradiol secretion.

Lipopolysaccharide Increases Expression of Inflammatory Mediators and Decreases Estradiol Secretion in Granulosa Cells from Large Follicles

To assess the impact of follicle size on the capacity of granulosa cells to respond to LPS, granulosa cells were isolated from large (<8 mm) follicles and exposed to effective doses of ultrapure LPS (10^3 or 10^4 ng/mL) or control medium for 24 h in the presence of 1 ng/mL FSH and 1 μM androstenedione (Fig. 4-5). Granulosa cells of large follicles displayed moderate *PTPRC* after initial isolation, but this expression was negligible 48 h after initial culture and before the application of treatment. The expression of the luteal marker *CYP17A1* was absent at the time of initial isolation, but steadily increased up to 72 h after the end of the treatment period, suggesting spontaneous luteinization similar to granulosa cells from small/medium follicles (Fig. A-7C-D).

Granulosa cells of large follicles increased expression of *CXCL8* and *IL6* after 24 h of exposure to 10^3 and 10^4 ng/mL of ultrapure LPS (Fig. 4-5A, B; $P \leq 0.05$). Expression of granulosa *HSD17B1* was decreased after LPS exposure compared to medium alone (Fig 4-5C; $P \leq 0.05$), while exposure to 10^4 ng/mL LPS reduced *CYP19A1* expression by 44.2% compared to medium alone (Fig 4-5D; $P > 0.05$). In the absence of LPS, granulosa cells 24 h estradiol secretion was 9.5 ± 4.7 ng/mL (Fig. 4-5E). Exposure to 10^4 ng/mL of ultrapure LPS reduced 24 h estradiol secretion by 27.7% compared to medium alone (Fig 4-5E; $P \leq 0.05$). Despite exposure to LPS reducing 24

h estradiol accumulation and *CYP19A1* gene expression in granulosa cells, LPS exposure had no affect aromatase abundance measured by western blot (Fig. 4-5F; $P > 0.05$).

Lipopolysaccharide Alters Transcription Factor CCAAT/Enhancer-Binding Protein Beta in Granulosa Cells

Expression of *CEBPB* was increased in granulosa cells of small/medium follicles exposed to 10^4 ng/mL of LPS for 24 h compared to medium alone (Fig. 4-6A; $P \leq 0.05$), but not in granulosa cells from large follicles (Fig. 4-6C). While CEBPβ protein was detected in granulosa cells of small/medium and large follicles by western blot, exposure to 10^4 ng/mL LPS for 24 h did not alter CEBPβ abundance (Fig. 4-6B, D).

Next the effect of LPS exposure on CEBPβ nuclear localization in granulosa cells was determined using immunocytochemistry. Granulosa cells from small/medium and large follicles were exposed to 10^4 ng/mL of LPS or medium alone for 6 or 24 h in the presence of 1 ng/mL FSH and 1 μM androstenedione. Exposure to LPS or duration of treatment did not affect the number of nuclei evaluated in granulosa cells of small/medium or large follicles (data not shown; $P > 0.05$). In granulosa cells of small/medium follicles CEBPβ nuclear localization was evaluated in 163.8 ± 24.8 cells per replicate (Fig. 4-7). Regardless of the duration of treatment, exposure of granulosa cells of small/medium follicles to LPS decreased nuclear abundance of CEBPβ by 27.3% compared to medium alone (Fig. 4-7M; $P \leq 0.05$). However, there was no difference in nuclear abundance of CEBPβ due to the duration of treatment or the interaction of LPS and duration of treatment (Fig. 4-7M; $P > 0.05$).

In granulosa cells of large follicles, CEBPβ nuclear localization was evaluated in 104.5 ± 77.3 cells per replicate (Fig. 4-8). Regardless of the duration of treatment,

exposure of granulosa cells of large follicles to LPS tended to decrease nuclear abundance of CEBPβ by 37.9% (Fig. 4-8M; $P = 0.09$). However, there was no difference in nuclear abundance of CEBPβ due to the duration of treatment or the interaction of LPS and duration of treatment (Fig. 4-8M; $P > 0.05$). Collectively, these data suggest that the effect of LPS exposure on CEBPβ nuclear localization in granulosa cells is follicle size dependent.

Discussion

Uterine infection-induced subfertility is caused by a myriad of factors and influences processes in organs other than the uterus, including the ovary. Despite the ovary being rarely infected, uterine diseases are associated with reduced dominant follicle growth and estradiol production (Sheldon et al., 2002). Previous work has shown that ovarian follicles from cows with a previous uterine infection have accumulated LPS weeks after the resolution of infection (Herath et al., 2007; Piersanti et al., 2019a). In fact, the transcriptome of granulosa cells is altered months after the initial disease insult (Piersanti et al., 2019a; Horlock et al., 2020). In vitro, granulosa cells mount a response to LPS with increased expression and production of inflammatory mediators such as IL-1β, IL-6, and IL-8 (Bromfield and Sheldon, 2011; Price et al., 2013).

Experiments in vitro have recapitulated what is apparent in vivo, where bovine granulosa cells exposed to LPS downregulate estradiol secretion (Herath et al., 2007; Shimizu et al., 2012; Price et al., 2013). Furthermore, these previous experiments report LPS decreases aromatase gene expression (*CYP19A1*), the final step in estradiol synthesis (Herath et al., 2007; Shimizu et al., 2012; Price et al., 2013). There have been few reports in the literature to delineate a connection between LPS exposure and decreased *CYP19A1* gene expression and estradiol synthesis in granulosa cells. In

buffalo, studies have described histone deacetylases or CEBPβ behaving as regulators of *CYP19A1* expression (Mehta et al., 2015; Yenuganti et al., 2017). More generally, work in rodents, has demonstrated *CEBPB* is critical for fertility, as granulosa cells from whole-body knockout mice cannot undergo luteinization and corpus luteum function fails, rendering female mice infertile (Sterneck et al., 1997). Therefore, we hypothesized that LPS stimulates altered CEBPβ signaling to downregulate *CYP19A1* expression and reduced estradiol secretion in bovine granulosa cells.

Bovine granulosa cells were isolated from small/medium follicles, 2-8 mm in diameter, and from large follicles, > 8 mm in diameter and exposed them to LPS in vitro. Granulosa cells exposed to LPS had increased gene expression of pro-inflammatory cytokines, *IL6* and *CXCL8*, compared to control medium, regardless of follicle size. Exposure of granulosa cells to concentrations of 10^3 ng/mL and 10^4 ng/mL LPS for 24 hours, decreased estradiol secretion in granulosa cells from small/medium follicles, while only 10^4 ng/mL of LPS reduced estradiol secretion in granulosa cells from large follicles. Interestingly, *CYP19A1* gene expression was reduced in granulosa cells from large follicles following exposure 10^4 ng/mL LPS for 24 hours, but not in granulosa cells from small/medium follicles. Aromatase protein abundance did not differ in granulosa cells after treatment with LPS, regardless of follicle size. In parallel, gene expression of *CEBPB* was increased after LPS exposure in granulosa cells from small/medium follicle but unchanged in granulosa cells from large follicles. Total protein abundance of CEBPβ in granulosa cells was not different due to LPS treatment from any size follicle, however, exposure to LPS reduced nuclear translocation of CEBPβ compared to control cells.

Granulosa cells begin expressing *CYP19A1* transcripts after recruitment (4 mm) and continue to increase aromatase expression and estradiol production until reaching a large preovulatory follicle (Xu et al., 1995). In response to a surge of luteinizing hormone, *CYP19A1* expression rapidly decreases in large preovulatory follicles in vivo (Richards, 1994; Komar et al., 2001). Previous work found a reduction in estradiol secretion from granulosa cells exposed to LPS at similar doses used here from small (< 5 mm), medium (4-8 mm) and large (>8 mm) follicles (Herath et al., 2007; Shimizu et al., 2012; Price et al., 2013). Similarly, in response to LPS, *CYP19A1* gene expression was reduced in granulosa cells from large follicles but not from small or medium follicles (Herath et al., 2007). Therefore, the developmental stage, as indicated by the size of follicle, that granulosa cells originate from can influence the response to LPS.

The transcription factor CEBPβ is involved in many cellular processes including the inflammatory response and fertility (Sterneck et al., 1997; Poli, 1998). Production of CEBPβ can be induced by cytokines such as IL-6 or TNFα (Akira et al., 1990; Greenwel et al., 2000). Furthermore, inflammatory mediators, including IL-6, IL-8, and TNFα, have consensus sequences for CEBPβ in their regulatory regions (Matsusaka et al., 1993; Stein and Yang, 1995; Wedel et al., 1996), suggesting these molecules are regulated by feedback loops.

While the transcription factor, CEBPβ, is imperative for fertility, there are differences in CEBPβ regulation in granulosa cells between species. In mice and rats, luteinizing hormone (mimicked experimentally using human chorionic gonadotropin; hCG) induces *CEBPB* expression in granulosa cells from antral follicles (Sirois and Richards, 1993), while in bovine granulosa cells from large follicles (8-12 mm) CEBPβ

abundance decreases following exposure to hCG (Liu et al., 1999). Following hCG treatment, aromatase expression remains elevated in female mice that lack *CEBPB* (Sterneck et al., 1997), thus indicating a potential relationship between CEBPβ and aromatase expression.

Aromatase expression is regulated by various promoters depending on tissue type, with proximal promoter II being the primary regulator of *CYP19A1* expression in granulosa cells of mice, humans, and cows (Means et al., 1991; Fürbass et al., 1997; Golovine et al., 2003). However, in bovine granulosa cells, promoter I.1 appears to contribute to *CYP19A1* expression (Fürbass et al., 1997; Lenz et al., 2004). There is strong sequence similarity (80%) between humans and cows for promoter II but not for promoter I.1 (< 50%). Interestingly, the bovine promoter I.1 contains two consensus sequences for CEBPβ and four CAAT transcription elements which are predicted to act as binding sites for CEBPβ, while promoter II contains three CAAT elements (Fürbass et al., 1997). Reports of the regulatory role of CEBPβ on promoter II of *CYP19A1* are contradictory. In human adipose fibroblasts, binding of CEBPβ to promoter II stimulates *CYP19A1* gene expression (Zhou et al., 2001). Similarly, in benign uterine tumors (leiomyomas), CEBPβ binds to *CYP19A1* promoter I.3/II sites and *CEBPB* knockdown in vitro decreases aromatase expression, demonstrating CEBPβ enhances aromatase gene expression and activity (Ishikawa et al., 2008). In contrast, overexpression of *CEBPB* in endometrial stromal cells drastically reduces *CYP19A1* promoter II activity (Yang et al., 2002). There does not appear to be a conserved CEBPβ mediated regulation of *CYP19A1* across cell types and species. Therefore, the relationship between a CEBPβ and *CYP19A1* expression in bovine granulosa cells is unclear.

In buffalo granulosa cells, there is a binding site for CEBPβ in the proximal promoter II of the *CYP19A1* gene, and treatment of granulosa cells from small/medium follicles with LPS increases CEBPβ binding to promoter II along with a concurrent reduction in *CYP19A1* expression and estradiol production (Yenuganti et al., 2017). Present data show that exposure to LPS for 24 hours decreases estradiol secretion, increases *CEBPB* gene expression, reduced CEBPβ nuclear localization, but does not change *CYP19A1* expression in granulosa cells from small/medium follicles. In contrast to our results, work in buffalo demonstrated exposure to LPS for 24 hours increased total protein abundance and nuclear localization of CEBPβ in granulosa cells from small/medium follicles (Yenuganti et al., 2017). However, here LPS exposure to granulosa cells from large follicles, did not alter gene expression or protein abundance of CEBPβ, but did decrease nuclear localization, while reducing *CYP19A1* expression and estradiol secretion. Although both cows and buffalo are part of the Bovidae family, there may be differences in CEBPβ activity in response to LPS.

The intracellular signaling cascade initiated when LPS binds to Toll-like receptor 4 on the granulosa cells employs a host of molecules that could additionally play a regulatory role in estradiol secretion. Previous research has shown LPS and IL-6 can upregulate transcription of *CEBPB* and CEBPβ regulates expression of inflammatory mediators such as IL-6 and TNFα, (Akira et al., 1990; Stein and Wang, 1995; Wedel et al., 1996; Liu et al., 2009; Yenuganti et al., 2017). Another example is the mice lacking *CEBPA* and *CEBPB* in their granulosa cells have seemingly normal downregulation of *CYP19A1* following the preovulatory LH surge, however mice lacking *ERK1/2* in their granulosa cells have erroneous *CYP19A1* downregulation following the preovulatory LH

surge (Fan et al., 2009, 2011). Perhaps, there are intermediary molecules, such as ERK1/2, which is downstream of TLR4 in the signaling cascade, that play a key role in *CYP19A1* regulation. Therefore, caution must be taken to interpret associations instead of causations within the present data.

In summary, we successfully cultured granulosa cells from both small/medium and large follicles in vitro. When these granulosa cells were treated with LPS, there was an increase in the inflammatory response, and decrease in estradiol secretion; however, there was no change in abundance of aromatase protein in granulosa cells exposed to LPS regardless of follicle size. Interestingly, the effects of LPS on *CEBPB* expression and CEBPβ nuclear translocation appear to be dependent on the developmental stage of follicle from which granulosa cells are isolated, suggesting stage specific mechanisms of estradiol regulation.

Further studies are warranted to determine the specific mechanisms by which CEBPβ may alter LPS mediated estradiol secretion in bovine granulosa cells. The use of siRNA technology to knock down *CEBPB* in granulosa cells would allow us to determine if it is involved in *CYP19A1* regulation and estradiol production. Additionally, the use of chromatin immunoprecipitation (ChIP) sequencing would determine the genes CEBPβ is regulating in response to LPS, as CEBPβ can be involved in many cellular processes. We cannot definitively conclude CEBPβ directly regulates a reduction in estradiol secretion in granulosa cells in response to LPS, however the data suggest CEBPβ signaling is altered in granulosa cells after LPS exposure that warrants further investigation.

Acknowledgements of Chapter 4

The authors would like to thank Eddie Cummings for driving long hours and collecting ovaries from the slaughterhouse and the graduate students from Dr. Peter Hansen's laboratory for the granulosa cells after collecting oocytes for their experiments.

Table 4-1. Primer sequences used for real time RT-PCR.

Gene	Primer Sequence	Accession number
AMH	5’ - GTGGTGCTGCTGCTAAAGATG	NM_173890.1
	3’ - TCGGACAGGCTGATGAGGAG	
ACTB	5’ - CAGAAGCACTCGTACGTGGG	NM_173979.3
	3’ - TTGGCCTTAGGGTTCAGGG	
CEBPB	5’ - ACAGCGACGAGTACAAGATCC	NM_176788.1
	3’ - GACAGTTGCTCCACCTTCTTCT	
CXCL8	5’ - GCAGGTATTTGTGAAGAGAGCTG	NM_173925.2
	3’ - CACAGAACATGAGGCACTGAA	
CYP17A1	5’ - CTCCAGCATTGGCGACCTTA	XM_024985958.1
	3’ - GAAGCGCTCGGGCATGAA	
CYP19A1	5’ - CGCAAAGCCTTAGAGGATGA	NM_174305.1
	3’ - ACCATGGCGATGTACTTTCC	
FSHR	5’ - GCAGTCGAACTGAGGTTTGTT	NM_174061.1
	3’ - TTGGAGAACACGTTTGCCTCT	
GAPDH	5’ - AGGTCGGAGTGAACGGATTC	NM_001034034.2
	3’ - ATGGCGACGATGTCCACTTT	
HDAC1	5’ - TTACGACGGGGATGTTGGAA	NM_001075460.1
	3’ - GGCTTTGTGAGGGCGATAGA	
HDAC10	5’ - CTCGGCTTCACTGTCAACCT	NM_001037444.2
	3’ - TCAGGGTCGAACTCAAAGGC	

Table 4-1. Continued

Gene	Primer Sequence	Accession number
HSD17B1	5’ - CGTGAGGGATGCAGATTCCA	NM_001102365.1
	3’ - GTTACACACCAGCACGTCCA	
IL6	5’ - ATGACTTCTGCTTTCCCTACCC	NM_173923.2
	3’ - GCTGCTTTCACACTCATCATTC	
LHCGR	5’- TGCCTTTGACAACCTCCTCAAT	NM_174381.1
	3’ - GATGCTTAGGTATTTTAACCGAGG	
PTPRC	5’- CTCGATGTTAAGCGAGAGGAAT	NM_001206523.1
	3’ - TCTTCATCTTCCACGCAGTCTA	
STAR	5’ - AGAAGGGTGTCATCAGAGCG	NM_174189.3
	3’ - TGGTCCTTGAGGGACTTCCA	

Table 4-2. Details of antibodies for immunodetection.

Protein	Size (kDa)	Product details (Catalog number, company)	Dilution	Species
Aromatase	55	MCA2077S; Bio-Rad, Hercules, CA	1:250	Mouse monoclonal
CEBPβ	38	NBP1-46179; Novus Biologicals, Littleton, CO	1:500 (ICC) 1:1000 (WB)	Rabbit polyclonal
Donkey anti-Mouse IgG	.	IRDye 680 RD anti-Mouse IgG (H+L), highly cross-adsorbed; 926-68072, Li-cor; Lincoln, NE	1:5000	Donkey polyclonal
Goat anti-Rabbit IgG	.	IRDye 800 CW anti-Rabbit IgG (H+L), highly cross-adsorbed; 926-32211, Li-cor; Lincoln, NE	1:5000	Goat polyclonal
Goat anti-Rabbit IgG	.	Goat anti-Rabbit IgG (H+L) Cross-Adsorbed Secondary Antibody Alexa Fluor 488 (Invitrogen)	1:800	Goat polyclonal

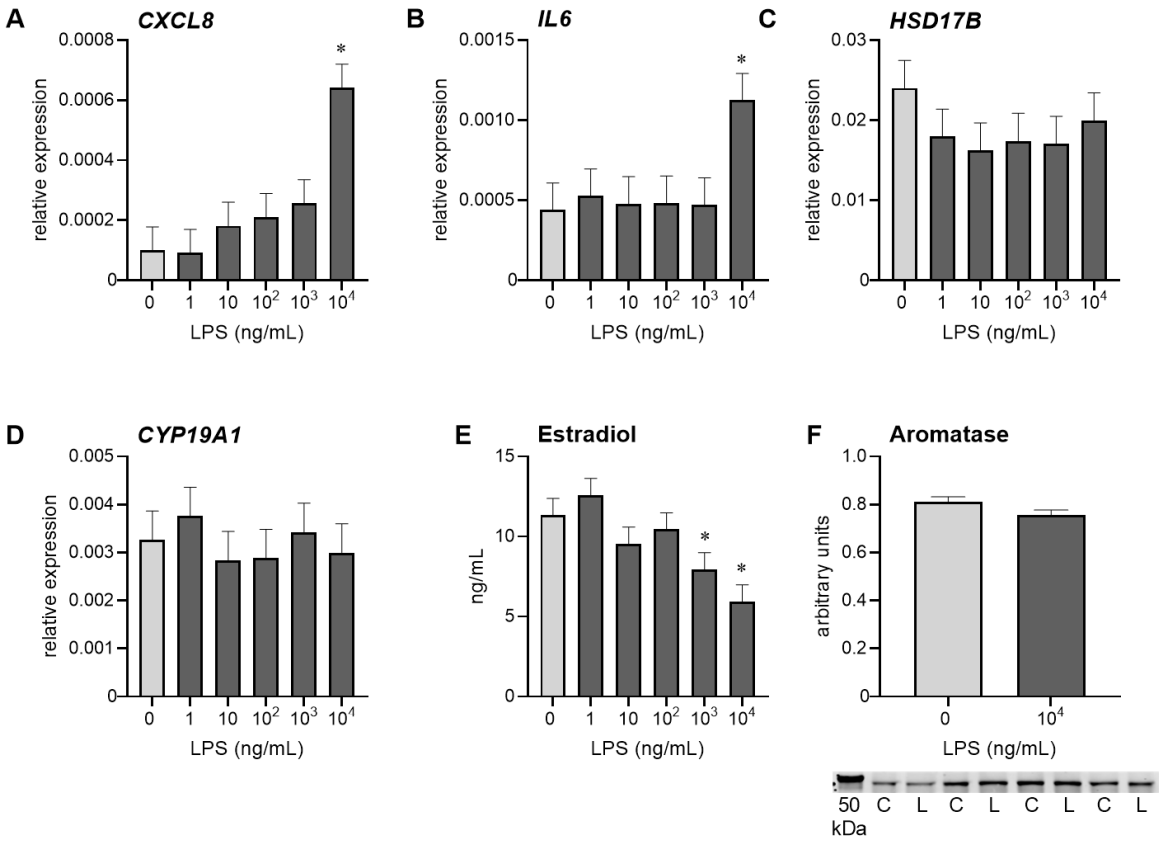

Figure 4-1. Lipopolysaccharide increases expression of inflammatory mediators and decreases estradiol secretion in granulosa cells from small/medium follicles. Bovine granulosa cells from small/medium diameter (2-8 mm) follicles were exposed to ultrapure LPS (1 to 10^4 ng/mL) for 24 h and gene expression for *CXCL8* (A), *IL6* (B), *HSD17B* (C) and *CYP19A1* (D) were quantified by PCR (n = 10), secretion of 17β-estradiol (E) was quantified using an ELISA (n = 10), and abundance of aromatase (F) was evaluated by western blot (n = 4; C represents control samples, L represents samples exposed to LPS). Gene expression data were log transformed for normality and a general linear model with fixed effect of dose and random effect of replicate followed by least significant difference pairwise comparisons were used to analyze each dose compared to the medium alone control. * indicates $P \leq 0.05$ compared to medium alone control. Blot of total protein is available in Fig. A-6A.

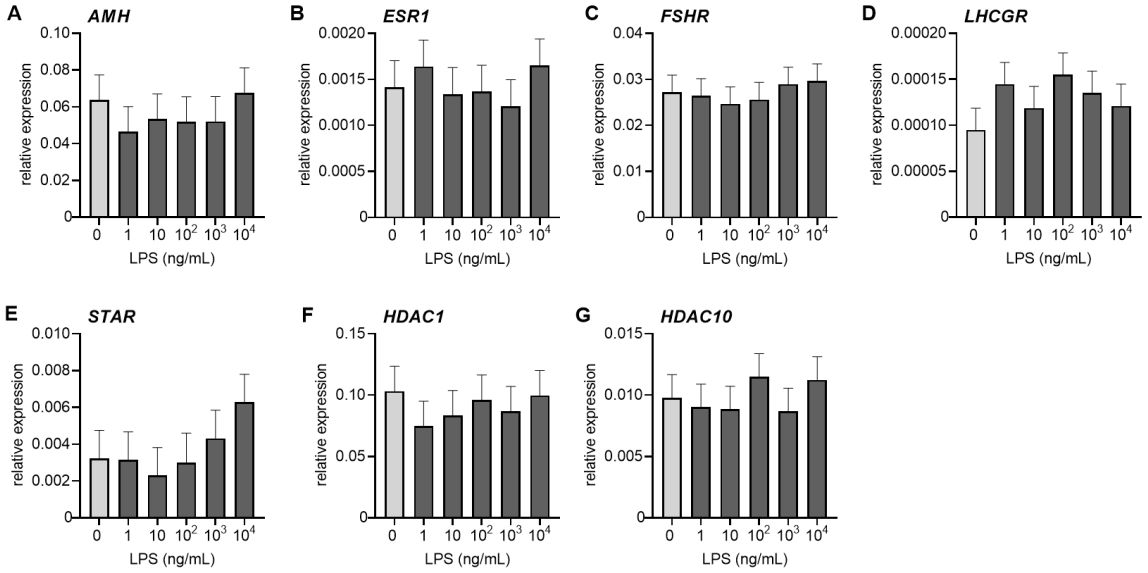

Figure 4-2. Effect of LPS exposure on expression of factors known to contribute to estradiol secretion in granulosa cells from small/medium follicles. Bovine granulosa cells from small/medium diameter (2-8 mm) follicles were exposed to ultrapure LPS (1 to 10^4 ng/mL) for 24 h and gene expression for *AMH* (A), *ESR1* (B), *FSHR* (C) and *LHCGR* (D), STAR (E), *HDAC1* (F), and *HDAC10* (G) were quantified by PCR (n = 10). Data were log transformed for normality and a general linear model with fixed effect of dose and random effect of replicate followed by least significant difference pairwise comparisons were used to analyze each dose compared to the medium alone control.

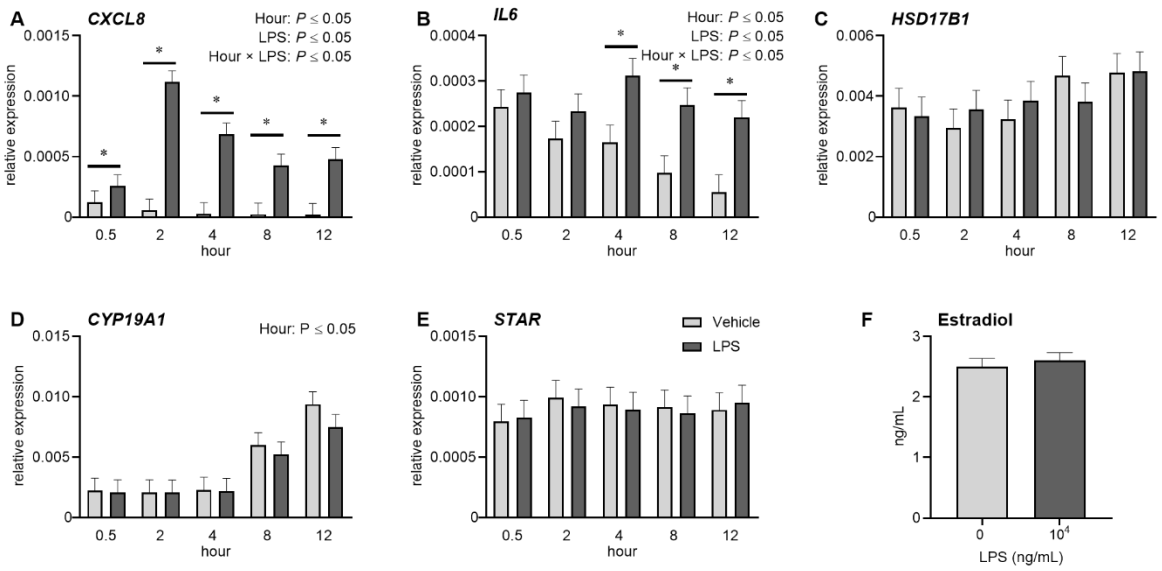

Figure 4-3. Effect of acute LPS exposure on expression of inflammatory mediators and estradiol secretion in granulosa cells from small/medium follicles. Bovine granulosa cells from small/medium diameter (2-8 mm) follicles were exposed to 10^4 ng/mL of ultrapure LPS for 0.5, 2, 4, 8, and 12 h and gene expression for *CXCL8* (A), *IL6* (B), *HSD17B* (C), *CYP19A1* (D) and *STAR* (E) were quantified by PCR (n = 6). Secretion of 12 h 17β-estradiol (F) was quantified using an ELISA (n = 6). Gene expression data were transformed and data were analyzed using a general linear model with replicate as a random effect and the fixed effects of LPS, hour, and the interaction of LPS and hour. Statistical significance for each test are listed for each individual graph and * indicates $P \leq 0.05$ compared to medium alone at a specific timepoint.

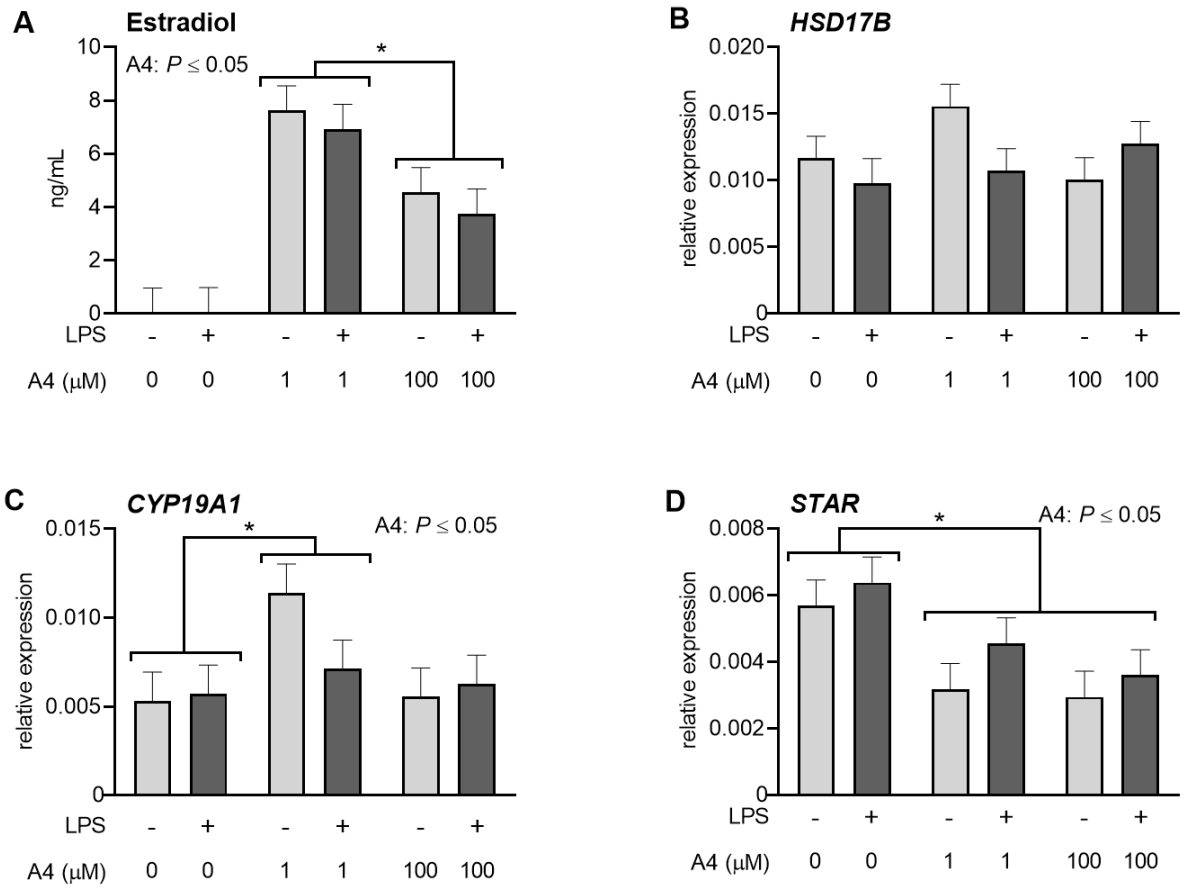

Figure 4-4. Excess androstenedione does not ameliorate LPS mediated estradiol secretion in granulosa cells from small/medium follicles. Bovine granulosa cells from small/medium diameter (2-8 mm) follicles were exposed to 10^4 ng/mL of ultrapure LPS for 24 h supplemented with 0, 1 or 100 μM androstenedione (A_4). Secretion of 17β-estradiol (A) was quantified using an ELISA and gene expression for *HSD17B* (B), *CYP19A1* (C) and *STAR* (D) were quantified by PCR (n = 6). Data were analyzed using a general linear model with replicate as a random effect and the main effects of LPS, androstenedione, and the interaction of LPS and androstenedione. Statistical significance for each test are listed for each individual graph and * indicates $P \leq 0.05$.

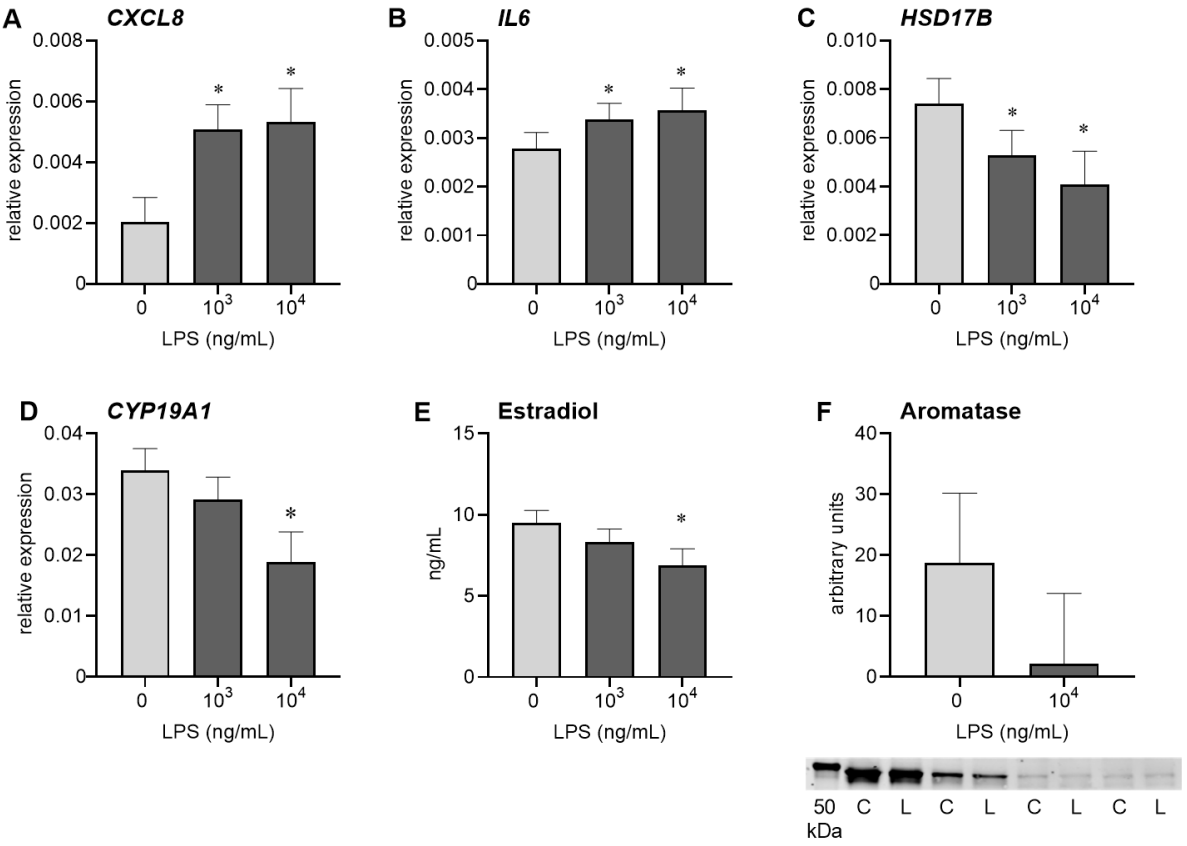

Figure 4-5. Lipopolysaccharide increases expression of inflammatory mediators and decreases estradiol secretion in granulosa cells from large follicles. Bovine granulosa cells from large (> 8 mm) follicles were exposed to ultrapure LPS (10^3 or 10^4 ng/mL) for 24 h and gene expression for *CXCL8* (A), *IL6* (B), *HSD17B* (C) and *CYP19A1* (D) were quantified by PCR (*n* = 9-14), secretion of 17β-estradiol (E) was quantified using an ELISA (*n* = 9-14), and abundance of aromatase (F) was evaluated by western blot (*n* = 4; C represents control samples, L represents samples exposed to LPS). Gene expression data were log transformed for normality and a general linear model with fixed effect of dose and random effect of replicate followed by least significant difference pairwise comparisons were used to analyze each dose compared to medium alone control. Statistical significance is depicted by * and indicates $P \leq 0.05$ compared to medium alone control. The blot of total protein is available in Fig. A-6B.

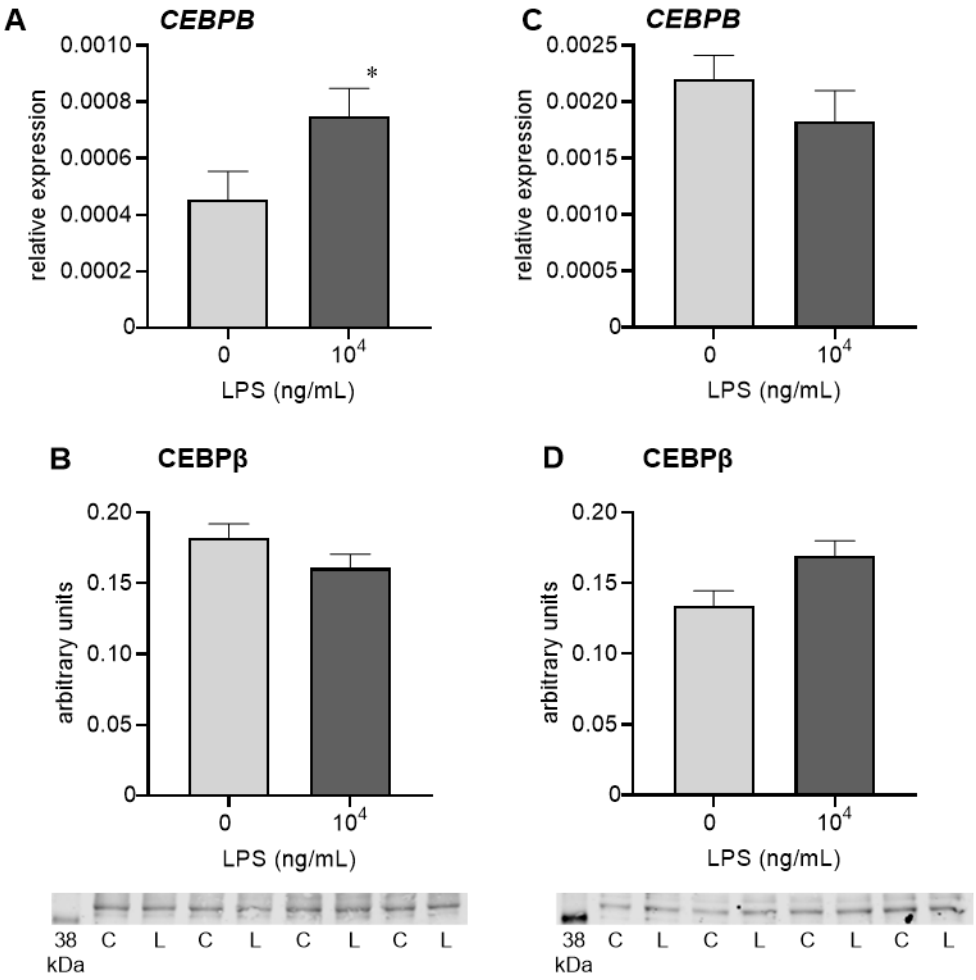

Figure 4-6. Gene expression and protein abundance of CCAAT/Enhancer-binding protein beta in granulosa cells exposed to LPS. Bovine granulosa cells from small/medium (A-B) follicles or large (C-D) follicles were exposed to ultrapure LPS (10^4 ng/mL) for 24 h and gene expression for *CEBPB* (A, C) was quantified by PCR (n = 6-9), and abundance of CEBPβ (B-D) was evaluated by Western blot (n = 4; C represents control samples, L represents samples exposed to LPS). Gene expression data were log transformed for normality and a general linear model with fixed effect of dose and random effect of replicate followed by least significant difference pairwise comparisons were used to analyze each dose compared to medium alone control. * indicates $P \leq 0.05$ compared to medium alone control. The blots of total protein are available in Fig. A-6C-D.

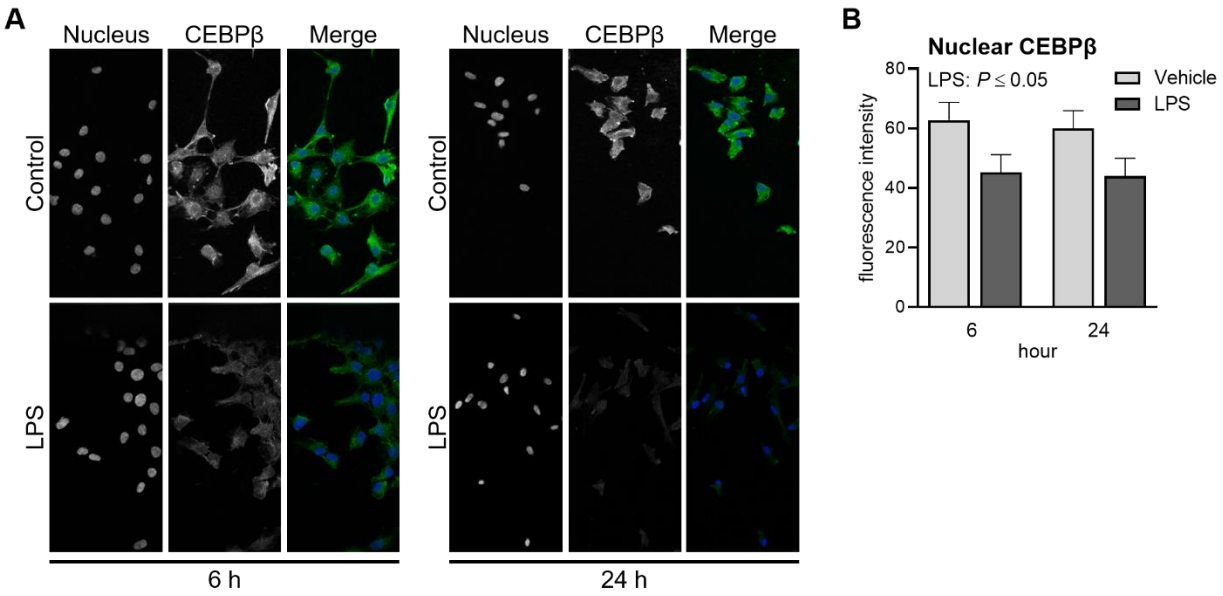

Figure 4-7. Lipopolysaccharide reduces CEBPβ nuclear translocation in granulosa cells from small/medium follicles. Bovine granulosa cells from small/medium diameter (2-8 mm) follicles were exposed to 10^4 ng/mL of ultrapure LPS for 6 or 24 h and nuclear localization of CEBPβ was assessed using immunocytochemistry (*n* = 5). (A) Representative images show individual nuclear and CEBPβ staining and a merge image showing nuclear (blue) and CEBPβ staining (green). (B) Nuclear translocation of CEBPβ was quantified using ImageJ. Data were analyzed using a general linear model with replicate as a random effect and the main effects of LPS.

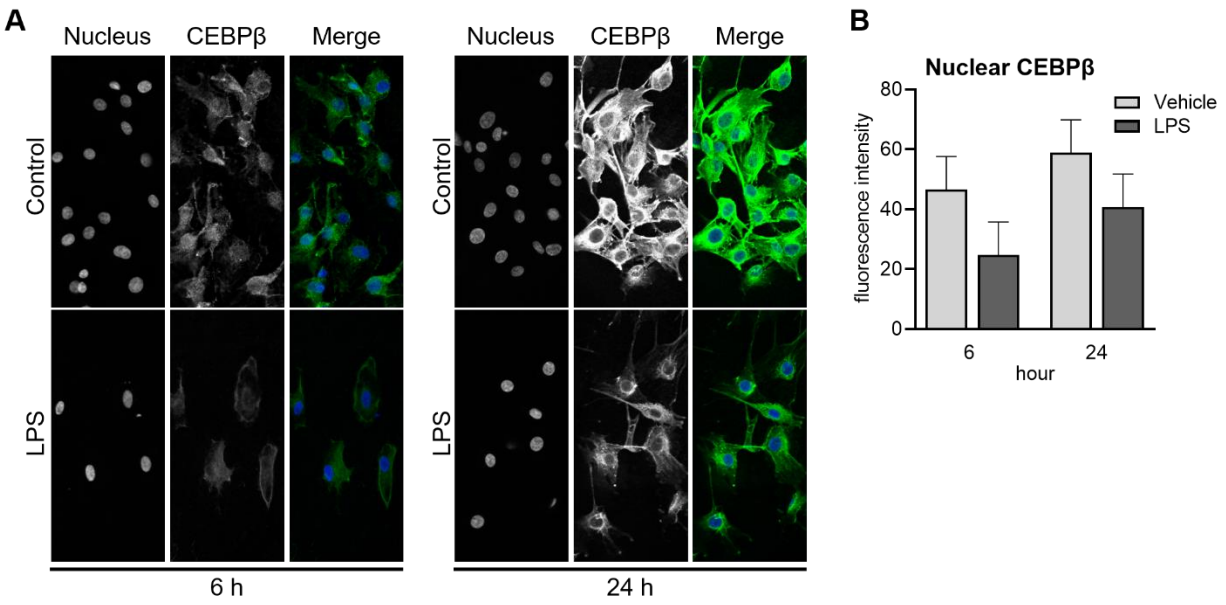

Figure 4-8. Lipopolysaccharide does not alter nuclear translocation of CEBPβ in granulosa cells from large follicles. Bovine granulosa cells from large diameter (> 8 mm) follicles were exposed to 10^4 ng/mL of ultrapure LPS for 6 or 24 h and nuclear localization of CEBPβ was assessed using immunocytochemistry (*n* = 7). (A) Representative images show individual nuclear and CEBPβ staining and a merge image showing nuclear (blue) and CEBPβ staining (green). (B) Nuclear translocation of CEBPβ was quantified using ImageJ. Data were analyzed using a general linear model with replicate as a random effect and the main effects of LPS.

CHAPTER 5
OVERALL DISCUSSION AND CONCLUSIONS

Approximately 90% of postpartum dairy cows have bacteria in the upper reproductive tract and nearly 40% of cows develop a uterine disease after calving (Elliott et al., 1968; Griffin et al., 1974; Sheldon et al., 2002). A substantial problem associated with uterine disease is that detrimental effects occur not only during active infection, but reproductive efficiency can be impaired long after the resolution of disease. Cows diagnosed with a uterine disease have altered ovarian function, decreased conception rates, and a higher incidence of abortion (Borsberry and Dobson, 1989; Ribeiro et al., 2016a). Even after resolution of clinical symptoms, infertility is often evident and reproductive failure is one of the major reasons for culling cows from dairy farms (Norman et al., 2009).

Large scale studies have associated uterine disease with a variety of atypical reproductive functions, such as slower dominant follicle growth, reduced estradiol production, decreased conception rates, and more frequent pregnancy loss (Sheldon et al., 2002; Ribeiro et al., 2016a; Edelhoff et al., 2020). Uterine infection leads to long-term alterations in the transcriptome of oocytes, granulosa cells, and the endometrium months after resolution of disease (Piersanti et al., 2019a, 2020; Horlock et al., 2020). While the exact mechanisms of how uterine disease causes long-term infertility are still obscure, previous work has suggested uterine disease alters the function of the ovary, possibly detrimental effects on the oocyte and surrounding granulosa cells, and the endometrium, potentially inhibiting the pregnancy establishment and maintenance. In vitro, oocytes exposed to the bacterial component, lipopolysaccharide (LPS), have increased rates of meiotic failure and are less likely to develop to an embryo (Soto et

al., 2003; Price et al., 2013). Furthermore, LPS decreases expression of *CYP19A1*, the final enzyme responsible for estradiol production, in granulosa cells (Herath et al., 2007; Price et al., 2013). While it is clear uterine infection has a wide range of effects on reproductive function, the knowledge of specific molecular pathways contributing to infection induced infertility are scant.

The overall objective of the studies reported in this dissertation was to ascertain mechanisms responsible for infection-induced infertility apparent after the resolution of uterine disease in dairy cattle. Specifically, I hypothesized that induced uterine infection reduces the competence of oocytes to develop into embryos independent of a perturbed uterine environment (chapter 2), and that uterine infection alters the endometrial transcriptome of cows that fail to become pregnant (chapter 3). Additionally, to better understand the mechanism by which uterine infection decreases estradiol production, I hypothesized that LPS stimulates altered CCAAT/enhancer-binding protein beta (CEBPβ) signaling which contributes to downregulation of *CYP19A1*, and subsequent estradiol production (chapter 4).

To investigate the initial hypotheses, uterine infection was experimentally induced in non-lactating cows using an intrauterine infusion of pathogenic bacteria previously isolated from cows with uterine disease or vehicle medium as controls. This uterine disease-induction model allowed for to study the direct impacts of a bacterial uterine infection on oocyte competence and the endometrial transcriptome independent of confounding variables, such as lactation, energy balance, or other diseases. To assess the long-term impact of uterine infection on oocyte quality, I collected oocytes for in vitro fertilization and embryo culture from the same cows at multiple timepoints after

infusion of bacteria. Bacteria infusion did not impact the number of oocytes collected or the fertilization rate in vitro compared to vehicle infused cows. Overall, putative zygotes from bacteria infused cows were less likely to develop to morulae compared to vehicle infused cows (Chapter 2). The data demonstrate that the observed reduction in conception rates due to uterine disease (Ribeiro et al., 2016a) is in part attributed to a reduction in oocyte competence.

The uterine disease-induction model allowed to assess oocyte quality over time, to understand if the developmental stage of the follicle present during infection altered the severity of impact on oocyte competence. In cows, follicle development takes between 120 to 200 days with approximately 42 days between antrum formation and ovulation (Lussier et al., 1987). In our experiment, all oocytes collected for in vitro fertilization were collected at the small antral follicle stage, approximately 20 days prior to potential ovulation. Aligning this knowledge with the oocyte collection timepoints in relation to induction of uterine infection, I found the largest reduction of oocyte competence at 24 days after bacteria infusion. Oocytes collected 24 days post infusion were likely to be at the secondary stage of follicle development during active disease. Oocytes collected at later timepoints after bacteria infusion were numerically less likely to develop into embryos, but the decrease was not as significant. Therefore, the data implies that oocytes in the secondary stage of follicle development could be more susceptible to damage from a uterine infection compared to follicles at earlier developmental stages during active infection.

Embryo transfer to cows with a previous case of uterine disease, which would circumvent any potentially damaged oocytes, does not rescue uterine infection-induced

infertility (Estrada-Cortés et al., 2019; Edelhoff et al., 2020), suggesting that the endometrium itself must harbor some long-term alterations due to previous disease. Using RNA sequencing, endometrial samples from cows previously infused with bacteria that were non-pregnant or pregnant following artificial insemination were analyzed. There was downregulation of genes in the non-pregnant endometrium mostly associated to interferon signaling, in alignment with a lack of interferon tau due to absence of a conceptus. To better understand potential differences in the endometrium of cows that failed to become pregnant following uterine infection, results were compared to previously published studies analyzing the difference between endometrial transcriptome of healthy cycling non-pregnant cows and healthy pregnant cows (Bauersachs et al., 2012; Cerri et al., 2012; Forde et al., 2012). A set of conserved genes that were consistently down-regulated in the endometrium of non-pregnant cows regardless of previous infection was identified, suggesting robust pregnancy-associated changes in the endometrium. Interestingly, there was a set of unique genes and altered pathways in the endometrium of non-pregnant cows previously infused with bacteria that were not in the endometrium of healthy non-pregnant cows. Of note, pathways involved in immune function were altered such as IL-7 signaling, TLR signaling, and iNOS signaling. Establishment of pregnancy requires a balance of pro- and anti-inflammatory processes that if dysregulated may be detrimental to pregnancy success (Mor et al., 2011). In fact, women with recurrent miscarriages or endometriosis have dysregulated iNOS production and endometrial *IL7* expression compared to healthy women (Osborn et al., 2002; Wu et al., 2016). Potentially there is a carryover effect from previous uterine infection and exacerbated inflammation that could influence

endometrial immune cell populations and signaling which hinders the establishment of pregnancy in cows with a previous uterine infection. Identifying pathways that are altered in the endometrium of non-pregnant cows infused with bacteria compared to non-pregnant healthy cows indicates that these pathways were perturbed by uterine infection and could contribute to pregnancy failure and infertility.

Previous work has found that cows with uterine disease have slower growth of the dominant follicle and reduced estradiol production (Sheldon et al., 2002). Interestingly, the bacterial component LPS, accumulates in follicular fluid of cows with uterine disease (Herath et al., 2007; Piersanti et al., 2019a). Using primary granulosa cell culture, I found that granulosa cells from small/medium and large follicles exposed to LPS mount an inflammatory response and increase expression of *IL6* and *IL8* as well as decrease estradiol secretion, which is in agreeance with previous studies (Herath et al., 2007; Bromfield and Sheldon, 2011; Price et al., 2013). I was also able to recapitulate what others have found in previous studies, where granulosa cells from large but not small/medium follicles reduced *CYP19A1* expression in response to LPS. Work in mice has demonstrated that the transcription factor CEBPβ is critical for fertility, as CEBPβ knockout mice are infertile due to failure of granulosa cells to luteinize (Sterneck et al., 1997). However other work has shown CEBPβ enhances *CYP19A1* expression and increases estradiol production (Ishikawa et al., 2008). Recent work in buffalo granulosa cells demonstrated that CEBPβ binds to the *CYP19A1* promoter and downregulates estradiol production (Yenuganti et al., 2017). In contrast, results from the experiment herein found LPS does not change total protein abundance of CEBPβ but does decrease nuclear localization in granulosa cells from small/medium follicles.

Although it cannot be concluded that CEBPβ directly regulates *CYP19A1* expression in bovine granulosa cells, exposure to LPS alters CEBPβ signaling in cells that reduce estradiol production. Future studies utilizing siRNA to knockdown *CEBPB* or chromatin immunoprecipitation sequencing would determine the role of CEBPβ in *CYP19A1* expression, and LPS mediated reductions in estradiol secretion.

In summary, I provided experimental evidence that intrauterine infusion of pathogenic bacteria alters oocyte competence and leaves a lasting impact on the endometrium. Uterine infection reduces oocyte competence even after disease resolution, with the severity of detrimental impact possibly dependent on the stage of follicular development present during infection. I found the endometrial transcriptome of non-pregnant cows following infusion of pathogenic bacteria is altered compared to the endometrium of non-pregnant healthy cows, specifically pathways related to immune function, demonstrating uterine infections leave a lasting impact on the endometrium and could contribute to pregnancy failure. Finally, exposing granulosa cells to LPS in vitro has allowed me to identify CEBPβ as a potential regulator of *CYP19A1* expression, which opens the door to potential targets to rescue estradiol production in cows with uterine disease.

Studies in this dissertation demonstrate the benefits of multiple models to determine the detrimental effects of uterine disease, from impact of LPS on granulosa cell function, to reduced oocyte competence due to intrauterine infusion of pathogenic bacteria, and long-term impacts of bacterial infusion on the endometrium in cows that fail to become pregnant. This comprehensive approach has allowed us to identify mechanistic responses to infection in oocytes, granulosa cells, and the endometrium.

Collectively, these findings provide critical evidence for future research to continue disentangling uterine infection induced infertility in dairy cows.

APPENDIX
SUPPLEMENTAL FIGURES AND TABLES

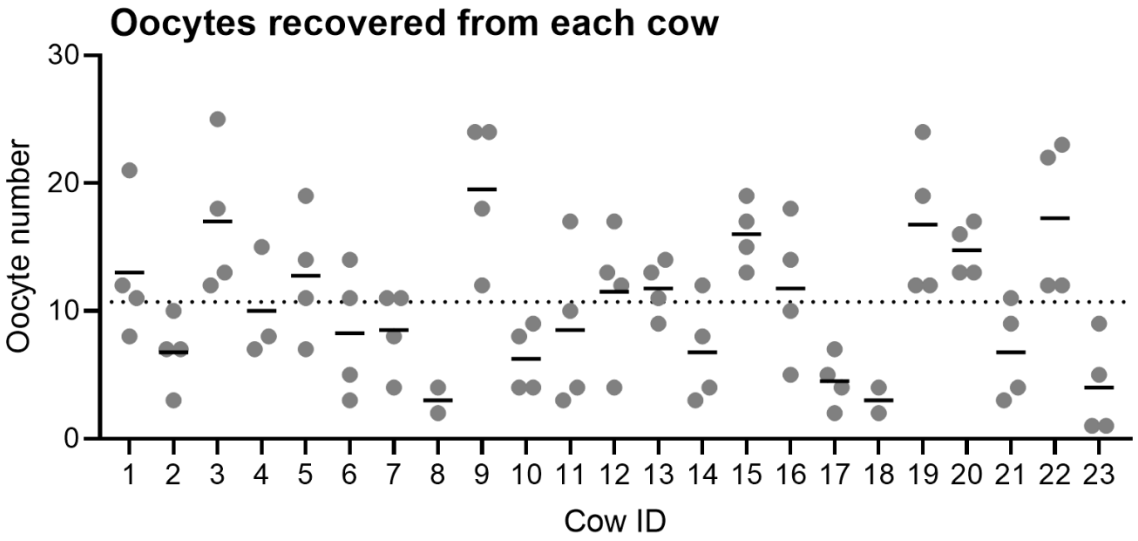

Figure A-1. Number of oocytes recovered from cows by follicle aspiration. Follicles (< 8 mm) were aspirated to facilitate oocyte collection using ultrasound guided transvaginal oocyte pick-up on day 2, 24, 45 and 66 relative to intrauterine infusion. Each cow is shown on the x-axis and each dot represents the number of oocytes isolated at each time point. The solid line represents the mean number of oocytes collected for each cow, and the dashed line depicts mean number of oocytes collected from all cows (10.7 oocytes).

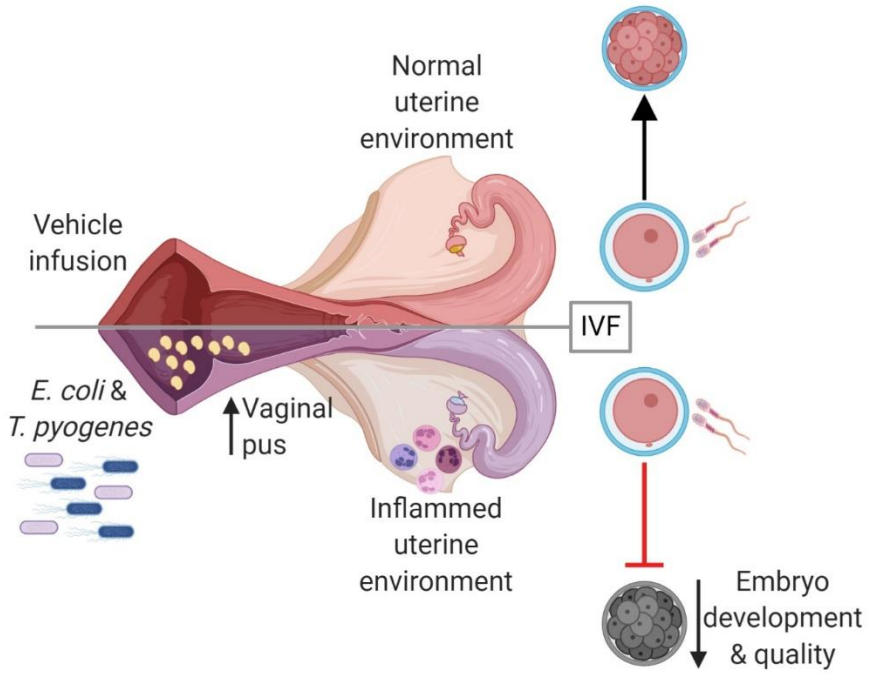

Figure A-2. Graphcial abstract for experimentally induced endometritis impairs the developmental capacity of bovine oocytes.

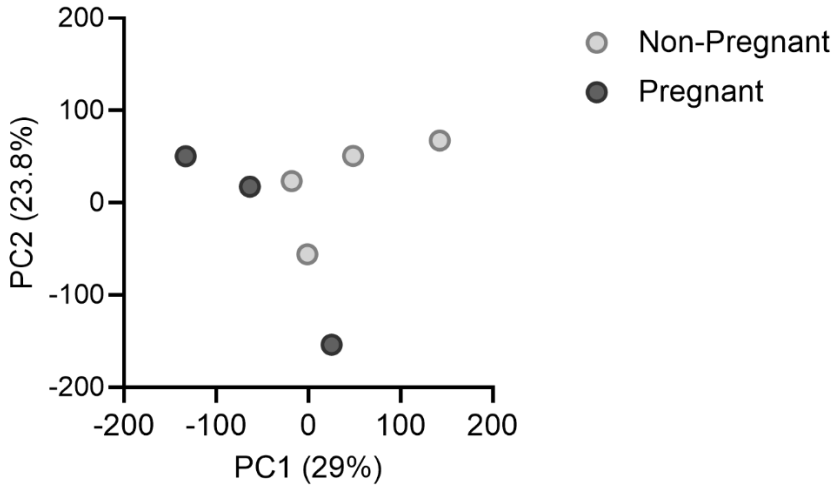

Figure A-3. Principal component analysis of endometrial transcript reads acquired from non-pregnant cows and pregnant cows after intrauterine infusion of pathogenic bacteria. Cows were inseminated 130 days after intrauterine infusion of pathogenic bacteria and endometrial tissue collected 16 days later. Based on the presence of an embryo and interferon tau cows were designated as pregnant (n = 3) or non-pregnant (n = 4). Endometrial tissue was subjected to RNA sequencing analysis. Read counts for all transcripts were subjected to principal component analysis. Principal component (PC) 1 and principal component 2 explain 29% and 23.8% of the total variance, respectively.

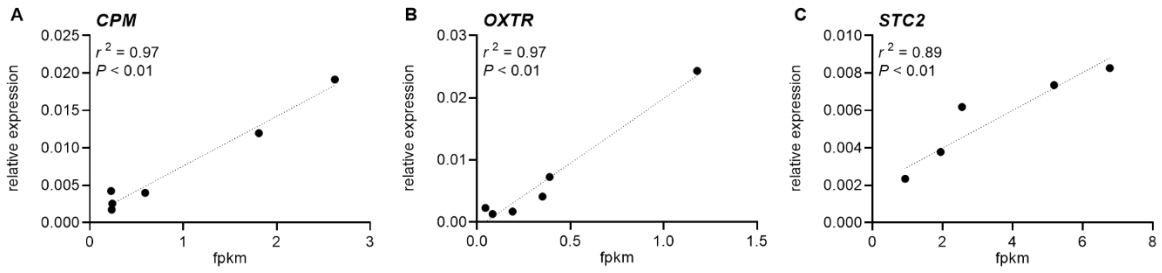

Figure A-4. Validation of RNA sequencing using real time RT-PCR. The validity of RNA sequencing of endometrial tissue was confirmed using real time RT-PCR. Linear regression using read counts and relative expression provides the correlation coefficient and *P*-value for the expression of (A) *CPM*, (B) *OXTR*, and (C) *STC2*.

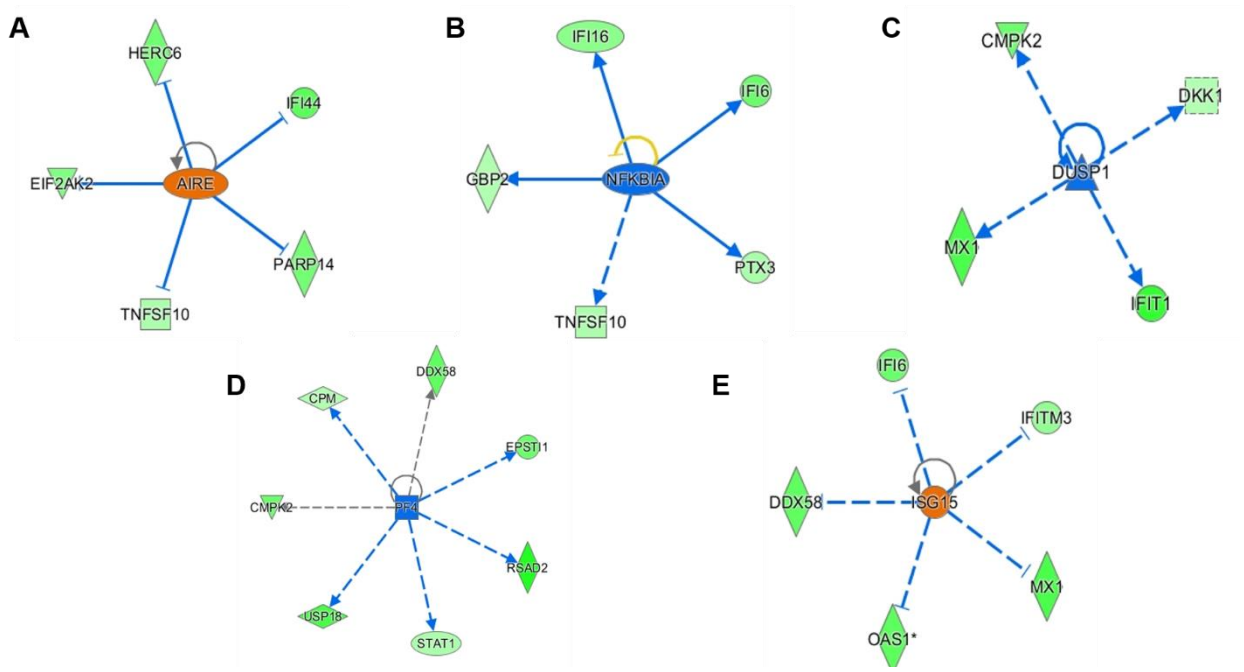

Figure A-5. Unique predicted upstream regulators of differentially expressed genes identified only in the non-pregnant endometrium after infusion with bacteria. Ingenuity Pathway Analysis identified five unique predicted upstream regulators in the endometrium of non-pregnant cows after infusion with bacteria that were not identified in not-pregnant healthy cows from previous studies. Each web depicts a single predicted upstream regulator and its associated differentially expressed genes that are downregulated (green) in non-pregnant cows compared to pregnant cows. (A) AIRE, (B) NFKBIA, (C) DUSP1, (D) PF4, and (E) ISG15. Orange color predicts activation (z-score ≥ 2) and blue predicts inhibition (z-score ≤ -2).

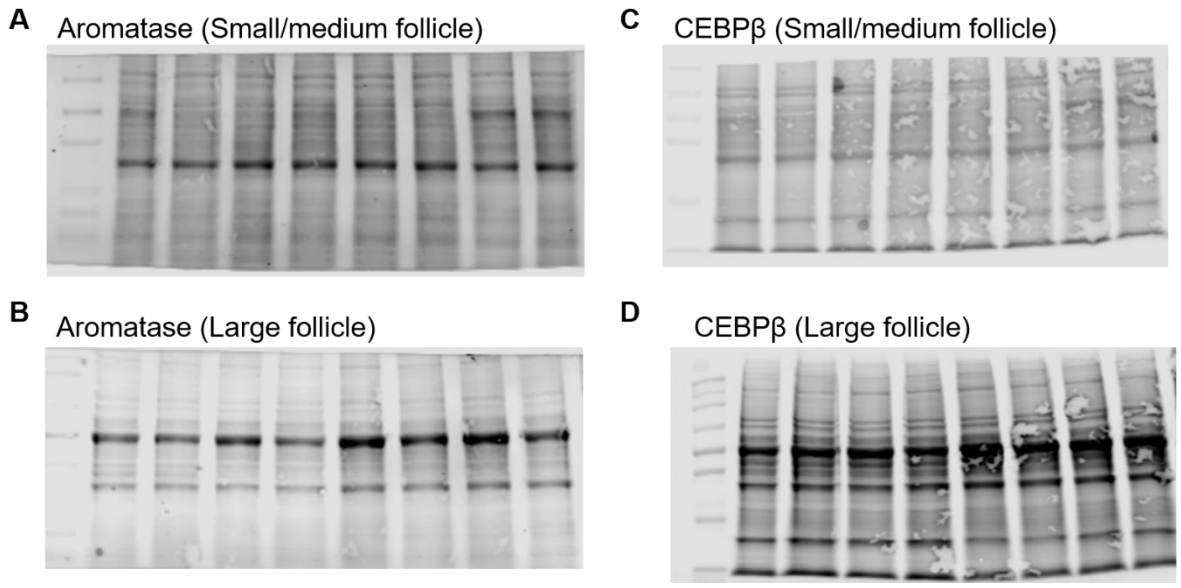

Figure A-6. Total protein stains from western blots. Each protein sample (10 µg) was loaded into a 10% gel and run for 1 h at 100 V. Proteins were transferred to nitrocellulose and stained for total protein. Membranes were imaged and quantified on the Li-Cor Odyessy CLx. Membranes used for western blot of granulosa cells from small/medium follicles (A, C) or large follicles (B, D) to detect aromatase (A-B) or CEBPβ (C-D) are shown and correspond to blots presented in the results section.

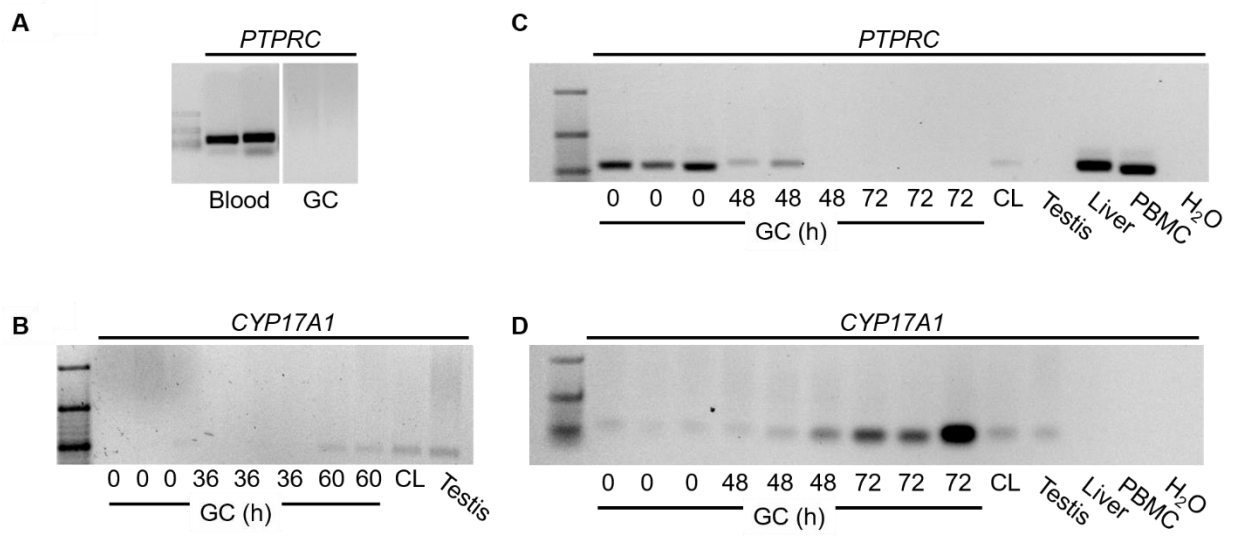

Figure A-7. Assessment of granulosa cell culture purity. Bovine granulosa cells (GC) from small/medium (A-B) follicles or large (C-D) follicles were tested for the expression of the immune cell marker *PTPRC* (A, C) or the luteal cell marker *CYP17A1* (B, D). Expression was evaluated after initial isolation or following a period of culture, as indicated. Whole blood, testis, liver, corpus luteum (CL), peripheral blood mononuclear cells (PBMC) and water (H_2O) were used as controls**.**

Table A-8. Primer details use for real time RT-PCR in bovine endometrium.

Gene Symbol	Primer Sequence	Primer Concentration	Accession number
ABHD1	5′ CTTTGTCCTACAGGCCCGC	500 nM	NM_001035094.2
	3′ CTTGGACTGGCTGCTTGGTA		
ACTB	5′ CAGAAGCACTCGTACGTGGG	500 nM	NM_173979.3
	3′ TTGGCCTTAGGGTTCAGGG		
CPM	5′ GGACTTCAGCTACCACCACC	300 nM	XM_003586067.4
	3′ CACGACGAGAACCCACAGG		
CXCL8	5′ GCAGGTATTTGTGAAGAGAGCTG	500 nM	NM_173925.2
	3′ CACAGAACATGAGGCACTGAA		
FAM135B	5′ CATCACACCTTGCGGGTCCGA	300 nM	NM_001078091.2
	3′ GGGACAGCTGGCTGTGGGTC		
FLRT1	5′ CCGGGTCTCCATCTGTGAGT	500 nM	XM_005227213.4
	3′ TAGCACATTGCGGTCTCAGG		
GAPDH	5′ AGGTCGGAGTGAACGGATTC	500 nM	NM_001034034.2
	3′ ATGGCGACGATGTCCACTTT		
IL6	5′ ATGACTTCTGCTTTCCCTACCC	500 nM	NM_173923.2
	3′ GCTGCTTTCACACTCATCATTC		
ISG15	5′ AGAGAGCCTGGCACCAGAAC	500 nM	NM_174366.1
	3′ TTCTGGGCGATGAACTGCTT		
MEF2B	5′ GTCCAGGTGGAGCAGACAAA	500 nM	NM_001145793.1
	3′ ATCAGCCCGAACTTTCGCTT		
MX1	5′ AGACGAGTGGAAAGGCAAAGTC	500 nM	NM_173940.2
	3′ GATGGCAATCTGGGCTTCAC		
OXTR	5′ AAGATCCGCACGGTCAAGAT	500 nM	NM_174134.2
	3′ TGAAAGGTGAGGCTTCCTTG		
RPL19	5′ ATGCCAACTCCCGCCAGCAGAT	500 nM	NM_001040516.2
	3′ TGTTTTTCCGGCATCGAGCCCG		
STC2	5′ CACTGTTTGGTCAACGCTGG	500 nM	NM_001192745.3
	3′ TGATGAACGACTTGCCCTGG		

Table A-8. Continued.

Gene Symbol	Primer Sequence	Primer Concentration	Accession number
TIMD4	5′ GGCCTCTGATTCTCTGGCTG 3′ AGTCACTGGCTGACCCAAAA	500 nM	NM_001075320.1
TRANK1	5′ CGAGCACCCAGATGGACC 3′ CCACTGGTACAACTGCAGGA	500 nM	XM_024983138.1

Table A-9. Differentially expressed endometrial genes at day 15 in the healthy non-pregnant cow compared to the pregnant cow from the previous study Bauersachs et al., 2012.

Gene ID	Symbol	Log_2FC	Adj *P* Value
510774	*ABHD1*	-1.513	0.002
505134	*ADAR*	-1.651	0.002
505518	*C15H11orf34*	-3.433	0.014
280678	*C4A*	-1.756	0.010
281044	*CCL8*	-2.354	0.001
511001	*CLEC4F*	-2.933	0.001
505167	*CRYM*	-1.537	0.017
615107	*CXCL10*	-2.951	0.001
504760	*DDX58*	-2.303	0.002
508378	*DHX58*	-2.572	0.001
504445	*DKK1*	-2.049	0.046
515051	*DTX3L*	-2.353	0.001
347700	*EIF2AK2*	-2.981	0.001
281751	*EIF4E*	-1.544	0.001
614555	*EPSTI1*	-2.743	0.001
281758	*FABP3*	-2.477	0.012
510874	*FBXO17*	-1.885	0.000
613313	*GBP4*	-2.592	0.035
516949	*GBP5*	-2.421	0.001
527520	*HERC6*	-1.661	0.010
506759	*IFI16*	-2.479	0.001
507138	*IFI27*	-3.076	0.002
508348	*IFI44*	-4.155	0.001
508347	*IFI44L*	-3.826	0.000
512913	*IFI6*	-2.461	0.001
535490	*IFIH1*	-2.440	0.002
515091	*IFIT5*	-2.203	0.000
353510	*IFITM1*	-1.886	0.021
100125591	*IRF7*	-2.148	0.001
509855	*IRF9*	-2.560	0.001
281871	*ISG15*	-5.243	0.001
506604	*ISG20*	-3.191	0.003
100139670	*LOC100139670*	-4.786	0.001
504861	*LOC504861*	-1.560	0.007
509283	*LOC509283*	-2.917	0.001
512486	*LOC512486*	-2.090	0.032

Table A-9. Continued

Gene ID	Symbol	Log_2FC	Adj *P* Value
618737	*LOC618737*	-4.536	0.001
281908	*MFAP5*	-1.653	0.015
280872	*MX1*	-3.642	0.004
280873	*MX2*	-5.321	0.000
654488	*OAS1Y*	-3.662	0.001
513185	*PARP12*	-2.122	0.001
540789	*PARP14*	-2.527	0.001
510532	*PARP9*	-1.795	0.001
767910	*PLAC8B*	-2.278	0.009
100138545	*PML*	-1.972	0.001
508877	*PNPT1*	-2.393	0.001
280701	*PPA1*	-1.644	0.001
506415	*RSAD2*	-4.842	0.001
532442	*RTP4*	-3.342	0.000
514205	*SAMD9*	-3.851	0.001
539759	*SIGLEC1*	-2.268	0.012
521795	*SLFN11*	-2.952	0.021
100140338	*SP100*	-2.393	0.003
510377	*SP140*	-1.629	0.002
510814	*STAT1*	-1.690	0.002
784029	*TDGF1*	1.581	0.045
783855	*TIFA*	-1.629	0.004
507549	*TIMD4*	-1.610	0.040
507215	*TNFSF10*	-1.772	0.005
523970	*TRAK2*	-2.419	0.008
509859	*TRANK1*	-1.567	0.001
497204	*UBA7*	-3.268	0.001
515202	*USP18*	-3.642	0.001
509740	*XAF1*	-2.687	0.001
508333	*ZBP1*	-2.973	0.001
539807	*ZNFX1*	-2.768	0.000

Table A-10. Differentially expressed endometrial genes at day 16 in the healthy non-pregnant cow compared to the pregnant cow from the previous study Forde et al., 2012.

Gene ID	Symbol	Log_2FC	Adj *P* Value
510774	*ABHD1*	-2.315	1.17E-47
505649	*ACCS*	1.515	4.98E-04
281672	*ACKR4*	-6.069	2.79E-04
532272	*ADAMTS13*	2.070	2.35E-07
505134	*ADAR*	-2.815	7.62E-47
525795	*AGRN*	-1.963	6.53E-16
327662	*ANXA1*	-1.644	1.05E-04
506045	*ATAD1*	-1.584	1.91E-05
512313	*ATP2A3*	1.890	2.25E-04
100137953	*ATP8B4*	-4.727	9.13E-15
280729	*B2M*	-1.813	1.38E-08
515585	*B3GNT2*	-1.527	4.32E-06
522469	*BATF2*	-3.435	1.70E-08
533338	*BCL2L12*	-1.535	1.01E-06
280734	*BPI*	-5.029	4.87E-05
280737	*BTC*	-1.522	1.69E-04
326579	*BZW2*	-2.220	6.45E-05
617435	*C1QB*	-1.897	1.22E-06
509968	*C1QC*	-1.683	4.58E-05
767827	*C1S*	-1.551	3.14E-06
515440	*C2*	-2.180	2.37E-09
540702	*C3AR1*	-1.892	8.91E-05
280678	*C4A*	-3.039	1.90E-09
515918	*CA8*	2.177	2.10E-06
338039	*CASP4*	-2.418	7.26E-07
507481	*CASP8*	-1.704	5.32E-13
529166	*CBLN3*	-1.892	6.78E-05
404072	*CCL11*	-3.810	2.20E-05
524530	*CCND1*	1.626	3.46E-05
533834	*CD274*	-4.545	3.00E-04
286849	*CD40*	-1.667	4.09E-04
505040	*CD53*	-2.075	5.26E-09
539690	*CD93*	2.163	5.05E-08
513265	*CDKN2AIP*	-1.627	5.72E-05
782472	*CGAS*	-2.481	1.13E-06
515280	*CHP2*	1.793	2.71E-04

Table A-10. Continued.

Gene ID	Symbol	Log_2FC	Adj *P* Value
508740	*CLEC12A*	-1.920	1.07E-03
511001	*CLEC4F*	-77.350	3.14E-26
784304	*CMPK2*	-10.265	4.07E-34
509620	*CMTR1*	-1.984	2.82E-36
784375	*CNTNAP3*	2.614	6.42E-04
613849	*COL13A1*	-1.622	9.59E-04
338086	*COX7A1*	-1.554	9.07E-08
785528	*CWH43*	-1.982	3.22E-06
615107	*CXCL10*	-4.553	1.55E-05
541171	*DIPK1A*	-1.502	7.70E-10
504445	*DKK1*	-2.794	4.54E-06
533992	*DRAM1*	-1.854	1.59E-06
515051	*DTX3L*	-4.780	3.23E-23
281750	*EDNRB*	-1.753	7.50E-04
347700	*EIF2AK2*	-5.511	1.75E-20
768233	*ELMOD1*	-2.068	1.21E-04
614555	*EPSTI1*	-9.560	5.29E-25
539571	*ESM1*	2.565	1.80E-04
280685	*F2*	1.775	5.35E-04
615144	*FAM171A2*	1.788	6.21E-04
514701	*FAM3B*	-1.985	3.23E-04
508561	*FAM83D*	2.668	7.61E-04
282227	*FCGR1A*	-1.987	4.65E-04
540142	*FOXS1*	-3.102	5.98E-14
510714	*FRMD4A*	1.593	5.19E-05
526127	*FRMD4B*	-1.603	1.14E-04
613313	*GBP4*	-7.114	1.57E-12
525937	*GDA*	-1.705	7.18E-04
508774	*GDAP2*	-1.626	5.06E-05
281797	*GNGT2*	-3.788	7.66E-04
517332	*GRAMD1B*	1.504	8.03E-04
510225	*GRINA*	-1.581	5.74E-05
513231	*GTF2B*	-1.836	1.01E-04
514373	*HERC5*	-3.576	3.77E-12
527520	*HERC6*	-10.559	4.73E-26
507480	*HES4*	-2.135	4.19E-04
616129	*HOXB2*	1.517	6.55E-04
768240	*HOXB4*	1.782	1.86E-04

Table A-10. Continued.

Gene ID	Symbol	Log_2FC	Adj *P* Value
100848273	*HSH2D*	-3.996	4.52E-05
506281	*IDO1*	-5.563	4.17E-07
506759	*IFI16*	-5.177	1.72E-21
507138	*IFI27*	-6.384	1.26E-28
510697	*IFI35*	-2.018	1.25E-13
508347	*IFI44L*	-18.086	8.82E-17
512913	*IFI6*	-8.766	5.15E-22
535490	*IFIH1*	-5.570	8.39E-20
527528	*IFIT2*	-12.752	3.57E-12
509678	*IFIT3*	-12.505	1.00E-19
515091	*IFIT5*	-5.410	6.67E-27
511022	*IL23A*	-1.955	8.47E-12
788637	*IQCN*	3.774	2.04E-04
516979	*IRF3*	-1.564	1.54E-16
509855	*IRF9*	-4.868	1.71E-70
281871	*ISG15*	-54.688	5.28E-69
506604	*ISG20*	-13.440	1.71E-13
509394	*ISYNA1*	1.580	4.29E-04
506526	*ITGA10*	-1.650	2.44E-05
521931	*KCNK12*	3.757	4.42E-04
514211	*KIAA1755*	-1.562	5.01E-13
281889	*KRT17*	-4.883	7.07E-05
520327	*KYNU*	-5.706	3.16E-04
531327	*LAMP3*	-2.308	2.84E-05
531137	*LGALS3BP*	-2.102	2.76E-12
510813	*LGALS9*	-2.579	1.33E-15
100125267	*LIPA*	-1.514	5.90E-04
100139670	*LOC100139670*	-42.135	2.46E-31
112441507	*LOC112441507*	-17.808	1.75E-44
112442826	*LOC112442826*	-2.743	3.94E-04
509283	*LOC509283*	-5.979	1.27E-21
511531	*LOC511531*	-4.251	1.32E-14
512672	*LOC512672*	-2.553	3.22E-06
513659	*LOC513659*	-2.170	2.73E-04
616948	*LOC616948*	-2.435	3.31E-07
506141	*LOC618409*	-3.188	1.18E-15
781710	*LOC781710*	-3.637	6.45E-09
516507	*LRRC66*	-2.141	1.01E-03

Table A-10. Continued.

Gene ID	Symbol	Log_2FC	Adj *P* Value
510977	*LY6E*	-1.804	2.75E-05
535622	*MAP3K8*	-1.873	1.47E-07
281296	*MAPT*	1.557	1.02E-03
505267	*MFNG*	1.521	8.86E-04
510644	*MICALL2*	1.514	4.44E-05
790225	*MLKL*	-2.102	8.83E-05
513807	*MORC3*	-1.757	2.42E-06
523206	*MOV10*	-1.555	7.37E-16
525504	*MST1R*	-1.589	2.24E-10
280872	*MX1*	-14.694	2.87E-29
280873	*MX2*	-52.595	4.86E-26
520472	*NAMPT*	-1.645	8.20E-04
614457	*NRIP2*	1.621	8.55E-05
525562	*NRTN*	1.796	1.09E-04
347699	*OAS1X*	-23.646	1.66E-10
654488	*OAS1Y*	-12.478	4.14E-48
519922	*OAS1Z*	-13.977	5.34E-30
529660	*OAS2*	-16.557	3.11E-43
534150	*OPTN*	-1.592	3.28E-05
281371	*OXTR*	7.406	4.49E-04
767936	*P2RY14*	1.541	6.76E-04
518368	*PARM1*	-1.658	3.62E-06
510991	*PARP10*	-2.749	1.01E-29
513185	*PARP12*	-3.201	4.58E-23
540789	*PARP14*	-6.324	1.22E-22
510532	*PARP9*	-3.647	1.62E-23
515067	*PGAM2*	1.712	1.78E-05
767910	*PLAC8B*	-6.858	4.74E-27
281983	*PLAUR*	-1.520	8.67E-04
510408	*PLCL2*	1.518	5.09E-04
524990	*PLVAP*	1.740	4.82E-04
617469	*PMEPA1*	1.501	1.03E-03
100138545	*PML*	-2.869	3.91E-32
508877	*PNPT1*	-3.411	3.58E-13
541218	*POLK*	-1.569	9.03E-06
280701	*PPA1*	-2.448	6.65E-12
282091	*PPP1R16B*	1.603	8.89E-04
100137803	*PRDM16*	2.647	1.02E-03

Table A-10. Continued.

Gene ID	Symbol	Log_2FC	Adj *P* Value
539141	*PSMA2*	-1.724	2.84E-11
509857	*PSME2*	-1.498	1.15E-07
617807	*PSMF1*	-2.138	1.04E-14
505285	*PTPRE*	-2.281	2.71E-05
513223	*RASEF*	-1.739	3.16E-06
617625	*RBM43*	-2.384	5.06E-06
507427	*RIPK3*	-1.629	7.72E-04
282341	*RNASE6*	-1.852	2.55E-07
100048947	*RNASEL*	-1.593	1.68E-07
513479	*RNF114*	-1.596	1.60E-57
767991	*RNF24*	1.508	3.73E-04
506415	*RSAD2*	-36.622	2.85E-47
511675	*RSPO1*	-7.054	2.48E-06
532442	*RTP4*	-5.497	1.13E-34
504467	*SASS6*	-2.012	9.44E-04
790815	*SCLY*	-1.592	4.30E-10
539321	*SERTAD1*	-1.584	1.25E-04
506155	*SGCG*	4.031	4.87E-07
539087	*SHFL*	-1.592	2.42E-06
616861	*SHISA5*	-1.955	1.05E-11
539759	*SIGLEC1*	-4.862	1.06E-34
513984	*SLC15A3*	-2.407	4.15E-18
282484	*SLC34A2*	1.677	9.58E-04
527023	*SLC40A1*	-1.985	7.20E-06
524085	*SLC41A3*	1.511	1.36E-04
506958	*SLC66A3*	-1.663	1.42E-04
514339	*SLC6A12*	-15.228	7.84E-04
508174	*SLC7A9*	-6.147	5.56E-05
521795	*SLFN11*	-9.479	3.60E-12
504287	*SOAT1*	-2.244	3.07E-04
515204	*SP110*	-3.186	2.60E-14
100139208	*SP140L*	-3.753	4.20E-23
510814	*STAT1*	-3.722	2.70E-33
511023	*STAT2*	-1.925	1.51E-11
540850	*SYT7*	1.580	1.55E-07
524959	*TAP1*	-1.808	1.07E-11
617047	*TCIM*	-1.609	1.46E-05
506702	*TDRD7*	-2.536	4.94E-15

Table A-10. Continued.

Gene ID	Symbol	Log_2FC	Adj *P* Value
533862	*TENT2*	-1.587	1.22E-04
783855	*TIFA*	-3.301	1.83E-11
507549	*TIMD4*	-3.009	6.65E-06
540975	*TIPARP*	-1.552	5.00E-05
533038	*TM4SF1*	-1.660	1.06E-07
508269	*TMEM106A*	-1.638	4.01E-07
515475	*TMEM140*	-1.756	3.05E-06
618298	*TMEM182*	-2.251	8.00E-04
507215	*TNFSF10*	-2.950	6.11E-07
504507	*TNFSF13B*	-5.113	3.82E-07
505683	*TPGS1*	1.641	3.81E-04
509859	*TRANK1*	-2.573	2.36E-29
506467	*TREM2*	2.225	4.52E-04
282099	*TREX1*	-2.000	1.12E-06
359715	*TRIM21*	-1.547	5.74E-04
510923	*TRIM25*	-1.656	4.92E-12
539820	*TRIM34*	-2.640	3.09E-10
514896	*TRIM56*	-1.595	8.36E-05
497204	*UBA7*	-8.616	1.82E-65
509471	*UBE2L6*	-2.113	6.09E-11
504557	*UPB1*	-2.913	8.33E-04
515202	*USP18*	-14.555	2.50E-33
524531	*USP25*	-1.596	2.25E-06
509740	*XAF1*	-6.623	7.87E-25
517417	*XRN2*	-1.502	1.06E-08
508333	*ZBP1*	-17.900	2.88E-32
509706	*ZNF74*	1.500	5.99E-08
539807	*ZNFX1*	-5.262	1.05E-81

Table A-11. Differentially expressed endometrial genes at day 17 in the healthy non-pregnant cow compared to the pregnant cow from the previous study Cerri et al., 2012.

Gene ID	Symbol	Log_2FC	Adj *P* Value
511515	*AATK*	-1.686	1.63E-06
510774	*ABHD1*	-3.209	3.52E-10
613794	*ABLIM3*	-1.552	3.51E-07
505134	*ADAR*	-2.083	6.89E-17
534286	*ALAS1*	-1.640	1.01E-10
407169	*ALOX12*	-3.504	8.58E-12
613869	*ALOX5AP*	-2.649	2.73E-10
518393	*AOX4*	-1.586	3.48E-04
518752	*ARG2*	-2.007	3.11E-07
616246	*ARHGAP15*	-2.559	9.90E-08
506075	*ARHGEF25*	1.531	9.61E-07
506045	*ATAD1*	-1.644	1.54E-07
515266	*ATF3*	-2.402	8.93E-10
790880	*ATXN3*	-2.187	1.47E-12
533338	*BCL2L12*	-2.421	9.62E-13
508365	*BCL2L14*	-1.653	7.97E-07
509786	*BCL2L15*	-2.537	7.98E-11
282534	*BOLA-DQA1*	-2.002	8.91E-03
282535	*BOLA-DQA2*	-3.793	8.12E-03
326579	*BZW2*	-1.613	3.35E-08
505518	*C15H11orf34*	-8.707	3.74E-15
617435	*C1QB*	-1.896	6.66E-12
509968	*C1QC*	-1.982	2.21E-10
515440	*C2*	-3.786	4.73E-11
529849	*C2CD4B*	-2.283	1.54E-07
515918	*CA8*	1.725	2.33E-07
616136	*CALHM6*	-2.725	2.73E-11
338039	*CASP4*	-2.179	9.77E-14
615922	*CCDC136*	-1.701	1.30E-09
281044	*CCL8*	-4.810	3.38E-12
510668	*CCR7*	-2.596	1.73E-06
286849	*CD40*	-1.621	4.73E-07
782186	*CD58*	-1.662	2.25E-06
281058	*CD69*	-1.827	1.33E-09
414345	*CD86*	-2.163	9.26E-09
539690	*CD93*	2.384	5.44E-09

Table A-11. Continued.

Gene ID	Symbol	Log_2FC	Adj *P* Value
514076	*CFB*	-1.556	7.71E-06
511001	*CLEC4F*	-8.660	5.65E-23
618591	*CLECL1*	-1.835	3.11E-06
536537	*CNOT9*	-1.545	1.65E-08
280752	*CNP*	-1.822	3.36E-06
781493	*COL14A1*	2.280	3.59E-08
534505	*CPXM2*	-1.943	6.13E-04
540605	*CREM*	-2.251	1.27E-10
281719	*CRYAB*	-2.267	4.46E-12
281724	*CRYGS*	-3.888	2.07E-08
505167	*CRYM*	-1.684	3.98E-05
615107	*CXCL10*	-3.530	3.05E-10
539047	*CYP26A1*	-2.079	2.53E-03
280762	*DDC*	-2.264	1.55E-06
504760	*DDX58*	-3.796	2.27E-14
508378	*DHX58*	-3.422	4.61E-14
504445	*DKK1*	-1.982	6.43E-08
512512	*DNASE1L3*	-2.473	1.98E-07
533992	*DRAM1*	-2.036	7.60E-13
513753	*EDN3*	1.819	7.11E-05
505206	*EHD4*	-1.641	5.58E-10
347700	*EIF2AK2*	-2.971	1.44E-09
282711	*EPAS1*	-1.897	1.32E-06
617442	*EVI2B*	-1.941	1.57E-07
281758	*FABP3*	-4.780	3.16E-11
514701	*FAM3B*	-1.735	1.29E-07
508882	*FAP*	1.621	2.21E-09
513483	*FBP1*	-3.960	5.64E-06
282227	*FCGR1A*	-2.413	9.36E-14
281812	*FGFBP1*	-4.156	7.52E-08
540142	*FOXS1*	-2.668	5.05E-17
505622	*GALNT17*	-1.612	1.65E-05
613313	*GBP4*	-2.690	1.32E-08
516949	*GBP5*	-4.104	1.92E-09
508774	*GDAP2*	-1.534	1.42E-12
523294	*GLT8D2*	1.868	4.07E-08
512826	*GPIHBP1*	1.611	3.00E-07
287025	*GPLD1*	-2.886	4.18E-06

Table A-11. Continued.

Gene ID	Symbol	Log_2FC	Adj *P* Value
533760	*GRIK1*	2.097	4.16E-05
525059	*GSS*	-1.884	4.69E-06
513971	*H1-2*	-1.633	1.82E-06
100126192	*H19*	1.687	2.75E-03
785042	*HOOK1*	-3.299	2.68E-13
506281	*IDO1*	-4.302	1.80E-12
506759	*IFI16*	-2.845	4.31E-17
507138	*IFI27*	-2.549	1.50E-10
510697	*IFI35*	-1.859	2.86E-15
508348	*IFI44*	-4.349	1.49E-12
508347	*IFI44L*	-5.090	5.60E-14
512913	*IFI6*	-2.789	8.22E-15
535490	*IFIH1*	-2.714	6.85E-13
527528	*IFIT2*	-6.395	9.72E-13
515091	*IFIT5*	-2.249	1.78E-14
353510	*IFITM1*	-1.755	2.56E-12
526461	*IFITM5*	-3.728	3.90E-13
537487	*IGSF10*	2.150	3.26E-08
100125591	*IRF7*	-3.950	6.74E-14
509855	*IRF9*	-2.728	5.30E-14
617420	*ISG12(B)*	-2.224	6.28E-06
281871	*ISG15*	-5.068	2.32E-11
506604	*ISG20*	-7.139	2.35E-15
515018	*ISLR*	1.940	1.16E-06
281889	*KRT17*	-3.494	3.50E-09
531137	*LGALS3BP*	-1.752	6.28E-08
510813	*LGALS9*	-1.988	1.09E-11
507402	*LOC100298356*	-5.486	2.79E-11
508666	*LOC508666*	1.563	5.87E-07
509283	*LOC509283*	-3.477	1.64E-11
510382	*LOC510382*	-2.754	9.39E-04
511531	*LOC511531*	-2.159	1.21E-06
512486	*LOC512486*	-2.922	4.01E-11
512672	*LOC512672*	-1.837	1.12E-09
514978	*LOC514978*	-4.788	1.80E-20
515676	*LOC515676*	-3.787	2.72E-06
616948	*LOC616948*	-2.236	1.77E-13
617696	*LOC617696*	-1.965	9.10E-12

Table A-11. Continued.

Gene ID	Symbol	Log_2FC	Adj *P* Value
539366	*LRFN5*	1.892	3.57E-04
510977	*LY6E*	-1.628	1.02E-12
505805	*LY6G6C*	-1.930	7.22E-07
281287	*LYZ1*	-1.603	2.31E-03
527595	*MCM10*	-2.503	1.08E-04
540701	*MEP1B*	-2.207	1.94E-07
282276	*MGAT4A*	-3.417	4.77E-11
790225	*MLKL*	-3.941	8.44E-12
539387	*MPZL1*	-1.602	1.01E-07
525504	*MST1R*	-2.443	6.85E-12
281187	*MSTN*	1.608	7.89E-06
280872	*MX1*	-3.177	1.77E-11
280873	*MX2*	-7.814	5.45E-13
522392	*MXRA8*	1.623	3.21E-10
505994	*NCDN*	-1.770	1.26E-05
281346	*NCF2*	-1.594	2.57E-08
510003	*NEDD4L*	-1.558	4.67E-12
782441	*NLRC5*	-2.451	6.05E-10
511280	*NMI*	-1.717	1.71E-13
511858	*NT5C3A*	-1.708	3.38E-10
347699	*OAS1*	-3.883	3.03E-13
514720	*OSMR*	-2.064	1.21E-05
281371	*OXTR*	2.334	2.70E-04
513185	*PARP12*	-2.386	4.02E-15
540789	*PARP14*	-3.131	4.02E-15
510532	*PARP9*	-2.256	1.35E-16
537453	*PATL1*	-2.953	4.43E-11
282856	*PCK2*	-1.624	1.49E-08
514168	*PDXK*	-2.621	2.22E-07
281401	*PIGR*	2.286	4.75E-07
509228	*PLAC8A*	-3.805	3.36E-09
767910	*PLAC8B*	-3.092	5.55E-14
510748	*PLEKHA4*	-1.996	2.12E-09
524990	*PLVAP*	1.988	3.84E-07
513533	*PMVK*	-1.952	2.74E-08
508877	*PNPT1*	-2.947	2.12E-19
280701	*PPA1*	-2.384	1.10E-17
282091	*PPP1R16B*	1.637	1.50E-09

Table A-11. Continued.

Gene ID	Symbol	Log_2FC	Adj *P* Value
282000	*PRELP*	1.699	2.12E-08
510394	*PRSS22*	-1.658	4.65E-05
617807	*PSMF1*	-1.771	4.07E-17
541148	*PTX3*	-3.056	1.44E-09
515860	*PXDN*	-5.464	9.44E-14
282846	*PYCARD*	-1.840	1.20E-08
282035	*RGS16*	-2.089	2.72E-10
282341	*RNASE6*	-1.761	3.23E-12
506415	*RSAD2*	-4.996	1.59E-10
532442	*RTP4*	-3.830	2.59E-11
282467	*S100A12*	-2.739	1.63E-08
514205	*SAMD9*	-4.594	5.36E-14
504467	*SASS6*	-1.904	4.92E-13
282348	*SCNN1A*	1.977	1.17E-06
513593	*SERINC2*	-1.673	4.72E-10
286871	*SERPINA14*	-3.337	7.19E-07
539321	*SERTAD1*	-1.589	1.01E-11
617797	*SH3BGR*	2.078	1.92E-08
617336	*SHISA2*	-2.980	7.54E-06
781091	*SHISA3*	-3.377	2.62E-08
616861	*SHISA5*	-2.145	1.57E-15
539759	*SIGLEC1*	-4.911	4.56E-20
286845	*SLC12A2*	-1.629	8.53E-07
521181	*SLC15A1*	-2.304	1.83E-05
505775	*SLC16A1*	-2.604	3.55E-09
535872	*SLC16A2*	1.661	5.02E-09
512495	*SLC38A5*	-1.951	5.52E-08
282361	*SLC5A1*	-1.545	3.64E-05
518699	*SMPDL3B*	-1.502	8.05E-07
518795	*SOCS1*	-1.858	4.33E-09
519439	*SOX18*	1.595	5.32E-07
510377	*SP140*	-1.921	5.19E-13
533103	*SPHK2*	1.641	2.38E-13
537972	*SPTLC2*	-1.536	1.32E-10
100125878	*SSLP1*	1.548	8.19E-08
512369	*STARD5*	-1.746	4.70E-08
510814	*STAT1*	-1.508	5.29E-14

Table A-11. Continued.

Gene ID	Symbol	Log_2FC	Adj *P* Value
511023	*STAT2*	-1.924	1.05E-15
534995	*SYNGR1*	-1.658	6.92E-05
404136	*TACR3*	-1.504	1.49E-04
539853	*TACSTD2*	-1.835	4.61E-09
524959	*TAP1*	-1.739	2.11E-12
506702	*TDRD7*	-2.157	4.56E-16
783855	*TIFA*	-2.962	1.20E-10
507549	*TIMD4*	-4.137	9.89E-13
404076	*TKDP1*	-3.104	9.18E-03
515475	*TMEM140*	-2.169	3.88E-12
533681	*TMEM156*	-1.531	2.19E-06
505490	*TMEM40*	-3.460	6.29E-06
510305	*TMEM45B*	-1.882	1.22E-07
617948	*TNFRSF13B*	-2.010	2.21E-09
504507	*TNFSF13B*	-3.035	3.04E-11
509859	*TRANK1*	-2.351	1.22E-13
282099	*TREX1*	-3.769	1.65E-13
539820	*TRIM34*	-2.010	6.03E-14
539001	*TSPAN2*	1.562	2.76E-05
497204	*UBA7*	-3.803	1.41E-13
509471	*UBE2L6*	-1.861	2.03E-11
535385	*UNC45B*	-2.387	4.35E-09
613535	*UNC93A*	-2.248	2.30E-07
282113	*UPK1B*	-2.005	8.40E-03
515202	*USP18*	-4.327	1.64E-14
613549	*VGLL1*	-1.918	7.56E-05
524159	*VWA8*	-3.179	1.58E-14
281576	*WARS*	-1.600	7.27E-11
509740	*XAF1*	-3.249	7.70E-16
539807	*ZNFX1*	-3.006	1.21E-15

.

Table A-12. Summary of read mapping for endometrial samples obtained from cows after intrauterine infusion of pathogenic bacteria.

Cow ID	Pregnany Status	RNA integrity number	Raw reads	Clean reads	Mapped reads	Mapped reads (%)	Mapped transcripts
7264	Non-Pregnant	7.3	75154822	72581934	68360501	94.18%	22535
7389	Non-Pregnant	6.9	60737768	58684410	56325262	95.98%	22238
7643	Non-Pregnant	8.6	64057526	62250658	59647818	95.82%	22481
8040	Non-Pregnant	6.8	67077856	65103720	62226869	95.58%	21566
7703	Pregnant	7.6	65462796	63716022	61279190	96.18%	22206
7895	Pregnant	8.3	63594128	61764160	59331566	96.06%	22727
8283	Pregnant	6.9	63075410	61662042	59330732	96.22%	21199

Table A-13. Most abundantly expressed endometrial genes in the cows after intrauterine infusion of pathogenic bacteria.

Gene ID	Symbol	Total read count	Type	Description
112444681	*LOC112444681*	5671146	pseudo	28S ribosomal RNA
493779	*RN18S1*	4984803	rRNA	18S ribosomal RNA
112442408	*LOC112442408*	850197	protein-coding	translation initiation factor IF-2-like
281850	*IGHG1*	767866	other	immunoglobulin heavy constant gamma 1
100498812	*MIR2887-1*	715869	ncRNA	microRNA 2887-1
104976804	*LOC104976804*	681736	ncRNA	uncharacterized LOC104976804
282220	*EEF1A1*	613568	protein-coding	eukaryotic translation elongation factor 1 alpha 1
510833	*COL3A1*	519490	protein-coding	collagen type III alpha 1 chain
539515	*SRRM2*	476649	protein-coding	serine/arginine repetitive matrix 2
511422	*COL6A1*	463255	protein-coding	collagen type VI alpha 1 chain
281387	*PENK*	374814	protein-coding	proenkephalin
326599	*TPT1*	365374	protein-coding	tumor protein, translationally-controlled 1
282194	*COL6A2*	341241	protein-coding	collagen type VI alpha 2 chain
282187	*COL1A1*	338835	protein-coding	collagen type I alpha 1 chain
786966	*PLEC*	334900	protein-coding	plectin

Table A-14. Differentially expressed endometrial genes in non-pregnant cows compared to pregnant cows after intrauterine infusion with pathogenic bacteria.

Gene ID	Symbol	Type	Log_2FC	Adj *P* Value
508284	*ACBD7*	protein-coding	-1.485	4.37E-02
505134	*ADAR*	protein-coding	-1.471	3.62E-07
327662	*ANXA1*	protein-coding	-1.301	4.05E-03
506045	*ATAD1*	protein-coding	-1.056	4.82E-02
100137953	*ATP8B4*	protein-coding	-2.088	4.83E-06
522469	*BATF2*	protein-coding	-1.678	3.54E-04
280734	*BPI*	protein-coding	-1.664	1.14E-02
511581	*C1R*	protein-coding	-1.152	1.07E-02
280678	*C4A*	protein-coding	-1.145	1.13E-02
529166	*CBLN3*	protein-coding	-1.598	1.10E-08
100848428	*CCDC188*	protein-coding	1.294	3.74E-02
101904723	*CCDC194*	protein-coding	-1.540	9.64E-03
522998	*CCDC6*	protein-coding	-0.894	2.54E-02
281044	*CCL8*	protein-coding	-1.943	4.31E-04
104971522	*CD160*	protein-coding	0.982	4.52E-02
338319	*CEBPB*	protein-coding	-0.796	2.57E-02
782472	*CGAS*	protein-coding	-1.478	4.05E-03
784304	*CMPK2*	protein-coding	-2.905	2.10E-13
509620	*CMTR1*	protein-coding	-0.876	4.10E-02
281702	*CNGB1*	protein-coding	-2.352	6.72E-06
280752	*CNP*	protein-coding	-1.110	3.73E-02
519501	*COL20A1*	protein-coding	1.237	2.43E-02
513281	*CPM*	protein-coding	-1.524	1.69E-02
534505	*CPXM2*	protein-coding	-1.369	2.61E-02
281105	*CTSB*	protein-coding	-0.919	4.55E-02
504760	*DDX58*	protein-coding	-3.146	1.75E-21
508378	*DHX58*	protein-coding	-2.279	1.27E-09
504445	*DKK1*	protein-coding	-1.502	6.30E-04
515051	*DTX3L*	protein-coding	-2.240	1.53E-06
522462	*EFHD1*	protein-coding	-0.770	3.04E-02
347700	*EIF2AK2*	protein-coding	-2.497	3.64E-11
614555	*EPSTI1*	protein-coding	-2.896	2.17E-18
618755	*FAM135B*	protein-coding	1.917	4.41E-06
514701	*FAM3B*	protein-coding	-2.058	2.06E-06
515085	*FCRL3*	protein-coding	-1.506	3.83E-02
508090	*FGL1*	protein-coding	-1.127	6.53E-03
788007	*FLRT1*	protein-coding	1.865	2.05E-04

Table A-14. Continued.

Gene ID	Symbol	Type	Log_2FC	Adj *P* Value
281797	*GNGT2*	protein-coding	-1.736	8.23E-04
516026	*GPRC5A*	protein-coding	-1.297	3.13E-02
510225	*GRINA*	protein-coding	-1.169	7.79E-03
514373	*HERC5*	protein-coding	-1.994	9.73E-07
527520	*HERC6*	protein-coding	-2.781	2.57E-14
112442653	*HOXB5*	protein-coding	0.887	4.88E-02
506759	*IFI16*	protein-coding	-2.261	2.44E-14
507138	*IFI27*	protein-coding	-2.510	3.64E-11
508348	*IFI44*	protein-coding	-3.223	9.88E-18
512913	*IFI6*	protein-coding	-2.925	9.25E-13
535490	*IFIH1*	protein-coding	-2.128	7.60E-09
515091	*IFIT5*	protein-coding	-2.250	1.46E-11
777594	*IFITM3*	protein-coding	-1.717	4.39E-07
282255	*IFITM3(1-8U)*	protein-coding	-2.097	4.64E-06
509855	*IRF9*	protein-coding	-1.757	2.12E-06
617420	*ISG12(B)*	protein-coding	-1.723	7.25E-03
531137	*LGALS3BP*	protein-coding	-1.307	1.37E-03
510813	*LGALS9*	protein-coding	-1.424	5.38E-04
520564	*LITAF*	protein-coding	-0.961	4.52E-02
100138660	*LOC100138660*	ncRNA	1.265	1.38E-02
100139670	*LOC100139670*	protein-coding	-3.996	2.42E-21
100141258	*LOC100141258*	protein-coding	-1.501	2.56E-02
100297676	*LOC100297676*	protein-coding	-1.364	2.43E-02
100336669	*LOC100336669*	protein-coding	-1.525	2.55E-03
100848246	*LOC100848246*	ncRNA	1.425	8.92E-03
100848263	*LOC100848263*	protein-coding	-1.512	3.72E-02
101903402	*LOC101903402*	ncRNA	-1.503	1.43E-03
101903765	*LOC101903765*	pseudo	-1.960	7.33E-04
101904136	*LOC101904136*	pseudo	1.451	3.94E-02
101905897	*LOC101905897*	ncRNA	0.943	2.57E-02
101907799	*LOC101907799*	ncRNA	-3.292	1.54E-15
104974749	*LOC104974749*	ncRNA	1.880	1.62E-03
104974750	*LOC104974750*	ncRNA	1.485	3.42E-02
104975106	*LOC104975106*	pseudo	1.658	5.13E-03
104975612	*LOC104975612*	ncRNA	1.596	1.21E-02
107132327	*LOC107132327*	protein-coding	-1.721	1.34E-03
107132911	*LOC107132911*	ncRNA	-1.427	1.69E-02
107133045	*LOC107133045*	ncRNA	1.494	2.30E-02

Table A-14. Continued.

Gene ID	Symbol	Type	Log_2FC	Adj *P* Value
112441507	*LOC112441507*	protein-coding	-3.974	1.88E-22
112441868	*LOC112441868*	ncRNA	1.109	5.45E-03
112442254	*LOC112442254*	ncRNA	1.465	3.90E-02
112442264	*LOC112442264*	ncRNA	1.749	4.86E-03
112446427	*LOC112446427*	protein-coding	-1.532	1.30E-04
112447832	*LOC112447832*	ncRNA	1.168	8.11E-03
112449099	*LOC112449099*	protein-coding	1.562	2.25E-02
509283	*LOC509283*	protein-coding	-2.527	1.00E-13
510382	*LOC510382*	pseudo	-3.738	4.77E-17
511531	*LOC511531*	protein-coding	-1.532	1.30E-02
511937	*LOC511937*	pseudo	-1.342	3.28E-02
512672	*LOC512672*	protein-coding	-1.366	5.69E-03
514978	*LOC514978*	protein-coding	-3.008	4.60E-14
614402	*LOC614402*	protein-coding	-2.056	2.73E-04
618409	*LOC618409*	protein-coding	-1.251	1.69E-02
618737	*LOC618737*	protein-coding	-3.015	4.40E-11
789503	*LOC789503*	protein-coding	1.441	2.94E-03
790255	*LOC790255*	protein-coding	1.506	2.30E-02
515494	*LRP10*	protein-coding	-0.883	1.88E-02
510977	*LY6E*	protein-coding	-1.364	1.88E-02
505805	*LY6G6C*	protein-coding	-1.506	2.57E-02
613856	*LY86*	protein-coding	-1.281	5.10E-03
507845	*MAPRE1*	protein-coding	-0.938	3.55E-02
100271851	*MEF2B*	protein-coding	1.662	1.15E-02
507921	*MFSD5*	protein-coding	-1.084	1.61E-02
280857	*MIA*	protein-coding	1.276	4.31E-03
533051	*MIC1*	protein-coding	-0.923	1.15E-02
790225	*MLKL*	protein-coding	-1.500	5.10E-03
512308	*MMRN2*	protein-coding	-1.202	5.38E-04
514667	*MST1*	protein-coding	0.941	2.09E-02
280872	*MX1*	protein-coding	-3.544	1.19E-27
280873	*MX2*	protein-coding	-4.386	1.58E-30
535092	*MYO7A*	protein-coding	1.475	4.96E-03
100125264	*NUP210*	protein-coding	1.036	1.10E-02
347699	*OAS1X*	protein-coding	-3.194	3.10E-21
654488	*OAS1Y*	protein-coding	-3.182	2.09E-21
519922	*OAS1Z*	protein-coding	-2.883	9.71E-13
529660	*OAS2*	protein-coding	-3.435	2.17E-19

Table A-14. Continued.

Gene ID	Symbol	Type	Log_2FC	Adj *P* Value
534150	*OPTN*	protein-coding	-1.251	9.33E-03
514720	*OSMR*	protein-coding	-1.088	2.89E-02
513185	*PARP12*	protein-coding	-2.088	1.98E-10
540789	*PARP14*	protein-coding	-2.742	3.54E-16
510532	*PARP9*	protein-coding	-1.731	2.01E-07
538371	*PAX5*	protein-coding	-1.707	8.08E-03
767910	*PLAC8B*	protein-coding	-1.988	2.05E-04
510748	*PLEKHA4*	protein-coding	-1.318	1.06E-02
280981	*PLIN2*	protein-coding	-1.145	1.65E-02
100138545	*PML*	protein-coding	-1.681	1.39E-05
538575	*PRSS23*	protein-coding	-0.883	6.37E-03
617807	*PSMF1*	protein-coding	-1.687	9.18E-06
541148	*PTX3*	protein-coding	-1.677	3.06E-04
521304	*RBFOX1*	protein-coding	1.564	2.11E-02
617625	*RBM43*	protein-coding	-1.101	7.42E-05
513479	*RNF114*	protein-coding	-1.284	5.13E-03
281898	*RPSA*	protein-coding	-1.244	2.57E-02
506415	*RSAD2*	protein-coding	-4.446	2.98E-32
511675	*RSPO1*	protein-coding	-1.270	4.97E-02
532442	*RTP4*	protein-coding	-2.728	1.32E-12
514205	*SAMD9*	protein-coding	-2.524	2.69E-09
504467	*SASS6*	protein-coding	-0.903	4.06E-02
521133	*SEC14L3*	protein-coding	-1.391	3.64E-02
286871	*SERPINA14*	protein-coding	-1.516	3.41E-02
539321	*SERTAD1*	protein-coding	-1.377	2.97E-03
617336	*SHISA2*	protein-coding	-1.493	4.15E-02
616861	*SHISA5*	protein-coding	-1.477	1.66E-04
539759	*SIGLEC1*	protein-coding	-2.050	4.04E-07
317704	*SLCO2B1*	protein-coding	-0.933	1.14E-02
616050	*SMYD3*	protein-coding	-0.870	4.88E-02
514207	*SNED1*	protein-coding	1.047	1.13E-02
515204	*SP110*	protein-coding	-2.190	2.54E-14
510377	*SP140*	protein-coding	-1.602	7.42E-05
100139208	*SP140L*	protein-coding	-1.408	5.15E-03
539299	*SPATS2L*	protein-coding	-1.065	3.85E-02
784460	*SPIB*	protein-coding	-1.663	1.05E-02
531014	*SPTBN5*	protein-coding	0.950	4.64E-02
510814	*STAT1*	protein-coding	-1.639	1.50E-03

Table A-14. Continued.

Gene ID	Symbol	Type	Log_2FC	Adj *P* Value
511023	*STAT2*	protein-coding	-1.080	4.99E-03
540573	*STC2*	protein-coding	-1.527	5.13E-03
540438	*STOML1*	protein-coding	-0.703	3.83E-02
506702	*TDRD7*	protein-coding	-1.397	3.57E-04
783855	*TIFA*	protein-coding	-1.524	1.21E-02
445425	*TKT*	protein-coding	-0.834	3.64E-02
515475	*TMEM140*	protein-coding	-1.427	2.88E-03
101902667	*TMEM210*	protein-coding	1.267	3.92E-02
507215	*TNFSF10*	protein-coding	-1.632	1.52E-04
510923	*TRIM25*	protein-coding	-1.266	1.37E-02
539820	*TRIM34*	protein-coding	-1.368	2.13E-03
514896	*TRIM56*	protein-coding	-1.186	4.32E-03
497204	*UBA7*	protein-coding	-2.442	4.37E-09
509471	*UBE2L6*	protein-coding	-1.473	6.39E-03
282113	*UPK1B*	protein-coding	-2.032	1.81E-04
515202	*USP18*	protein-coding	-3.589	7.16E-28
509740	*XAF1*	protein-coding	-2.597	4.21E-13
508333	*ZBP1*	protein-coding	-2.565	3.04E-09
787099	*ZCCHC2*	protein-coding	-1.284	2.01E-07
539807	*ZNFX1*	protein-coding	-2.720	2.16E-16

Table A-15. Canonical pathways and related genes altered in the endometrium of non-pregnant cows compared to the pregnant cows after infusion of pathogenic bacteria.

Canonical Pathways	-Log (*P* value)	z-score	Differentially expressed genes in pathway
Interferon Signaling	10.4	-2.646	*IFI6, IFIT1, IFITM3, IRF9, MX1, OAS1, STAT1, STAT2*
Activation of IRF by Cytosolic Pattern Recognition Receptors	8.35	-1.414	*ADAR, DDX58, DHX58, IFIH1, IRF9, STAT1, STAT2, ZBP1*
Role of Pattern Recognition Receptors in Recognition of Bacteria and Viruses	4.35	nd[a]	*DDX58, EIF2AK2, IFIH1, OAS1, OAS2, PTX3, TNFSF10*
Necroptosis Signaling Pathway	4.3	-2.646	*EIF2AK2, IRF9, MLKL, STAT1, STAT2, TNFSF10, ZBP1*
Role of PKR in Interferon Induction and Antiviral Response	4.09	-2.449	*DDX58, EIF2AK2, IFIH1, IRF9, STAT1, STAT2*
Role of RIG1-like Receptors in Antiviral Innate Immunity	3.83	-1	*DDX58, DHX58, IFIH1, TRIM25*
Retinoic acid Mediated Apoptosis Signaling	3.31	-2	*PARP12, PARP14, PARP9, TNFSF10*
Death Receptor Signaling	2.63	-2	*PARP12, PARP14, PARP9, TNFSF10*
UVA-Induced MAPK Signaling	2.52	nd	*PARP12, PARP14, PARP9, STAT1*
T Cell Exhaustion Signaling Pathway	2.36	-1.342	*IRF4, IRF9, LGALS9, STAT1, STAT2*
Acute Phase Response Signaling	2.32	nd	*C1R, C4A/C4B, CEBPB, LBP, OSMR*
Role of JAK1, JAK2 and TYK2 in Interferon Signaling	2.03	nd	*STAT1, STAT2*
Role of JAK family kinases in IL-6-type Cytokine Signaling	2	nd	*OSMR, STAT1*
JAK/Stat Signaling	1.89	nd	*CEBPB, STAT1, STAT2*
Complement System	1.67	nd	*C1R, C4A/C4B*
Systemic Lupus Erythematosus In B Cell Signaling Pathway	1.58	-2.236	*IFIH1, IRF9, STAT1, STAT2, TNFSF10*
Oncostatin M Signaling	1.55	nd	*OSMR, STAT1*

Table A-15. Continued.

Canonical Pathways	-Log (*P* value)	z-score	Differentially expressed genes in pathway
BAG2 Signaling Pathway	1.55	nd	*CTSB, PSMF1*
iNOS Signaling	1.51	nd	*LBP, STAT1*
p38 MAPK Signaling	1.45	nd	*MEF2B, STAT1, TIFA*
Pentose Phosphate Pathway (Non-oxidative Branch)	1.44	nd	*TKT*
Phototransduction Pathway	1.38	nd	*CNGB1, GNGT2*
IL-12 Signaling and Production in Macrophages	1.33	nd	*CEBPB, MST1, STAT1*

[a]nd means Ingenuity Pathway Analysis could not determine a z-score.

Table A-16. Gene networks altered in the endometrium of non-pregnant cows compared to the pregnant cows after infusion of pathogenic bacteria.

Gene network[a]	Score[b]	Molecules in network
Connective Tissue Disorders, Immunological Disease, Inflammatory Disease	60	ADAR, BPI, CCL8, CD160, CGAS, CMTR1, cytochrome C, DTX3L, EPSTI1, HERC5, HERC6, Hsp27, Ifi27, IFITM3, Ifn gamma, Interferon alpha, LGALS9, LITAF, LRP10, MLKL, NFkB (complex), OPTN, PARP, PARP12, PARP14, RNF114, SAMD9, SEC14L3, SPATS2L, TMEM140, Tnf (family), TRIM56, UBE2L6, USP18, XAF1
Dermatological Diseases and Conditions, Immunological Disease, Organismal Injury and Abnormalities	46	Akt, BCR (complex), Collagen type II, CYP2J2, DDX58, FAM3B, GBP1, GBP2, IFI27, IFI44, IFI6, IFIT1, IFN Beta, IgG1, IgG2b, Igm, Ikb, Interferon-α Induced, IRF4, JAK, JAK1/2, LY86, MHC CLASS I (family), MX1, MX2, PARP9, PAX5, PLAC8, SIGLEC1, SP110, SP140, SPIB, TIFA, TKT, TNFSF10
Antimicrobial Response, Infectious Diseases, Inflammatory Response	38	2' 5' oas, Alpha 1 antitrypsin, C1R, C4A/C4B, CCDC6, Complement component 1, DHX58, ERK1/2, IFIH1, IFN alpha/beta, IFN type 1, Ifnar, IRF9, Isg, ISGF3, LBP, MIA, MST1, MUC5B, nucleotidyltransferase, Oas, OAS1, OAS2, OSMR, PRSS23, PTX3, RSAD2, RTP4, SAA, Serine Protease, STAT-1/2, Stat1-Stat2, STAT2, UBA7, ZBP1
Antimicrobial Response, Cell Signaling, Inflammatory Response	26	26s Proteasome, Alp, AMPK, BATF2, BST2, caspase, Cbp/p300, CEBPB, CMPK2, Creb, CTSB, Cyclin A, Cyclin E, EIF2AK2, ERK, Hdac, HISTONE, Hsp70, IFI16, IFIT5, Ifn, IRF, MICB, PDGF BB, Pias, PML, PP2A, PSMF1, Rb, RBFOX1, RPSA, STAT1, STAT5a/b, TRIM6-TRIM34, Ubiquitin
Inflammatory Response, Molecular Transport, Small Molecule Biochemistry	26	ACBD7, ADGRF3, ATAD1, beta-estradiol, chemokine, CX3CR1, FAM135B, FGL1, GRINA, H2-T24, IFNG, IL1B, IL6, KAT5, LILRA4, LOC100911216/Pcsk1, MEF2B, MFSD5, MMRN2, MX, MX2, PLEKHA4, progesterone, SASS6, SIGLEC1, SNED1, SPAG17, SRC, TCFL5, TNFRSF1A, TRIM25, TRPV1, VDR, WDPCP, Wfdc17
Cell Cycle, Cell Death and Survival, Nervous System Development and Function	22	APP, CALML3, CBLN1, CBLN3, CHURC1, CNP, CNTN3, CPM, E2F1, EFHD1, EPB41L4A, ERMN, ESR2, FLRT1, FLRT3, GIMAP8, HAGH, HSPD1, LY6G6C, MAPRE1, MIB1, PCDH17, RBM43, RNF123, RNF213, SERTAD1, SLFN13, SNX31, STOML1, TBC1D30, TDRD7, TP63, UPK1B, UPK2, ZNF740

Table A-16. Continued.

Gene network[a]	Score[b]	Molecules in network
Lipid Metabolism, Molecular Transport, Small Molecule Biochemistry	20	Alpha catenin, CG, Ck2, CNGB1, DKK1, FSH, GPRC5A, Gsk3, Histone h3, Histone h4, HOXB5, IgG, IKK (complex), Insulin, LGALS3BP, Lh, MYO7A, PI3K (complex), PI3K (family), Pka, Pkc(s), PRC2, RAS, RNA polymerase II, Rnr, RSPO1, SHISA2, SLCO2B1, SMYD3, SRC (family), STAT, STC2, TCR, Vegf, ZNFX1
Connective Tissue Disorders, Lipid Metabolism, Small Molecule Biochemistry	10	ANXA1, Ap1, CD3, COL20A1, collagen, collagen type i (family), Collagen(s), cytokine, estrogen receptor, FCRL3, Growth hormone, Hsp90, Ige, IL1, IL12 (complex), IL12 (family), Immunoglobulin, Jnk, LDL, LY6E, Mapk, Mek, MHC Class I (complex), MHC Class II (complex), N-cor, Nfat (family), Nr1h, P38 MAPK, PLAAT3, PLIN2, Pro-inflammatory Cytokine, Rxr, SHISA5, Tgf beta, Tlr
Infectious Diseases, Molecular Transport, Post-Translational Modification	10	ADGRL1, ATP11A, ATP1B3, ATP8B4, CANX, CNNM2, DDX60L, GNB1, GNGT2, GNPTAB, HS6ST1, MCF2L, NDC1, NUP210, NUP37, OPRD1, PIGT, PRSS21, SDF2, SECTM1, SLFN12, SPATS2L, SPCS3, SPTBN5, ST3GAL2, STT3A, TEX2, TMED7, TMEM30A, TMTC3, TOR1A, UBE4A, UQCRB, VIRMA, ZCCHC2
Endocrine System Development and Function, Endocrine System Disorders, Nervous System Development and Function	2	ARNT2, CPXM2, OTX2, SIM1

[a]Enriched gene networks determined by Ingenuity Pathway Analysis using significantly differentially expressed genes only.

[b]Network score is derived from a P value and indicates the likelihood of the genes in a network being found together due to random chance. A network score of 2 or greater gives a 99% confidence the network and genes not being generated by random chance alone.

Table A-17. Predicted upstream regulators identified in the endometrium of non-pregnant cows compared to the pregnant cows after infusion of pathogenic bacteria.

Upstream Regulator	Type of molecule	Predicted state	z-score	*P*-value	Target molecules in dataset
MAPK1	kinase	Activated	4.919	8.52E-27	ADAR, BST2, CTSB, DDX58, EIF2AK2, GBP1, GBP2, HERC5, IFI16, IFI27, IFI44, IFI6, IFIH1, IFIT1, IFIT5, IFITM3, IRF9, LGALS3BP, MX2, NUP210, OAS1, OAS2, PARP12, PML, SP110, STAT1, STAT2, TDRD7, TNFSF10, TRIM25, UBE2L6, USP18
NKX2-3	transcription regulator	Activated	4.796	1.05E-21	BATF2, CMPK2, DDX58, DHX58, EIF2AK2, GBP1, GBP2, LY6E, PARP12, PARP14, PARP9, PLEKHA4, RNF213, RTP4, SAMD9, SP110, STAT1, STAT2, UBA7, UBE2L6, USP18, XAF1, ZNFX1
IL1RN	cytokine	Activated	4.583	5.76E-24	DDX58, GBP1, HERC6, IFI27, IFI44, IFI6, IFIH1, IFIT5, IRF9, LGALS9, MX1, MX2, OAS1, OAS2, PML, RSAD2, RTP4, SAMD9, STAT2, TNFSF10, USP18
TRIM24	transcription regulator	Activated	4.416	1.05E-23	CMPK2, DDX58, DHX58, EPSTI1, GBP2, HERC6, IFI44, IFIH1, IRF9, LGALS3BP, OAS1, PARP12, PLAC8, RTP4, SHISA5, STAT1, STAT2, TRIM6-TRIM34, UBA7, USP18
PNPT1	enzyme	Activated	4.333	1.02E-29	CMPK2, DDX58, EIF2AK2, GBP2, IFI16, IFI44, IFIH1, LGALS3BP, OAS1, PARP12, PARP14, PARP9, RNF213, RTP4, STAT1, STAT2, UBE2L6, USP18, XAF1
RC3H1	enzyme	Activated	4.243	1.7E-24	BST2, DDX58, IFI16, IFI27, IFI44, IFI6, IFIT1, IFITM3, IRF9, MX1, OAS1, OAS2, PARP9, RSAD2, STAT1, STAT2, TRIM25, TRIM56

Table A-17. Continued.

Upstream Regulator	Type of molecule	Predicted state	z-score	*P*-value	Target molecules in dataset
SIRT1	transcription regulator	Activated	4.121	1.16E-14	ADAR, CEBPB, CMPK2, DDX58, DHX58, DKK1, IFI44, IFITM3, LGALS3BP, LY6E, OAS1, OAS2, PARP12, PARP14, PML, RNF213, RSAD2, RTP4, SP110, STAT1, UBA7, USP18
PTGER4	G-protein coupled receptor	Activated	3.568	1.26E-11	CMPK2, DDX58, GBP2, HERC6, IFI16, IFIH1, PARP14, RNF213, RSAD2, RTP4, TNFSF10, USP18, XAF1
SOCS1	other	Activated	3.552	5.75E-12	DDX58, H2-T24, IFI16, IFI27, IFI44, IFIH1, IFIT1, MX1, OAS1, OAS2, RSAD2, STAT1, USP18
ACKR2	G-protein coupled receptor	Activated	3.464	2.97E-17	ADAR, DDX58, DHX58, EIF2AK2, IFI16, IFI44, OAS1, OAS2, RSAD2, STAT1, STAT2, USP18
SP110	transcription regulator	Activated	3.317	1.46E-09	BST2, CTSB, IFI27, IFI6, IFIH1, IFIT1, IFITM3, IRF9, MX1, OAS1, STAT1
mir-21	microRNA	Activated	3.111	1.31E-05	C1R, DHX58, GBP2, IFI16, OAS2, SIGLEC1, STAT1, STAT2, UBA7, UBE2L6
IL4	cytokine	Activated	2.977	1.68E-05	ANXA1, CCL8, CMPK2, DHX58, EIF2AK2, GBP2, IFI16, IFI44, IFIH1, IFITM3, IRF4, IRF9, LGALS3BP, PAX5, PLIN2, RNF213, STAT1, STAT2, ZBP1
IRF4	transcription regulator	Activated	2.971	6.18E-08	GBP1, IRF4, IRF9, MAPRE1, OAS1, PAX5, SPIB, STAT1, STAT2, TNFSF10
NRAS	enzyme	Activated	2.804	5.56E-07	GBP2, IFI16, Ifi27, IFIH1, IFIT1, LBP, LY86, PTX3, STAT1, USP18
IKZF3	transcription regulator	Activated	2.646	3.12E-07	DDX58, DKK1, IFI27, IFI6, IFIT5, RNF213, RTP4
USP18	peptidase	Activated	2.588	7.61E-10	IFI6, IFIH1, IFITM3, IRF9, MX1, OAS1, TNFSF10

Table A-17. Continued.

Upstream Regulator	Type of molecule	Predicted state	z-score	*P*-value	Target molecules in dataset
IL10RA	transmembrane receptor	Activated	2.53	2.85E-05	BATF2, GBP2, IFI16, MLKL, PLAAT3, RNF213, RSAD2, SLCO2B1, STAT1, ZBP1
KRAS	enzyme	Activated	2.514	2.14E-05	ADAR, CEBPB, EIF2AK2, IFI6, IFIT1, IFITM3, IRF9, MICB, MX1, MX2, OAS1, RPSA, STAT1, STAT2, TNFSF10
STAT6	transcription regulator	Activated	2.492	1.56E-09	ANXA1, CCL8, CMPK2, CTSB, DHX58, EIF2AK2, GBP2, IFI16, IFI44, IFIH1, IFITM3, IRF4, IRF9, LGALS3BP, RNF213, STAT2, ZBP1
miR-199a-5p (and other miRNAs w/seed CCAGUGU)	mature microRNA	Activated	2.449	7.13E-06	CMPK2, GPRC5A, IFI27, MX2, RSAD2, ZBP1
TAB1	enzyme	Activated	2.433	3.54E-08	GBP1, GBP2, IFIH1, IFIT1, TNFSF10, XAF1
IKZF1	transcription regulator	Activated	2.419	6.69E-08	CYP2J2, DKK1, DTX3L, EPSTI1, IFI16, IFI27, IFI6, IFIT5, IRF4, PAX5, RNF213, RTP4
TREX1	enzyme	Activated	2.405	1.97E-09	IFI16, IFI44, IFIT1, MX1, OAS1, USP18
NGLY1	enzyme	Activated	2.386	7.64E-08	IFI27, IFI44, IFIT1, OAS1, RSAD2, USP18
MYC	transcription regulator	Activated	2.261	1.45E-07	CNP, CTSB, DKK1, GBP2, HERC5, IFI16, IFI27, IFI44, IFI6, IFIH1, IFIT1, IFIT5, IRF4, IRF9, MX1, MX2, OAS1, PAX5, PML, RPSA, RSAD2, STAT1, TKT, TNFSF10, USP18
PIK3CG	kinase	Activated	2.236	5.51E-04	GBP2, OAS2, STAT1, TNFSF10, ZBP1
ISG15	other	Activated	2.222	1.88E-10	DDX58, IFI6, IFITM3, MX1, OAS1
GAPDH	enzyme	Activated	2.2	2.91E-06	IFI6, OAS1, OAS2, STAT1, UBE2L6
mir-155	microRNA	Activated	2.198	9.31E-04	CEBPB, IRF4, IRF9, MX1, STAT1
PRDM1	transcription regulator	Activated	2.184	2.30E-04	CD160, IRF4, PAX5, PLAC8, RSAD2, SLCO2B1, SPIB, TNFSF10

Table A-17. Continued.

Upstream Regulator	Type of molecule	Predicted state	z-score	*P*-value	Target molecules in dataset
CLDN7	other	Activated	2.157	1.10E-06	DKK1, GRINA, IFI44, IFI6, MX1, PLAAT3, PRSS23, UBE2L6
BCL6	transcription regulator	Activated	2.156	1.69E-05	CGAS, HERC5, HERC6, IRF4, IRF9, LITAF, PRSS23, STAT1, UBA7
BTK	kinase	Activated	2.121	7.03E-07	CEBPB, IFIT1, IRF4, IRF9, MX1, MX2, OAS2, STAT1
Irgm1	other	Activated	2	1.97E-04	IFI16, OAS2, RSAD2, USP18
SAMHD1	enzyme	Activated	2	1.01E-06	DDX58, IFI27, IFI6, MX1
Brd4	kinase	Inhibited	-2	1.21E-03	C1R, H2-T24, LY86, TNFSF10
DOCK8	other	Inhibited	-2	9.34E-04	CMPK2, RSAD2, STAT1, STAT2
SYVN1	transporter	Inhibited	-2	1.24E-02	GPRC5A, HERC5, IFI44, LGALS3BP
TNK1	kinase	Inhibited	-2	3.31E-06	IFI16, IFIH1, OAS2, TNFSF10
P38 MAPK	group	Inhibited	-2.024	2.61E-03	BATF2, CCL8, CEBPB, GBP1, MUC5B, PML, STAT1, TNFSF10
REL	transcription regulator	Inhibited	-2.169	3.95E-03	IRF4, PARP14, PLAAT3, RSAD2, SASS6, TNFSF10
CGAS	enzyme	Inhibited	-2.199	4.34E-07	IFI44, IFIT1, OAS1, RSAD2, USP18
IFNA5	cytokine	Inhibited	-2.2	1.73E-08	CCL8, IFIH1, IFIT1, MX1, ZBP1
IFNA6	cytokine	Inhibited	-2.2	1.73E-08	CCL8, IFIH1, IFIT1, MX1, ZBP1
IFNA7	cytokine	Inhibited	-2.2	1.73E-08	CCL8, IFIH1, IFIT1, MX1, ZBP1
IFNA8	cytokine	Inhibited	-2.2	2.58E-08	CCL8, IFIH1, IFIT1, MX1, ZBP1
IFNA10	cytokine	Inhibited	-2.2	1.73E-08	CCL8, IFIH1, IFIT1, MX1, ZBP1
IFNA14	cytokine	Inhibited	-2.2	1.73E-08	CCL8, IFIH1, IFIT1, MX1, ZBP1
IFNA16	cytokine	Inhibited	-2.2	2.58E-08	CCL8, IFIH1, IFIT1, MX1, ZBP1
IFNA21	cytokine	Inhibited	-2.2	1.73E-08	CCL8, IFIH1, IFIT1, MX1, ZBP1

Table A-17. Continued.

Upstream Regulator	Type of molecule	Predicted state	z-score	*P*-value	Target molecules in dataset
CHUK	kinase	Inhibited	-2.211	1.11E-02	CEBPB, CTSB, GBP2, IFI16, PTX3
IRF9	transcription regulator	Inhibited	-2.213	9.41E-15	GBP1, IFI27, IFIT1, IFITM3, MX1, OAS2, RTP4, STAT1, STAT2, TNFSF10, ZBP1
IL1A	cytokine	Inhibited	-2.219	2.09E-02	C4A/C4B, CCL8, GBP1, LGALS9, PTX3
JAK1/2	group	Inhibited	-2.219	8.44E-05	EIF2AK2, GBP2, MX1, PLAC8, RSAD2
PARP9	enzyme	Inhibited	-2.219	7.25E-08	IFI44, IFIT1, OAS2, SP110, STAT1
IFNL3	cytokine	Inhibited	-2.23	9.50E-07	DDX58, MX1, RSAD2, STAT1, USP18
DUSP1	phosphatase	Inhibited	-2.236	8.30E-04	CMPK2, DKK1, IFIT1, MX1, PLIN2
SAMSN1	other	Inhibited	-2.236	2.73E-04	CMPK2, PML, RSAD2, STAT1, STAT2
SASH1	other	Inhibited	-2.236	8.44E-05	CMPK2, PML, RSAD2, STAT1, STAT2
SNCA	enzyme	Inhibited	-2.236	5.48E-02	CTSB, GBP2, MX1, PLAC8, RSAD2
OSM	cytokine	Inhibited	-2.268	1.29E-05	ANXA1, C1R, CPM, GBP1, GBP2, IRF9, LBP, LITAF, LY6G6C, MX1, OAS1, OSMR, STAT1, UBE2L6
IFN alpha/ beta	group	Inhibited	-2.39	1.21E-05	IFI16, LY6E, RSAD2, STAT1, STAT2, TNFSF10
TICAM1	other	Inhibited	-2.408	3.11E-04	CMPK2, DDX58, IFI16, IFIT1, RSAD2, TNFSF10
IKBKB	kinase	Inhibited	-2.423	9.91E-03	CEBPB, CTSB, GBP2, IFI16, MX1, PTX3
STAT4	transcription regulator	Inhibited	-2.433	5.57E-04	DDX58, IFIH1, IRF4, PLAC8, SERTAD1, STAT1, STC2
IKBKG	kinase	Inhibited	-2.438	2.38E-04	CEBPB, CTSB, GBP2, IFI16, PTX3, TNFSF10
IFNAR2	transmembr ane receptor	Inhibited	-2.449	1.12E-18	DDX58, HERC5, IFI44, IFI6, IFIH1, MX2, OAS1, OAS2, TNFSF10, UBA7, UBE2L6, USP18, XAF1
IFNK	cytokine	Inhibited	-2.449	5.05E-09	EIF2AK2, IFIH1, MX1, OAS1, STAT1, ZBP1

Table A-17. Contined.

Upstream Regulator	Type of molecule	Predicted state	z-score	*P*-value	Target molecules in dataset
JAK1	kinase	Inhibited	-2.449	2.83E-07	EIF2AK2, IRF9, MX1, OSMR, STAT1, STAT2, USP18
MSC	transcription regulator	Inhibited	-2.449	1.52E-06	EPSTI1, IFI27, IFI44, IFIT1, PAX5, XAF1
SMARCB1	transcription regulator	Inhibited	-2.449	7.68E-04	C4A/C4B, EIF2AK2, IFI16, LBP, MX1, OAS1
DDX58	enzyme	Inhibited	-2.541	7.35E-13	DDX58, EIF2AK2, IFI27, IFI44, IFIH1, IFIT1, OAS1, RSAD2, STAT1, STAT2, TNFSF10
STING1	other	Inhibited	-2.586	4.35E-09	CGAS, IFI16, IFI44, IFITM3, OAS1, PLEKHA4, RSAD2, USP18
NFkB (complex)	complex	Inhibited	-2.591	7.71E-04	C1R, CCL8, CEBPB, GBP2, HERC5, IRF4, LITAF, MUC5B, PTX3, RSAD2, SPIB, TNFSF10
IFNL4	cytokine	Inhibited	-2.624	3.87E-14	DDX58, DHX58, IFIH1, MX1, OAS1, OAS2, STAT1
PAF1	other	Inhibited	-2.646	2.26E-08	DDX58, HERC5, IFI44, IFITM3, OAS2, SERTAD1, ZNFX1
IL21	cytokine	Inhibited	-2.714	1.59E-08	CMPK2, EIF2AK2, HERC6, IFI16, IFIT1, IRF4, OAS2, PAX5, RSAD2, STAT2, USP18
TLR4	transmembrane receptor	Inhibited	-2.752	1.09E-06	BPI, CCL8, CMPK2, GBP2, IFI16, IFITM3, MX1, PML, PTX3, RSAD2, STAT1, STAT2, TNFSF10
Ifn gamma	complex	Inhibited	-2.777	2.07E-07	ADAR, EIF2AK2, GBP1, LGALS9, PML, STAT1, TNFSF10, XAF1
IL27	cytokine	Inhibited	-2.788	3.98E-06	BST2, EIF2AK2, GBP2, MX1, OAS1, STAT1, STAT2, TNFSF10
IFNE	cytokine	Inhibited	-2.795	2.36E-10	BST2, HERC5, IFIH1, IFITM3, MX2, STAT1, USP18, ZBP1
FADD	other	Inhibited	-2.828	9.01E-08	DDX58, DHX58, EIF2AK2, IFIH1, LY6E, RNF114, STAT1, STAT2

Table A-17. Continued.

Upstream Regulator	Type of molecule	Predicted state	z-score	*P*-value	Target molecules in dataset
JAK	group	Inhibited	-2.828	2.36E-10	DDX58, EIF2AK2, IFI6, IFIH1, IFIT1, IFITM3, RSAD2, STAT1
IFNA4	cytokine	Inhibited	-2.93	1.05E-11	CCL8, GBP2, H2-T24, IFIH1, IFIT1, MX1, RSAD2, USP18, ZBP1
TNFSF10	cytokine	Inhibited	-2.95	1.62E-08	CTSB, EIF2AK2, IFI16, IFI27, IFI6, IFIT1, IRF9, STAT1, TNFSF10
IFNAR1	transmembrane receptor	Inhibited	-2.969	9.9E-17	CGAS, CMPK2, EIF2AK2, IFI16, IFI44, IFI6, IFIH1, MX2, OAS1, OAS2, PARP12, RSAD2, RTP4, STAT1, TNFSF10, USP18, XAF1
ELAVL1	other	Inhibited	-3	6.78E-09	CCL8, IFI16, Ifi27, IFI44, IFIH1, IFITM3, IRF9, LGALS3BP, OAS1, OAS2, STAT1, USP18
CD3	complex	Inhibited	-3.022	2.69E-06	ANXA1, BST2, C1R, GBP1, GPRC5A, IFIT1, IRF4, IRF9, MST1, PLIN2, PSMF1, STAT1, TNFSF10, TRIM25, UBE2L6, XAF1
IL6	cytokine	Inhibited	-3.073	1.33E-04	ANXA1, BST2, CEBPB, FGL1, GBP2, IFI16, IFIT1, IFITM3, IRF4, IRF9, LBP, LY86, SP110, STAT1, TNFSF10
TLR7	transmembrane receptor	Inhibited	-3.138	1.28E-08	CEBPB, DKK1, IFI44, IFIT1, IRF9, MX1, MX2, OAS2, PTX3, RSAD2, STAT1, STAT2
SMARCA4	transcription regulator	Inhibited	-3.24	4.59E-05	CEBPB, CNP, CPM, CTSB, GBP1, IFI16, IFI27, IFIT1, IFITM3, MICB, PLIN2, PTX3, SERTAD1, TNFSF10
TLR3	transmembrane receptor	Inhibited	-3.26	1.89E-17	CMPK2, CPM, DDX58, DHX58, EIF2AK2, GBP2, HERC5, IFI16, IFI44, IFI6, IFIH1, IFIT1, MX1, MX2, OAS1, PTX3, RSAD2, STAT1, TNFSF10, USP18, ZNFX1
IFN type 1	group	Inhibited	-3.264	5.1E-18	BST2, CGAS, DDX58, DHX58, EIF2AK2, IFI16, IFIH1, IFIT1, PML, STAT1, STAT2, TNFSF10, UBA7

Table A-17. Continued.

Upstream Regulator	Type of molecule	Predicted state	z-score	*P*-value	Target molecules in dataset
TLR9	transmembrane receptor	Inhibited	-3.302	4.84E-09	CPM, IFI16, IFIT1, IRF4, IRF9, MX1, MX2, OAS2, RSAD2, STAT1, STAT2, TNFSF10, USP18
PML	transcription regulator	Inhibited	-3.44	6.13E-10	BST2, EPSTI1, HERC6, IFI27, IFI44, IFIH1, IFIT1, MX1, OAS1, OAS2, PML, STAT1
Ifn	group	Inhibited	-3.53	7.25E-13	DDX58, DHX58, EIF2AK2, IFI16, IFIH1, IFIT1, IFITM3, MX1, OAS2, PML, RSAD2, STAT1, ZBP1
IL1B	cytokine	Inhibited	-3.669	5.79E-11	ANXA1, C1R, CCL8, CEBPB, CMPK2, CTSB, GBP1, GBP2, HERC5, IFI16, IFIT1, IRF4, LBP, LGALS9, MEF2B, MIA, MUC5B, MX1, OAS2, OSMR, PTX3, RPSA, RSAD2, STAT1, TNFSF10, UBE2L6, USP18
MAVS	other	Inhibited	-3.691	2.27E-19	ADAR, CGAS, CMPK2, DDX58, DHX58, IFIT1, IFITM3, OAS1, OAS2, PARP12, RSAD2, STAT1, STAT2, UBE2L6, USP18
SPI1	transcription regulator	Inhibited	-3.695	1.27E-11	CMPK2, IFI27, IFI44, IFI6, IFIT1, IFITM3, IRF4, IRF9, LY6E, MX1, PARP12, PML, RSAD2, SP110, TNFSF10, USP18
EIF2AK2	kinase	Inhibited	-3.705	4.96E-17	CEBPB, DDX58, EIF2AK2, IFI27, IFI6, IFIT1, IFIT5, LGALS3BP, OAS1, PARP12, PARP9, SP140, STAT1, UBE2L6, USP18
IRF5	transcription regulator	Inhibited	-3.791	2.34E-19	CMPK2, DDX58, DHX58, IFI44, IFIH1, IFIT1, IFITM3, OAS1, OAS2, PARP12, RSAD2, SP110, STAT1, STAT2, TNFSF10, UBE2L6
TGM2	enzyme	Inhibited	-3.86	1.63E-11	IFI6, IFIT1, IFIT5, IRF9, LGALS9, LY6E, OAS1, OAS2, PARP14, PARP9, RNF213, SP110, STAT1, UBA7, XAF1

Table A-17. Continued.

Upstream Regulator	Type of molecule	Predicted state	z-score	*P*-value	Target molecules in dataset
RNY3	other	Inhibited	-3.873	6.86E-27	BATF2, EPSTI1, HERC5, IFI44, IFIT1, IFITM3, LY6E, MX1, OAS1, OAS2, RSAD2, RTP4, SIGLEC1, SPATS2L, XAF1
APP	other	Inhibited	-3.906	1.97E-06	C1R, C4A/C4B, CMPK2, CTSB, DDX58, DKK1, GBP2, HERC6, IFI16, IFIH1, IRF4, LBP, PARP14, PAX5, RNF213, RSAD2, RTP4, TNFSF10, USP18, XAF1
IFNA1/IFNA13	cytokine	Inhibited	-3.914	1.51E-22	CCL8, DHX58, EIF2AK2, IFI27, IFI6, IFIH1, IFIT1, MX1, OAS1, OAS2, RSAD2, SIGLEC1, STAT1, STAT2, UBE2L6, ZBP1
Ifnar	group	Inhibited	-4.165	4.37E-22	DDX58, EIF2AK2, GBP2, IFI16, IFIH1, IFITM3, IRF9, OAS1, OAS2, RNF213, RSAD2, STAT1, STAT2, TNFSF10, UBE2L6, USP18, XAF1, ZBP1
IRF1	transcription regulator	Inhibited	-4.679	2.95E-26	C1R, CMPK2, DDX58, EIF2AK2, GBP2, IFI27, IFI44, IFI6, IFIH1, IFIT1, IFIT5, IFITM3, IRF4, IRF9, MX1, OAS1, OAS2, PLAAT3, PML, RSAD2, SP110, STAT1, STAT2, TNFSF10, XAF1
IFN Beta	group	Inhibited	-4.687	5.5E-26	BST2, CEBPB, DDX58, EIF2AK2, HERC5, IFI16, IFI27, IFI44, IFI6, IFIH1, IFIT1, IRF9, MX1, MX2, OAS1, OAS2, RSAD2, STAT1, STAT2, TNFSF10, USP18, XAF1, ZBP1

Table A-17. Continued.

Upstream Regulator	Type of molecule	Predicted state	z-score	*P*-value	Target molecules in dataset
TNF	cytokine	Inhibited	-4.73	2.55E-14	ANXA1, BST2, C4A/C4B, CEBPB, CNP, CTSB, DDX58, DKK1, EIF2AK2, GBP1, GBP2, HERC5, IFI16, IFI27, IFI6, IFIH1, IFIT1, IFIT5, IRF4, LBP, LGALS9, LITAF, MIA, MST1, MX1, OAS1, OAS2, OPTN, OSMR, PARP14, PLAAT3, PLIN2, PML, PRSS23, PTX3, RPSA, SAMD9, SLCO2B1, STAT1, TDRD7, TIFA, TNFSF10, TRIM56
IFNB1	cytokine	Inhibited	-4.804	3.61E-25	BST2, CMPK2, DDX58, DHX58, EIF2AK2, GBP2, HERC5, IFI16, IFI27, IFI6, IFIH1, IFIT1, IRF9, MX1, OAS1, OAS2, PARP12, PARP14, PML, RSAD2, STAT1, STAT2, TNFSF10, TRIM6-TRIM34, UBA7, USP18, XAF1, ZBP1
STAT1	transcription regulator	Inhibited	-4.872	8.7E-29	BATF2, BST2, C1R, C4A/C4B, CMPK2, EIF2AK2, EPSTI1, GBP1, GBP2, HERC6, IFI16, IFI27, IFI44, IFI6, IFIH1, IFIT1, IFITM3, IRF9, LY6E, MX1, OAS1, OAS2, PARP9, RNF213, RSAD2, RTP4, SP110, STAT1, STAT2, TNFSF10, USP18, XAF1, ZBP1
IRF3	transcription regulator	Inhibited	-5.062	2.56E-28	ADAR, CMPK2, DDX58, DHX58, EIF2AK2, GBP1, IFI16, IFI27, IFI44, IFI6, IFIH1, IFIT1, IFITM3, OAS1, OAS2, PARP12, PARP14, PLAC8, PML, RSAD2, STAT1, STAT2, TDRD7, TNFSF10, UBE2L6, USP18, ZBP1

Table A-17. Continued.

Upstream Regulator	Type of molecule	Predicted state	z-score	*P*-value	Target molecules in dataset
IFNL1	cytokine	Inhibited	-5.536	2.17E-49	BST2, CMPK2, DDX58, EIF2AK2, GBP1, HERC5, HERC6, IFI27, IFI44, IFI6, IFIH1, IFIT1, IFIT5, IFITM3, IRF9, LGALS3BP, MLKL, MX1, OAS1, OAS2, PML, RSAD2, RTP4, SAMD9, SP110, STAT1, STAT2, TDRD7, TMEM140, UBE2L6, USP18, XAF1
Interferon alpha	group	Inhibited	-5.589	2.68E-44	ADAR, BST2, CGAS, CMTR1, DDX58, DHX58, EIF2AK2, EPSTI1, GBP1, GBP2, HERC5, HERC6, IFI16, IFI27, Ifi27, IFI44, IFI6, IFIH1, IFIT1, IFITM3, IRF4, IRF9, LGALS9, MX1, MX2, OAS1, OAS2, PARP12, PARP14, PARP9, PML, RNF213, RSAD2, RTP4, SAMD9, SEC14L3, SIGLEC1, SP110, STAT1, STAT2, TDRD7, TMEM140, TNFSF10, UBA7, UBE2L6, USP18, ZBP1
IRF7	transcription regulator	Inhibited	-5.605	3.68E-40	ADAR, CCL8, CMPK2, DDX58, DHX58, GBP1, HERC5, IFI16, IFI44, IFI6, IFIH1, IFIT1, IFITM3, IRF9, MICB, MX1, MX2, OAS1, OAS2, PARP12, PARP14, PLAC8, RSAD2, RTP4, STAT1, STAT2, TDRD7, TNFSF10, UBA7, UBE2L6, USP18, XAF1, ZBP1
PRL	cytokine	Inhibited	-6.037	1.79E-38	ADAR, BST2, CMPK2, CTSB, DDX58, DHX58, DTX3L, EIF2AK2, EPSTI1, HERC5, HERC6, IFI44, IFI6, IFIH1, IFIT1, IFIT5, IRF9, LY6E, MLKL, MX2, OAS1, OAS2, PARP12, PARP14, RPSA, RSAD2, SAMD9, SHISA5, SP110, STAT1, STAT2, TDRD7, TMEM140, TRIM25, USP18, XAF1, ZCCHC2

Table A-17. Continued.

Upstream Regulator	Type of molecule	Predicted state	z-score	*P*-value	Target molecules in dataset
IFNA2	cytokine	Inhibited	-6.207	1.6E-47	ANXA1, BST2, C1R, CCL8, CMPK2, CNP, DDX58, EIF2AK2, GBP1, GBP2, HERC5, HERC6, IFI16, IFI27, IFI44, IFI6, IFIH1, IFIT1, IFIT5, IFITM3, IRF9, LGALS3BP, LY6E, MX1, MX2, OAS1, OAS2, PARP12, PARP9, PML, RSAD2, SAMD9, SP110, STAT1, TDRD7, TNFSF10, UBA7, UBE2L6, USP18, XAF1, ZBP1
IFNG	cytokine	Inhibited	-7.075	2.54E-26	BATF2, BST2, C1R, C4A/C4B, CCL8, CEBPB, CGAS, CMPK2, CTSB, DDX58, DKK1, DTX3L, EIF2AK2, GBP1, GBP2, HERC6, IFI16, IFI27, IFI44, IFI6, IFIH1, IFIT1, IFIT5, IFITM3, IRF4, IRF9, LGALS3BP, LGALS9, LY6E, MLKL, MX1, MX2, OAS1, OAS2, OPTN, PARP14, PARP9, PLAAT3, PML, PSMF1, PTX3, RNF114, RSAD2, RTP4, SAMD9, SP110, STAT1, STAT2, TNFSF10, UBE2L6, USP18, XAF1

Table A-18. Differentially expressed endometrial genes in non-pregnant cows compared to pregnant cows after intrauterine infusion with pathogenic bacteria ($Log_2FC \geq 1.5$ or ≤ -1.5).

Gene ID	Symbol	Type	Log_2FC	Adj *P* Value
100137953	*ATP8B4*	protein-coding	-2.088	4.83E-06
522469	*BATF2*	protein-coding	-1.678	3.54E-04
280734	*BPI*	protein-coding	-1.664	1.14E-02
529166	*CBLN3*	protein-coding	-1.598	1.10E-08
101904723	*CCDC194*	protein-coding	-1.540	9.64E-03
281044	*CCL8*	protein-coding	-1.943	4.31E-04
784304	*CMPK2*	protein-coding	-2.905	2.10E-13
281702	*CNGB1*	protein-coding	-2.352	6.72E-06
513281	*CPM*	protein-coding	-1.524	1.69E-02
504760	*DDX58*	protein-coding	-3.146	1.75E-21
508378	*DHX58*	protein-coding	-2.279	1.27E-09
504445	*DKK1*	protein-coding	-1.502	6.30E-04
515051	*DTX3L*	protein-coding	-2.240	1.53E-06
347700	*EIF2AK2*	protein-coding	-2.497	3.64E-11
614555	*EPSTI1*	protein-coding	-2.896	2.17E-18
618755	*FAM135B*	protein-coding	1.917	4.41E-06
514701	*FAM3B*	protein-coding	-2.058	2.06E-06
515085	*FCRL3*	protein-coding	-1.506	3.83E-02
788007	*FLRT1*	protein-coding	1.865	2.05E-04
281797	*GNGT2*	protein-coding	-1.736	8.23E-04
514373	*HERC5*	protein-coding	-1.994	9.73E-07
527520	*HERC6*	protein-coding	-2.781	2.57E-14
506759	*IFI16*	protein-coding	-2.261	2.44E-14
507138	*IFI27*	protein-coding	-2.510	3.64E-11
508348	*IFI44*	protein-coding	-3.223	9.88E-18
512913	*IFI6*	protein-coding	-2.925	9.25E-13
535490	*IFIH1*	protein-coding	-2.128	7.60E-09
515091	*IFIT5*	protein-coding	-2.250	1.46E-11
777594	*IFITM3*	protein-coding	-1.717	4.39E-07
282255	*IFITM3(1-8U)*	protein-coding	-2.097	4.64E-06
509855	*IRF9*	protein-coding	-1.757	2.12E-06
617420	*ISG12(B)*	protein-coding	-1.723	7.25E-03
100139670	*LOC100139670*	protein-coding	-3.996	2.42E-21
100141258	*LOC100141258*	protein-coding	-1.501	2.56E-02
100336669	*LOC100336669*	protein-coding	-1.525	2.55E-03
100848263	*LOC100848263*	protein-coding	-1.512	3.72E-02

Table A-18 Continued.

Gene ID	Symbol	Type	Log_2FC	Adj *P* Value
101903402	*LOC101903402*	ncRNA	-1.503	1.43E-03
101903765	*LOC101903765*	pseudo	-1.960	7.33E-04
101907799	*LOC101907799*	ncRNA	-3.292	1.54E-15
104974749	*LOC104974749*	ncRNA	1.880	1.62E-03
104975106	*LOC104975106*	pseudo	1.658	5.13E-03
104975612	*LOC104975612*	ncRNA	1.596	1.21E-02
107132327	*LOC107132327*	protein-coding	-1.721	1.34E-03
112441507	*LOC112441507*	protein-coding	-3.974	1.88E-22
112442264	*LOC112442264*	ncRNA	1.749	4.86E-03
112446427	*LOC112446427*	protein-coding	-1.532	1.30E-04
112449099	*LOC112449099*	protein-coding	1.562	2.25E-02
509283	*LOC509283*	protein-coding	-2.527	1.00E-13
510382	*LOC510382*	pseudo	-3.738	4.77E-17
511531	*LOC511531*	protein-coding	-1.532	1.30E-02
514978	*LOC514978*	protein-coding	-3.008	4.60E-14
614402	*LOC614402*	protein-coding	-2.056	2.73E-04
618737	*LOC618737*	protein-coding	-3.015	4.40E-11
790255	*LOC790255*	protein-coding	1.506	2.30E-02
505805	*LY6G6C*	protein-coding	-1.506	2.57E-02
100271851	*MEF2B*	protein-coding	1.662	1.15E-02
790225	*MLKL*	protein-coding	-1.500	5.10E-03
280872	*MX1*	protein-coding	-3.544	1.19E-27
280873	*MX2*	protein-coding	-4.386	1.58E-30
347699	*OAS1X*	protein-coding	-3.194	3.10E-21
654488	*OAS1Y*	protein-coding	-3.182	2.09E-21
519922	*OAS1Z*	protein-coding	-2.883	9.71E-13
529660	*OAS2*	protein-coding	-3.435	2.17E-19
513185	*PARP12*	protein-coding	-2.088	1.98E-10
540789	*PARP14*	protein-coding	-2.742	3.54E-16
510532	*PARP9*	protein-coding	-1.731	2.01E-07
538371	*PAX5*	protein-coding	-1.707	8.08E-03
767910	*PLAC8B*	protein-coding	-1.988	2.05E-04
100138545	*PML*	protein-coding	-1.681	1.39E-05
617807	*PSMF1*	protein-coding	-1.687	9.18E-06
541148	*PTX3*	protein-coding	-1.677	3.06E-04
521304	*RBFOX1*	protein-coding	1.564	2.11E-02
506415	*RSAD2*	protein-coding	-4.446	2.98E-32

Table A-18. Continued.

Gene ID	Symbol	Type	Log_2FC	Adj *P* Value
532442	*RTP4*	protein-coding	-2.728	1.32E-12
514205	*SAMD9*	protein-coding	-2.524	2.69E-09
286871	*SERPINA14*	protein-coding	-1.516	3.41E-02
539759	*SIGLEC1*	protein-coding	-2.050	4.04E-07
515204	*SP110*	protein-coding	-2.190	2.54E-14
510377	*SP140*	protein-coding	-1.602	7.42E-05
784460	*SPIB*	protein-coding	-1.663	1.05E-02
510814	*STAT1*	protein-coding	-1.639	1.50E-03
540573	*STC2*	protein-coding	-1.527	5.13E-03
783855	*TIFA*	protein-coding	-1.524	1.21E-02
507215	*TNFSF10*	protein-coding	-1.632	1.52E-04
497204	*UBA7*	protein-coding	-2.442	4.37E-09
282113	*UPK1B*	protein-coding	-2.032	1.81E-04
515202	*USP18*	protein-coding	-3.589	7.16E-28
509740	*XAF1*	protein-coding	-2.597	4.21E-13
508333	*ZBP1*	protein-coding	-2.565	3.04E-09
539807	*ZNFX1*	protein-coding	-2.720	2.16E-16

Table A-19. Differentially expressed genes in the endometrium of non-pregnant cows compared to pregnant cows in using previously published studies (Log_2FC compared to pregnant).

Gene ID	Symbol	Type	Infected d 16	Healthy d 15	Healthy d 16	Healthy d 17
504445	*DKK1*	protein-coding	-1.50	-2.05	-2.79	-1.98
347700	*EIF2AK2*	protein-coding	-2.49	-2.98	-5.51	-2.97
506759	*IFI16*	protein-coding	-2.26	-2.48	-5.18	-2.85
507138	*IFI27*	protein-coding	-2.51	-3.08	-6.38	-2.55
512913	*IFI6*	protein-coding	-2.93	-2.46	-8.77	-2.79
535490	*IFIH1*	protein-coding	-2.13	-2.44	-5.57	-2.71
515091	*IFIT5*	protein-coding	-2.25	-2.20	-5.41	-2.25
509855	*IRF9*	protein-coding	-1.76	-2.56	-4.87	-2.73
509283	*LOC509283*	protein-coding	-3.74	-2.92	-5.98	-3.48
280872	*MX1*	protein-coding	-3.54	-3.64	-14.69	-3.18
280873	*MX2*	protein-coding	-4.39	-5.32	-52.59	-7.81
513185	*PARP12*	protein-coding	-2.09	-2.12	-3.20	-2.39
540789	*PARP14*	protein-coding	-2.74	-2.53	-6.32	-3.13
510532	*PARP9*	protein-coding	-1.73	-1.80	-3.65	-2.26
767910	*PLAC8B*	protein-coding	-1.99	-2.28	-6.86	-3.09
506415	*RSAD2*	protein-coding	-4.45	-4.84	-36.62	-5.00
532442	*RTP4*	protein-coding	-2.73	-3.34	-5.50	-3.83
539759	*SIGLEC1*	protein-coding	-2.05	-2.27	-4.86	-4.91
510814	*STAT1*	protein-coding	-1.64	-1.69	-3.72	-1.51
783855	*TIFA*	protein-coding	-1.52	-1.63	-3.30	-2.96
497204	*UBA7*	protein-coding	-2.44	-3.27	-8.62	-3.80
515202	*USP18*	protein-coding	-3.59	-3.64	-14.55	-4.33
509740	*XAF1*	protein-coding	-2.60	-2.69	-6.62	-3.25
539807	*ZNFX1*	protein-coding	-2.72	-2.77	-5.26	-3.01
101904723	*CCDC194*	protein-coding	-1.54			

Table A-19. Continued.

Gene ID	Symbol	Type	Infected d 16	Healthy d 15	Healthy d 16	Healthy d 17
281702	*CNGB1*	protein-coding	-2.35			
513281	*CPM*	protein-coding	-1.52			
618755	*FAM135B*	protein-coding	1.92			
515085	*FCRL3*	protein-coding	-1.51			
788007	*FLRT1*	protein-coding	1.87			
777594	*IFITM3*	protein-coding	-1.72			
282255	*IFITM3(1-8U)*	protein-coding	-2.10			
100141258	*LOC100141258*	protein-coding (uncharacterized)	-1.50			
100336669	*LOC100336669*	protein-coding (*GBP4*)	-1.53			
100848263	*LOC100848263*	protein-coding (*SLFN12*)	-1.51			
101903402	*LOC101903402*	ncRNA	-1.50			
101903765	*LOC101903765*	pseudo	-1.96			
101907799	*LOC101907799*	ncRNA	-3.29			
104974749	*LOC104974749*	ncRNA	1.88			
104975106	*LOC104975106*	pseudo	1.66			
104975612	*LOC104975612*	ncRNA	1.60			
107132327	*LOC107132327*	protein-coding (*CYP2J2L*)	-1.72			
112442264	*LOC112442264*	ncRNA	1.75			
112446427	*LOC112446427*	protein-coding (uncharacterized)	-1.53			
112449099	*LOC112449099*	protein-coding (uncharacterized)	1.56			
614402	*LOC614402*	protein-coding (*HRASLS3*)	-2.06			
790255	*LOC790255*	protein-coding (*LILRA6*)	1.51			
100271851	*MEF2B*	protein-coding	1.66			
538371	*PAX5*	protein-coding	-1.71			
521304	*RBFOX1*	protein-coding	1.56			
784460	*SPIB*	protein-coding	-1.66			

Table A-19. Continued.

Gene ID	Symbol	Type	Infected d 16	Healthy d 15	Healthy d 16	Healthy d 17
540573	*STC2*	protein-coding	-1.53			
510774	*ABHD1*	protein-coding		-1.51	-2.31	-3.21
505134	*ADAR*	protein-coding		-1.65	-2.81	-2.08
511001	*CLEC4F*	protein-coding		-2.93	-77.35	-8.66
615107	*CXCL10*	protein-coding		-2.95	-4.55	-3.53
613313	*GBP4*	protein-coding		-2.59	-7.11	-2.69
508347	*IFI44L*	protein-coding		-3.83	-18.09	-5.09
281871	*ISG15*	protein-coding		-5.24	-54.69	-5.07
506604	*ISG20*	protein-coding		-3.19	-13.44	-7.14
508877	*PNPT1*	protein-coding		-2.39	-3.41	-2.95
280701	*PPA1*	protein-coding		-1.64	-2.45	-2.38
507549	*TIMD4*	protein-coding		-1.64	-3.01	-4.14
509859	*TRANK1*	protein-coding		-1.57	-2.57	-2.35

Table A-20. Altered canonical pathways in the endometrium of non-pregnant cows compared to pregnant cows using previously published studies. Infected day 16[a], Healthy day 15[b], Healthy day 16[c], Healthy day 17[d].

	Bacteria infused day 16		Healthy day 15		Healthy day 16		Healthy day 17	
Canonical Pathways	$-Log_{10}(P)$ z-score	Molecules	$-Log_{10}(P)$ z-score	Molecules	$-Log_{10}(P)$ z-score	Molecules	$-Log_{10}(P)$ z-score	Molecules
Interferon Signaling	10.7 -2.45	IFI6, IFIT1, IFITM3, IRF9, MX1, OAS1, STAT1	13.00 -2.65	IFI6, IFIT1, IFITM1, IRF9, ISG15, MX1, OAS1, STAT1	13.8 -3.16	IFI35, IFI6, IFIT1, IFIT3, IRF9, ISG15, MX1, OAS1, STAT1, STAT2, TAP1	14 -2.53	IFI35, IFI6, IFITM1, IRF9, ISG15, MX1, OAS1, SOCS1, STAT1, STAT2, TAP1
Activation of IRF by Cytosolic Pattern Recognition Receptors	7.32 -1.63	DDX58, DHX58, IFIH1, IRF9, STAT1, ZBP1	12.70 -1.00	ADAR, DDX58, DHX58, IFIH1, IRF7, IRF9, ISG15, STAT1, ZBP1	9.54 -1.90	ADAR, CD40, IFIH1, IFIT2, IRF3, IRF9, ISG15, STAT1, STAT2, ZBP1	11.1 -1.51	ADAR, CD40, DDX58, DHX58, IFIH1, IFIT2, IRF7, IRF9, ISG15, STAT1, STAT2
Role of PKR in Interferon Induction and Antiviral Response	4.45 -2.24	DDX58, EIF2AK2, IFIH1, IRF9, STAT1	4.61 -2.24	DDX58, EIF2AK2, IFIH1, IRF9, STAT1	4.89 -2.83	CASP8, EIF2AK2, FCGR1A, IFIH1, IRF3, IRF9, STAT1, STAT2	6.02 -2.838	ATF3, DDX58, EIF2AK2, FCGR1A, IFIH1, IRF9, PYCARD, STAT1, STAT2
Role of Pattern Recognition Receptors in Recognition of Bacteria and Viruses	6.24 nd[a]	DDX58, EIF2AK2, IFIH1, OAS1, OAS2, PTX3, TNFSF10	5.21 -2.00	DDX58, EIF2AK2, IFIH1, IRF7, OAS1, TNFSF10	6.71 -2.24	C1QB, C1QC, C3AR1, EIF2AK2, IFIH1, IRF3, OAS1, OAS2, RNASEL, TNFSF10, TNFSF13B	5.03 -2.449	C1QB, C1QC, DDX58, EIF2AK2, IFIH1, IRF7, OAS1, PTX3, TNFSF13B
Systemic Lupus Erythematosus In B Cell Signaling Pathway	2.74 -2.24	IFIH1, IRF9, LILRA6, STAT1, TNFSF10	4.79 -2.65	IFIH1, IRF7, IRF9, ISG15, ISG20, STAT1, TNFSF10	5.76 -3.05	CCND1, CD40, IFIH1, IFIT2, IFIT3, IRF3, IRF9, ISG15, ISG20, STAT1, STAT2, TNFSF10, TNFSF13B	3.77 -3.16	CD40, IFIH1, IFIT2, IRF7, IRF9, ISG15, ISG20, STAT1, STAT2, TNFSF13B

Table A-20. Continued.

	Bacteria infused day 16		Healthy day 15		Healthy day 16		Healthy day 17	
Canonical Pathways	-Log10 (*P*) z-score	Molecules	-Log10 (*P*) z-score	Molecules	-Log10 (*P*) z-score	Molecules	-Log10 (*P*) z-score	Molecules
Role of RIG1-like Receptors in Antiviral Innate Immunity	3.44 nd	DDX58, DHX58, IFIH1	5.07 -1.00	DDX58, DHX58, IFIH1, IRF7	3.15 -2	CASP8, IFIH1, IRF3, TRIM25	3.22 -1	DDX58, DHX58, IFIH1, IRF7
Coronavirus Pathogenesis Pathway	1.92 nd	DDX58, IRF9, STAT1	4.09 2.24	DDX58, EIF4E, IRF7, IRF9, STAT1	3.31 1.134	CASP8, CCND1, IRF3, IRF9, STAT1, STAT2, TRIM25	2.67 1.633	DDX58, IRF7, IRF9, PYCARD, STAT1, STAT2
Necroptosis Signaling Pathway	4.97 -2.45	EIF2AK2, IRF9, MLKL, STAT1, TNFSF10, ZBP1	4.00 -2.24	EIF2AK2, IRF9, STAT1, TNFSF10, ZBP1	5.70 -2.53	CASP8, EIF2AK2, IRF3, IRF9, MLKL, RIPK3, STAT1, STAT2, TNFSF10, ZBP1	2.57 -2.45	EIF2AK2, IRF9, MLKL, PYCARD, STAT1, STAT2
UVA-Induced MAPK Signaling	3.57 nd	PARP12, PARP14, PARP9, STAT1	3.69 nd	PARP12, PARP14, PARP9, STAT1	4.47 nd	PARP10, PARP12, PARP14, PARP9, PLCL2, STAT1, TIPARP	1.96 nd	PARP12, PARP14, PARP9, STAT1
Retinoic acid Mediated Apoptosis Signaling	4.4 -2.00	PARP12, PARP14, PARP9, TNFSF10	4.53 -2.00	PARP12, PARP14, PARP9, TNFSF10	5.89 -2.646	CASP8, PARP10, PARP12, PARP14, PARP9, TIPARP, TNFSF10	1.80 nd	PARP12, PARP14, PARP9
Death Receptor Signaling	3.70 -2	PARP12, PARP14, PARP9, TNFSF10	3.82 -2.00	PARP12, PARP14, PARP9, TNFSF10	4.68 -2.646	CASP8, PARP10, PARP12, PARP14, PARP9, TIPARP, TNFSF10	1.33 nd	PARP12, PARP14, PARP9

Table A-20. Continued.

	Bacteria infused day 16		Healthy day 15		Healthy day 16		Healthy day 17	
Canonical Pathways	-Log_{10} (*P*) z-score	Molecules	-Log_{10} (*P*) z-score	Molecules	-Log_{10} (*P*) z-score	Molecules	-Log_{10} (*P*) z-score	Molecules
iNOS Signaling	2.05 nd	LBP, STAT1						
Phototransduction Pathway	1.91 nd	CNGB1, GNGT2						
Toll-like receptor signaling	1.62 nd	EIF2AK2, LBP						
IL-7 signaling pathway	1.60 nd	PAX5, STAT1						
Salvage pathways of pyrimidine ribonucleotides	1.41 nd	CMPK2, EIF2AK2						

[a]nd means Ingenuity Pathway Analysis could not determine a z-score.

Table A-21. Predicted upstream regulators in the endometrium of non-pregnant cows compared to pregnant cows using previously published studies. Predicted activation state was either activated (+) or inhibited (-).

	Bacteria infused day 16		Healthy day 15		Healthy day 16		Healthy day 17	
Predicted upstream regulator	+/- z -score *P* value	Molecules	+/- z -score *P* value	Molecules	+/- z -score *P* value	Molecules	+/- z -score *P* value	Molecules
ACKR2	+ 3.16 1.21E-16	DDX58, DHX58, EIF2AK2, IFI16, IFI44, OAS1, OAS2, RSAD2, STAT1, USP18	+ 3.74 9.28E-26	ADAR, CXCL10, DDX58, DHX58, EIF2AK2, IFI16, IFI44, IRF7, ISG15, ISG20, OAS1, RSAD2, STAT1, USP18	+ 3.87 3.53E-20	ADAR, CCL11, CXCL10, EIF2AK2, IFI16, IFIT2, IFIT3, ISG15, ISG20, OAS1, OAS2, RSAD2, STAT1, STAT2, USP18	+ 4.00 2.30E-22	ADAR, CXCL10, DDX58, DHX58, EIF2AK2, IFI16, IFI44, IFIT2, IRF7, ISG15, ISG20, OAS1, RSAD2, STAT1, STAT2, USP18
APP	- -3.78 5.41E-08	CMPK2, DDX58, DKK1, GBP2, HERC6, IFI16, IFIH1, LBP, PARP14, PAX5, RNF213, RSAD2, RTP4, TNFSF10, USP18, XAF1	- -3.90 3.35E-11	C4A/C4B, CRYM, CXCL10, DDX58, DKK1, FABP3, GBP4, HERC6, IFI16, IFIH1, IRF7, ISG20, PARP14, RNF213, RSAD2, RTP4, TNFSF10, USP18, XAF1	- -3.90 7.10E-12	C1S, C4A/C4B, CCL11, CCND1, CD40, CMPK2, COL13A1, CXCL10, DKK1, FCGR1A, GBP2, GBP4, GBP6, HERC6, IDO1, IFI16, IFI35, IFIH1, IFIT2, IRF3, IRF4, ISG20, KYNU, MAPT, NAMPT, PARP14, RNASEL, RNF213, RNF24, RSAD2, RTP4, TNFSF10, TRIM21, USP18, XAF1	- -3.49 6.42E-10	CD40, CD69, CD86, CRYM, CXCL10, DDX58, DKK1, EPAS1, FABP3, FAP, FCGR1A, GBP4, H19, IDO1, IFI16, IFI35, IFIH1, IFIT2, IRF7, ISG20, MCM10, NCDN, PARP14, PYCARD, RNF213, RSAD2, RTP4, SHISA3, SOCS1, USP18, XAF1

Table A-21. Continued.

	Bacteria infused day 16		Healthy day 15		Healthy day 16		Healthy day 17	
Predicted upstream regulator	+/- z -score *P* value	Molecules	+/- z -score *P* value	Molecules	+/- z -score *P* value	Molecules	+/- z -score *P* value	Molecules
BTK	+ 2.45 2.13E-06	IFIT1, IRF9, MX1, MX2, OAS2, STAT1	+ 3.16 2.03E-12	CXCL10, IFI44L, IFIT1, IFITM1, IRF9, ISG15, ISG20, MX1, MX2, STAT1	+ 3.86 3.49E-13	CD274, CD40, CXCL10, IFI35, IFI44L, IFIT1, IFIT3, IRF4, IRF9, ISG15, ISG20, MX1, MX2, OAS2, STAT1	+ 3.42 2.76E-12	CCR7, CD40, CD69, CD86, CXCL10, IFI35, IFI44L, IFITM1, IRF9, ISG15, ISG20, MX1, MX2, STAT1
CD3	- -2.55 1.08E-03	BST2, GBP1, IFIT1, IRF9, PSMF1, STAT1, TNFSF10, XAF1	- -2.52 4.25E-07	BST2, CXCL10, EIF4E, GBP1, IFIT1, IFITM1, IRF9, PPA1, SP100, STAT1, TNFSF10, XAF1	- -3.20 5.24E-08	ANXA1, C2, CASP8, CCND1, CD274, CD53, COX7A1, CXCL10, GBP1, IFI35, IFIT1, IRF4, IRF9, MAP3K8, NAMPT, PPA1, PSMF1, STAT1, SYT7, TNFSF10, TRIM25, UBE2L6, XAF1	- -3.18 2.16E-05	ALAS1, C2, CD69, CD86, CREM, CXCL10, GBP1, H19, IFI35, IFITM1, IRF9, PPA1, PSMF1, SMPDL3B, SOCS1, STAT1, UBE2L6, XAF1
CGAS	- -2.20 1.59E-08	IFI44, IFIT1, OAS1, RSAD2, USP18	- -2.97 2.40E-17	CXCL10, IFI44, IFI44L, IFIT1, IRF7, ISG15, OAS1, RSAD2, USP18	- -2.95 9.80E-13	CXCL10, IFI44L, IFIT1, IFIT2, IFIT3, ISG15, OAS1, RSAD2, USP18	- -2.97 6.04E-13	CXCL10, IFI44, IFI44L, IFIT2, IRF7, ISG15, OAS1, RSAD2, USP18
DDX58	- -2.38 2.70E-14	DDX58, EIF2AK2, IFI27, IFI44, IFIH1, IFIT1, OAS1, RSAD2, STAT1, TNFSF10	- -3.04 2.68E-22	CXCL10, DDX58, EIF2AK2, IFI27, IFI44, IFIH1, IFIT1, IRF7, ISG15, ISG20, OAS1, RSAD2, STAT1, TNFSF10	- -3.63 1.52E-19	CASP4, CXCL10, EIF2AK2, IFI27, IFI35, IFIH1, IFIT1, IFIT2, IFIT3, IRF3, ISG15, ISG20, OAS1, RSAD2, STAT1, STAT2, TNFSF10	- -3.17 1.51E-21	CASP4, CXCL10, DDX58, EIF2AK2, IFI27, IFI35, IFI44, IFIH1, IFIT2, IRF7, ISG15, ISG20, NMI, OAS1, RSAD2, SOCS1, STAT1, STAT2

Table A-21. Continued.

	Bacteria infused day 16		Healthy day 15		Healthy day 16		Healthy day 17	
Predicted upstream regulator	+/- z -score *P* value	Molecules	+/- z -score *P* value	Molecules	+/- z -score *P* value	Molecules	+/- z -score *P* value	Molecules
EIF2AK2	- -3.43 3.46E-16	DDX58, EIF2AK2, IFI27, IFI6, IFIT1, IFIT5, OAS1, PARP12, PARP9, SP140, STAT1, USP18	- -3.82 4.61E-22	DDX58, EIF2AK2, IFI27, IFI6, IFIT1, IFIT5, IFITM1, ISG15, ISG20, OAS1, PARP12, PARP9, SP140, STAT1, USP18	- -3.82 1.25E-15	CCND1, EIF2AK2, IFI27, IFI35, IFI6, IFIT1, IFIT5, ISG15, ISG20, LGALS3BP, OAS1, PARP12, PARP9, STAT1, UBE2L6, USP18	- -4.28 2.84E-20	ATF3, DDX58, EIF2AK2, IFI27, IFI35, IFI6, IFIT5, IFITM1, ISG15, ISG20, LGALS3BP, NMI, OAS1, PARP12, PARP9, SP140, STAT1, UBE2L6, USP18
Ifn	- -3.53 1.07E-16	DDX58, DHX58, EIF2AK2, IFI16, IFIH1, IFIT1, IFITM3, MX1, OAS2, PML, RSAD2, STAT1, ZBP1	- -3.92 2.90E-24	CXCL10, DDX58, DHX58, EIF2AK2, IFI16, IFIH1, IFIT1, IFITM1, IRF7, ISG15, ISG20, MX1, PML, RSAD2, SP100, STAT1, ZBP1	- -4.57 1.44E-23	B2M, CASP8, CD40, CXCL10, EIF2AK2, IDO1, IFI16, IFIH1, IFIT1, IL23A, IRF3, ISG15, ISG20, MX1, OAS2, PML, RNASEL, RSAD2, STAT1, TAP1, TNFSF13B, TRIM21, ZBP1	- -4.15 3.16E-21	CD40, CD58, CD69, CD86, CXCL10, DDX58, DHX58, EIF2AK2, IDO1, IFI16, IFIH1, IFITM1, IRF7, ISG15, ISG20, MX1, RSAD2, SOCS1, STAT1, TAP1, TNFSF13B
IFN Beta	- -4.59 2.71E-31	BST2, CMPK2, DDX58, EIF2AK2, HERC5, IFI16, IFI27, IFI44, IFI6, IFIH1, IFIT1, IRF9, MX1, MX2, OAS1, OAS2, RSAD2, STAT1, TNFSF10, USP18, XAF1, ZBP1	- -4.70 4.87E-36	BST2, CXCL10, DDX58, EIF2AK2, IFI16, IFI27, IFI44, IFI6, IFIH1, IFIT1, IFITM1, IRF7, IRF9, ISG15, MX1, MX2, OAS1, PNPT1, RSAD2, STAT1, TNFSF10, USP18, XAF1, ZBP1	- -5.45 1.32E-34	C3AR1, CASP4, CD274, CD40, CMPK2,CXCL10,EIF2AK2,HERC5,IDO1, IFI16,IFI27, IFI35,IFI6,IFIH1,IFIT1,IFIT2,IFIT3,IRF9,ISG15,MX1,MX2, OAS1,OAS2,PNPT1,RSAD2,STAT1,STAT2,TNFSF10, USP18, USP25, XAF1, ZBP1	- -5.01 7.85E-34	ATF3, CASP4, CCR7, CD40, CD69, CD86, CXCL10, DDX58, EIF2AK2, IDO1,IFI16,IFI27,IFI35,IFI44,IFI6,IFIH1,IFIT2,IFITM1,IRF7, IRF9,ISG15,MX1,MX2,OAS1,PNPT1,RSAD2,SOCS1,STAT1,STAT2,USP18, XAF1

Table A-21. Continued.

	Bacteria infused day 16		Healthy day 15		Healthy day 16		Healthy day 17	
Predicted upstream regulator	+/- z -score *P* value	Molecules	+/- z -score *P* value	Molecules	+/- z -score *P* value	Molecules	+/- z -score *P* value	Molecules
Ifn gamma	-2.42 8.41E-07	EIF2AK2, GBP1, PML, STAT1, TNFSF10, XAF1	-2.95 1.70E-11	ADAR,CXCL10,EIF2AK2,GBP1,IFI44L,PML,STAT1,TNFSF10,XAF1	-3.26 2.75E-09	ADAR,CXCL10,EIF2AK2,GBP1,IFI44L,LGALS9,PML,PSME2,STAT1,TNFSF10,XAF1	-2.48 2.24E-08	ADAR,CD86,CXCL10,EIF2AK2,GBP1,IFI44L,LGALS9,SOCS1,STAT1,XAF1
IFN type 1	+3.11 8.25E-18	BST2, DDX58, DHX58, EIF2AK2, IFI16, IFIH1, IFIT1, PML, STAT1, TNFSF10, UBA7	+3.37 2.26E-22	BST2,CXCL10,DDX58,DHX58,EIF2AK2,IFI16,IFIH1,IFIT1,ISG15,PML,STAT1,TNFSF10,UBA7	+3.38 6.95E-19	CGAS,CXCL10,EIF2AK2,IDO1,IFI16,IFIH1,IFIT1,IFIT2,ISG15,PML,STAT1,STAT2,TNFSF10,TNFSF13B,UBA7	+3.38 1.47E-17	CD69,CXCL10,DDX58,DHX58,EIF2AK2,IDO1,IFI16,IFIH1,IFIT2,ISG15,STAT1,STAT2,TNFSF13B,UBA7
IFNA1/ IFNA13	-3.66 3.47E-23	CCL8, DHX58, EIF2AK2, IFI27, IFI6, IFIH1, IFIT1, MX1, OAS1, OAS2, RSAD2, SIGLEC1, STAT1, ZBP1	-4.01 2.97E-30	CCL8,CXCL10,DHX58,EIF2AK2,IFI27,IFI6,IFIH1,IFIT1,IFITM1,IRF7,ISG15,MX1,OAS1,RSAD2,SIGLEC1,STAT1,ZBP1	-4.27 1.21E-24	CD274,CD40,CXCL10,EIF2AK2,IFI27,IFI6,IFIH1,IFIT1,IFIT2,ISG15,MX1,OAS1,OAS2,RSAD2,SIGLEC1,STAT1,STAT2,UBE2L6,ZBP1	-4.57 1.39E-30	CCL8,CD40,CD69,CD86,CXCL10,DHX58,EIF2AK2,IFI27,IFI6,IFIH1,IFIT2,IFITM1,IRF7,ISG15,MX1,OAS1,RSAD2,SIGLEC1,SOCS1,STAT1,STAT2,UBE2L6
IFNA10	-2.20 6.16E-10	CCL8, IFIH1,IFIT1, MX1, ZBP1	-2.59 5.69E-15	CCL8,CXCL10,IFIH1,IFIT1,ISG15,MX1,ZBP1	-2.40 1.97E-09	CXCL10,IFIH1,IFIT1,ISG15,MX1,ZBP1	-2.19 1.07E-07	CCL8,CXCL10,IFIH1,ISG15,MX1
IFNA14	-2.20 6.16E-10	CCL8, IFIH1,IFIT1, MX1, ZBP1	-2.59 5.69E-15	CCL8,CXCL10,IFIH1,IFIT1,ISG15,MX1,ZBP1	-2.40 1.97E-09	CXCL10,IFIH1,IFIT1,ISG15,MX1,ZBP1	-2.19 1.07E-07	CCL8,CXCL10,IFIH1,ISG15,MX1
IFNA16	-2.20 9.21E-10	CCL8, IFIH1,IFIT1, MX1, ZBP1	-2.59 1.06E-14	CCL8,CXCL10,IFIH1,IFIT1,ISG15,MX1,ZBP1	-2.40 3.26E-09	CXCL10,IFIH1,IFIT1,ISG15,MX1,ZBP1	-2.19 1.60E-07	CCL8,CXCL10,IFIH1,ISG15,MX1

Table A-21. Continued.

	Bacteria infused day 16		Healthy day 15		Healthy day 16		Healthy day 17	
Predicted upstream regulator	+/- z -score *P* value	Molecules	+/- z -score *P* value	Molecules	+/- z -score *P* value	Molecules	+/- z -score *P* value	Molecules
IFNA2	-5.71 5.88E-48	BST2, CCL8, CMPK2, DDX58, EIF2AK2, GBP1, GBP2, HERC5, HERC6, IFI16, IFI27, IFI44, IFI6, IFIH1, IFIT1, IFIT5, IFITM3, IRF9, MX1, MX2, OAS1, OAS2, PARP12, PARP9, PML, RSAD2, SAMD9, SP110, STAT1, TNFSF10, UBA7, USP18, XAF1, ZBP1	-5.90 1.73E-53	BST2, CCL8, CXCL10,DDX58, EIF2AK2,GBP1, GBP4,HERC6, IFI16,IFI27,IFI44, IFI44L,IFI6,IFIH1, IFIT1,IFIT5,IFITM1,IRF7,IRF9,ISG15,ISG20,MX1,MX2,OAS1, PARP12, PARP9,PML, RSAD2,SAMD9, SP100,STAT1, TNFSF10,UBA7, USP18,XAF1, ZBP1	-7.02 9.08E-56	ANXA1,B2M,C1S, CD274,CMPK2, CXCL10,EIF2AK2, GBP1,GBP2,GBP4,HERC5,HERC6, HSH2D,IDO1,IFI16,IFI27,IFI35,IFI44L, IFI6,IFIH1,IFIT1, IFIT2,IFIT3,IFIT5, IRF9,ISG15,ISG20, LAMP3,LGALS3BP,LY6E,MX1,MX2, OAS1,OAS2,PARP12,PARP9,PML, RSAD2,SHFL, SLC15A3,SP110, STAT1,TAP1, TDRD7,TNFSF10, TREX1,TRIM21, UBA7,UBE2L6,USP18,XAF1,ZBP1	-6.45 3.03E-43	BCL2L14,CCL8,CD69,CD86,CNP,CXCL10,DDX58,EIF2AK2,GBP1,GBP4,IDO1,IFI16,IFI27,IFI35,IFI44,IFI44L,IFI6,IFIH1,IFIT2,IFIT5,IFITM1,IRF7,IRF9,ISG15,ISG20,LGALS3BP,LY6E,MX1,MX2,OAS1,PARP12,PARP9,RSAD2,SAMD9,SOCS1,STAT1,TAP1,TDRD7,TREX1,UBA7,UBE2L6,USP18,XAF1
IFNA21	-2.20 6.16E-10	CCL8, IFIH1, IFIT1, MX1, ZBP1	-2.59 5.69E-15	CCL8, CXCL10, IFIH1, IFIT1, ISG15,MX1,ZBP1	-2.40 1.97E-09	CXCL10,IFIH1, IFIT1,ISG15,MX1, ZBP1	-2.18 1.07E-07	CCL8,CXCL10, IFIH1,ISG15,MX1
IFNA4	-2.76 2.37E-12	CCL8, GBP2, IFIH1, IFIT1, MX1, RSAD2, USP18, ZBP1	-3.06 1.52E-16	CCL8, CXCL10, GBP5, IFIH1, IFIT1,ISG15,MX1,RSAD2,USP18, ZBP1	-3.17 8.57E-18	CD274,CXCL10, GBP2, H2-T24, IFIH1,IFIT1,IFIT2,ISG15,MAP3K8,MX1,PMEPA1,RSAD2, USP18,ZBP1	-3.37 8.41E-15	CCL8,CD69,CD86, CXCL10,GBP5, H2-T24, IFIH1,IFIT2,ISG15, MX1,RSAD2, USP18

Table A-21. Continued.

	Bacteria infused day 16		Healthy day 15		Healthy day 16		Healthy day 17	
Predicted upstream regulator	+/- z -score *P* value	Molecules	+/- z -score *P* value	Molecules	+/- z -score *P* value	Molecules	+/- z -score *P* value	Molecules
IFNA5	- -2.20 6.16E-10	CCL8, IFIH1, IFIT1, MX1, ZBP1	- -2.59 5.69E-15	CCL8,CXCL10, IFIH1,IFIT1,ISG15 , MX1,ZBP1	- -2.40 1.97E-09	CXCL10,IFIH1, IFIT1,ISG15,MX1, ZBP1	- -2.19 1.07E-07	CCL8,CXCL10, IFIH1,ISG15,MX 1
IFNA6	- -2.20 6.16E-10	CCL8, IFIH1, IFIT1, MX1, ZBP1	- -2.59 5.69E-15	CCL8, CXCL10, IFIH1, IFIT1, ISG15, MX1, ZBP1	- -2.40 1.97E-09	CXCL10, IFIH1, IFIT1, ISG15, MX1, ZBP1	- -2.19 1.07E-07	CCL8, CXCL10, IFIH1, ISG15, MX1
IFNA7	- -2.20 6.16E-10	CCL8, IFIH1, IFIT1, MX1, ZBP1	- -2.59 5.69E-15	CCL8, CXCL10, IFIH1, IFIT1, ISG15, MX1, ZBP1	- -2.40 1.97E-09	CXCL10, IFIH1, IFIT1, ISG15, MX1, ZBP1	- -2.19 1.07E-07	CCL8, CXCL10, IFIH1, ISG15, MX1
IFNA8	- -2.20 9.21E-10	CCL8, IFIH1, IFIT1, MX1, ZBP1	- -2.60 1.06E-14	CCL8, CXCL10, IFIH1, IFIT1, ISG15, MX1, ZBP1	- -2.41 3.26E-09	CXCL10, IFIH1, IFIT1, ISG15, MX1, ZBP1	- -2.20 1.60E-07	CCL8, CXCL10, IFIH1, ISG15, MX1
Ifnar	- -3.92 1.41E-23	DDX58, EIF2AK2, GBP2, IFI16, IFIH1, IFITM3, IRF9, OAS1, OAS2, RNF213, RSAD2, STAT1, TNFSF10, USP18, XAF1, ZBP1	- -4.13 4.31E-28	CXCL10, DDX58, EIF2AK2, IFI16, IFIH1, IRF7, IRF9, ISG15, ISG20, OAS1, PNPT1, RNF213, RSAD2, STAT1, TNFSF10, USP18, XAF1, ZBP1	- -5.28 6.08E-36	B2M, CD274, CD40, CXCL10, EIF2AK2, GBP2, IDO1, IFI16, IFI35, IFIH1, IFIT2, IFIT3, IRF9, ISG15, ISG20, OAS1, OAS2, PNPT1, RNF213, RSAD2, STAT1, STAT2, TAP1, TNFSF10, TRIM21, UBE2L6, USP18, XAF1, ZBP1	- -4.89 7.33E-30	CD40, CD86, CXCL10, DDX58, EIF2AK2, IDO1, IFI16, IFI35, IFIH1, IFIT2, IRF7, IRF9, ISG15, ISG20, NLRC5, OAS1, PNPT1, RNF213, RSAD2, STAT1, STAT2, TAP1, UBE2L6, USP18, XAF1

Table A-21. Continued.

	Bacteria infused day 16		Healthy day 15		Healthy day 16		Healthy day 17	
Predicted upstream regulator	+/- z -score *P* value	Molecules	+/- z -score *P* value	Molecules	+/- z -score *P* value	Molecules	+/- z -score *P* value	Molecules
IFNAR1	- -2.80 5.42E-20	CMPK2, EIF2AK2, IFI16, IFI44, IFI6, IFIH1, MX2, OAS1, OAS2, PARP12, RSAD2, RTP4, STAT1, TNFSF10, USP18, XAF1	- -2.96 8.61E-26	CXCL10, EIF2AK2, GBP4, IFI16, IFI44, IFI6, IFIH1, IFITM1, IRF7, ISG15, MX2, OAS1, PARP12, RSAD2, RTP4, STAT1, TNFSF10, USP18, XAF1	- -3.47 1.48E-30	B2M, CD274, CD40, CGAS, CMPK2, CXCL10, EIF2AK2, F2, GBP4, HSH2D, IDO1, IFI16, IFI6, IFIH1, IFIT2, IFIT3, ISG15, LAMP3, MX2, OAS1, OAS2, PARP12, RSAD2, RTP4, STAT1, TNFSF10, TNFSF13B, USP18, USP25, XAF1	- -3.55 1.68E-25	ATF3, BCL2L14, CD40, CD86, CXCL10, EIF2AK2, GBP4, IDO1, IFI16, IFI44, IFI6, IFIH1, IFIT2, IFITM1, IRF7, ISG15, MX2, OAS1, PARP12, RSAD2, RTP4, SOCS1, STAT1, TNFSF13B, USP18, XAF1
IFNAR2	- -2.24 1.89E-20	DDX58, HERC5, IFI44, IFI6, IFIH1, MX2, OAS1, OAS2, TNFSF10, UBA7, USP18, XAF1	- -2.24 2.82E-25	CXCL10, DDX58, GBP4, IFI44, IFI6, IFIH1, IFITM1, ISG15, MX2, OAS1, TNFSF10, UBA7, USP18, XAF1	- -2.65 4.51E-25	CXCL10, GBP4, HERC5, HSH2D, IDO1, IFI6, IFIH1, ISG15, LAMP3, MX2, OAS1, OAS2, PSME2, TNFSF10, UBA7, UBE2L6, USP18, XAF1	- -2.45 8.39E-22	BCL2L14, CXCL10, DDX58, GBP4, IDO1, IFI44, IFI6, IFIH1, IFITM1, ISG15, MX2, OAS1, UBA7, UBE2L6, USP18, XAF1

Table A-21. Continued.

	Bacteria infused day 16		Healthy day 15		Healthy day 16		Healthy day 17	
Predicted upstream regulator	+/- z -score *P* value	Molecules	+/- z -score *P* value	Molecules	+/- z -score *P* value	Molecules	+/- z -score *P* value	Molecules
IFNB1	- -4.70 8.18E-31	BST2, CMPK2, DDX58, DHX58, EIF2AK2, GBP2, HERC5, IFI16, IFI27, IFI6, IFIH1, IFIT1, IRF9, MX1, OAS1, OAS2, PARP12, PARP14, PML, RSAD2, STAT1, TNFSF10, UBA7, USP18, XAF1, ZBP1	- -5.06 4.65E-37	BST2, CXCL10, DDX58, DHX58, EIF2AK2, GBP4, GBP5, IFI16, IFI27, IFI6, IFIH1, IFIT1, IFITM1, IRF7, IRF9, ISG15, ISG20, MX1, OAS1, PARP12, PARP14, PML, RSAD2, STAT1, TNFSF10, UBA7, USP18, XAF1, ZBP1	- -5.67 6.60E-32	CASP8, CD274, CD40, CMPK2, CXCL10, EIF2AK2, GBP2, GBP4, GBP6, HERC5, IDO1, IFI16, IFI27, IFI6, IFIH1, IFIT1, IFIT2, IFIT3, IRF3, IRF9, ISG15, ISG20, MX1, OAS1, OAS2, PARP12, PARP14, PML, RNASEL, RSAD2, STAT1, STAT2, TNFSF10, TRIM21, UBA7, USP18, XAF1, ZBP1	- -5.35 5.44E-29	CD40, CD86, CREM, CRYAB, CXCL10, DDX58, DHX58, EIF2AK2, GBP4, GBP5, IDO1, IFI16, IFI27, IFI6, IFIH1, IFIT2, IFITM1, IRF7, IRF9, ISG15, ISG20, MCM10, MX1, NMI, NT5C3A, OAS1, PARP12, PARP14, RSAD2, SOCS1, STAT1, STAT2,UBA7, USP18,XAF1
IFNE	- -2.80 1.10E-12	BST2, HERC5, IFIH1, IFITM3, MX2, STAT1, USP18, ZBP1	- -3.13 4.39E-19	BST2, CXCL10, EIF4E, IFIH1, ISG15, ISG20, MX2, SLC7A2, STAT1, USP18, ZBP1	- -3.13 2.00E-13	CD40, CXCL10, HERC5, IFIH1, IFIT2, ISG15, ISG20, MX2, STAT1, USP18, ZBP1	- -2.97 4.28E-12	CD40, CD86, CXCL10, IFIH1, IFIT2, ISG15, ISG20, MX2, STAT1, USP18

Table A-21. Continued.

	Bacteria infused day 16		Healthy day 15		Healthy day 16		Healthy day 17	
Predicted upstream regulator	+/- z -score *P* value	Molecules	+/- z -score *P* value	Molecules	+/- z -score *P* value	Molecules	+/- z -score *P* value	Molecules
IFNG	- -6.13 1.93E-27	BATF2, BST2, CCL8, CMPK2, DDX58, DKK1, DTX3L, EIF2AK2, GBP1, GBP2, HERC6, IFI16, IFI27, IFI44, IFI6, IFIH1, IFIT1, IFIT5, IFITM3, IRF9, MLKL, MX1, MX2, OAS1, OAS2,PARP14, PARP9,PLAAT3, PML,PSMF1, PTX3,RSAD2, RTP4, SAMD9,SP110, STAT1,TNFSF10, USP18,XAF1	- -6.16 4.54E-29	BST2, C4A/C4B, CCL8,CXCL10, DDX58,DKK1,DTX3L,EIF2AK2, GBP1, GBP4,GBP5, HERC6,IFI16, IFI27,IFI44,IFI44L, IFI6,IFIH1,IFIT1, IFIT5,IFITM1,IRF7,IRF9,ISG15,ISG20,MX1,MX2,OAS1, PARP14,PARP9, PML,RSAD2,RTP4,SAMD9,SP100, STAT1,TNFSF10,USP18,XAF1	- -7.69 3.22E-46	AGRN,B2M,BATF2, C1QB,C1QC,C2,C4A/C4B,CASP4,CASP8,CCL11,CCND1, CD274,CD40,CGAS,CMPK2,CXCL10, DKK1,DTX3L,EDNRB,EIF2AK2,ESM1, FCGR1A,GBP1,GBP2,GBP4,GBP6,HERC6,IDO1,IFI16,IFI27,IFI35,IFI44L,IFI6,IFIH1,IFIT1,IFIT2,IFIT3,IFIT5,IL23A,IRF3,IRF4,IRF9,ISG15,ISG20,KRT17,KYNU,LAMP3,LGALS3BP,LGALS9,LY6E, MAP3K8,MLKL,MST1R,MX1,MX2,NAMPT,OAS1,OAS2, OPTN,P2RY14,PARP14,PARP9,PLAUR,PML,PSMA2,PSME2,PSMF1,RNF114,RSAD2,RTP4,SCLY,SLC15A3,SLC40A1,SOAT1,SP110,STAT1,STAT2,SYT7,TAP1,TNFSF10, TNFSF13B,TREM2, TRIM21,UBE2L6, USP18,XAF1	- -7.42 8.60E-33	ABLIM3,ALOX12, ALOX5AP,ARG2, ATF3,C1QB,C1QC, C2,CALHM6, CASP4,CCL8, CD40,CD86,CFB, CREM,CXCL10, DDX58,DKK1, EIF2AK2,FBP1, FCGR1A,GBP1, GBP4,GBP5,IDO1, IFI16,IFI27,IFI35, IFI44,IFI44L,IFI6, IFIH1,IFIT2,IFIT5, IFITM1,IRF7,IRF9, ISG15,ISG20, KRT17,LGALS3BP, LGALS9,LY6E, MLKL,MST1R,MX1,MX2,NCF2,NLRC5,NMI,OAS1, PARP14,PARP9, PIGR,PSMF1, PTX3,RSAD2, RTP4,SAMD9, SCNN1A,SLC12A2,SOCS1,STAT1,STAT2,TAP1,TNFSF13B,UBE2L6,USP18,WARS1,XAF1

Table A-21. Continued.

	Bacteria infused day 16		Healthy day 15		Healthy day 16		Healthy day 17	
Predicted upstream regulator	+/- z -score *P* value	Molecules	+/- z -score *P* value	Molecules	+/- z -score *P* value	Molecules	+/- z -score *P* value	Molecules
IFNK	-2.45 9.20E-11	EIF2AK2,IFIH1,MX1,OAS1,STAT1,ZBP1	-2.45 3.98E-13	CXCL10,EIF2AK2,IFIH1,MX1,OAS1,STAT1,ZBP1	-2.65 2.59E-11	CD40,CXCL10,EIF2AK2,IFIH1,MX1,OAS1,STAT1,ZBP1	-2.65 1.69E-11	CD40,CD86,CXCL10,EIF2AK2,IFIH1,MX1,OAS1,STAT1
IFNL1	-5.08 3.49E-48	BST2,CMPK2,DDX58,EIF2AK2,GBP1,HERC5,HERC6,IFI27,IFI44,IFI6,IFIH1,IFIT1,IFIT5,IFITM3,IRF9,MLKL,MX1,OAS1,OAS2,PML,RSAD2,RTP4,SAMD9,SP110,STAT1,USP18,XAF1	-5.19 1.21E-51	BST2,CXCL10,DDX58,EIF2AK2,GBP1,GBP5,HERC6,IFI27,IFI44,IFI44L,IFI6,IFIH1,IFIT1,IFIT5,IFITM1,IRF9,ISG15,ISG20,MX1,OAS1,PML,RSAD2,RTP4,SAMD9,SP100,STAT1,USP18,XAF1	-6.04 1.24E-54	CD40,CMPK2,CXCL10,EIF2AK2,GBP1,HERC5,HERC6,IFI27,IFI35,IFI44L,IFI6,IFIH1,IFIT1,IFIT2,IFIT3,IFIT5,IRF9,ISG15,ISG20,LAMP3,LGALS3BP,MLKL,MX1,OAS1,OAS2,PML,RSAD2,RTP4,SHFL,SLC15A3,SP110,STAT1,STAT2,TDRD7,TMEM140,UBE2L6,USP18,XAF1	-5.71 1.16E-47	ATF3,CCR7,CD40,CXCL10,DDX58,EIF2AK2,GBP1,GBP5,IFI27,IFI35,IFI44,IFI44L,IFI6,IFIH1,IFIT2,IFIT5,IFITM1,IRF9,ISG15,ISG20,LGALS3BP,MLKL,MX1,OAS1,RSAD2,RTP4,SAMD9,STAT1,STAT2,TDRD7,TMEM140,UBE2L6,USP18,XAF1
IFNL3	-2.42 6.57E-10	DDX58,IFIH1,MX1,RSAD2,STAT1,USP18	-2.60 4.19E-12	DDX58,IFIH1,ISG20,MX1,RSAD2,STAT1,USP18	-2.76 3.90E-10	IFIH1,IL23A,ISG20,MX1,RNASEL,RSAD2,STAT1,USP18	-2.00 8.17E-06	CXCL10,IRF7,MX1,RSAD2
IFNL4	-2.80 4.08E-18	DDX58,DHX58,IFIH1,IFIT1,MX1,OAS1,OAS2,STAT1	-2.97 2.66E-21	CXCL10,DDX58,DHX58,IFIH1,IFIT1,ISG15,MX1,OAS1,STAT1	-2.80 2.86E-14	CXCL10,IFIH1,IFIT1,ISG15,MX1,OAS1,OAS2,STAT1	-2.79 2.55E-10	DDX58,IFIH1,ISG20,MX1,RSAD2,SOCS1,STAT1,USP18
IKBKG	-2.00 1.07E-03	GBP2,IFI16,PTX3,TNFSF10	-2.20 6.20E-05	CXCL10,IFI16,IRF7,ISG15,TNFSF10	-2.21 1.05E-02	CXCL10,GBP2,IFI16,ISG15,TNFSF10	-2.80 1.85E-14	CXCL10,DDX58,DHX58,IFIH1,ISG15,MX1,OAS1,STAT1

Table A-21. Continued.

	Bacteria infused day 16		Healthy day 15		Healthy day 16		Healthy day 17	
Predicted upstream regulator	+/- z -score *P* value	Molecules	+/- z -score *P* value	Molecules	+/- z -score *P* value	Molecules	+/- z -score *P* value	Molecules
IKZF1	+ 2.75 5.43E-10	CYP2J2,DKK1,DTX3L,EPSTI1,IFI16,IFI27,IFI6,IFIT5,PAX5,RNF213,RTP4	+ 2.95 6.70E-08	DKK1,DTX3L,EPSTI1,IFI16,IFI27,IFI6,IFIT5,RNF213,RTP4	+ 3.09 9.75E-07	B2M,DIPK1A,DKK1,DTX3L,EPSTI1,IFI16,IFI27,IFI6,IFIT3,IFIT5,IRF4,RNF213,RTP4	+ 2.61 8.16E-03	DKK1,IFI16,IFI27,IFI6,IFIT5,RNF213,RTP4
IKZF3	+ 2.65 3.20E-09	DDX58,DKK1,IFI27,IFI6,IFIT5,RNF213,RTP4	+ 2.83 4.19E-11	DDX58,DKK1,IFI27,IFI6,IFIT5,IRF7,RNF213,RTP4	+ 2.63 5.13E-06	DKK1,IFI27,IFI6,IFIT3,IFIT5,RNF213,RTP4	+ 2.83 2.52E-07	DDX58,DKK1,IFI27,IFI6,IFIT5,IRF7,RNF213,RTP4
IL10RA	+ 3.00 7.59E-07	BATF2,GBP2,IFI16,MLKL,PLAAT3,RNF213,RSAD2,STAT1,ZBP1	+ 2.65 4.36E-05	GBP5,IFI16,IRF7,RNF213,RSAD2,STAT1,ZBP1	+ 3.76 1.30E-09	BATF2,CD40,CLEC12A,DRAM1,EDNRB,GBP2,GBP6,GDA,IFI16,IL23A,MLKL,NAMPT,RIPK3,RNF213,RSAD2,STAT1,TAP1,ZBP1	+ 4.12 3.98E-09	ARG2,CALHM6,CCR7,CD40,CD69,CFB,COL14A1,DRAM1,GBP5,IFI16,IRF7,MLKL,NLRC5,RNF213,RSAD2,STAT1,TAP1
IL1B	- -3.20 6.99E-08	CCL8,CMPK2,GBP1,GBP2,HERC5,IFI16,IFIT1,LBP,MEF2B,MX1,OAS2,PTX3,RSAD2,STAT1,TNFSF10,USP18	- -3.32 1.00E-06	CCL8,CXCL10,EIF4E,GBP1,IFI16,IFIT1,IRF7,ISG15,ISG20,MX1,RSAD2,STAT1,TNFSF10,USP18	- -5.39 5.10E-13	ANXA1,B2M,CASP4,CCL11,CD274,CD40,CMPK2,CXCL10,GBP1,GBP2,GBP6,HERC5,IDO1,IFI16,IFIT1,IFIT3,IL23A,IRF4,ISG15,ISG20,LGALS9,MAP3K8,MAPT,MX1,NAMPT,OAS2,OXTR,PSME2,RSAD2,SCLY,STAT1,TCIM,TNFSF10,TNFSF13B,TREM2,UBE2L6,USP18	- -4.66 1.10E-11	ATF3,CASP4,CCL8,CCR7,CD40,CD69,CD86,CFB,CREM,CRYAB,CXCL10,EPAS1,GBP1,H19,IDO1,IFI16,IRF7,ISG15,ISG20,LGALS9,MX1,NMI,OSMR,OXTR,PIGR,PTX3,RGS16,RSAD2,SCNN1A,SOCS1,STAT1,TNFSF13B,UBE2L6,USP18

Table A-21. Continued.

	Bacteria infused day 16		Healthy day 15		Healthy day 16		Healthy day 17	
Predicted upstream regulator	+/- z -score *P* value	Molecules	+/- z -score *P* value	Molecules	+/- z -score *P* value	Molecules	+/- z -score *P* value	Molecules
IL1RN	+ 4.36 9.22E-27	DDX58,GBP1,HERC6,IFI27,IFI44,IFI6,IFIH1,IFIT5,IRF9,MX1,MX2,OAS1,OAS2,PML,RSAD2,RTP4,SAMD9,TNFSF10,USP18	+ 4.69 2.77E-33	DDX58,GBP1,HERC6,IFI27,IFI44,IFI44L,IFI6,IFIH1,IFIT5,IRF7,IRF9,ISG20,MX1,MX2,OAS1,PML,RSAD2,RTP4,SAMD9,SP100,TNFSF10,USP18	+ 4.80 3.15E-24	GBP1,HERC6,IFI27,IFI44L,IFI6,IFIH1,IFIT3,IFIT5,IL23A,IRF9,ISG20,LAMP3,LGALS9,MX1,MX2,OAS1,OAS2,PML,RSAD2,RTP4,SLC15A3,STAT2,TNFSF10,USP18	+ 4.58 1.52E-20	ATF3,DDX58,GBP1,IFI27,IFI44,IFI44L,IFI6,IFIH1,IFIT5,IRF7,IRF9,ISG20,LGALS9,MX1,MX2,OAS1,RSAD2,RTP4,SAMD9,STAT2,USP18
IL21	- -2.33 5.97E-09	CMPK2,EIF2AK2,HERC6,IFI16,IFIT1,OAS2,PAX5,RSAD2,USP18	- -2.53 1.39E-10	CXCL10,EIF2AK2,GBP5,HERC6,IFI16,IFIT1,IRF7,ISG15,RSAD2,USP18	- -2.93 5.12E-16	CCL11,CMPK2,CXCL10,EIF2AK2,GBP6,HERC6,HSH2D,IDO1,IFI16,IFIT1,IFIT2,IFIT3,IL23A,IRF4,ISG15,OAS2,RSAD2,STAT2,TAP1,USP18	- -3.29 3.94E-14	ARG2,CALHM6,CCR7,CD69,CD86,CXCL10,EIF2AK2,GBP5,IDO1,IFI16,IFIT2,IRF7,ISG15,RSAD2,SOCS1,STAT2,TAP1,USP18
IL27	- -2.61 4.81E-07	BST2,EIF2AK2,GBP2,MX1,OAS1,STAT1,TNFSF10	- -2.61 2.94E-07	BST2,CXCL10,EIF2AK2,MX1,OAS1,STAT1,TNFSF10	- -3.41 1.65E-08	B2M,CD274,CXCL10,EIF2AK2,GBP2,MX1,OAS1,STAT1,STAT2,TAP1,TNFSF10,TNFSF13B	- -3.11 9.41E-08	CD69,CD86,CXCL10,EIF2AK2,MX1,OAS1,SOCS1,STAT1,STAT2,TAP1,TNFSF13B

Table A-21. Continued.

	Bacteria infused day 16		Healthy day 15		Healthy day 16		Healthy day 17	
Predicted upstream regulator	+/- z -score *P* value	Molecules	+/- z -score *P* value	Molecules	+/- z -score *P* value	Molecules	+/- z -score *P* value	Molecules
Interferon alpha	- -5.05 1.09E-41	BST2,DDX58,DHX58,EIF2AK2,EPSTI1,GBP1,GBP2,HERC5,HERC6,IFI16,IFI27,IFI44,IFI6,IFIH1,IFIT1,IFITM3,IRF9,MX1,MX2,OAS1,OAS2,PARP12,PARP14,PARP9,PML,RNF213,RSAD2,RTP4,SAMD9,SIGLEC1,SP110,STAT1,TNFSF10,UBA7,USP18,ZBP1	- -5.51 2.38E-54	ADAR,BST2,CXCL10,DDX58,DHX58,EIF2AK2,EPSTI1,GBP1,GBP5,HERC6,IFI16,IFI27,IFI44,IFI44L,IFI6,IFIH1,IFIT1,IFITM1,IRF7,IRF9,ISG15,ISG20,MX1,MX2,OAS1,PARP12,PARP14,PARP9,PML,PNPT1,RNF213,RSAD2,RTP4,SAMD9,SIGLEC1,SP100,STAT1,TNFSF10,TRANK1,UBA7,USP18,ZBP1	- -6.57 1.62E-59	ADAR,B2M,C3AR1,CASP8,CCND1,CD274,CD40,CGAS,CMTR1,COX7A1,CXCL10,EIF2AK2,EPSTI1,FCGR1A,GBP1,GBP2,GBP6,HERC5,HERC6,IDO1,IFI16,IFI27,IFI35,IFI44L,IFI6,IFIH1,IFIT1,IFIT2,IFIT3,IRF4,IRF9,ISG15,ISG20,LAMP3,LGALS9,MX1,MX2,OAS1,OAS2,PARP10,PARP12,PARP14,PARP9,PML,PNPT1,RNASEL,RNF213,RSAD2,RTP4,SHFL,SIGLEC1,SP110,STAT1,STAT2,TAP1,TDRD7,TMEM140,TNFSF10,TNFSF13B,TRANK1,TRIM21,UBA7,UBE2L6,USP18,USP25,ZBP1	- -6.28 3.71E-46	ADAR,ATF3,CCR7,CD40,CD69,CD86,CXCL10,DDX58,DHX58,EIF2AK2,FCGR1A,GBP1,GBP5,IDO1,IFI16,IFI27,IFI35,IFI44,IFI44L,IFI6,IFIH1,IFIT2,IFITM1,IRF7,IRF9,ISG15,ISG20,LGALS9,MX1,MX2,NMI,NT5C3A,OAS1,PARP12,PARP14,PARP9,PNPT1,RNF213,RSAD2,RTP4,SAMD9,SIGLEC1,SLC5A1,SOCS1,STAT1,STAT2,TAP1,TDRD7,TMEM140,TNFSF13B,TRANK1,UBA7,UBE2L6,USP18,WARS1

Table A-21. Continued.

	Bacteria infused day 16		Healthy day 15		Healthy day 16		Healthy day 17	
Predicted upstream regulator	+/- z -score *P* value	Molecules	+/- z -score *P* value	Molecules	+/- z -score *P* value	Molecules	+/- z -score *P* value	Molecules
IRF1	- -4.50 9.49E-29	CMPK2,DDX58,EIF2AK2,GBP2,IFI27,IFI44,IFI6,IFIH1,IFIT1,IFIT5,IFITM3,IRF9,MX1,OAS1,OAS2,PLAAT3,PML,RSAD2,SP110,STAT1,TNFSF10,XAF1	- -4.48 9.54E-28	CXCL10,DDX58,EIF2AK2,IFI27,IFI44,IFI44L,IFI6,IFIH1,IFIT1,IFIT5,IFITM1,IRF7,IRF9,ISG15,MX1,OAS1,PML,RSAD2,STAT1,TNFSF10,XAF1	- -5.47 1.31E-36	B2M,CASP8,CCND1,CD274,CD40,CMPK2,CXCL10,EIF2AK2,GBP2,IDO1,IFI27,IFI35,IFI44L,IFI6,IFIH1,IFIT1,IFIT2,IFIT3,IFIT5,IRF4,IRF9,ISG15,MX1,OAS1,OAS2,PML,PSME2,RSAD2,SP110,STAT1,STAT2,TAP1,TNFSF10,TNFSF13B,TRIM21,XAF1	- -4.53 4.58E-26	CD40,CFB,CXCL10,DDX58,EIF2AK2,IDO1,IFI27,IFI35,IFI44,IFI44L,IFI6,IFIH1,IFIT2,IFIT5,IFITM1,IRF7,IRF9,ISG15,MX1,OAS1,PIGR,RSAD2,SOCS1,STAT1,STAT2,TAP1,TNFSF13B,XAF1
IRF3	- -4.67 9.84E-30	CMPK2,DDX58,DHX58,EIF2AK2,GBP1,IFI16,IFI27,IFI44,IFI6,IFIH1,IFIT1,IFITM3,OAS1,OAS2,PARP12,PARP14,PLAC8,PML,RSAD2,STAT1,TNFSF10,USP18,ZBP1	- -5.03 4.21E-38	ADAR,CXCL10,DDX58,DHX58,EIF2AK2,GBP1,GBP5,IFI16,IFI27,IFI44,IFI44L,IFI6,IFIH1,IFIT1,IRF7,ISG15,ISG20,OAS1,PARP12,PARP14,PLAC8,PML,RSAD2,STAT1,TNFSF10,USP18,ZBP1	- -5.73 7.33E-37	ADAR,B2M,CD274,CD40,CMPK2,CXCL10,EIF2AK2,FCGR1A,GBP1,IFI16,IFI27,IFI44L,IFI6,IFIH1,IFIT1,IFIT2,IFIT3,IL23A,IRF3,ISG15,ISG20,OAS1,OAS2,PARP12,PARP14,PLAC8,PML,RSAD2,STAT1,STAT2,TAP1,TDRD7,TNFSF10,TREX1,UBE2L6,USP18,ZBP1	- -5.89 2.92E-39	ADAR,ARG2,CALHM6,CD40,CD58,CD69,CD86,CXCL10,DDX58,DHX58,EIF2AK2,FCGR1A,GBP1,GBP5,IFI16,IFI27,IFI44,IFI44L,IFI6,IFIH1,IFIT2,IRF7,ISG15,ISG20,NLRC5,NT5C3A,OAS1,PARP12,PARP14,PLAC8,RSAD2,STAT1,STAT2,TAP1,TDRD7,TREX1,UBE2L6,USP18

Table A-21. Continued.

	Bacteria infused day 16		Healthy day 15		Healthy day 16		Healthy day 17	
Predicted upstream regulator	+/- z -score *P* value	Molecules	+/- z -score *P* value	Molecules	+/- z -score *P* value	Molecules	+/- z -score *P* value	Molecules
IRF4	+ 2.62 2.53E-06	GBP1,IRF9,OAS1,PAX5,SPIB,STAT1,TNFSF10	+ 2.42 5.07E-09	CXCL10,GBP1,IRF7,IRF9,ISG15,ISG20,OAS1,STAT1,TNFSF10	+ 3.10 3.60E-10	B2M,CXCL10,GBP1,IRF4,IRF9,ISG15,ISG20,OAS1,PLAUR,PSMA2,STAT1,STAT2,TNFSF10,TNFSF13B,TRIM21	+ 2.63 8.18E-06	CXCL10,GBP1,IRF7,IRF9,ISG15,ISG20,OAS1,STAT1,STAT2,TNFSF13B
IRF5	- -3.53 2.04E-20	CMPK2,DDX58,DHX58,IFI44,IFIH1,IFIT1,IFITM3,OAS1,OAS2,PARP12,RSAD2,SP110,STAT1,TNFSF10	- -3.52 6.89E-21	CXCL10,DDX58,DHX58,IFI44,IFIH1,IFIT1,IRF7,ISG15,ISG20,OAS1,PARP12,RSAD2,STAT1,TNFSF10	- -4.14 8.85E-21	CMPK2,CXCL10,IFIH1,IFIT1,IFIT2,IFIT3,IL23A,ISG15,ISG20,NAMPT,OAS1,OAS2,PARP12,RSAD2,SP110,STAT1,STAT2,TNFSF10,UBE2L6	- -3.91 8.81E-17	CXCL10,DDX58,DHX58,IFI44,IFIH1,IFIT2,IRF7,ISG15,ISG20,NT5C3A,OAS1,PARP12,RSAD2,STAT1,STAT2,UBE2L6
IRF7	- -5.16 4.75E-41	CCL8,CMPK2,DDX58,DHX58,GBP1,HERC5,IFI16,IFI44,IFI6,IFIH1,IFIT1,IFITM3,IRF9,MX1,MX2,OAS1,OAS2,PARP12,PARP14,PLAC8,RSAD2,RTP4,STAT1,TNFSF10,UBA7,USP18,XAF1,ZBP1	- -5.59 8.71E-53	ADAR,CCL8,CXCL10,DDX58,DHX58,GBP1,GBP4,GBP5,IFI16,IFI44,IFI44L,IFI6,IFIH1,IFIT1,IFITM1,IRF7,IRF9,ISG15,ISG20,MX1,MX2,OAS1,PARP12,PARP14,PLAC8,RSAD2,RTP4,STAT1,TNFSF10,UBA7,USP18,XAF1,ZBP1	- -6.60 5.54E-56	ADAR,CASP4,CD40,CMPK2,CXCL10,FCGR1A,GBP1,GBP4,HERC5,IDO1,IFI16,IFI35,IFI44L,IFI6,IFIH1,IFIT1,IFIT2,IFIT3,IRF9,ISG15,ISG20,MAP3K8,MX1,MX2,NAMPT,OAS1,OAS2,PARP12,PARP14,PLAC8,PSME2,RSAD2,RTP4,STAT1,STAT2,TAP1,TDRD7,TNFSF10,TNFSF13B,TREX1,TRIM21,UBA7,UBE2L6,USP18,USP25,XAF1,ZBP1	- -6.68 3.41E-57	ADAR,CALHM6,CASP4,CCL8,CD40,CD69,CXCL10,DDX58,DHX58,FCGR1A,GBP1,GBP4,GBP5,IDO1,IFI16,IFI35,IFI44,IFI44L,IFI6,IFIH1,IFIT2,IFITM1,IRF7,IRF9,ISG15,ISG20,MX1,MX2,NMI,NT5C3A,OAS1,PARP12,PARP14,PLAC8,RSAD2,RTP4,SOCS1,STAT1,STAT2,TAP1,TDRD7,TNFSF13B,TREX1,UBA7,UBE2L6,USP18,XAF1

Table A-21. Continued.

	Bacteria infused day 16		Healthy day 15		Healthy day 16		Healthy day 17	
Predicted upstream regulator	+/- z -score *P* value	Molecules	+/- z -score *P* value	Molecules	+/- z -score *P* value	Molecules	+/- z -score *P* value	Molecules
Irgm1	+ 2.00 1.38E-05	IFI16,OAS2,RSAD2,USP18	+ 2.24 2.43E-07	CXCL10,IFI16,IRF7,RSAD2,USP18	+ 2.65 2.16E-07	CXCL10,IFI16,IFIT2,IFIT3,OAS2,RSAD2,USP18	+ 2.45 3.07E-06	CXCL10,IFI16,IFIT2,IRF7,RSAD2,USP18
JAK	- -2.83 1.10E-12	DDX58,EIF2AK2,IFI6,IFIH1,IFIT1,IFITM3,RSAD2,STAT1	- -3.00 6.34E-15	CXCL10,DDX58,EIF2AK2,IFI6,IFIH1,IFIT1,ISG15,RSAD2,STAT1	- -3.16 2.00E-13	CD40,CXCL10,EIF2AK2,IFI6,IFIH1,IFIT1,IFIT2,IFIT3,ISG15,RSAD2,STAT1	- -3.00 1.11E-13	CD40,CXCL10,DDX58,EIF2AK2,IFI6,IFIH1,IFIT2,ISG15,RSAD2,SOCS1,STAT1
JAK1	- -2.24 3.23E-06	EIF2AK2,IRF9,MX1,STAT1,USP18	- -2.24 6.89E-08	EIF2AK2,IRF7,IRF9,MX1,STAT1,USP18	- -2.99 1.21E-09	CD40,EIF2AK2,IFIT2,IRF9,MAP3K8,MX1,STAT1,STAT2,TAP1,USP18	- -2.99 3.38E-11	CD40,EIF2AK2,IFIT2,IRF7,IRF9,MX1,OSMR,STAT1,STAT2,TAP1,USP18
JAK1/2	- -2.22 3.47E-06	EIF2AK2,GBP2,MX1,PLAC8,RSAD2	- -2.63 1.92E-09	EIF2AK2,GBP5,IRF7,ISG15,MX1,PLAC8,RSAD2	- -2.63 5.13E-06	EIF2AK2,GBP2,GDA,ISG15,MX1,PLAC8,RSAD2	- -2.81 2.52E-07	CD69,EIF2AK2,GBP5,IRF7,ISG15,MX1,PLAC8,RSAD2
KRAS	+ 3.15 7.65E-06	CPM,CYP2J2,EIF2AK2,IFI6,IFIT1,IFITM3,IRF9,MX1,MX2,OAS1,STAT1,TNFSF10	+ 3.30 1.72E-09	ADAR,CXCL10,EIF2AK2,EIF4E,IFI6,IFIT1,IFITM1,IRF9,ISG15,MX1,MX2,OAS1,SP100,STAT1,TNFSF10	+ 2.86 5.59E-10	ADAR,AGRN,B2M,BTC,BZW2,CCND1,CD274,CXCL10,EIF2AK2,IDO1,IFI6,IFIT1,IRF9,ISG15,LAMP3,MX1,MX2,OAS1,P2RY14,PGAM2,SLC34A2,SOAT1,STAT1,STAT2,TAP1,TNFSF10,XRN2	+ 3.05 1.31E-06	ADAR,ATF3,BCL2L14,BZW2,CRYAB,CXCL10,EIF2AK2,H1-2,IDO1,IFI6,IFITM1,IRF9,ISG15,MX1,MX2,NCF2,OAS1,PYCARD,STAT1,STAT2,TAP1

Table A-21. Continued.

	Bacteria infused day 16		Healthy day 15		Healthy day 16		Healthy day 17	
Predicted upstream regulator	+/- z -score *P* value	Molecules	+/- z -score *P* value	Molecules	+/- z -score *P* value	Molecules	+/- z -score *P* value	Molecules
MAPK1	+ 4.77 1.18E-24	BST2,DDX58,EIF2AK2,GBP1,GBP2,HERC5,IFI16,IFI27,IFI44,IFI6,IFIH1,IFIT1,IFIT5,IFITM3,IRF9,MX2,OAS1,OAS2,PARP12,PML,SP110,STAT1,TNFSF10,USP18	+ 5.07 3.11E-30	ADAR,BST2,DDX58,EIF2AK2,GBP1,GBP5,IFI16,IFI27,IFI44,IFI6,IFIH1,IFIT1,IFIT5,IFITM1,IRF7,IRF9,ISG15,ISG20,MX2,OAS1,PARP12,PML,SP100,STAT1,TNFSF10,TRANK1,USP18	+ 6.28 6.80E-31	ADAR,C1S,CCND1,EIF2AK2,GBP1,GBP2,GRAMD1B,HERC5,IFI16,IFI27,IFI35,IFI6,IFIH1,IFIT1,IFIT2,IFIT3,IFIT5,IRF9,ISG15,ISG20,KRT17,LAMP3,LGALS3BP,MX2,OAS1,OAS2,PARP12,PML,PSME2,SP110,STAT1,STAT2,TAP1,TDRD7,TNFSF10,TRANK1,TRIM21,TRIM25,TRIM34,UBE2L6,USP18	+ 4.58 2.59E-28	ADAR,ARG2,ATF3,CD69,CFB,DDX58,EIF2AK2,GBP1,GBP5,IFI16,IFI27,IFI35,IFI44,IFI6,IFIH1,IFIT2,IFIT5,IFITM1,IRF7,IRF9,ISG15,ISG20,KRT17,LGALS3BP,MX2,NMI,OAS1,PARP12,RGS16,SCNN1A,STAT1,STAT2,TAP1,TDRD7,TRANK1,TRIM34,UBE2L6,USP18
MAVS	- -3.27 3.57E-16	CMPK2,DDX58,DHX58,IFIT1,IFITM3,OAS1,OAS2,PARP12,RSAD2,STAT1,USP18	- -3.39 2.16E-20	ADAR,CXCL10,DDX58,DHX58,IFIT1,IRF7,ISG15,ISG20,OAS1,PARP12,RSAD2,STAT1,USP18	- -3.92 1.17E-19	ADAR,CGAS,CMPK2,CXCL10,IFIT1,IFIT2,IFIT3,ISG15,ISG20,OAS1,OAS2,PARP12,RSAD2,STAT1,STAT2,UBE2L6,USP18	- -3.91 4.63E-20	ADAR,CXCL10,DDX58,DHX58,IFIT2,IRF7,ISG15,ISG20,NT5C3A,OAS1,PARP12,RSAD2,SOCS1,STAT1,STAT2,UBE2L6,USP18
mir-21	+ 2.60 3.99E-05	DHX58,GBP2,IFI16,OAS2,SIGLEC1,STAT1,UBA7	+ 2.78 2.37E-06	CXCL10,DHX58,GBP5,IFI16,PPA1,SIGLEC1,STAT1,UBA7	+ 4.30 4.01E-11	CASP4,CCND1,CD274,CXCL10,FCGR1A,GBP2,GBP6,IDO1,IFI16,OAS2,PPA1,PSME2,SIGLEC1,STAT1,STAT2,TAP1,TREM2,UBA7,UBE2L6	+ 3.83 5.58E-08	CASP4,CXCL10,DHX58,FCGR1A,GBP5,IDO1,IFI16,NLRC5,PPA1,SIGLEC1,STAT1,STAT2,TAP1,UBA7,UBE2L6
MSC	- -2.45 3.03E-08	EPSTI1,IFI27,IFI44,IFIT1,PAX5,XAF1	- -2.65 3.96E-10	EPSTI1,IFI27,IFI44,IFI44L,IFIT1,IRF7,XAF1	- -2.24 2.10E-04	EPSTI1,IFI27,IFI44L,IFIT1,XAF1	- -2.24 1.64E-04	IFI27,IFI44,IFI44L,IRF7,XAF1

Table A-21. Continued.

	Bacteria infused day 16		Healthy day 15		Healthy day 16		Healthy day 17	
Predicted upstream regulator	+/- z -score *P* value	Molecules	+/- z -score *P* value	Molecules	+/- z -score *P* value	Molecules	+/- z -score *P* value	Molecules
NFATC2	- -2.00 4.72E-03	CMPK2,PML,RSAD2,STAT1	- -2.65 2.15E-07	CXCL10,GBP4,IRF7,ISG15,ISG20,PML,RSAD2,STAT1	- -2.70 1.72E-11	CASP4,CD274,CD40,CMPK2,CXCL10,GBP4,IFIT2,IFIT3,IRF4,ISG15,ISG20,PML,RSAD2,STAT1,STAT2,TNFSF13B,USP25	- -2.50 7.29E-12	CASP4,CCR7,CD40,CD86,CRYAB,CXCL10,GBP4,IFIT2,IRF7,ISG15,ISG20,NMI,RSAD2,SOCS1,STAT1,STAT2,TNFSF13B
NFkB (complex)	- -2.40 5.00E-03	CCL8,GBP2,HERC5,PTX3,RSAD2,SPIB,TNFSF10	- -2.16 1.35E-02	CCL8,CXCL10,IRF7,ISG15,RSAD2,TNFSF10	- -3.92 3.21E-09	CASP4,CASP8,CCL11,CCND1,CD274,CD40,CXCL10,EDNRB,FCGR1A,GBP2,HERC5,IDO1,IL23A,IRF3,IRF4,ISG15,KRT17,KYNU,MAP3K8,NAMPT,RSAD2,SCLY,SOAT1,TAP1,TNFSF10	- -4.01 2.41E-08	ATF3,CASP4,CCL8,CCR7,CD40,CD69,CD86,CFB,CREM,CXCL10,EPAS1,FCGR1A,IDO1,IRF7,ISG15,KRT17,MSTN,NCF2,PTX3,RGS16,RSAD2,SOCS1,TAP1
NGLY1	+ 2.39 1.43E-09	IFI27,IFI44,IFIT1,OAS1,RSAD2,USP18	+ 2.76 1.01E-13	CXCL10,IFI27,IFI44,IFI44L,IFIT1,OAS1,RSAD2,USP18	+ 2.91 3.12E-11	CXCL10,IFI27,IFI44L,IFIT1,IFIT2,IFIT3,OAS1,RSAD2,USP18	+ 2.76 7.37E-10	CXCL10,IFI27,IFI44,IFI44L,IFIT2,OAS1,RSAD2,USP18
NKX2-3	+ 4.36 3.22E-22	BATF2,CMPK2,DDX58,DHX58,EIF2AK2,GBP1,GBP2,PARP12,PARP14,PARP9,RNF213,RTP4,SAMD9,SP110,STAT1,UBA7,USP18,XAF1,ZNFX1	+ 4.00 4.04E-18	DDX58,DHX58,EIF2AK2,GBP1,PARP12,PARP14,PARP9,PNPT1,RNF213,RTP4,SAMD9,STAT1,UBA7,USP18,XAF1,ZNFX1	+ 4.75 6.23E-26	BATF2,CMPK2,EIF2AK2,GBP1,GBP2,IDO1,LY6E,MFNG,PARP10,PARP12,PARP14,PARP9,PNPT1,PTPRE,RNF213,RTP4,SHFL,SLC40A1,SP110,STAT1,STAT2,TAP1,TCIM,TIPARP,TRIM21,UBA7,UBE2L6,USP18,XAF1,ZNFX1	+ 4.60 2.39E-20	C2CD4B,CRYAB,DDX58,DHX58,EIF2AK2,GBP1,IDO1,LY6E,NT5C3A,PARP12,PARP14,PARP9,PLEKHA4,PNPT1,RNF213,RTP4,SAMD9,STAT1,STAT2,TAP1,UBA7,UBE2L6,USP18,XAF1,ZNFX1

Table A-21. Continued.

	Bacteria infused day 16		Healthy day 15		Healthy day 16		Healthy day 17	
Predicted upstream regulator	+/- z -score *P* value	Molecules	+/- z -score *P* value	Molecules	+/- z -score *P* value	Molecules	+/- z -score *P* value	Molecules
NRAS	+ 2.62 2.80E-07	GBP2,IFI16,IFIH1,IFIT1,LBP,PTX3,STAT1,USP18	+ 2.21 3.19E-05	IFI16,IFIH1,IFIT1,ISG15,STAT1,USP18	+ 2.74 8.25E-09	AGRN,B2M,CCND1,GBP2,IFI16,IFI35,IFIH1,IFIT1,ISG15,RNASE6,SLC66A3,STAT1,TAP1,USP18	+ 2.18 2.95E-07	CD86,EPAS1,IFI16,IFI35,IFIH1,ISG15,NCF2,PTX3,RNASE6,STAT1,TAP1,USP18
P38 MAPK	- -2.40 1.40E-03	BATF2,CCL8,GBP1,PML,STAT1,TNFSF10	- -2.60 1.40E-04	CCL8,CXCL10,GBP1,IRF7,PML,STAT1,TNFSF10	- -2.87 7.01E-05	BATF2,CCL11,CCND1,CD40,CXCL10,EDNRB,GBP1,IL23A,PLAUR,PML,SLC6A12,STAT1,TNFSF10	- -2.77 8.90E-06	ARG2,ATF3,CCL8,CCR7,CD40,CD69,CD86,CXCL10,DDC,GBP1,IRF7,S100A12,SCNN1A,STAT1
PAF1	- -2.45 1.19E-08	DDX58,HERC5,IFI44,IFITM3,OAS2,ZNFX1	- -2.45 7.72E-09	DDX58,IFI44,IFI44L,ISG15,ISG20,ZNFX1	- -3.16 2.97E-11	HERC5,IDO1,IFI44L,IFIT3,ISG15,ISG20,OAS2,PLAUR,SERTAD1,ZNFX1	- -2.83 1.27E-08	DDX58,IDO1,IFI44,IFI44L,ISG15,ISG20,SERTAD1,ZNFX1
PARP9	- -2.22 2.61E-09	IFI44,IFIT1,OAS2,SP110,STAT1	- -2.21 1.81E-09	IFI44,IFIT1,IRF7,ISG15,STAT1	- -2.63 1.88E-10	IFIT1,IFIT2,IFIT3,ISG15,OAS2,SP110,STAT1	- -2.21 4.46E-07	IFI44,IFIT2,IRF7,ISG15,STAT1
PIK3CG	+ 2.24 2.47E-05	GBP2,OAS2,STAT1,TNFSF10,ZBP1	+ 2.45 8.23E-07	CXCL10,GBP4,GBP5,STAT1,TNFSF10,ZBP1	+ 3.29 5.73E-09	B2M,C2,CXCL10,GBP2,GBP4,GBP6,OAS2,STAT1,TAP1,TNFSF10,ZBP1	+ 2.65 5.07E-05	C2,CXCL10,GBP4,GBP5,NLRC5,STAT1,TAP1
PML	- -3.44 2.03E-13	BST2,EPSTI1,HERC6,IFI27,IFI44,IFIH1,IFIT1,MX1,OAS1,OAS2,PML,STAT1	- -3.99 3.50E-20	BST2,EPSTI1,HERC6,IFI27,IFI44,IFI44L,IFIH1,IFIT1,IFITM1,IRF7,ISG15,ISG20,MX1,OAS1,PML,STAT1	- -4.08 4.00E-13	CCND1,EPSTI1,HERC6,IFI27,IFI35,IFI44L,IFIH1,IFIT1,IFIT3,ISG15,ISG20,MX1,OAS1,OAS2,PML,STAT1,TAP1	- -3.59 3.61E-09	IFI27,IFI35,IFI44,IFI44L,IFIH1,IFITM1,IRF7,ISG15,ISG20,MX1,OAS1,STAT1,TAP1

Table A-21. Continued.

	Bacteria infused day 16		Healthy day 15		Healthy day 16		Healthy day 17	
Predicted upstream regulator	+/- z -score *P* value	Molecules	+/- z -score *P* value	Molecules	+/- z -score *P* value	Molecules	+/- z -score *P* value	Molecules
PNPT1	+ 3.97 1.17E-28	CMPK2,DDX58,EIF2AK2,GBP2,IFI16,IFI44,IFIH1,OAS1,PARP12,PARP14,PARP9,RNF213,RTP4,STAT1,USP18,XAF1	+ 4.22 6.26E-34	CXCL10,DDX58,EIF2AK2,GBP4,IFI16,IFI44,IFIH1,IRF7,ISG15,OAS1,PARP12,PARP14,PARP9,RNF213,RTP4,STAT1,USP18,XAF1	+ 4.77 8.39E-34	AGRN,CMPK2,CXCL10,EIF2AK2,GBP2,GBP4,GBP6,IFI16,IFIH1,IFIT3,ISG15,LGALS3BP,OAS1,PARP12,PARP14,PARP9,RNF213,RTP4,STAT1,STAT2,UBE2L6,USP18,XAF1	+ 4.56 2.17E-30	CXCL10,DDX58,EIF2AK2,GBP4,IFI16,IFI44,IFIH1,IRF7,ISG15,LGALS3BP,OAS1,PARP12,PARP14,PARP9,RNF213,RTP4,STAT1,STAT2,UBE2L6,USP18,XAF1
PRL	- -5.20 5.94E-33	BST2,CMPK2,DDX58,DHX58,DTX3L,EIF2AK2,EPSTI1,HERC5,HERC6,IFI44,IFI6,IFIH1,IFIT1,IFIT5,IRF9,MLKL,MX2,OAS1,OAS2,PARP12,PARP14,RSAD2,SAMD9,SP110,STAT1,USP18,XAF1	- -5.45 2.18E-39	ADAR,BST2,CXCL10,DDX58,DHX58,DTX3L,EIF2AK2,EPSTI1,HERC6,IFI44,IFI44L,IFI6,IFIH1,IFIT1,IFIT5,IFITM1,IRF7,IRF9,ISG15,MX2,OAS1,PARP12,PARP14,PNPT1,RSAD2,SAMD9,SP100,STAT1,USP18,XAF1	- -5.68 1.43E-40	ADAR,B2M,CCND1,CD40,CMPK2,CXCL10,DTX3L,EIF2AK2,EPSTI1,HERC5,HERC6,IFI35,IFI44L,IFI6,IFIH1,IFIT1,IFIT3,IFIT5,IRF9,ISG15,LAMP3,LY6E,MLKL,MX2,OAS1,OAS2,PARM1,PARP10,PARP12,PARP14,PNPT1,PSME2,RSAD2,SHFL,SHISA5,SP110,STAT1,STAT2,TDRD7,TMEM140,TNFSF13B,TRIM25,USP18,XAF1	- -5.46 1.42E-29	ADAR,CD40,CD69,CXCL10,DDX58,DHX58,EIF2AK2,IFI35,IFI44,IFI44L,IFI6,IFIH1,IFIT5,IFITM1,IRF7,IRF9,ISG15,LY6E,MLKL,MX2,OAS1,PARP12,PARP14,PNPT1,RSAD2,SAMD9,SHISA5,SOCS1,STAT1,STAT2,TDRD7,TMEM140,TNFSF13B,USP18,XAF1

Table A-21. Continued.

	Bacteria infused day 16		Healthy day 15		Healthy day 16		Healthy day 17	
Predicted upstream regulator	+/- z -score *P* value	Molecules	+/- z -score *P* value	Molecules	+/- z -score *P* value	Molecules	+/- z -score *P* value	Molecules
PTGER4	+ 3.57 2.42E-15	CMPK2,DDX58,GBP2,HERC6,IFI16,IFIH1,PARP14,RNF213,RSAD2,RTP4,TNFSF10,USP18,XAF1	+ 3.84 4.47E-19	CXCL10,DDX58,GBP4,HERC6,IFI16,IFIH1,IRF7,ISG20,PARP14,RNF213,RSAD2,RTP4,TNFSF10,USP18,XAF1	+ 3.59 3.43E-21	CD40,CMPK2,CXCL10,GBP2,GBP4,GBP6,HERC6,IFI16,IFI35,IFIH1,IFIT2,IL23A,ISG20,PARP14,RNASEL,RNF213,RNF24,RSAD2,RTP4,TNFSF10,TRIM21,USP18,XAF1	+ 4.32 8.56E-18	CCR7,CD40,CD69,CXCL10,DDX58,GBP4,IFI16,IFI35,IFIH1,IFIT2,IRF7,ISG20,NCF2,PARP14,RNF213,RSAD2,RTP4,SHISA3,USP18,XAF1
RC3H1	+ 3.87 1.00E-23	BST2,DDX58,IFI16,IFI27,IFI44,IFI6,IFIT1,IFITM3,IRF9,MX1,OAS1,OAS2,PARP9,RSAD2,STAT1	+ 4.00 2.59E-26	BST2,DDX58,IFI16,IFI27,IFI44,IFI44L,IFI6,IFIT1,IFITM1,IRF9,ISG15,MX1,OAS1,PARP9,RSAD2,STAT1	+ 4.47 3.10E-24	IFI16,IFI27,IFI44L,IFI6,IFIT1,IFIT2,IFIT3,IRF9,ISG15,MX1,OAS1,OAS2,PARP9,RSAD2,SHFL,STAT1,STAT2,TRIM21,TRIM25,TRIM56	+ 4.00 7.85E-20	CCR7,DDX58,IFI16,IFI27,IFI44,IFI44L,IFI6,IFIT2,IFITM1,IRF9,ISG15,MX1,OAS1,PARP9,RSAD2,STAT1,STAT2
RNY3	- -3.61 2.77E-26	BATF2,EPSTI1,HERC5,IFI44,IFIT1,IFITM3,MX1,OAS1,OAS2,RSAD2,RTP4,SIGLEC1,XAF1	- -3.46 3.50E-24	CXCL10,EPSTI1,IFI44,IFI44L,IFIT1,ISG15,MX1,OAS1,RSAD2,RTP4,SIGLEC1,XAF1	- -4.24 8.77E-31	BATF2,CXCL10,EPSTI1,HERC5,HES4,IFI44L,IFIT1,IFIT3,ISG15,LAMP3,LY6E,MX1,OAS1,OAS2,RSAD2,RTP4,SIGLEC1,XAF1	- -3.32 2.85E-16	CXCL10,IFI44,IFI44L,ISG15,LY6E,MX1,OAS1,RSAD2,RTP4,SIGLEC1,XAF1
SAMSN1	- -2.00 2.21E-04	CMPK2,PML,RSAD2,STAT1	- -2.65 1.12E-08	CXCL10,IRF7,ISG15,ISG20,PML,RSAD2,STAT1	- -3.74 1.86E-13	CD40,CMPK2,CXCL10,IFIT2,IFIT3,IL23A,ISG15,ISG20,PML,RSAD2,STAT1,STAT2,TRIM21,USP25	- -3.32 6.27E-10	CD40,CXCL10,IFIT2,IRF7,ISG15,ISG20,NMI,RSAD2,SOCS1,STAT1,STAT2
SASH1	- -2.00 8.45E-05	CMPK2,PML,RSAD2,STAT1	- -2.65 1.92E-09	CXCL10,IRF7,ISG15,ISG20,PML,RSAD2,STAT1	- -3.61 1.32E-13	CD40,CMPK2,CXCL10,IFIT2,IFIT3,ISG15,ISG20,PML,RSAD2,STAT1,STAT2,TRIM21,USP25	- -3.32 3.97E-11	CD40,CXCL10,IFIT2,IRF7,ISG15,ISG20,NMI,RSAD2,SOCS1,STAT1,STAT2

Table A-21. Continued.

	Bacteria infused day 16		Healthy day 15		Healthy day 16		Healthy day 17	
Predicted upstream regulator	+/- z -score *P* value	Molecules	+/- z -score *P* value	Molecules	+/- z -score *P* value	Molecules	+/- z -score *P* value	Molecules
SIRT1	+ 3.62 9.97E-16	CMPK2,DDX58,DHX58,DKK1,IFI44,IFITM3,OAS1,OAS2,PARP12,PARP14,PML,RNF213,RSAD2,RTP4,SP110,STAT1,UBA7,USP18	+ 3.34 8.21E-14	ADAR,DDX58,DHX58,DKK1,IFI44,IRF7,OAS1,PARP12,PARP14,PML,RNF213,RSAD2,RTP4,STAT1,UBA7,USP18	+ 3.84 1.31E-11	ADAR,CCND1,CMPK2,DKK1,GBP6,IFIT3,LGALS3BP,LY6E,MAPT,OAS1,OAS2,PARP12,PARP14,PML,PRDM16,RNF213,RSAD2,RTP4,SP110,STAT1,TAP1,UBA7,USP18	+ 4.03 7.30E-14	ADAR,DDX58,DHX58,DKK1,EPAS1,IFI44,IRF7,LGALS3BP,LY6E,NEDD4L,NLRC5,OAS1,PARP12,PARP14,PCK2,RGS16,RNF213,RSAD2,RTP4,SCNN1A,STAT1,TACSTD2,TAP1,UBA7,USP18
SOCS1	+ 3.42 3.04E-14	DDX58,IFI16,IFI27,IFI44,IFIH1,IFIT1,MX1,OAS1,OAS2,RSAD2,STAT1,USP18	+ 3.82 2.61E-21	CXCL10,DDX58,GBP5,IFI16,IFI27,IFI44,IFIH1,IFIT1,IRF7,ISG15,ISG20,MX1,OAS1,RSAD2,STAT1,USP18	+ 3.76 1.01E-16	CCND1,CD40,CXCL10,GBP6,H2-T24,IFI16,IFI27,IFIH1,IFIT1,IFIT2,IFIT3,ISG15,ISG20,MX1,OAS1,OAS2,RSAD2,STAT1,USP18	+ 3.98 3.94E-21	CCR7,CD40,CD69,CD86,CXCL10,DDX58,GBP5,H2-T24,IFI16,IFI27,IFI44,IFIH1,IFIT2,IRF7,ISG15,ISG20,MX1,OAS1,RSAD2,SOCS1,STAT1,USP18
SP110	+ 3.16 3.02E-11	BST2,IFI27,IFI6,IFIH1,IFIT1,IFITM3,IRF9,MX1,OAS1,STAT1	+ 3.32 4.47E-13	BST2,CXCL10,IFI27,IFI6,IFIH1,IFIT1,IFITM1,IRF9,MX1,OAS1,STAT1	+ 2.71 1.13E-07	BCL2L12,CXCL10,IFI27,IFI6,IFIH1,IFIT1,IFIT3,IRF9,MX1,OAS1,STAT1	+ 2.71 6.58E-08	ATF3,BCL2L12,CXCL10,IFI27,IFI6,IFIH1,IFITM1,IRF9,MX1,OAS1,STAT1
SPI1	- -3.56 2.97E-13	CMPK2,IFI27,IFI44,IFI6,IFIT1,IFITM3,IRF9,MX1,PARP12,PML,RSAD2,SP110,TNFSF10,USP18	- -3.95 6.39E-18	CXCL10,IFI27,IFI44,IFI44L,IFI6,IFIT1,IFITM1,IRF7,IRF9,ISG15,ISG20,MX1,PARP12,PML,RSAD2,TNFSF10,USP18	- -4.53 3.20E-16	C1QC,C3AR1,CCND1,CMPK2,CXCL10,IFI27,IFI44L,IFI6,IFIT1,IFIT2,IFIT3,IRF4,IRF9,ISG15,ISG20,LAMP3,LY6E,MX1,PARP12,PML,RSAD2,SP110,TNFSF10,USP18	- -3.87 1.09E-11	C1QC,CCR7,CXCL10,IFI27,IFI44,IFI44L,IFI6,IFIT2,IFITM1,IRF7,IRF9,ISG15,ISG20,LY6E,MX1,NCF2,PARP12,RSAD2,USP18

Table A-21. Continued.

	Bacteria infused day 16		Healthy day 15		Healthy day 16		Healthy day 17	
Predicted upstream regulator	+/- z -score *P* value	Molecules	+/- z -score *P* value	Molecules	+/- z -score *P* value	Molecules	+/- z -score *P* value	Molecules
STAT1	- -4.56 4.49E-33	BATF2,BST2,CMPK2,EIF2AK2,EPSTI1,GBP1,GBP2,HERC6,IFI16,IFI27,IFI44,IFI6,IFIH1,IFIT1,IFITM3,IRF9,MX1,OAS1,OAS2,PARP9,RNF213,RSAD2,RTP4,SP110,STAT1,TNFSF10,USP18,XAF1,ZBP1	- -4.75 1.24E-37	BST2,C4A/C4B,CXCL10,EIF2AK2,EPSTI1,GBP1,GBP4,GBP5,HERC6,IFI16,IFI27,IFI44,IFI44L,IFI6,IFIH1,IFIT1,IFITM1,IRF7,IRF9,ISG15,MX1,OAS1,PARP9,RNF213,RSAD2,RTP4,STAT1,TNFSF10,USP18,XAF1,ZBP1	- -5.75 6.21E-46	B2M,BATF2,C1S,C4A/C4B,CASP4,CASP8,CCND1,CD274,CD40,CMPK2,CXCL10,EIF2AK2,EPSTI1,FCGR1A,GBP1,GBP2,GBP4,GBP6,HERC6,IDO1,IFI16,IFI27,IFI35,IFI44L,IFI6,IFIH1,IFIT1,IFIT2,IFIT3,IL23A,IRF9,ISG15,LY6E,MX1,OAS1,OAS2,PARP9,PSME2,RNF213,RSAD2,RTP4,SOAT1,SP110,STAT1,STAT2,TAP1,TNFSF10,TNFSF13B,TRIM21,USP18,XAF1,ZBP1	- -5.54 4.63E-34	CALHM6,CASP4,CCR7,CD40,CD86,CFB,CREM,CXCL10,EIF2AK2,FCGR1A,GBP1,GBP4,GBP5,IDO1,IFI16,IFI27,IFI35,IFI44,IFI44L,IFI6,IFIH1,IFIT2,IFITM1,IRF7,IRF9,ISG15,LY6E,MX1,NLRC5,OAS1,PARP9,RNF213,RSAD2,RTP4,SOCS1,STAT1,STAT2,TAP1,TNFSF13B,USP18,WARS1,XAF1
STAT4	- -2.22 8.32E-04	DDX58,IFIH1,PLAC8,STAT1,STC2	- -2.63 5.29E-06	CXCL10,DDX58,IFIH1,ISG15,ISG20,PLAC8,STAT1	- -2.35 1.12E-05	CXCL10,IFIH1,IFIT2,IRF4,ISG15,ISG20,MAP3K8,PLAC8,PRDM16,SERTAD1,STAT1	- -3.29 6.77E-06	ARHGAP15,CXCL10,DDX58,IFIH1,IFIT2,ISG15,ISG20,PLAC8,RGS16,SERTAD1,STAT1
STING1	- -2.20 3.37E-08	IFI16,IFI44,IFITM3,OAS1,RSAD2,USP18	- -2.93 9.79E-14	CXCL10,GBP5,IFI16,IFI44,IRF7,ISG15,OAS1,RSAD2,USP18	- -2.93 3.32E-09	CGAS,CXCL10,IFI16,IFIT2,IFIT3,ISG15,OAS1,RSAD2,USP18	- -3.52 3.12E-15	CD86,CXCL10,GBP5,IFI16,IFI44,IFIT2,IRF7,ISG15,OAS1,PLEKHA4,RGS16,RSAD2,USP18
TAB1	+ 2.43 8.07E-10	GBP1,GBP2,IFIH1,IFIT1,TNFSF10,XAF1	+ 2.63 5.34E-12	CXCL10,GBP1,IFIH1,IFIT1,IRF7,TNFSF10, XAF1	+ 2.81 5.16E-10	CXCL10,GBP1,GBP2,IFIH1,IFIT1,TNFSF10,TNFSF13B,XAF1	+ 2.65 1.23E-08	CFB,CXCL10,GBP1,IFIH1,IRF7,TNFSF13B,XAF1

Table A-21. Continued.

	Bacteria infused day 16		Healthy day 15		Healthy day 16		Healthy day 17	
Predicted upstream regulator	+/- z -score *P* value	Molecules	+/- z -score *P* value	Molecules	+/- z -score *P* value	Molecules	+/- z -score *P* value	Molecules
TGM2	- -3.59 4.52E-13	IFI6,IFIT1,IFIT5,IRF9,OAS1,OAS2,PARP14,PARP9,RNF213,SP110,STAT1,UBA7,XAF1	- -3.05 1.71E-13	CXCL10,IFI6,IFIT1,IFIT5,IRF9,OAS1,PARP14,PARP9,RNF213,SLC7A2,STAT1,UBA7,XAF1	- -3.56 4.17E-17	CCND1,CD93,CXCL10,IFI35,IFI6,IFIT1,IFIT2,IFIT3,IFIT5,IRF9,LGALS9,LY6E,OAS1,OAS2,PARP14,PARP9,PPP1R16B,RNF213,SP110,STAT1,TAP1,UBA7,XAF1	- -3.29 2.20E-15	CD86,CD93,CXCL10,IFI35,IFI6,IFIT2,IFIT5,IRF9,LGALS9,LY6E,NCF2,OAS1,PARP14,PARP9,PPP1R16B,RNF213,SLC16A1,STAT1,TAP1,UBA7,XAF1
TICAM1	+ -2.41 7.46E-06	CMPK2,DDX58,IFI16,IFIT1,RSAD2,TNFSF10	+ -3.09 1.79E-11	CXCL10,DDX58,IFI16,IFIT1,IRF7,ISG15,ISG20,RSAD2,SLC7A2,TNFSF10	+ -3.77 8.56E-12	CASP4,CD40,CMPK2,CXCL10,EDNRB,IFI16,IFIT1,IFIT2,IFIT3,IL23A,IRF3,ISG15,ISG20,RSAD2,TNFSF10	+ -3.51 6.75E-10	CASP4,CD40,CD86,CFB,CXCL10,DDX58,IFI16,IFIT2,IRF7,ISG15,ISG20,RSAD2,SOCS1
TLR3	- -3.26 7.37E-24	CMPK2,CPM,DDX58,DHX58,EIF2AK2,GBP2,HERC5,IFI16,IFI44,IFI6,IFIH1,IFIT1,MX1,MX2,OAS1,PTX3,RSAD2,STAT1,TNFSF10,USP18,ZNFX1	- -3.09 3.08E-26	CXCL10,DDX58,DHX58,EIF2AK2,GBP4,IFI16,IFI44,IFI44L,IFI6,IFIH1,IFIT1,IRF7,ISG15,ISG20,MX1,MX2,OAS1,RSAD2,STAT1,TNFSF10,USP18,ZNFX1	- -4.15 1.16E-23	CD274,CD40,CMPK2,CXCL10,EIF2AK2,GBP2,GBP4,HERC5,IFI16,IFI44L,IFI6,IFIH1,IFIT1,IFIT2,IFIT3,IL23A,IRF3,ISG15,ISG20,LIPA,MAP3K8,MX1,MX2,OAS1,RSAD2,STAT1,TNFSF10,TNFSF13B,USP18,ZNFX1	- -4.14 1.35E-25	ARG2,ATF3,CD40,CD69,CD86,CFB,CXCL10,DDX58,DHX58,EIF2AK2,GBP4,IFI16,IFI44,IFI44L,IFI6,IFIH1,IFIT2,IRF7,ISG15,ISG20,MX1,MX2,NMI,OAS1,PTX3,RSAD2,SOCS1,STAT1,TNFSF13B,USP18,ZNFX1

Table A-21. Continued.

	Bacteria infused day 16		Healthy day 15		Healthy day 16		Healthy day 17	
Predicted upstream regulator	+/- z -score *P* value	Molecules	+/- z -score *P* value	Molecules	+/- z -score *P* value	Molecules	+/- z -score *P* value	Molecules
TLR4	- -2.75 4.32E-09	BPI,CCL8,CMPK2,GBP2,IFI16,IFITM3,MX1,PML,PTX3,RSAD2,STAT1,TNFSF10	- -2.56 2.28E-08	CCL8,CXCL10,IFI16,IRF7,ISG15,ISG20,MX1,PML,RSAD2,STAT1,TNFSF10	- -3.50 5.86E-14	BPI,CASP8,CD274,CD40,CMPK2,CXCL10,GBP2,IFI16,IFIT2,IFIT3,IL23A,IRF3,ISG15,ISG20,MX1,OXTR,PML,RSAD2,SLC6A12,STAT1,STAT2,TNFSF10,TREM2,TRIM21,USP25	- -3.51 1.42E-13	ATF3,CCL8,CCR7,CD40,CD86,CFB,CXCL10,IFI16,IFIT2,IRF7,ISG15,ISG20,MX1,NMI,OXTR,PTX3,RGS16,RSAD2,SMPDL3B,SOCS1,SPTLC2,STAT1,STAT2,TNFRSF13B
TLR7	- -2.81 2.09E-09	DKK1,IFI44,IFIT1,IRF9,MX1,MX2,OAS2,PTX3,RSAD2,STAT1	- -3.41 3.07E-15	CXCL10,DKK1,IFI44,IFI44L,IFIT1,IFITM1,IRF7,IRF9,ISG15,ISG20,MX1,MX2,RSAD2,STAT1	- -4.14 2.19E-15	CCND1,CD274,CD40,CXCL10,DKK1,ESM1,IDO1,IFI35,IFI44L,IFIT1,IFIT3,IL23A,IRF9,ISG15,ISG20,MX1,MX2,OAS2,RSAD2,STAT1,STAT2	- -4.46 3.73E-18	ATF3,CCR7,CD40,CD69,CD86,CXCL10,DKK1,IDO1,IFI35,IFI44,IFI44L,IFITM1,IRF7,IRF9,ISG15,ISG20,MX1,MX2,PTX3,RSAD2,SOCS1,STAT1,STAT2
TLR9	- -3.15 3.86E-10	CPM,IFI16,IFIT1,IRF9,MX1,MX2,OAS2,RSAD2,STAT1,TNFSF10,USP18	- -3.65 5.81E-16	CXCL10,IFI16,IFI44L,IFIT1,IFITM1,IRF7,IRF9,ISG15,ISG20,MX1,MX2,RSAD2,STAT1,TNFSF10,USP18	- -4.30 7.35E-20	CCND1,CD274,CD40,CXCL10,IDO1,IFI16,IFI35,IFI44L,IFIT1,IFIT2,IFIT3,IL23A,IRF4,IRF9,ISG15,ISG20,MX1,MX2,NAMPT,OAS2,RSAD2,STAT1,STAT2,TNFSF10,TNFSF13B,USP18	- -4.98 4.32E-24	ARG2,ATF3,CCR7,CD40,CD69,CD86,CXCL10,IDO1,IFI16,IFI35,IFI44L,IFIT2,IFITM1,IRF7,IRF9,ISG15,ISG20,MX1,MX2,PYCARD,RSAD2,SMPDL3B,SOCS1,SPTLC2,STAT1,STAT2,TNFRSF13B,TNFSF13B,USP18

Table A-21. Continued.

	Bacteria infused day 16		Healthy day 15		Healthy day 16		Healthy day 17	
Predicted upstream regulator	+/- z -score *P* value	Molecules	+/- z -score *P* value	Molecules	+/- z -score *P* value	Molecules	+/- z -score *P* value	Molecules
TNF	-4.04 4.42E-10	BST2,DDX58,DKK1,EIF2AK2,GBP1,GBP2,HERC5,IFI16,IFI27,IFI6,IFIH1,IFIT1,IFIT5,LBP,MX1,OAS1,OAS2,PARP14,PLAAT3,PML,PTX3,SAMD9,STAT1,TIFA,TNFSF10	-4.50 1.05E-11	BST2,C4A/C4B,CXCL10,DDX58,DKK1,EIF2AK2,GBP1,GBP4,IFI16,IFI27,IFI6,IFIH1,IFIT1,IFIT5,IFITM1,IRF7,ISG15,MX1,OAS1,PARP14,PML,SAMD9,SLC7A2,STAT1,TIFA,TNFSF10	-5.35 9.79E-19	ANXA1,B2M,C3AR1,C4A/C4B,CASP4,CASP8,CCL11,CCND1,CD274,CD40,CXCL10,DKK1,EDNRB,EIF2AK2,ESM1,FRMD4A,GBP1,GBP2,GBP4,GBP6,HERC5,IDO1,IFI16,IFI27,IFI6,IFIH1,IFIT1,IFIT3,IFIT5,IL23A,IRF4,ISG15,ITGA10,KYNU,LAMP3,LGALS9,MAP3K8,MST1R,MX1,NAMPT,OAS1,OAS2,OPTN,PARP14,PLAUR,PLVAP,PML,PSMA2,PSME2,SLC15A3,SLC40A1,SOAT1,STAT1,TAP1,TCIM,TDRD7,TIFA,TM4SF1,TNFSF10,TNFSF13B,TREM2,TRIM56	-4.75 3.67E-14	AATK,ALOX5AP,ATF3,CASP4,CCR7,CD40,CD69,CD86,CFB,CNP,CREM,CRYAB,CXCL10,DDX58,DKK1,EIF2AK2,GBP1,GBP4,H19,IDO1,IFI16,IFI27,IFI6,IFIH1,IFIT5,IFITM1,IRF7,ISG15,LGALS9,MST1R,MSTN,MX1,NCF2,OAS1,OSMR,PARP14,PCK2,PIGR,PLVAP,PTX3,PYCARD,RGS16,S100A12,SAMD9,SCNN1A,SLC16A2,SOCS1,STAT1,TAP1,TDRD7,TIFA,TMEM40,TNFSF13B
TNFSF10	-2.78 1.32E-09	EIF2AK2,IFI16,IFI27,IFI6,IFIT1,IRF9,STAT1,TNFSF10	-3.27 1.06E-14	EIF2AK2,IFI16,IFI27,IFI6,IFIT1,IFITM1,IRF9,ISG15,SP100,STAT1,TNFSF10	-3.23 3.42E-09	CASP8,EIF2AK2,IFI16,IFI27,IFI6,IFIT1,IRF9,ISG15,PSME2,STAT1,TNFSF10	-2.13 3.42E-07	CD69,EIF2AK2,IFI16,IFI27,IFI6,IFITM1,IRF9,ISG15,STAT1
TNK1	-2.00 2.36E-07	IFI16,IFIH1,OAS2,TNFSF10	-2.24 1.31E-09	IFI16,IFIH1,IRF7,ISG20,TNFSF10	-2.45 7.92E-09	IFI16,IFIH1,IFIT2,ISG20,OAS2,TNFSF10	-2.24 3.25E-07	IFI16,IFIH1,IFIT2,IRF7,ISG20

Table A-21. Continued.

	Bacteria infused day 16		Healthy day 15		Healthy day 16		Healthy day 17	
Predicted upstream regulator	+/- z -score *P* value	Molecules	+/- z -score *P* value	Molecules	+/- z -score *P* value	Molecules	+/- z -score *P* value	Molecules
TP53	- -2.19 2.16E-02	DKK1,GBP1,HERC5,IFI16,IRF9,MX1,OAS1,PLAAT3,PML,STAT1,TNFSF10,XAF1	- -2.28 1.70E-03	CXCL10,DKK1,FABP3,GBP1,IFI16,IRF7,IRF9,ISG15,MX1,OAS1,PML,STAT1,TNFSF10,XAF1	- -2.66 5.92E-06	ANXA1,C1QC,C2,CASP4,CASP8,CCND1,COL13A1,COX7A1,CXCL10,DKK1,DRAM1,FAM83D,FRMD4A,GBP1,GDA,HERC5,IFI16,IFI35,IRF9,ISG15,LAMP3,MAP3K8,MX1,NAMPT,OAS1,P2RY14,PGAM2,PLAUR,PMEPA1,PML,POLK,PSMA2,PTPRE,SHISA5,SLC66A3,STAT1,TAP1,TNFSF10,XAF1	- -3.01 1.25E-03	ATF3,C1QC,C2,CASP4,COL14A1,CRYAB,CXCL10,DKK1,DRAM1,EPAS1,FABP3,FGFBP1,GBP1,H19,IFI16,IFI35,IRF7,IRF9,ISG15,MX1,OAS1,PYCARD,RGS16,SCNN1A,SHISA5,SLC16A1,SPHK2,SPTLC2,STAT1,TAP1,XAF1
TREX1	+ 2.41 4.97E-11	IFI16,IFI44,IFIT1,MX1,OAS1,USP18	+ 3.09 1.10E-20	CXCL10,IFI16,IFI44,IFI44L,IFIT1,ISG15,ISG20,MX1,OAS1,USP18	+ 3.08 1.61E-15	CXCL10,IFI16,IFI44L,IFIT1,IFIT2,ISG15,ISG20,MX1,OAS1,USP18	+ 3.07 8.10E-18	CD86,CXCL10,IFI16,IFI44,IFI44L,IFIT2,ISG15,ISG20,MX1,OAS1,USP18
TRIM24	+ 3.94 2.26E-22	CMPK2,DDX58,DHX58,EPSTI1,GBP2,HERC6,IFI44,IFIH1,IRF9,OAS1,PARP12,PLAC8,RTP4,STAT1,UBA7,USP18	+ 4.19 1.02E-26	CXCL10,DDX58,DHX58,EPSTI1,GBP4,HERC6,IFI44,IFIH1,IRF7,IRF9,ISG15,OAS1,PARP12,PLAC8,RTP4,STAT1,UBA7,USP18	+ 4.95 2.64E-27	AGRN,CMPK2,CXCL10,EPSTI1,GBP2,GBP4,HERC6,IFI35,IFIH1,IFIT2,IFIT3,IRF9,ISG15,LGALS3BP,MOV10,OAS1,PARP12,PLAC8,RTP4,SHISA5,STAT1,STAT2,TAP1,UBA7,USP18	+ 4.95 6.64E-28	CALHM6,CXCL10,DDX58,DHX58,GBP4,IFI35,IFI44,IFIH1,IFIT2,IRF7,IRF9,ISG15,LGALS3BP,NMI,OAS1,PARP12,PLAC8,RTP4,SHISA5,SOCS1,STAT1,STAT2,TAP1,UBA7,USP18
USP18	+ 2.59 7.01E-12	IFI6,IFIH1,IFITM3,IRF9,MX1,OAS1,TNFSF10	+ 2.94 2.33E-16	CXCL10,IFI6,IFIH1,IRF7,IRF9,ISG15,MX1,OAS1,TNFSF10	+ 2.77 3.90E-10	CXCL10,IFI6,IFIH1,IRF9,ISG15,MX1,OAS1,TNFSF10	+ 2.96 5.69E-12	CXCL10,IFI6,IFIH1,IRF7,IRF9,ISG15,MX1,OAS1,SOCS1

Table A-21. Continued.

	Bacteria infused day 16		Healthy day 15		Healthy day 16		Healthy day 17	
Predicted upstream regulator	+/- z -score *P* value	Molecules	+/- z -score *P* value	Molecules	+/- z -score *P* value	Molecules	+/- z -score *P* value	Molecules
VCAN	- -2.53 1.27E-10	IFI44,IFI6,IFIT1, LBP,MX1,MX2, OAS2,PARP14, STAT1,XAF1	- -2.71 2.21E-12	C4A/C4B,IFI44,I FI44L,IFI6,IFIT1 ,IFITM1,MX1,M X2,PARP14,ST AT1,XAF1	- -2.51 5.95E-09	AGRN,C1S,C4A/C4B ,IFI44L,IFI6,IFIT1,IFIT 2,MX1,MX2,OAS2,PA RP14,STAT1,XAF1	- -2.89 3.13E-08	IFI44,IFI44L,IFI6,IFI T2,IFITM1,MX1,MX2 ,PARP14,PRELP,S MPDL3B,STAT1,XA F1
ISG15	+ 2.22 6.58E-12	DDX58,IFI6,IFIT M3,MX1,OAS1						
AIRE	+ 2.24 6.66E-06	EIF2AK2,HERC 6,IFI44,PARP14, TNFSF10						
PF4	- -2.22 5.19E-09	CMPK2,CPM,D DX58,EPSTI1,R SAD2,STAT1,U SP18						
DUSP1	- -2.00 5.58E-04	CMPK2,DKK1,IF IT1,MX1						
NFKBIA	- -2.18 1.45E-02	GBP2,IFI16,IFI6, PTX3,TNFSF10						
CNOT7			+ 2.21 6.65E-21	BST2,HERC6,IF I27,IFI44L,IFI6,I FIT5,IFITM1,IS G15,OAS1,PAR P12,STAT1	+ 2.22 5.43E-27	B2M,CMPK2,HERC6, IFI27,IFI35,IFI44L,IFI 6,IFIT5,ISG15,LGALS 3BP,OAS1,OAS2,PA RP12,SP110,STAT1, TAP1,UBE2L6	+ 2.21 3.23E-19	IFI27,IFI35,IFI44L,IF I6,IFIT5,IFITM1,ISG 15,LGALS3BP,OAS 1,PARP12,STAT1,T AP1,UBE2L6
DNASE2			+ 2.60 3.96E-18	CXCL10,DHX58 ,IRF7,ISG15,OA S1,RSAD2,RTP 4,TNFSF10,US P18,ZBP1	+ 2.40 5.37E-13	ACKR4,CXCL10,IFIT 3,ISG15,OAS1,RSAD 2,RTP4,TNFSF10,US P18,ZBP1	+ 2.20 5.73E-10	CXCL10,DHX58,IRF 7,ISG15,OAS1,RSA D2,RTP4,USP18

Table A-21. Continued.

	Bacteria infused day 16		Healthy day 15		Healthy day 16		Healthy day 17	
Predicted upstream regulator	+/- z -score *P* value	Molecules	+/- z -score *P* value	Molecules	+/- z -score *P* value	Molecules	+/- z -score *P* value	Molecules
DOCK8			- -2.45 6.31E-08	CXCL10,IRF7,ISG15,ISG20,RSAD2,STAT1	- -3.46 2.25E-12	CD40,CMPK2,CXCL10,IFIT2,IFIT3,ISG15,ISG20,RSAD2,STAT1,STAT2,TRIM21,USP25	- -3.32 2.87E-11	CD40,CXCL10,IFIT2,IRF7,ISG15,ISG20,NMI,RSAD2,SOCS1,STAT1,STAT2
IFI16			- -2.21 3.88E-06	CXCL10,DDX58,IFI16,ISG15,OAS1	- -2.20 1.01E-04	CCND1,CXCL10,IFI16,ISG15,OAS1,STAT2	- -2.42 7.55E-05	CXCL10,DDX58,IFI16,ISG15,OAS1,STAT2
IFIH1			- -2.40 1.91E-16	CXCL10,IFI27,IFI44L,IFIT1,IRF7,ISG15,OAS1,RSAD2,SIGLEC1,USP18	- -2.40 2.39E-11	CXCL10,IFI27,IFI44L,IFIT1,ISG15,OAS1,OAS2,RSAD2,SIGLEC1,USP18	- -2.20 4.14E-10	CXCL10,IFI27,IFI44L,IRF7,ISG15,OAS1,RSAD2,SIGLEC1,USP18
IFN alpha/ beta			- -2.39 1.66E-07	CXCL10,IFI16,IRF7,RSAD2,STAT1,TNFSF10	- -3.52 7.86E-13	CD40,CXCL10,IDO1,IFI16,IFIT2,IFIT3,LY6E,RSAD2,STAT1,STAT2,TNFSF10,TNFSF13B,TRIM21	- -3.79 6.20E-16	CCR7,CD40,CD69,CD86,CXCL10,IDO1,IFI16,IFIT2,IRF7,LY6E,RSAD2,SOCS1,STAT1,STAT2,TNFSF13B
IFNL2			- -2.24 6.40E-10	CXCL10,IFIT1,IRF7,MX1,RSAD2	- -2.00 1.01E-05	CXCL10,IFIT1,MX1,RSAD2	- -2.00 8.17E-06	CXCL10,IRF7,MX1,RSAD2
MAP2K3			- -2.62 1.92E-09	CCL8,CXCL10,IRF9,ISG15,PPA1,STAT1,TNFSF10	- -2.43 5.97E-05	CXCL10,IRF9,ISG15,PPA1,STAT1,TNFSF10	- -2.62 3.61E-06	ARG2,CCL8,CXCL10,IRF9,ISG15,PPA1,STAT1
mir-155			+ 2.21 3.18E-05	CXCL10,IRF7,IRF9,MX1,STAT1	+ 2.00 1.55E-04	CCND1,CXCL10,IFIT3,IRF4,IRF9,MX1,STAT1	+ 2.59 1.11E-04	CD69,CXCL10,IRF7,IRF9,MX1,SOCS1,STAT1

Table A-21. Continued.

	Bacteria infused day 16		Healthy day 15		Healthy day 16		Healthy day 17	
Predicted upstream regulator	+/- z -score *P* value	Molecules	+/- z -score *P* value	Molecules	+/- z -score *P* value	Molecules	+/- z -score *P* value	Molecules
MYD88			-2.32 1.77E-04	CXCL10,IRF7,ISG15,RSAD2,SLC7A2,USP18	-3.39 1.31E-05	CASP4,CD274,CD40,CMPK2,CXCL10,EDNRB,IFIT2,IL23A,ISG15,RSAD2,TNFSF13B,USP18	-3.32 7.62E-06	CASP4,CD40,CD86,CXCL10,IFIT2,IRF7,ISG15,RSAD2,SOCS1,TNFRSF13B,TNFSF13B,USP18
OSM			-2.71 2.94E-04	CXCL10,GBP1,IRF7,IRF9,ISG20,MX1,OAS1,STAT1	-4.10 1.18E-07	ANXA1,B2M,BTC,C1S,CASP4,CCL11,CCND1,CXCL10,GBP1,GBP2,IFI35,IRF9,ISG20,KRT17,MX1,NAMPT,OAS1,STAT1,TAP1,TM4SF1,UBE2L6	-3.50 9.54E-09	ATF3,CASP4,CXCL10,GBP1,IFI35,IRF7,IRF9,ISG20,KRT17,LY6G6C,MX1,NEDD4L,OAS1,OSMR,PIGR,S100A12,SLC15A1,SLC16A1,SOCS1,STAT1,TAP1,UBE2L6
PRDM16			+2.18 1.11E-09	CXCL10,GBP4,IFI44,IRF7,MX2,STAT1	+2.40 4.27E-08	CXCL10,GBP4,IFIT2,MX2,OAS2,STAT1,STAT2	+2.58 9.41E-10	CXCL10,GBP4,IFI44,IFIT2,IRF7,MX2,STAT1,STAT2
SOCS3			+2.21 9.23E-06	CXCL10,IFIT1,ISG20,MX1,OAS1	+2.89 1.40E-09	CCND1,CD40,CXCL10,FCGR1A,IFIT1,IFIT2,IL23A,ISG20,MX1,OAS1,OAS2	+2.37 1.22E-08	ATF3,CD40,CD86,CXCL10,FCGR1A,IFIT2,ISG20,MX1,OAS1,SOCS1
STAT2			-2.01 5.80E-30	CXCL10,GBP1,IFI27,IFI6,IFIT1,IFITM1,IRF7,IRF9,ISG15,MX1,OAS1,RSAD2,RTP4,STAT1,TNFSF10,USP18,ZBP1	-2.39 7.64E-28	CD40,CXCL10,GBP1,GBP6,IFI27,IFI35,IFI6,IFIT1,IFIT2,IFIT3,IRF9,ISG15,MX1,OAS1,OAS2,RSAD2,RTP4,STAT1,TNFSF10,USP18,ZBP1	-2.80 1.52E-26	CD40,CD86,CXCL10,GBP1,IFI27,IFI35,IFI6,IFIT2,IFITM1,IRF7,IRF9,ISG15,MX1,OAS1,RSAD2,RTP4,SOCS1,STAT1,USP18,WARS1

LIST OF REFERENCES

Adashi, E.Y., C.E. Resnick, A.J. D'Ercole, M.E. Svoboda, and J.J. van Wyk. 1985. Insulin-like growth factors as intraovarian regulators of granulosa cell growth and function. Endocr. Rev. 6:400–420. doi:10.1210/edrv-6-3-400.

Adashi, E.Y., C.E. Resnick, and B. Jastorff. 1990. Blockade of granulosa cell differentiation by an antagonistic analog of adenosine 3',5'-cyclic monophosphate (cAMP): central but non-exclusive intermediary role of cAMP in follicle-stimulating hormone action. Mol. Cell. Endocrinol. 72:1–11. doi:10.1016/0303-7207(90)90234-Y.

Akira, S., H. Isshiki, T. Sugita, O.S. Tanabe Kinoshita, Y. Nishio, T. Nakajima, T. Hirano, and T. Kishimoto. 1990. A nuclear factor for IL-6 expression (NF-IL6) is a member of a C/EBP family. EMBO J. 9:1897–1906. doi:10.1002/j.1460-2075.1990.tb08316.x.

Akira, S., K. Takeda, and T. Kaisho. 2001. Toll-like receptors: critical proteins linking innate and acquired immunity. Nature 2:675–680.

Allen, E., and E.A. Doisy. 1923. An ovarian hormone: preliminary report on its localization, extraction and partial purification and action in test animals. J. Am. Med. Assoc. 81:819–821.

Allen, E., B.F. Francis, L.L. Robertson, C.E. Colgate, and C.G. Johnston. 1924. The hormone of the ovarian follicle; its localization and action in test animals, and additional points bearing upon the internal secretion of the ovary. Am. J. Anat. 34:133–181.

Amos, M.R., G.D. Healey, R.J. Goldstone, S.M. Mahan, A. Duval, H.J. Schuberth, O. Sandra, P. Zieger, I. Dieuzy-Labaye, D.G.E. Smith, and I.M. Sheldon. 2014. Differential endometrial cell sensitivity to a cholesterol-dependent cytolysin links Trueperella pyogenes to uterine disease in cattle. Biol. Reprod. 90:1–13. doi:10.1095/biolreprod.113.115972.

Asaf, S., G. Leitner, O. Furman, Y. Lavon, D. Kalo, D. Wolfenson, and Z. Roth. 2014. Effects of Escherichia coli- and Staphylococcus aureus-induced mastitis in lactating cows on oocyte developmental competence. Reproduction 147:33–43. doi:10.1530/REP-13-0383.

Babicki, S., D. Arndt, A. Marcu, Y. Liang, J.R. Grant, A. Maciejewski, and D.S. Wishart. 2016. Heatmapper: web-enabled heat mapping for all. Nucleic Acids Res. 44:W147–W153. doi:10.1093/nar/gkw419.

Baker, T.G. 1963. A quantitative and cytological study of germ cells in human ovaries. Proc R.Soc L. B Biol Sci 158:417–433. doi:10.1098/rspb.1963.0055.

Barański, W., K. Łukasik, D. Skarzyński, M. Sztachańska, S. Zduńczyk, and T. Janowski. 2013. Secretion of prostaglandins and leukotrienes by endometrial cells in cows with subclinical and clinical endometritis. Theriogenology 80:766–772. doi:10.1016/j.theriogenology.2013.07.001.

Barkema, H.W., J.D. Westrik, K.A.S. van Keulen, Y.H. Schukken, and A. Brand. 1994. The effects of lameness on reproductive performance, milk production and culling in Dutch dairy farms. Prev. Vet. Med. 20:249–259. doi:10.1016/0167-5877(94)90058-2.

Barker, A.R., F.N. Schrick, M.J. Lewis, H.H. Dowlen, and S.P. Oliver. 1998. Influence of clinical mastitis during early lactation on reproductive performance of Jersey cows. J. Dairy Sci. 81:1285–1290. doi:10.3168/jds.S0022-0302(98)75690-5.

Barlow, D.P., R. Stoger, B.G. Herrmann, K. Saitot, and N. Schweifer. 1991. The mouse insulin-like growth factor type-2 receptor is imprinted and closely linked to the Tme locus. Nature 349:84–87.

Barroso, R.P., C. Osuamkpe, M. Nagamani, and C. Yallampalli. 1998. Nitric oxide inhibits development of embryos and implantation in mice. Mol. Hum. Reprod. 4:503–507. doi:10.1093/molehr/4.5.503.

Battaglia, D.F., A.B. Beaver, T.G. Harris, E. Tanhehco, C. Viguié, and F.J. Karsch. 1999. Endotoxin disrupts the estradiol-induced luteinizing hormone surge: Interference with estradiol signal reading, not surge release. Endocrinology 140:2471–2479. doi:10.1210/endo.140.6.6739.

Battaglia, D.F., J.M. Bowen, H.B. Krasa, L.A. Thrun, C. Viguié, and F.J. Karsch. 1997. Endotoxin inhibits the reproductive neuroendocrine axis while stimulating adrenal steroids: A simultaneous view from hypophyseal portal and peripheral blood. Endocrinology 138:4273–4281. doi:10.1210/en.138.10.4273.

Battaglia, D.F., H.B. Krasa, V. Padmanabhan, C. Viguié, and F.J. Karsch. 2000. Endocrine alterations that underlie endotoxin-induced disruption of the follicular phase in ewes. Biol. Reprod. 62:45–53. doi:10.1095/BIOLREPROD62.1.45.

Bauersachs, S., C.A. Simintiras, R.G. Sturmey, S. Krebs, J. Bick, H. Blum, E. Wolf, P. Lonergan, and N. Forde. 2017. Effect of metabolic status on conceptus–maternal interactions on day 19 in dairy cattle: II. Effects on the endometrial transcriptome. Biol. Reprod. 97:413–425. doi:10.1093/biolre/iox095.

Bauersachs, S., S.E. Ulbrich, K. Gross, S.E.M. Schmidt, H.H.D. Meyer, R. Einspanier, H. Wenigerkind, M. Vermehren, H. Blum, F. Sinowatz, and E. Wolf. 2005. Gene expression profiling of bovine endometrium during the oestrous cycle: Detection of molecular pathways involved in functional changes. J. Mol. Endocrinol. 34:889–908. doi:10.1677/jme.1.01799.

Bauersachs, S., S.E. Ulbrich, H.-D. Reichenbach, M. Reichenbach, M. Büttner, H.H.. Meyer, T.E. Spencer, M. Minten, G. Sax, G. Winter, and E. Wolf. 2012. Comparison of the effects of early pregnancy with human interferon, alpha 2 (IFNA2), on gene expression in bovine endometrium. Biol. Reprod. 86:1–15. doi:10.1095/biolreprod.111.094771.

Bauman, D.E., and B.W. Currie. 1980. Partitioning of nutrients during pregnancy and lactation: a review of mechanisms involving homeostasis and homeorhesis. J. Dairy Sci. 63:1514–1529. doi:10.3168/jds.S0022-0302(80)83111-0.

Bazer, F.W., T.E. Spencer, and T.L. Ott. 1997. Interferon tau: a novel pregnancy recognition signal. Am. J. Reprod. Immunol. 37:412–420. doi:10.1111/j.1600-0897.1997.tb00253.x.

Beam, S.W., and W.R. Butler. 1999. Effects of energy balance on follicular development and first ovulation in postpartum dairy cows. J. Reprod. Fertil. Suppl. 54:411–424. doi:10.1530/biosciprocs.4.032.

Bell, A.W. 1995. Regulation of organic nutrient metabolism during transition from late pregnancy to early lactation. J. Anim. Sci. 73:2804. doi:10.2527/1995.7392804x.

Bikfalvi, A. 2004. Platelet factor 4: An inhibitor of angiogenesis. Semin. Thromb. Hemost. 30:379–385. doi:10.1055/s-2004-831051.

Bilge-Dagalp, S., E. Gungor, A.B. Demir, D. Pinar-Muz, V. Yilmaz, T.Ç. Oguzoglu, V.S. Ataseven, and F. Alkan. 2010. The investigation of the presence of bovine herpesvirus type 4 (BoHV-4) in cows with metritis in a dairy herd. Ankara Univ. Vet. Fak. Derg. 57:87–91. doi:10.1501/vetfak_0000002316.

Bjersing, L., and H. Carstensen. 1964. The role of the granulosa cell in the biosynthesis of ovarian steroid hormones. Biochim. Biophys. Acta 86:639–640.

Bjersing, L., and H. Carstensen. 1967. Biosynthesis of steroids by granulosa cells of the porcine ovary in vitro. J. Reprod. Fertil. 14:101–111. doi:10.1530/jrf.0.0140101.

Bondurant, R.H. 1999. Inflammation in the bovine female reproductive tract.. J. Anim. Sci. 77 Suppl 2:101–110. doi:10.2527/1999.77suppl_2101x.

Borsberry, S., and H. Dobson. 1989. Peripartureint diseases and their effect on reproductive performance in five dairy herds. Vet. Rec. 124:217–219.

Brick, T.A., G.M. Schuenemann, S. Bas, J.B. Daniels, C.R. Pinto, D.M. Rings, and P.J. Rajala-Schultz. 2012. Effect of intrauterine dextrose or antibiotic therapy on reproductive performance of lactating dairy cows diagnosed with clinical endometritis. J. Dairy Sci. 95:1894–1905. doi:10.3168/jds.2011-4892.

Britt, J.H. 1992. Impacts of early postpartum metabolism on follicular development and fertility. Am. Assoc. Bov. Pr. 39–43.

Britt, J.H., R.A. Cushman, C.D. Dechow, H. Dobson, P. Humblot, M.F. Hutjens, G.A. Jones, P.S. Ruegg, I.M. Sheldon, and J.S. Stevenson. 2018. Invited review: Learning from the future—A vision for dairy farms and cows in 2067. J. Dairy Sci. 101:3722–3741. doi:10.3168/jds.2017-14025.

Bromfield, J.J., and I.M. Sheldon. 2011. Lipopolysaccharide initiates inflammation in bovine granulosa cells via the TLR4 pathway and perturbs oocyte meiotic progression in vitro. Endocrinology 152:5029–5040. doi:10.1210/en.2011-1124.

Brooks, G. 2000. Comparison of two intrauterine treatments for bovine endometritis. Vet. Rec. 146:25. doi:10.1136/vr.146.1.25.

Broome, A.W., A.J. Winter, S.H. McNutt, and L.E. Casida. 1960. Variations in uterine response to experimental infection due to the hormonal state of the ovaries II. The mobilization of leukocytes and their importance in uterine bactericidal activity. Am. J. Vet. Res. 675–681.

Bustin, S.A., V. Benes, J.A. Garson, J. Hellemans, J. Huggett, M. Kubista, R. Mueller, T. Nolan, M.W. Pfaffl, G.L. Shipley, J. Vandesompele, and C.T. Wittwer. 2009. The MIQE guidelines: minimum information for publication of quantitative real-time PCR experiments. Clin. Chem. 55:611–622. doi:10.1373/clinchem.2008.112797.

Butler, W.R. 1998. Review: effect of protein nutrition on ovarian and uterine physiology in dairy cattle.. J. Dairy Sci. 81:2533–2539. doi:10.3168/jds.S0022-0302(98)70146-8.

Butler, W.R., and R.D. Smith. 1989. Interrelationships between energy balance and postpartum reproductive function in dairy cattle. J. Dairy Sci. 72:767–783. doi:10.3168/jds.S0022-0302(89)79169-4.

Carvalho, M.R., F. Peñagaricano, J.E.P. Santos, T.J. Devries, B.W. Mcbride, and E.S. Ribeiro. 2019. Long-term effects of postpartum clinical disease on milk production, reproduction, and culling of dairy cows. J. Dairy Sci. doi:10.3168/jds.2019-17025.

Carvalho, P.D., A.H. Souza, M.C. Amundson, K.S. Hackbart, M.J. Fuenzalida, M.M. Herlihy, H. Ayres, A.R. Dresch, L.M. Vieira, J.N. Guenther, R.R. Grummer, P.M. Fricke, R.D. Shaver, and M.C. Wiltbank. 2014. Relationships between fertility and postpartum changes in body condition and body weight in lactating dairy cows. J. Dairy Sci. 97:3666–3683. doi:10.3168/jds.2013-7809.

Centers for Disease Control and Prevention. 2018. Sexually transmitted disease surveillance 2017. Atlanta, GA.

Cerri, R.L.A., I.M. Thompson, I.H. Kim, A.D. Ealy, P.J. Hansen, C.R. Staples, J.L. Li, J.E.P. Santos, and W.W. Thatcher. 2012. Effects of lactation and pregnancy on gene expression of endometrium of Holstein cows at day 17 of the estrous cycle or pregnancy. J. Dairy Sci. 95:5657–5675. doi:10.3168/jds.2011-5114.

Channing, C.P., and S.P. Coudert. 1976. Contribution of granulosa cells and follicular fluid to ovarian estrogen secretion in the rhesus monkey in vivo. Endocrinology 98:590–597. doi:10.1210/endo-98-3-590.

Chen, F.C.K., N. Sarioglu, U. Büscher, and J.W. Dudenhausen. 2009. Lipopolysaccharide binding protein in the early diagnosis of intraamniotic infection of pregnant women with premature rupture of the membranes. J. Perinat. Med. 37:135–139. doi:10.1515/JPM.2009.004.

Chenault, J.R., J.F. McAllister, T.S. Chester Jr, K.J. Dame, F.M. Kausche, and E.J. Robb. 2004. Efficacy of ceftiofur hydrochloride sterile suspension administered parenterally for the treatment of acute postpartum metritis in dairy cows. Sci. Rep. 224:1634–1639.

Czaplicki, G., and E. Thiry. 1998. An association exists between bovine herpesvirus-4 seropositivity and abortion in cows. Prev. Vet. Med. 33:235–240. doi:10.1016/S0167-5877(97)00036-6.

Davies, D., K.G. Meade, S. Herath, P.D. David, D. Gonzalez, J.O. White, R.S. Steven, C. O'Farrelly, and I.M. Martin. 2008. Toll-like receptor and antimicrobial peptide expression in the bovine endometrium. Reprod. Biol. Endocrinol. 6:1–12. doi:10.1186/1477-7827-6-53.

Deb, K., M.M. Chaturvedi, and Y.K. Jaiswal. 2004. Comprehending the role of LPS in Gram-negative bacterial vaginosis: ogling into the causes of unfulfilled child-wish.. Arch. Gynecol. Obstet. 270:133–146. doi:10.1007/s00404-004-0623-0.

DeChiara, T.M., A. Efstratiadis, and E.J. Robertsen. 1990. A growth-deficiency phenotype in heterozygous mice carrying an insulin-like growth factor II gene disrupted by targeting. Nature 345:78–80. doi:10.1038/345078a0.

Del Vecchio, R.P., D.J. Matsas, S. Fortin, D.P. Sponenberg, and G.S. Lewis. 1994. Spontaneous uterine infections are associated with elevated prostaglandin F2α metabolite concentrations in postpartum dairy cows. Theriogenology 41:413–421. doi:10.1016/0093-691X(94)90077-V.

Dematawewa, C.M.B., and P.J. Berger. 1998. Genetic and phenotypic parameters for 305-day yield, fertility, and survival in Holsteins. J. Dairy Sci. 81:2700–2709. doi:10.3168/jds.S0022-0302(98)75827-8.

Deori, S., H. Kumar, M.C. Yadav, M. Rawat, and S.K. Srivastava. 2004. Intrauterine administration of bacterial modulins: an alternative therapy for endometrits. J. Appl. Anim. Res. 26:117–1121. doi:10.1080/09712119.2004.9706519.

Descombes, P., and U. Schibler. 1991. A liver-enriched transcriptional activator protein, LAP, and a transcriptional inhibitory protein, LIP, are translated from the same mRNA. Cell 67:569–579. doi:10.1016/0092-8674(91)90531-3.

Dickson, M.J., R.L. Piersanti, R. Ramirez-Hernandez, E.B. de Oliveira, J.V. Bishop, T.R. Hansen, Z. Ma, K.C.C. Jeong, J.E.P. Santos, M.I. Sheldon, J. Block, and J.J. Bromfield. 2020. Experimentally induced endometritis impairs the developmental capacity of bovine oocytes. Biol. Reprod. 103:508–520. doi:10.1093/biolre/ioaa129.

Dohmen, M.J.W., K. Joop, A. Sturk, P.E.J. Bols, and J.A.C.M. Lohuis. 2000. Relationship between intra-uterine bacterial contamination, endotoxin levels and the development of endometritis in postpartum cows with dystocia or retained placenta. Theriogenology 54:1019–1032. doi:10.1016/S0093-691X(00)00410-6.

Donofrio, G., S. Herath, C. Sartori, S. Cavirani, C.F. Flammini, and I.M. Sheldon. 2007. Bovine herpesvirus 4 is tropic for bovine endometrial cells and modulates endocrine function. Reproduction 134:183–197. doi:10.1530/REP-07-0065.

Dorrington, J.H., and D.T. Armstrong. 1975. Follicle-stimulating hormone stimulates estradiol-17B synthesis in cultured Sertoli cells. Cell Biol. 72:2677–2681.

Dorrington, J.H., Y.S. Moon, and D.T. Armstrong. 1975. Estradiol-17B biosynthesis in cultured granulosa cells from hypophysectomized immature rats; stimulation by follicle-stimulating hormone. Endocrinology 1328:1328–1331.

Drackley, J.K. 1999. Biology of dairy cows during the transition period: the final frontier?. J. Dairy Sci. 82:2259–2273. doi:10.3168/jds.s0022-0302(99)75474-3.

Drillich, M., D. Raab, M. Wittke, and W. Heuwieser. 2005. Treatment of chronic endometritis in dairy cows with an intrauterine application of enzymes: A field trial. Theriogenology 63:1811–1823. doi:10.1016/j.theriogenology.2004.05.031.

Dubuc, J., T.F. Duffield, K.E. Leslie, J.S. Walton, and S.J. LeBlanc. 2011. Randomized clinical trial of antibiotic and prostaglandin treatments for uterine health and reproductive performance in dairy cows. J. Dairy Sci. 94:1325–1338. doi:10.3168/jds.2010-3757.

Edelhoff, I.N.F., M.H.C. Pereira, J.J. Bromfield, J.L.M. Vasconcelos, and J.E.P. Santos. 2020. Inflammatory diseases in dairy cows: Risk factors and associations with pregnancy after embryo transfer. J. Dairy Sci. 103:11970–11987. doi:10.3168/jds.2020-19070.

Edwards, J.L., A.D. Ealy, V.H. Monterroso, and P.J. Hansen. 1997. Ontogeny of temperature-regulated heat shock protein 70 synthesis in preimplantation bovine embryos. Mol. Reprod. Dev. 48:25–33. doi:10.1002/(SICI)1098-2795(199709)48:1<25::AID-MRD4>3.0.CO;2-R.

Elliott, L., K.J. McMahon, H.T. Gier, and G.B. Marion. 1968. Uterus of the cow after parturition: bacterial content . Am. J. Vet. Res. 29:77–81.

Erb, H.N., S.W. Martin, N. Ison, and S. Swaminathan. 1981. Interrelationships between production and reproductive diseases in Holstein cows. Conditional relationships between production and disease. J. Dairy Sci. 64:272–281. doi:10.3168/jds.S0022-0302(81)82564-7.

Erickson, B.H. 1966. Development and senescence of the postnatal bovine ovary. J. Anim. Sci. 25:800–805. doi:10.2527/jas1966.253800x.

Erickson, G.F., and A.J.W. Hsueh. 1978. Stimulation of aromatase activity by follicle stimulating hormone in rat granulosa cells in vivo and in vitro. Endocrinology 102:1275–1282. doi:10.1210/endo-102-4-1275.

Erickson, G.F., and K.J. Ryan. 1975. The effect of LH/FSH, dibutyryl cyclic AMP, and prostaglandins on the production of estrogens by rabbit granulosa cells in vitro. Endocrinology 97:108–113. doi:10.1210/endo-97-1-108.

Erickson, G.F., and K.J. Ryan. 1976. Stimulation of testosterone production in isolated rabbit thecal tissue by LH/FSH, dibutyryl cyclic AMP, PGF2alpha, and PGE2. Endocrinology 99:452–8. doi:10.1210/endo-99-2-452.

Estrada-Cortés, E., W.G. Ortiz, R.C. Chebel, E.A. Jannaman, J.I. Moss, F.C. De Castro, A.M. Zolini, C.R. Staples, and P.J. Hansen. 2019. Embryo and cow factors affecting pregnancy per embryo transfer for multiple-service, lactating Holstein recipients. Transl. Anim. Sci. 3:60–65. doi:10.1093/tas/txz009.

Ezz, M.A., M.A. Marey, A.E. Elweza, T. Kawai, M. Heppelmann, C. Pfarrer, A.Z. Balboula, A. Montaser, K. Imakawa, S.M. Zaabel, M. Shimada, and A. Miyamoto. 2019. TLR2/4 signaling pathway mediates sperm-induced inflammation in bovine endometrial epithelial cells in vitro. PLoS One 14:1–17. doi:10.1371/journal.pone.0214516.

Falck, B. 1959. Site of production of oestrogen in rat ovary as studied in micro-transplants. Acta Physiol. Scand. Suppl. 47:1–101.

Fan, H.Y., Z. Liu, P.F. Johnson, and J.A.S. Richards. 2011. CCAAT/enhancer-binding proteins (C/EBP)-α and -β are essential for ovulation, luteinization, and the expression of key target genes. Mol. Endocrinol. 25:253–268. doi:10.1210/me.2010-0318.

Farin, P.W., L. Ball, J.D. Olson, R.G. Mortimer, R.L. Jones, W.S. Adney, and A.E. McChesney. 1989. Effect of Actinomyces pyogenes on gram-negative anaerobic bacteria on the development of bovine placenta. Theriogenology 31:979–989.

Faust, M.A., B.T. McDaniel, O.W. Robison, J.H. Britt, and A.H. Rakes. 1988. Environmental and Yield Effects on Reproduction in Primiparous Holsteins. J. Dairy Sci. 71:3092–3099. doi:10.3168/jds.S0022-0302(88)79909-9.

Fischer, C., M. Drillich, S. Odau, W. Heuwieser, R. Einspanier, and C. Gabler. 2010. Selected pro-inflammatory factor transcripts in bovine endometrial epithelial cells are regulated during the oestrous cycle and elevated in case of subclinical or clinical endometritis. Reprod. Fertil. Dev. 22:818–829. doi:10.1071/RD09120.

Földi, J., M. Kulcsár, A. Pécsi, B. Huyghe, C. de Sa, J.A.C.M. Lohuis, P. Cox, and G. Huszenicza. 2006. Bacterial complications of postpartum uterine involution in cattle. Anim. Reprod. Sci. 96:265–281. doi:10.1016/j.anireprosci.2006.08.006.

Fonseca, F.A., J.H. Britt, B.T. McDaniel, J.C. Wilk, A.H. Rakes, N.J. Moeller, and H. Karg. 1983. Reproductive traits of Holsteins and Jerseys. Effects of age, milk yield, and clinical abnormalities on involution of cervix and uterus, ovulation, estrous cycles, detection of estrus, conception rate, and days open. J. Dairy Sci. 66:1128–47. doi:10.3168/jds.S0022-0302(83)81910-9.

Forde, N., F. Carter, T.E. Spencer, F.W. Bazer, O. Sandra, N. Mansouri-Attia, L.A. Okumu, P.A. McGettigan, J.P. Mehta, R. McBride, P. O'Gaora, J.F. Roche, and P. Lonergan. 2011. Conceptus-induced changes in the endometrial transcriptome: How soon does the cow know she is pregnant?. Biol. Reprod. 85:144–156. doi:10.1095/biolreprod.110.090019.

Forde, N., G.B. Duffy, P.A. McGettigan, J.A. Browne, J.P. Mehta, A.K. Kelly, N. Mansouri-Attia, O. Sandra, B.J. Loftus, M.A. Crowe, T. Fair, J.F. Roche, P. Lonergan, and A.C.O. Evans. 2012. Evidence for an early endometrial response to pregnancy in cattle: Both dependent upon and independent of interferon tau. Physiol. Genomics 44:799–810. doi:10.1152/physiolgenomics.00067.2012.

Fortune, J.E. 1986. Bovine theca and granulosa cells interact to promote androgen production.. Biol. Reprod. 35:292–9.

Fortune, J.E., and D.T. Armstrong. 1977. Androgen production by theca and granulosa isolated from proestrous rat follicles. Endocrinology 100:1341–1347. doi:10.1210/endo-100-5-1341.

Frazier, K., M. Pence, M.J. Mauel, A. Liggett, M.E. Hines II, L. Sangster, H.D. Lehmkuhl, D. Miller, E. Styer, J. West, and C.A. Baldwin. 2001. Endometritis in postparturient cattle associated with bovine herpesvirus-4 infection: 15 cases. J. Veterniary Diagnostic Investig. 13:502–508.

Freick, M., M. Zenker, O. Passarge, and J. Weber. 2018. Reducing the incidence of acute puerperal metritis in primiparous cows by application of pegbovigrastim in a Holstein dairy herd. Vet. Med. (Praha). 63:151–160. doi:10.17221/2/2018-VETMED.

Fry, T.J., and C.L. Mackall. 2005. The Many Faces of IL-7: From Lymphopoiesis to Peripheral T Cell Maintenance. J. Immunol. 174:6571–6576. doi:10.4049/jimmunol.174.11.6571.

Fürbass, R., C. Kalbe, and J. Vanselow. 1997. Tissue-specific expression of the bovine aromatase-encoding gene uses multiple transcriptional start sites and alternative first exons. Endocrinology 138:2813–2819. doi:10.1210/endo.138.7.5257.

Gabler, C., M. Drillich, C. Fischer, C. Holder, W. Heuwieser, and R. Einspanier. 2009. Endometrial expression of selected transcripts involved in prostaglandin synthesis in cows with endometritis. Theriogenology 71:993–1004. doi:10.1016/j.theriogenology.2008.11.009.

Gallagher, J.T., and L. Ball. 1980. Effect of infusion of uterine purulent. Theriogenology 13:311–320.

Galvão, K.N., R.C. Bicalho, and S.J. Jeon. 2019. Symposium review: The uterine microbiome associated with the development of uterine disease in dairy cows. J. Dairy Sci. 102:11786–11797. doi:10.3168/jds.2019-17106.

Galvão, K.N., M. Frajblat, S.B. Brittin, W.R. Butler, C.L. Guard, and R.O. Gilbert. 2009a. Effect of prostaglandin F2α on subclinical endometritis and fertility in dairy cows. J. Dairy Sci. 92:4906–4913. doi:10.3168/jds.2008-1984.

Galvão, K.N., L.F. Greco, J.M. Vilela, M.F. Sá Filho, and J.E.P. Santos. 2009b. Effect of intrauterine infusion of ceftiofur on uterine health and fertility in dairy cows. J. Dairy Sci. 92:1532–1542. doi:10.3168/jds.2008-1615.

Gicquel, C., and Y. Le Bouc. 2006. Hormonal regulation of fetal growth. Horm. Res. 65:28–33. doi:10.1159/000091503.

Gilbert, R.O., and N.R. Santos. 2016. Dynamics of postpartum endometrial cytology and bacteriology and their relationship to fertility in dairy cows. Theriogenology 85:1367–1374. doi:10.1016/j.theriogenology.2015.10.045.

Gilbert, R.O., S.T. Shin, C.L. Guard, H.N. Erb, and M. Frajblat. 2005. Prevalence of endometritis and its effects on reproductive performance of dairy cows. Theriogenology 64:1879–1888. doi:10.1016/j.theriogenology.2005.04.022.

Gillund, P., O. Reksen, Y.T. Gröhn, and K. Karlberg. 2001. Body condition related to ketosis and reproductive performance in Norwegian dairy cows. J. Dairy Sci. 84:1390–1396. doi:10.3168/jds.S0022-0302(01)70170-1.

Giuliodori, M.J., R.P. Magnasco, D. Becu-Villalobos, I.M. Lacau-Mengido, C.A. Risco, and R.L. De la Sota. 2013. Metritis in dairy cows: Risk factors and reproductive performance. J. Dairy Sci. 96:3621–3631. doi:10.3168/jds.2012-5922.

Goldstone, R.J., M. Amos, R. Talbot, H.-J. Schuberth, O. Sandra, I.M. Sheldon, and D.G.E. Smith. 2014a. Draft genome sequence of Escherichia coli MS499, isolated from the infected uterus of a postpartum cow with metritis. Genome Announc. 2:e00217-14. doi:10.1128/genomeA.00194-14.

Goldstone, R.J., M. Amos, R. Talbot, H.-J. Schuberth, O. Sandra, I.M. Sheldon, and D.G.E. Smith. 2014b. Draft genome sequence of Trueperella pyogenes, isolated from the infected uterus of a postpartum cow with metritis. Genome Announc. 2:e00194-14. doi:10.1128/genomeA.00194-14.

Golovine, K., M. Schwerin, and J. Vanselow. 2003. Three different promoters control expression of the aromatase cytochrome P450 gene (Cyp19) in mouse gonads and brain. Biol. Reprod. 68:978–984. doi:10.1095/biolreprod.102.008037.

Gong, J.G., W.J. Lee, P.C. Garnsworthy, and R. Webb. 2002. Effect of dietary-induced increases in circulating insulin concentrations during the early postpartum period on reproductive function in dairy cows. Reproduction 123:419–427. doi:10.1530/rep.0.1230419.

Gougeon, A. 1996. Regulation of ovarian follicular development in primates: facts and hypotheses. Endocr. Rev. 17:121–155. doi:10.1210/edrv-17-2-121.

Greenwel, P., S. Tanaka, D. Penkov, W. Zhang, M. Olive, J. Moll, C. Vinson, M. Di Liberto, and F. Ramirez. 2000. Tumor necrosis factor alpha inhibits type I collagen synthesis through repressive CCAAT/Enhancer-binding proteins. Mol. Cell. Biol. 20:912–918.

Griffin, J.F.T., P.J. Hartigan, and W.R. Nunn. 1974. Non-specific uterine infection and bovine infertility. Theriogenology 1:91–106.

Hageman, W.H., G.E. Shook, and W.J. Tyler. 1991. Reproductive performance in genetic lines selected for high or average milk yield. J. Dairy Sci. 74:4366–4376. doi:10.3168/jds.S0022-0302(91)78633-5.

Hansen, L.B., A.E. Freeman, and P.J. Berger. 1983. Association of heifer fertility with cow fertility and yield in dairy cattle. J. Dairy Sci. 66:306–314. doi:10.3168/jds.S0022-0302(83)81790-1.

Hansen, T.R., L.D.P. Sinedino, and T.E. Spencer. 2017. Paracrine and endocrine actions of interferon tau (IFNT). Reproduction 154:F45–F59. doi:10.1530/REP-17-0315.

Hawk, H.W., T.H. Brinsfield, G.D. Turner, G.W. Whitemore, and M.A. Norcross. 1964. Effect of ovarian status on induced acute inflammatory responses in cattle uteri. Am. J. Vet. Res. 25:362–366.

Hawk, H.W., G.D. Turner, and J.F. Sykes. 1960. The effect of ovarian hormones on the uterine disease mechanism during the early stages of induced infection. Am. J. Vet. Res. 644–8.

Haziak, K., A.P. Herman, and D. Tomaszewska-Zaremba. 2014. Effects of central injection of anti-LPS antibody and blockade of TLR4 on GnRH/LH secretion during immunological stress in anestrous ewes. Mediators Inflamm. 2014:1–10. doi:10.1155/2014/867170.

Heard, R.D.., P.H. Jellinck, and V.J. O'Donnell. 1955. Biogenesis of the estrogens: the conversion of testosterone-4-C14 to estrone in the pregnant mare. Endocrinology 57:200–204.

Heppelmann, M., M. Weinert, S.E. Ulbrich, A. Brömmling, M. Piechotta, S. Merbach, H.A. Schoon, M. Hoedemaker, and H. Bollwein. 2016. The effect of puerperal uterine disease on histopathologic findings and mRNA expression of proinflammatory cytokines of the endometrium in dairy cows. Theriogenology 85:1348–1356. doi:10.1016/j.theriogenology.2015.12.022.

Herath, S., D.P. Fischer, D. Werling, E.J. Williams, S.T. Lilly, H. Dobson, C.E. Bryant, and I.M. Sheldon. 2006. Expression and function of toll-like receptor 4 in the endometrial cells of the uterus. Endocrinology 147:562–570. doi:10.1210/en.2005-1113.

Herath, S., S.T. Lilly, D.P. Fischer, E.J. Williams, H. Dobson, C.E. Bryant, and I.M. Sheldon. 2009a. Bacterial lipopolysaccharide induces an endocrine switch from prostaglandin F2α to prostaglandin E2 in bovine endometrium. Endocrinology 150:1912–1920. doi:10.1210/en.2008-1379.

Herath, S., S.T. Lilly, N.R. Santos, R.O. Gilbert, L. Goetze, C.E. Bryant, J.O. White, J. Cronin, and I.M. Sheldon. 2009b. Expression of genes associated with immunity in the endometrium of cattle with disparate postpartum uterine disease and fertility. Reprod. Biol. Endocrinol. 7:55. doi:10.1186/1477-7827-7-55.

Herath, S., E.J. Williams, S.T. Lilly, R.O. Gilbert, H. Dobson, C.E. Bryant, and I.M. Sheldon. 2007. Ovarian follicular cells have innate immune capabilities that modulate their endocrine function. Reproduction 134:683–693. doi:10.1530/REP-07-0229.

Hernandez-Ledezma, J.J., J.D. Sikes, C.N. Murphy, A.J. Watson, G.A. Schultz, and R.M. Roberts. 1992. Expression of bovine trophoblast interferon in conceptuses derived by in vitro techniques. Biol. Reprod. 47:374–380. doi:10.1095/biolreprod47.3.374.

Hernandez, J.A., E.J. Garbarino, J.K. Shearer, C.A. Risco, and W.W. Thatcher. 2005. Comparison of the calving-to-conception interval in dairy cows with different degrees of lameness during the prebreeding postpartum period. J. Am. Vet. Med. Assoc. 227:1284–1291. doi:10.2460/javma.2005.227.1284.

Hertl, J.A., Y.T. Gröhn, J.D.G. Leach, D. Bar, G.J. Bennett, R.N. González, B.J. Rauch, F.L. Welcome, L.W. Tauer, and Y.H. Schukken. 2010. Effects of clinical mastitis caused by gram-positive and gram-negative bacteria and other organisms on the probability of conception in New York State Holstein dairy cows. J. Dairy Sci. 93:1551–60. doi:10.3168/jds.2009-2599.

Hill, J., and R. Gilbert. 2008. Reduced quality of bovine embryos cultured in media conditioned by exposure to an inflamed endometrium. Aust. Vet. J. 86:312–316. doi:10.1111/j.1751-0813.2008.00326.x.

Hirschfield, A. 1991. Development of follicles in the mammalian ovary. Int. Rev. Cytol. 124:43–101. doi:10.1016/s0074-7696(08)61524-7.

Horlock, A.D., R.L. Piersanti, R. Ramirez-Hernandez, F. Yu, Z. Ma, K.C. Jeong, M.J.D. Clift, J. Block, J.E.P. Santos, J.J. Bromfield, and I.M. Sheldon. 2020. Uterine infection alters the transcriptome of the bovine reproductive tract three months later. Reproduction 160:93–107. doi:10.1530/REP-19-0564.

Huber, R., D. Pietsch, T. Panterodt, and K. Brand. 2012. Regulation of C/EBPβ and resulting functions in cells of the monocytic lineage. Cell. Signal. 24:1287–1296. doi:10.1016/j.cellsig.2012.02.007.

Hussain, A.M., and R.C.W. Daniel. 1992. Effects of intrauterine infusion of Escherichia coli endotoxin in normal cows and in cows with endometritis induced by experimental infection with Streptococcus agalactiae. Theriogenology 37:791–810.

Huszenicza, G., M. Fodor, M. Gacs, M. Kulcsar, M.J.W. Dohmen, M. Vamos, L. Porkolab, T. Kegl, J. Bartyik, J. Lohuis, S. Janosi, and G. Szita. 1999. Uterine bacteriology, resumption of cyclic ovarian activity and fertility in postpartum cows kept in large-scale dairy herds. Reprod. Domest. Anim. 34:237–245. doi:10.1111/j.1439-0531.1999.tb01246.x.

International mouse phenotyping consortium: Trank1. Accessed March 9, 2021. https://www.mousephenotype.org/data/genes/MGI:1341834#phenotypesTab.

Ishikawa, H., V. Fencki, E.E. Marsh, P. Yin, D. Chen, Y.-H. Cheng, S. Reisterd, Z. Lin, and S.E. Bulun. 2008. CCAAT/Enhancer binding protein β regulates aromatase expression via multiple and novel cis-regulatory sequences in uterine leiomyoma. J. Clin. Endocrinol. Metab. 93:981–991. doi:10.1210/jc.2007-2507.

Janowski, T., W. Baranski, K. Lukasik, D. Skarzynski, M. Rudowska, and S. Zdunczyk. 2013. Prevalence of subclinical endometritis in repeat breeding cows and mRNA expression of tumor necrosis factor α and inducible nitric oxide synthase in the endometrium of repeat breeding cows with and without subclinical endometritis. Pol. J. Vet. Sci. 16:693–699. doi:10.2478/pjvs-2013-0098.

Jasti, S., B.D. Warren, L.K. McGinnis, W.H. Kinsey, B.K. Petroff, and M.G. Petroff. 2012. The autoimmune regulator prevents premature reproductive senescence in female mice. Biol. Reprod. 86:1–9. doi:10.1095/biolreprod.111.097501.

Jiang, X., S.D. Detera-Wadleigh, N. Akula, B.S. Mallon, T. Xiao, G. Felsenfeld, X. Gu, and F.J. McMahon. 2019. Sodium valproate rescues expression of TRANK1 in iPSC-derived neural cells that carry a genetic variant associated with serious mental illness. Mol. Psychiatry 24:613–624. doi:10.1038/s41380-018-0207-1.Sodium.

Jorritsma, R., H. Jorritsma, Y.H. Schukken, and G.H. Wentink. 2000. Relationships between fatty liver and fertility and some periparturient diseases in commercial dutch dairy herds. Theriogenology 54:1065–1074. doi:10.1017/CBO9781107415324.004.

Jost, B.H., and S.J. Billington. 2005. Arcanobacterium pyogenes: Molecular pathogenesis of an animal opportunist. Antonie Van Leeuwenhoek 88:87–102. doi:10.1007/s10482-005-2316-5.

Kaneko, K., and S. Kawakami. 2008. Influence of experimental intrauterine infusion of arcanobacterium pyogenes solution on ovarian activity in cycling cows. J. Vet. Med. Sci. 70:77–83.

Kasimanickam, R., T.F. Duffield, R.A. Foster, C.J. Gartley, K.E. Leslie, J.S. Walton, and W.H. Johnson. 2004. Endometrial cytology and ultrasonography for the detection of subclinical endometritis in postpartum dairy cows. Theriogenology 62:9–23. doi:10.1016/j.theriogenology.2003.03.001.

Kasimanickam, R., T.F. Duffield, R.A. Foster, C.J. Gartley, K.E. Leslie, J.S. Walton, and W.H. Johnson. 2005. The effect of a single administration of cephapirin or cloprostenol on the reproductive performance of dairy cows with subclinical endometritis. Theriogenology 63:818–830. doi:10.1016/j.theriogenology.2004.05.002.

Kellis, J.T., and L.E. Vickery. 1987. Purification and characterization of human placental aromatase cytochrome P-450. J. Biol. Chem. 262:4413–4420.

Kim, I., and H. Kang. 2003. Risk factors for postpartum endometritis and the effect of endometritis on reproductive performance in dairy cows in Korea. J. Reprod. Dev. 49:485–491.

Knutti, B., U. Küpfer, and A. Busato. 2000. Reproductive efficiency of cows with endometritis after treatment with intrauterine infusions or prostaglandin injections, or no treatment. J. Vet. Med. Ser. A Physiol. Pathol. Clin. Med. 47:609–615. doi:10.1046/j.1439-0442.2000.00324.x.

Kolena, J., and C.P. Channing. 1972. Stimulatory effects of LH, FSH and prostaglandins upon cyclic 3′,5′-AMP levels in porcine granulosa cells. Endocrinology 90:1543–1550. doi:10.1210/endo-90-6-1543.

Komar, C.M., A.K. Berndtson, A.C.O. Evans, and J.E. Fortune. 2001. Decline in circulating estradiol during the periovulatory period is correlated with decreases in estradiol and androgen, and in messenger RNA for P450 aromatase and P450 17α-hydroxylase, in bovine preovulatory follicles. Biol. Reprod. 64:1797–1805. doi:10.1095/biolreprod64.6.1797.

Kotani, S., Y. Kamada, K. Shimizu, A. Sakamoto, M. Nakatsuka, Y. Hiramatsu, and H. Masuyama. 2020. Increased plasma levels of platelet factor 4 and β-thromboglobulin in women with recurrent pregnancy loss. Acta Med. Okayama 74:115–122. doi:10.18926/AMO/58269.

Krämer, A., J. Green, J. Pollard, and S. Tugendreich. 2014. Systems biology Causal analysis approaches in Ingenuity Pathway Analysis 30:523–530. doi:10.1093/bioinformatics/btt703.

Kreisel, K., E. Torrone, K. Bernstein, J. Hong, and R. Gorwitz. 2017. Prevalence of pelvic inflammatory disease in sexually experienced women of reproductive age — United States, 2013-2014. Morb. Mortal. Wkly. Rep. 66:80–83. doi:10.15585/mmwr.mm6603a3.

Kujjo, L.L., W.T. Bosu, and G.I. Perez. 1995. Opioid peptides involvement in endotoxin-induced suppression of LH secretion in ovariectomized Holstein heifers. Reprod. Toxicol. 9:169–174. doi:10.1016/0890-6238(94)00068-9.

Kwon, H., G. Wu, C.J. Meininger, F.W. Bazer, and T.E. Spencer. 2004. Developmental changes in nitric oxide synthesis in the ovine placenta. Biol. Reprod. 70:679–686. doi:10.1095/biolreprod.103.023184.

Lacroix, E., W. Eechaute, and I. Leusen. 1974. The biosynthesis of estrogens by cow follicles. J. Chem. Inf. Model. 53:337–355. doi:10.1017/CBO9781107415324.004.

Lavon, Y., G. Leitner, T. Goshen, R. Braw-Tal, S. Jacoby, and D. Wolfenson. 2008. Exposure to endotoxin during estrus alters the timing of ovulation and hormonal concentrations in cows. Theriogenology 70:956–967. doi:10.1016/j.theriogenology.2008.05.058.

LeBlanc, S.J., T.F. Duffield, K.E. Leslie, K.G. Bateman, G.P. Keefe, J.S. Walton, and W.H. Johnson. 2002a. Defining and diagnosing postpartum clinical endometritis and its impact on reproductive performance in dairy cows. J. Dairy Sci. 85:2223–2236. doi:10.3168/jds.S0022-0302(02)74302-6.

LeBlanc, S.J., T.F. Duffield, K.E. Leslie, K.G. Bateman, G.P. Keefe, J.S. Walton, and W.H. Johnson. 2002b. The effect of treatment of clinical endometritis on reproductive performance in dairy cows. J. Dairy Sci. 85:2237–2249. doi:10.3168/jds.S0022-0302(02)74303-8.

Lenz, S., R. Pöhland, F. Becker, and J. Vanselow. 2004. Expression of the bovine aromatase cytochrome P450 gene (Cyp19) is primarily regulated by promoter 2 in bovine follicles and by promoter 1.1 in corpora lutea. Mol. Reprod. Dev. 67:406–413. doi:10.1002/mrd.20000.

Leroy, J.L.M.R., T. Vanholder, B. Mateusen, A. Christophe, G. Opsomer, A. de Kruif, G. Genicot, and A. Van Soom. 2005. Non-esterified fatty acids in follicular fluid of dairy cows and their effect on developmental capacity of bovine oocytes in vitro. Reproduction 130:485–495. doi:10.1530/rep.1.00735.

Lewis, G.S. 1997. Uterine health and disorders. J. Dairy Sci. 80:984–994. doi:10.3168/jds.S0022-0302(97)76024-7.

Li, H., S. Guo, L. Cai, W. Ma, and Z. Shi. 2017. Lipopolysaccharide and heat stress impair the estradiol biosynthesis in granulosa cells via increase of HSP70 and inhibition of smad3 phosphorylation and nuclear translocation. Cell. Signal. 30:130–141. doi:10.1016/j.cellsig.2016.12.004.

Li, W., X. Cai, H.J. Li, M. Song, C.Y. Zhang, Y. Yang, L. Zhang, L. Zhao, W. Liu, L. Wang, M. Shao, Y. Zhang, C. Zhang, J. Cai, D.S. Zhou, X. Li, L. Hui, Q.F. Jia, N. Qu, B.L. Zhong, S.F. Zhang, J. Chen, B. Xia, Y. Li, X. Song, Fan, X. Xiao, M. Li, L. Lv, and H. Chang. 2020. Independent replications and integrative analyses confirm TRANK1 as a susceptibility gene for bipolar disorder. Neuropsychopharmacology 10:1–10. doi:10.1038/s41386-020-00788-4.

Lima, F.S., L.F. Greco, R.S. Bisinotto, E.S. Ribeiro, N.M. Martinez, W.W. Thatcher, J.E.P. Santos, M.K. Reinhard, and K.N. Galvão. 2015. Effects of intrauterine infusion of Trueperella pyogenes on endometrial mRNA expression of proinflammatory cytokines and luteolytic cascade genes and their association with luteal life span in dairy cows. Theriogenology 84:1263–1272. doi:10.1016/j.theriogenology.2015.07.004.

Lima, F.S., J.A. Snodgrass, A. De Vries, and J.E.P. Santos. 2019. Economic comparison of systemic antimicrobial therapies for metritis in dairy cows. J. Dairy Sci. 102:7345–7358. doi:10.3168/jds.2018-15383.

Lima, F.S., A. Vieira-Neto, G.S.F.M. Vasconcellos, R.D. Mingoti, E. Karakaya, E. Solé, R.S. Bisinotto, N. Martinez, C.A. Risco, K.N. Galvão, and J.E.P. Santos. 2014. Efficacy of ampicillin trihydrate or ceftiofur hydrochloride for treatment of metritis and subsequent fertility in dairy cows. J. Dairy Sci. 97:5401–5414. doi:10.3168/jds.2013-7569.

Liu, J.J., M. Antaya, D. Boerboom, J.G. Lussier, D.W. Silversides, and J. Sirois. 1999. The delayed activation of the prostaglandin G/H synthase-2 promoter in bovine granulosa cells is associated with down-regulation of truncated upstream stimulatory factor-2. J. Biol. Chem. 274:35037–35045. doi:10.1074/jbc.274.49.35037.

Liu, X., L. Zhang, J. Cui, S. Che, Y. Liu, Y. Zhang, B. Cao, and Y. Song. 2019. The mRNA and lncRNA landscape of the non-pregnant endometrium during the oestrus cycle in dairy goat. Anim. Prod. Sci. 59:1803–1813. doi:10.1071/AN18426.

Liu, Y.X., and A.J.W. Hsueh. 1986. Synergism between granulosa and theca-interstitial cells in estrogen biosynthesis by gonadotropin-treated rat ovaries: studies on the two-cell, two-gonadotropin hypothesis using steroid antisera. Biol. Reprod. 35:27–36. doi:10.1095/biolreprod35.1.27.

Loeffler, S.H., M.J. De Vries, and Y.H. Schukken. 1999. The effects of time of disease occurrence, milk yield, and body condition on fertility of dairy cows. J. Dairy Sci. 82:2589–2604. doi:10.3168/jds.S0022-0302(99)75514-1.

Lucey, S., G.J. Rowlands, and A.M. Russell. 1986. The association between lameness and fertility in dairy cows.. Vet. Rec. 118:628–31. doi:10.1136/VR.118.23.628.

Lucy, M.C. 2001. Reproductive loss in high-producing dairy cattle: where will it end?. J. Dairy Sci. 84:1277–1293.

Lussier, J.G., P. Matton, and J.J. Dufour. 1987. Growth rates of follicles in the ovary of the cow. J. Reprod. Fertil. 81:301–307. doi:10.1530/jrf.0.0810301.

Machado, V.S., G. Oikonomou, E.K. Ganda, L. Stephens, M. Milhomem, G.L. Freitas, M. Zinicola, J. Pearson, M. Wieland, C. Guard, R.O. Gilbert, and R.C. Bicalho. 2015. The effect of intrauterine infusion of dextrose on clinical endometritis cure rate and reproductive performance of dairy cows. J. Dairy Sci. 98:3849–3858. doi:10.3168/jds.2014-9046.

Machado, V.S., G. Oikonomou, S.F. Lima, M.L.S. Bicalho, C. Kacar, C. Foditsch, M.J. Felippe, R.O. Gilbert, and R.C. Bicalho. 2014a. The effect of injectable trace minerals (selenium, copper, zinc, and manganese) on peripheral blood leukocyte activity and serum superoxide dismutase activity of lactating Holstein cows. Vet. J. 200:299–304. doi:10.1016/j.tvjl.2014.02.026.

Machado, V.S., M.L. De Souza Bicalho, E.B. De Souza Meira, R. Rossi, B.L. Ribeiro, S. Lima, T. Santos, A. Kussler, C. Foditsch, E.K. Ganda, G. Oikonomou, S.H. Cheong, R.O. Gilbert, and R.C. Bicalho. 2014b. Subcutaneous immunization with inactivated bacterial components and purified protein of Escherichia coli, Fusobacterium necrophorum and Trueperella pyogenes prevents puerperal metritis in Holstein dairy cows. PLoS One 9. doi:10.1371/journal.pone.0091734.

Magata, F., M. Horiuchi, A. Miyamoto, and T. Shimizu. 2014. Lipopolysaccharide (LPS) inhibits steroid production in theca cells of bovine follicles in vitro: distinct effect of LPS on theca cell function. J. Reprod. Dev. 60:280–287.

Makris, A., and K.J. Ryan. 1975. Progesterone, androstenedione, testosterone, estrone, and estradiol synthesis in hamster ovarian follicle cells. Endocrinology 96:694–701.

Mamo, S., J.P. Mehta, N. Forde, P. McGettigan, and P. Lonergan. 2012. Conceptus-endometrium crosstalk during maternal recognition of pregnancy in cattle. Biol. Reprod. 87:1–9. doi:10.1095/biolreprod.112.099945.

Maquivar, M.G., A.A. Barragan, J.S. Velez, H. Bothe, and G.M. Schuenemann. 2015. Effect of intrauterine dextrose on reproductive performance of lactating dairy cows diagnosed with purulent vaginal discharge under certified organic management. J. Dairy Sci. 98:3876–3886. doi:10.3168/jds.2014-9081.

Markusfeld, O. 1987. Periparturient traits in seven high dairy herds. Incidence rates, association with parity, and interrelationships among traits. J. Dairy Sci. 70:158–166. doi:10.3168/jds.S0022-0302(87)79990-1.

Martinez, N., C.A. Risco, F.S. Lima, R.S. Bisinotto, L.F. Greco, E.S. Ribeiro, F. Maunsell, K. Galvão, and J.E.P. Santos. 2012. Evaluation of peripartal calcium status, energetic profile, and neutrophil function in dairy cows at low or high risk of developing uterine disease. J. Dairy Sci. 95:7158–7172. doi:10.3168/jds.2012-5812.

Mateus, L., L. Lopes da Costa, P. Diniz, and A.J. Ziecik. 2003. Relationship between endotoxin and prostaglandin (PGE2 and PGFM) concentrations and ovarian function in dairy cows with puerperal endometritis. Anim. Reprod. Sci. 76:143–154. doi:10.1016/S0378-4320(02)00248-8.

Matsusaka, T., K. Fujikawa, Y. Nishio, N. Mukaida, K. Matsushima, T. Kishimoto, and S. Akira. 1993. Transcription factors NF-IL6 and NF-κB synergistically activate transcription of the inflammatory cytokines, interleukin 6 and interleukin 8. Proc. Natl. Acad. Sci. U. S. A. 90:10193–10197. doi:10.1073/pnas.90.21.10193.

Mauleon, P. 1969. Oogenesis and folliculogenesis. 2nd ed. H.H. Cole and P.T. Cupps, ed.

McCarthy, M.M., and M.W. Overton. 2018. Short communication: Model for metritis severity predicts that disease misclassification underestimates projected milk production losses. J. Dairy Sci. 101:5434–5438. doi:10.3168/jds.2017-14164.

McDougall, S., M. de Boer, C. Compton, and S.J. LeBlanc. 2013. Clinical trial of treatment programs for purulent vaginal discharge in lactating dairy cattle in New Zealand. Theriogenology 79:1139–1145. doi:10.1016/j.theriogenology.2013.02.002.

McLaughlin, C.L., E. Stanisiewski, M.J. Lucas, C.P. Cornell, J. Watkins, L. Bryson, J.K.S. Tena, J. Hallberg, and J.R. Chenault. 2012. Evaluation of two doses of ceftiofur crystalline free acid sterile suspension for treatment of metritis in lactating dairy cows. J. Dairy Sci. 95:4363–4371. doi:10.3168/jds.2011-5111.

McNatty, K.P., D.T. Baird, A. Bolton, P. Chambers, C.S. Corker, and H. McLean. 1976. Concentration of oestrogens and androgens in human ovarian venous plasma and follicular fluid throughout the menstrual cycle. J. Endocrinol. 71:77–85.

Means, G.D., M.W. Kilgore, M.S. Mahendroo, C.R. Mendelson, and E.R. Simpson. 1991. Tissue-specific promoters regulate aromatase cytochrome P450 gene expression in human ovary and fetal tissues. Mol. Endocrinol. 5:2005–2013.

Mehta, A., Ravinder, S.K. Onteru, and D. Singh. 2015. HDAC inhibitor prevents LPS mediated inhibition of CYP19A1 expression and 17β-estradiol production in granulosa cells. Mol. Cell. Endocrinol. 414:73–81. doi:10.1016/j.mce.2015.07.002.

Mejía, M.E., and I.M. Lacau-Mengido. 2005. Endometritis treatment with a PGF2α analog does not improve reproductive performance in a large dairy herd in Argentina. Theriogenology 63:1266–1276. doi:10.1016/j.theriogenology.2004.05.023.

Melendez, P., J. Bartolome, L.F. Archbald, and A. Donovan. 2003. The association between lameness, ovarian cysts and fertility in lactating dairy cows. Theriogenology 59:927–937. doi:10.1016/S0093-691X(02)01152-4.

Mendelson, C.R., E.E. Wright, C.T. Evans, J.C. Porter, and E.R. Simpson. 1985. Preparation and characterization of polyclonal and monoclonal antibodies against human aromatase cytochrome P-450 (P-450AROM), and their use in its purification. Arch. Biochem. Biophys. 243:480–491. doi:10.1016/0003-9861(85)90525-9.

Menzies, M., and A. Ingham. 2006. Identification and expression of Toll-like receptors 1-10 in selected bovine and ovine tissues. Vet. Immunol. Immunopathol. 109:23–30. doi:10.1016/j.vetimm.2005.06.014.

Metsalu, T., and J. Vilo. 2015. ClustVis: a web tool for visualizing clustering of multivariate data using Principal Component Analysis and heatmap. Web Serv. issue Publ. online 43. doi:10.1093/nar/gkv468.

Miller, A.N.A., E.J. Williams, K. Sibley, S. Herath, E.A. Lane, J. Fishwick, D.M. Nash, A.N. Rycroft, H. Dobson, C.E. Bryant, and I.M. Sheldon. 2007. The effects of Arcanobacterium pyogenes on endometrial function in vitro, and on uterine and ovarian function in vivo. Theriogenology 68:972–980. doi:10.1016/j.theriogenology.2007.07.013.

Miller, D., M. Gershater, R. Slutsky, R. Romero, and N. Gomez-Lopez. 2020. Maternal and fetal T cells in term pregnancy and preterm labor. Cell. Mol. Immunol. 17:693–704. doi:10.1038/s41423-020-0471-2.

Miller, W.L. 2007. Steroidogenic acute regulatory protein (StAR), a novel mitochondrial cholesterol transporter. Biochim. Biophys. Acta - Mol. Cell Biol. Lipids 1771:663–676. doi:10.1016/j.bbalip.2007.02.012.

Miller, W.L., and R.J. Auchus. 2011. The molecular biology, biochemistry, and physiology of human steroidogenesis and its disorders. Endocr. Rev. 32:81–151. doi:10.1210/er.2010-0013.

Mincheva-Nilsson, L. 2003. Pregnancy and gamma/delta T cells: Taking on the hard questions. Reprod. Biol. Endocrinol. 1. doi:10.1186/1477-7827-1-120.

Mitko, K., S.E. Ulbrich, H. Wenigerkind, F. Sinowatz, H. Blum, E. Wolf, and S. Bauersachs. 2008. Dynamic changes in messenger RNA profiles of bovine endometrium during the oestrous cycle. Reproduction 135:225–240. doi:10.1530/REP-07-0415.

Monge, A., L. Elvira, J. V. Gonzalez, S. Astiz, and G.J. Wellenberg. 2006. Bovine herpesvirus 4-associated postpartum metritis in a Spanish dairy herd. Res. Vet. Sci. 80:120–125. doi:10.1016/j.rvsc.2005.04.001.

Monniaux, D., C. Huet, N. Besnard, F. Clement, M. Bosc, C. Pisselet, P. Monget, and J.C. Mariana. 1997. Follicular growth and ovarian dynamics in mammals. J. Reprod. Fertil. Suppl. 51:3–23.

Moon, Y.S., J.H. Dorringtont, and D.T. Armstrong. 1975. Stimulatory action of follicle-stimulating hormone on estradiol-17b secretion by hypophysectomized rat ovaries in organ culture. Endocrinology 97:244–247.

Moore, D.A., J.S. Cullor, R.H. Bondurant, and W.M. Sischo. 1991. Preliminary field evidence for the association of clinical mastitis with altered interestrus intervals in dairy cattle. Theriogenology 36:257–265. doi:10.1016/0093-691X(91)90384-P.

Mor, G., I. Cardenas, V. Abrahams, and S. Guller. 2011. Inflammation and pregnancy: the role of the immune system at the implantation site. Ann. N. Y. Acad. Sci. 1221:80–87. doi:10.1111/j.1749-6632.2010.05938.x.

Mor, G., R. Romero, P.B. Aldo, and V.M. Abrahams. 2005. Is the trophoblast an immune regulator? The role of toll-like receptors during pregnancy. Crit. Rev. Immunol. 25:375–388. doi:10.1615/CritRevImmunol.v25.i5.30.

Moran, B., S.T. Butler, S.G. Moore, D.E. MacHugh, and C.J. Creevey. 2015. Differential gene expression in the endometrium reveals a complex of cytoskeletal and immunological genes in lactating dairy cows genetically divergent for fertility traits. Reprod. Fertil. Dev. 29:274–282. doi:10.1016/b978-0-08-102933-6.00007-x.

Mudunuri, U., A. Che, M. Yi, and R.M. Stephens. 2009. bioDBnet: The biological database network. Bioinformatics 25:555–556. doi:10.1093/bioinformatics/btn654.

Murakami, S., Y. Miyamoto, D.J. Skarzynski, and K. Okuda. 2001. Effects of tumor necrosis factor-α on secretion of prostaglandins E2 and F2α in bovine endometrium throughout the estrous cycle. Theriogenology 55:1667–1678. doi:10.1016/S0093-691X(01)00511-8.

Murray, R., J. Allison, and R. Gard. 1990. Bovine endometritis: comparative efficacy of alfaprostol and intrauterine therapies, and other factors influencing clinical success. Vet. Rec. 127:86–90.

Naftolin, F., K.J. Ryan, and I.J. Davies. 1975. The formation of estrogens by central neuroendocrine tissues. Recent Prog. Horm. Res. Vol.31:295–319. doi:10.1016/b978-0-12-571131-9.50012-8.

Nakao, T., M. Moriyoshi, and K. Kawata. 1988. Effect of postpartum intrauterine treatment with 2 % polyvinyl-pyrrolidone-iodine solution on reproductive efficiency in cows. Theriogenology 30:1033–1043. doi:10.1016/0093-691X(88)90277-4.

Noakes, D.E., L.M. Wallace, and G.R. Smith. 1990. Pyometra in a Friesian heifer: bacteriological and endometrial changes. Vet. Rec. 126:509.

Norman, H.D., L.M. Walton, and J.W. Dürr. Reproductive Status of DHI Cows (2017). Accessed February 1, 2021. https://queries.uscdcb.com/publish/dhi/dhi19/reproall.html.

Norman, H.D., J.R. Wright, S.M. Hubbard, R.H. Miller, and J.L. Hutchison. 2009. Reproductive status of Holstein and Jersey cows in the United States. J. Dairy Sci. 92:3517–3528. doi:10.3168/jds.2008-1768.

de Oliveira, E.B., F. Cunha, R. Daetz, C.C. Figueiredo, R.C. Chebel, J.E. Santos, C.A. Risco, K.C. Jeong, V.S. Machado, and K.N. Galvão. 2020. Using chitosan microparticles to treat metritis in lactating dairy cows. J. Dairy Sci. 103:7377–7391. doi:10.3168/jds.2019-18028.

Oltenacu, P.A., J.H. Britt, R.K. Braun, and R.W. Mellenberger. 1983. Relationships among type of parturition, type of discharge from genital tract, involution of cervix, and subsequent reproductive performance in Holstein cows. J. Dairy Sci. 66:612–619. doi:10.3168/jds.S0022-0302(83)81832-3.

Onnureddy, K., Ravinder, S.K. Onteru, and D. Singh. 2015. IGF-1 attenuates LPS induced pro-inflammatory cytokines expression in buffalo (Bubalus bubalis) granulosa cells. Mol. Immunol. 64:136–143. doi:10.1016/j.molimm.2014.11.008.

Opsomer, G., Y.T. Gröhn, J. Hertl, M. Coryn, H. Deluyker, and A. De Kruif. 2000. Risk factors for post partum ovarian dysfunction in high producing dairy cows in Belgium: a field study. Theriogenology 53:841–857. doi:10.1016/S0093-691X(00)00234-X.

Osborn, B.H., A.F. Haney, M.A. Misukonis, and J.B. Weinberg. 2002. Inducible nitric oxide synthase expression by peritoneal macrophages in endometriosis-associated infertility. Fertil. Steril. 77:46–51. doi:10.1016/S0015-0282(01)02940-5.

Ossipow, V., P. Descombes, and U. Schibler. 1993. CCAAT/enhancer-binding protein mRNA is translated into multiple proteins with different transcription activation potentials. Proc. Natl. Acad. Sci. U. S. A. 90:8219–8223. doi:10.1073/pnas.90.17.8219.

Owusu-Edusei, K., H.W. Chesson, T.L. Gift, G. Tao, R. Mahajan, M.C.B. Ocfemia, and C.K. Kent. 2013. The estimated direct medical cost of selected sexually transmitted infections in the United States, 2008. Sex. Transm. Dis. 40:197–201. doi:10.1097/OLQ.0b013e318285c6d2.

Paisley, L.G., W.D. Mickelsen, and P.B. Anderson. 1986. Mechanisms and therapy for retained fetal membranes and uterine infections of cows: A review. Theriogenology 25:353–381. doi:10.1016/0093-691X(86)90045-2.

Parks, J.B., and J.W. Kendrick. 1973. The isolation and partial characterization of a herpesvirus from a case of bovine metritis. Arch. Gesamte Virusforsch. 41:211–215. doi:10.1007/BF01252768.

Pasanen, M., and O. Pelkonen. 1981. Solubilization and partial purification of human placental cytochromes P-450. Biochem. Biophys. Res. Commun. 103:1310–1317.

Pepper, R.T., and H. Dobson. 1987. Preliminary results of treatment and endocrinology of chronic endometritis in the dairy cow.. Vet. Rec. 120:53–56. doi:10.1136/vr.120.3.53.

Perniola, R. 2018. Twenty years of AIRE. Front. Immunol. 9. doi:10.3389/fimmu.2018.00098.

Peter, A.T., W.T. Bosu, and R.J. DeDecker. 1989. Suppression of preovulatory luteinizing hormone surges in heifers after intrauterine infusions of Escherichia coli endotoxin. Am. J. Vet. Res. 50:368–73.

Peter, A.T., and W.T.K. Bosu. 1987. Effects of intrauterine infection on the function of the corpora lutea formed after first postpartum ovulations in dairy cows. Theriogenology 27:593–609.

Peter, A.T., J.E. Simon, C.W. Luker, and W.T.K. Bosu. 1990. Site of action for endotoxin-induced cortisol release in the suppression of preovulatory luteinizing hormone surges. Theriogenology 33:637–643. doi:10.1016/0093-691X(90)90540-A.

Peter, S., G. Michel, A. Hahn, M. Ibrahim, A. Lubke-Becker, M. Jung, R. Einspanier, and C. Gabler. 2015. Puerperal influence of bovine uterine health status on the mRNA expression of pro-inflammatory factors. J. Physiol. Pharmacol. 66:449–462.

Piersanti, R.L., J. Block, Z. Ma, K.C. Jeong, J.E.P. Santos, F. Yu, I.M. Sheldon, and J.J. Bromfield. 2020. Uterine infusion of bacteria alters the transcriptome of bovine oocytes. FASEB BioAdvances 2:506–520. doi:10.1096/fba.2020-00029.

Piersanti, R.L., A.D. Horlock, J. Block, J.E.P. Santos, I.M. Sheldon, and J.J. Bromfield. 2019a. Persistent effects on bovine granulosa cell transcriptome after resolution of uterine disease. Reproduction 158:35–46. doi:10.1530/REP-19-0037.

Piersanti, R.L., R. Zimpel, P.C.C. Molinari, M.J. Dickson, Z. Ma, K.C. Jeong, J.E.P. Santos, I.M. Sheldon, and J.J. Bromfield. 2019b. A model of clinical endometritis in Holstein heifers using pathogenic Escherichia coli and Trueperella pyogenes. J. Dairy Sci. 102:2686–2697. doi:10.3168/jds.2018-15595.

Poli, V. 1998. The role of C/EBP isoforms in the control of inflammatory and native immunity functions. J. Biol. Chem. 273:29279–29282. doi:10.1074/jbc.273.45.29279.

Ponce, C., M. Torres, C. Galleguillos, H. Sovino, M.A. Boric, A. Fuentes, and M.C. Johnson. 2009. Nuclear factor κB pathway and interleukin-6 are affected in eutopic endometrium of women with endometriosis. Reproduction 137:727–737.

Potter, T.J., J. Guitian, J. Fishwick, P.J. Gordon, and I.M. Sheldon. 2010. Risk factors for clinical endometritis in postpartum dairy cattle. Theriogenology 74:127–134. doi:10.1016/j.theriogenology.2010.01.023.

Price, J.C., J.J. Bromfield, and I.M. Sheldon. 2013. Pathogen-asssociated molecular patterns initiate inflammation and perturb the endocrine function of bovine granulosa cells from ovarian dominant follicles via TLR2 and TLR4 Pathways. Endocrinology 154:3377–3386. doi:10.1210/en.2013-1102.

Price, J.C., and I.M. Sheldon. 2013. Granulosa cells from emerged antral follicles of the bovine ovary initiate inflammation in response to bacterial pathogen-associated molecular patterns via Toll-Like receptor pathways. Biol. Reprod. 89:1–12. doi:10.1095/biolreprod.113.110965.

Purcell, T.L., R. Given, K. Chwalisz, and R.E. Garfield. 1999. Nitric oxide synthase distribution during implantation in the mouse. Mol. Hum. Reprod. 5:467–475. doi:10.1093/molehr/5.5.467.

Rajala, P.J., and Y.T. Gröhn. 1998. Effects of dystocia, retained placenta, and metritis on milk yield in dairy cows. J. Dairy Sci. 81:3172–3181. doi:10.3168/jds.S0022-0302(98)75883-7.

Ramji, D.P., and P. Foka. 2002. CCAAT/enhancer-binding proteins: structure, function and regulation. Biochem. J. 575:561–575. doi:10.1042/BJ20020508.

Regassa, F., I.M. Sheldon, and D.E. Noakes. 2002. Effect of experimentally induced metritis on uterine involution, acute phase protein response and PGFM secretion in the postpartum ewe. Vet. Rec. 150:605–607.

Ribeiro, E.S. 2018. Symposium review: Lipids as regulators of conceptus development: Implications for metabolic regulation of reproduction in dairy cattle. J. Dairy Sci. 101:3630–3641. doi:10.3168/jds.2017-13469.

Ribeiro, E.S., G. Gomes, L.F. Greco, R.L.A. Cerri, A. Vieira-Neto, P.L.J. Monteiro, F.S. Lima, R.S. Bisinotto, W.W. Thatcher, and J.E.P. Santos. 2016a. Carryover effect of postpartum inflammatory diseases on developmental biology and fertility in lactating dairy cows. J. Dairy Sci. 99:2201–2220. doi:10.3168/jds.2015-10337.

Ribeiro, E.S., L.F. Greco, R.S. Bisinotto, F.S. Lima, W.W. Thatcher, and J.E. Santos. 2016b. Biology of preimplantation conceptus at the onset of elongation in dairy cows. Biol. Reprod. 94:1–18. doi:10.1095/biolreprod.115.134908.

Ribeiro, E.S., F.S. Lima, L.F. Greco, R.S. Bisinotto, A.P.A. Monteiro, M. Favoreto, H. Ayres, and R.S. Marsola. 2013. Prevalence of periparturient diseases and effects on fertility of seasonally calving grazing dairy cows supplemented with concentrates. J. Dairy Sci. 96:5682–5697. doi:10.3168/jds.2012-6335.

Richards, J.S. 1994. Hormonal control of gene expression in the ovary. Endocr. Rev. 15:725–751. doi:10.1210/edrv-15-6-725.

Richards, J.S., Y.A. Ren, N. Candelaria, J.E. Adams, and A. Rajkovic. 2018. Ovarian Follicular Theca Cell Recruitment, Differentiation, and Impact on Fertility: 2017 Update. Endocr. Rev. 39:1–20. doi:10.1210/er.2017-00164.

Rizos, D., F. Ward, P. Duffy, M.P. Boland, and P. Lonergan. 2002. Consequences of bovine oocyte maturation, fertilization or early embryo development in vitro versus in vivo: implications for blastocyst yield and blastocyst quality. Mol. Reprod. Dev. 61:234–248. doi:10.1002/mrd.1153.

Rocha, A., R.D. Randel, J.R. Broussard, J.M. Lim, R.M. Blair, J.D. Roussel, R.A. Godke, and W. Hansel. 1998. High environmental temperature and humidity decrease oocyte quality in Bos taurus but not in Bos indicus cows. Theriogenology 49:657–665. doi:10.1016/S0093-691X(98)00016-8.

Rodgers, R.J., and H.F. Irving-Rodgers. 2010. Formation of the ovarian follicular antrum and follicular fluid. Biol. Reprod. 82:1021–1029. doi:10.1095/biolreprod.109.082941.

Roselli, C.E., L.E. Horton, and J.A. Resko. 1985. Distribution and regulation of aromatase activity in the rat hypothalamus and limbic system. Endocrinology 117:2471–2477.

Roth, Z., A. Dvir, O. Furman, Y. Lavon, D. Kalo, G. Leitner, and D. Wolfenson. 2020. Oocyte maturation in plasma or follicular fluid obtained from lipopolysaccharide-treated cows disrupts its developmental competence. Theriogenology 141:120–127. doi:10.1016/j.theriogenology.2019.09.021.

Roth, Z., A. Dvir, D. Kalo, Y. Lavon, O. Krifucks, D. Wolfenson, and G. Leitner. 2013. Naturally occurring mastitis disrupts developmental competeance of bovine oocytes. J. Dairy Sci. 96:6499–6505. doi:10.3168/jds.2013-6903.

Roth, Z., R. Meidan, R. Braw-Tal, and D. Wolfenson. 2000. Immediate and delayed effects of heat stress on follicular development and its association with plasma FSH and inhibin concentration in cows. J Reprod Fertil 120:83–90.

Rowson, L.E., and G.E. Lamming. 1953. Influence of ovarian hormones on uterine infection. Nature 171:749–750.

Ryan, K.J. 1959. Biological aromatization of steroids. J. Biol. Chem. 234:268–272.

Ryan, K.J., and Z. Petro. 1966. Steroid biosynthesis by human ovarian granulosa and thecal cells. Obstet. Gynecol. Surv. 21:635–638.

Ryan, K.J., Z. Petro, and J. Kaiser. 1968. Steroid formation by isolated and recombined ovarian granulosa and thecal cells.. J. Clin. Endocrinol. Metab. 28:355–358. doi:10.1210/jcem-28-3-355.

Ryan, K.J., and R. V. Short. 1965. Formation of estradiol by granulosa and theca cells of the equine ovarian follicle. Endocrinology 76:108–114. doi:10.1210/endo-76-1-108.

Rytkönen, K.T., E.M. Erkenbrack, M. Poutanen, L.L. Elo, M. Pavlicev, and G.P. Wagner. 2019. Decidualization of Human Endometrial Stromal Fibroblasts is a Multiphasic Process Involving Distinct Transcriptional Programs. Reprod. Sci. 26:323–336. doi:10.1177/1933719118802056.

Sagirkaya, H., M. Misirlioglu, A. Kaya, N.L. First, J.J. Parrish, and E. Memili. 2006. Developmental and molecular correlates of bovine preimplantation embryos. Reproduction 131:895–904. doi:10.1530/rep.1.01021.

Salasel, B., A. Mokhtari, and T. Taktaz. 2010. Prevalence, risk factors for and impact of subclinical endometritis in repeat breeder dairy cows. Theriogenology 74:1271–1278. doi:10.1016/j.theriogenology.2010.05.033.

Salilew-Wondim, D., M. Hölker, F. Rings, N. Ghanem, M. Ulas-Cinar, J. Peippo, E. Tholen, C. Looft, K. Schellander, and D. Tesfaye. 2010. Bovine pretransfer endometrium and embryo transcriptome fingerprints as predictors of pregnancy success after embryo transfer. Physiol. Genomics 42:201–218. doi:10.1152/physiolgenomics.00047.2010.

Salilew-Wondim, D., S. Ibrahim, S. Gebremedhn, D. Tesfaye, M. Heppelmann, H. Bollwein, C. Pfarrer, E. Tholen, C. Neuhoff, K. Schellander, and M. Hoelker. 2016. Clinical and subclinical endometritis induced alterations in bovine endometrial transcriptome and miRNome profile. BMC Genomics 17:1–21. doi:10.1186/s12864-016-2513-9.

Santen, R.J., H. Brodie, E.R. Simpson, P.K. Siiteri, and A. Brodie. 2009. History of aromatase: Saga of an important biological mediator and therapeutic target. Endocr. Rev. 30:343–375. doi:10.1210/er.2008-0016.

Santos, J.E.P., R.S. Bisinotto, E.S. Ribeiro, F.S. Lima, L.F. Greco, C.R. Staples, and W.W. Thatcher. 2010. Applying nutrition and physiology to improve reproduction in dairy cattle.. Soc. Reprod. Fertil. Suppl. 67:387–403.

Santos, J.E.P., R.L. Cerri, M.A. Ballou, G.E. Higginbotham, and J.H. Kirk. 2004. Effect of timing of first clinical mastitis occurrence on lactational and reproductive performance of Holstein dairy cows.. Anim. Reprod. Sci. 80:31–45. doi:10.1016/S0378-4320(03)00133-7.

Sartori, R., R. Sartor-Bergfelt, S.A. Mertens, J.N. Guenther, J.J. Parrish, and M.C. Wiltbank. 2002. Fertilization and early embryonic development in heifers and lactating cows in summer and lactating and dry cows in winter. J. Dairy Sci. 85:2803–2812. doi:10.3168/jds.S0022-0302(02)74367-1.

Schneider, C.A., W.S. Rasband, and K.W. Eliceiri. 2012. NIH Image to ImageJ: 25 years of image analysis. Nat. Methods 9:671–675. doi:10.1038/nmeth.2089.

Schrick, F.N., M.E. Hockett, A.M. Saxton, M.J. Lewis, H.H. Dowlen, and S.P. Oliver. 2001. Influence of subclinical mastitis during early lactation on reproductive parameters.. J. Dairy Sci. 84:1407–12. doi:10.3168/jds.S0022-0302(01)70172-5.

Shah, S., E.M. King, A. Chandrasekhar, and R. Newton. 2014. Roles for the mitogen-Activated protein kinase (MAPK) phosphatase, DUSP1, in feedback control of inflammatory gene expression and repression by dexamethasone. J. Biol. Chem. 289:13667–13679. doi:10.1074/jbc.M113.540799.

Shalgi, R., P. Kraicer, A. Rimon, M. Pinto, and N. Soferman. 1973. Proteins of human follicular fluid: the blood-follicle barrier. Fertil. Steril. 24:429–34.

Sheldon, I.M. 2004. The postpartum uterus. Vet. Clin. North Am. - Food Anim. Pract. 20:569–591. doi:10.1016/j.cvfa.2004.06.008.

Sheldon, I.M., J. Cronin, L. Goetze, G. Donofrio, and H.J. Schuberth. 2009. Defining postpartum uterine disease and the mechanisms of infection and immunity in the female reproductive tract in cattle. Biol. Reprod. 81:1025–1032. doi:10.1095/biolreprod.109.077370.

Sheldon, I.M., J.G. Cronin, and J.J. Bromfield. 2019. Tolerance and innate immunity shape the development of postpartum uterine disease and the impact of endometritis in dairy cattle. Annu. Rev. Anim. Biosci. 7:361–384. doi:10.1146/annurev-animal-020518-115227.

Sheldon, I.M., and H. Dobson. 2004. Postpartum uterine health in cattle. Anim. Reprod. Sci. 82–83:295–306. doi:10.1016/j.anireprosci.2004.04.006.

Sheldon, I.M., G.S. Lewis, S. LeBlanc, and R.O. Gilbert. 2006. Defining postpartum uterine disease in cattle. Theriogenology 65:1516–1530. doi:10.1016/j.theriogenology.2005.08.021.

Sheldon, I.M., and D.E. Noakes. 1998. Comparison of three treatments for bovine endometritis. Vet. Rec. 142:575–579. doi:10.1136/vr.142.21.575.

Sheldon, I.M., D.E. Noakes, A.N. Rycroft, D.U. Pfeiffer, and H. Dobson. 2002. Influence of uterine bacterial contamination after parturition on ovarian dominant follicle selection and follicle growth and function in cattle. Reproduction 123:837–845.

Sheldon, I.M., A.N. Rycroft, B. Dogan, M. Craven, J.J. Bromfield, A. Chandler, M.H. Roberts, S.B. Price, R.O. Gilbert, and K.W. Simpson. 2010. Specific strains of Escherichia coli are pathogenic for the endometrium of cattle and cause pelvic inflammatory disease in cattle and mice. PLoS One 5. doi:10.1371/journal.pone.0009192.

Shimizu, T., R. Echizenya, and A. Miyamoto. 2016. Effect of lipopolysaccharide on progesterone production during luteinization of granulosa and theca cells in vitro. J. Biochem. Mol. Toxicol. 30:206–211. doi:10.1002/jbt.21783.

Shimizu, T., K. Miyauchi, K. Shirasuna, H. Bollwein, F. Magata, C. Murayama, and a Miyamoto. 2012. Effects of lipopolysaccharide (LPS) and peptidoglycan (PGN) on estradiol production in bovine granulosa cells from small and large follicles. Toxicol. Vitr. 26:1134–1142. doi:http://dx.doi.org/10.1016/j.tiv.2012.06.014.

Siiteri, P.K. 1982. Review of studies on estrogen biosynthesis in the human. Cancer Res. 42:3269–3274.

Simerl, N.A., C.J. Wilcox, and W.W. Thatcher. 1992. Postpartum performance of dairy heifers freshening at young ages. J. Dairy Sci. 75:590–595. doi:10.3168/jds.S0022-0302(92)77796-0.

Simpson, E.R., M.S. Mahendroof, G.D. Means, M.W. Kilgoref, M.M. Hinshelwoodf, S. Graham-Lorence, B. Amarneh, Y. Ito, C.R. Fisher, M.D. Michaelt, C.R. Mendelson, and S.E. Bulun. 1994. Aromatase cytochrome P450, the enzyme responsible for estrogen biosynthesis. Endocr. Rev. 15:342–355.

Singh, J., S.S. Sidhu, G.S. Dhaliwal, G.R. Pangaonkar, A.S. Nanda, and A.S. Grewal. 2000. Effectiveness of lipopolysaccharide as an intrauterine immunomodulator in curing bacterial endometritis in repeat breeding cross-bred cows. Anim. Reprod. Sci. 59:159–166.

Sirois, J., and J.S. Richards. 1993. Transcriptional regulation of the rat prostaglandin endoperoxide synthase 2 gene in granulosa cells. Evidence for the role of a cis-acting C/EBPβ promoter element. J. Biol. Chem. 268:21931–21938. doi:10.1016/s0021-9258(20)80630-9.

Snijders, S.E.M., P. Dillon, D. O'Callaghan, and M.P. Boland. 2000. Effect of genetic merit, milk yield, body condition and lactation number on in vitro oocyte development in dairy cows. Theriogenology 53:981–989. doi:10.1016/S0093-691X(00)00244-2.

Södersten, P., D. Crews, C. Logan, and R.W. Soukup. 2014. Eugen Steinach: The first neuroendocrinologist. Endocrinology 155:688–695. doi:10.1210/en.2013-1816.

Soto, P., R.P. Natzke, and P.J. Hansen. 2003. Identification of possible mediators of embryonic mortality caused by mastitis: actions of lipopolysaccharide, prostaglandin F2α, and the nitric oxide generator, sodium nitroprusside dihydrate, on oocyte maturation and embryonic development in cattle. Am. J. Reprod. Immunol. 50:263–272. doi:10.1034/j.1600-0897.2003.00085.x.

Soumya, V., R.A. Padmanabhan, S. Titus, and M. Laloraya. 2016. Murine uterine decidualization is a novel function of autoimmune regulator—beyond immune tolerance. Am. J. Reprod. Immunol. 76:224–234. doi:10.1111/aji.12538.

Souza, A.H., H. Ayres, R.M. Ferreira, and M.C. Wiltbank. 2008. A new presynchronization system (Double-Ovsynch) increases fertility at first postpartum timed AI in lactating dairy cows. Theriogenology 70:208–215. doi:10.1016/j.theriogenology.2008.03.014.

Sprecher, D.J., D.E. Hostetler, and J.B. Kaneene. 1997. A lameness scoring system that uses posture and gait to predict dairy cattle reporductive performance. Theriogenology 47:1179–1187.

Staples, C.R., W.W. Thatcher, and J.H. Clark. 1990. Relationship between ovarian activity and energy status during the early postpartum period of high producing dairy cows. J. Dairy Sci. 73:938–947. doi:10.3168/jds.S0022-0302(90)78750-4.

Steffan, J., M. Agric, S. Adriamanga, and M. Thibier. 1984. Treatment of metritis with antibiotics or prostaglandin F(2α) and influence of ovarian cyclicity in dairy cows. Am. J. Vet. Res. 45:1090–1094.

Stein, B., and M.X. Yang. 1995. Repression of the interleukin-6 promoter by estrogen receptor is mediated by NF-kappa B and C/EBP beta.. Mol. Cell. Biol. 15:4971–4979. doi:10.1128/mcb.15.9.4971.

Steinach, E., and H. Kun. 1937. Transformation of male sex hormones into a substance with action of a female hormone. Lancet 945.

Steinkampf, M.P., C.R. Mendelson, and E.R. Simpson. 1987. Regulation by follicle-stimulating hormone of the synthesis of aromatase cytochrome p-450 in human granulosa cells. Mol. Endocrinol. 1:465–471. doi:10.1210/mend-1-7-465.

Steinkampf, M.P., C.R. Mendelson, and E.R. Simpson. 1988. Effects of epidermal growth factor and insulin-like growth factor I on the levels of mRNA encoding aromatase cytochrome P-450 of human ovarian granulosa cells. Mol. Cell. Endocrinol. 59:93–99. doi:10.1016/0303-7207(88)90199-2.

Sterneck, E., L. Tessarollo, and P.F. Johnson. 1997. An essential role for C/EBPB in female reproduction. Genes Dev. 11:2153–2162.

Stocco, C. 2012. Tissue physiology and pathology of aromatase. Steroids 77:27–35. doi:10.1016/j.steroids.2011.10.013.Tissue.

Su, L., R. Liu, W. Cheng, M. Zhu, X. Li, S. Zhao, and M. Yu. 2014. Expression patterns of microRNAs in porcine endometrium and their potential roles in embryo implantation and placentation. PLoS One 9. doi:10.1371/journal.pone.0087867.

Suzuki, C., K. Yoshioka, S. Iwamura, and H. Hirose. 2001. Endotoxin induces delayed ovulation following endocrine aberration during the proestrous phase in Holstein heifers. Domest. Anim. Endocrinol. 20:267–278. doi:10.1016/S0739-7240(01)00098-4.

Tagoma, A., K. Haller-Kikkatalo, K. Roos, A. Oras, A. Kirss, J. Ilonen, and R. Uibo. 2019. Interleukin-7, T helper 1, and regulatory T-cell activity-related cytokines are increased during the second trimester of healthy pregnancy compared to non-pregnant women. Am. J. Reprod. Immunol. 82:1–10. doi:10.1111/aji.13188.

Tanabe, T.Y., H.W. Hawk, and J.F. Hasler. 1985. Comparative fertility of normal and repeat-breeding cows as embryo recipients. Theriogenology 23:687–696. doi:10.1016/0093-691X(85)90203-1.

Thatcher, W.W., A. Guzeloglu, R. Mattos, M. Binelli, T.R. Hansen, and J.K. Pru. 2001. Uterine-conceptus interactions and reproductive failure in cattle. Theriogenology 56:1435–1450.

Thatcher, W.W., P.J. Hansen, T.S. Gross, S.D. Helmer, C. Plante, and F.W. Bazer. 1989. Antiluteolytic effects of bovine trophoblast protein-1. J Reprod Fertil Suppl 37:91–99.

Theilen, L.H., H.D. Campbell, S.L. Mumford, A.C. Purdue-Smithe, L.A. Sjaarda, N.J. Perkins, J.G. Radoc, R.M. Silver, and E.F. Schisterman. 2020. Platelet activation and placenta-mediated adverse pregnancy outcomes: an ancillary study to the effects of aspirin in gestation and reproduction trial. Am. J. Obstet. Gynecol. 223:741.e1-741.e12. doi:10.1016/j.ajog.2020.05.026.

Torbé, A., M. Sokołowska, S. Kwiatkowski, R. Rzepka, B. Torbé, and R. Czajka. 2011. Maternal plasma lipopolysaccharide binding protein (LBP) concentrations in pregnancy complicated by preterm premature rupture of membranes. Eur. J. Obstet. Gynecol. Reprod. Biol. 156:153–157. doi:10.1016/j.ejogrb.2011.01.024.

Torres-Júnior, J.R. d. S., M. de F.A. Pires, W.F. de Sá, A. de M. Ferreira, J.H.M. Viana, L.S.A. Camargo, A.A. Ramos, I.M. Folhadella, J. Polisseni, C. de Freitas, C.A.A. Clemente, M.F. de Sá Filho, F.F. Paula-Lopes, and P.S. Baruselli. 2008. Effect of maternal heat-stress on follicular growth and oocyte competence in Bos indicus cattle. Theriogenology 69:155–166. doi:10.1016/j.theriogenology.2007.06.023.

Torry, D.S., J. Leavenworth, M. Chang, V. Maheshwari, K. Groesch, E.R. Ball, and R.J. Torry. 2007. Angiogenesis in implantation. J. Assist. Reprod. Genet. 24:303–315. doi:10.1007/s10815-007-9152-7.

Tríbulo, P., M.B. Rabaglino, M.B. Bo, L. de R. Carvalheira, J. V. Bishop, T.R. Hansen, and P.J. Hansen. 2019. Dickkopf-related protein 1 is a progestomedin acting on the bovine embryo during the morula-to-blastocyst transition to program trophoblast elongation. Sci. Rep. 9:11816. doi:10.1038/s41598-019-48374-z.

Tsai-Morris, C.H., D.R. Aquilano, and M.L. Dufau. 1985. Gonadotropic regulation of aromatase activity in the adult rat testis. Endocrinology 116:31–37. doi:10.1210/endo-116-1-31.

Tsevat, D.G., H.C. Wiesenfeld, C. Parks, and J.F. Peipert. 2017. Sexually transmitted diseases and infertility. Am. J. Obstet. Gynecol. 216:1–9. doi:10.1016/j.ajog.2016.08.008.

Udofa, E.A., B.W. Stringer, P. Gade, D. Mahony, M.S. Buzza, D. V. Kalvakolanu, and T.M. Antalis. 2013. The transcription factor C/EBP-β mediates constitutive and LPS-inducible transcription of murine serpinB2. PLoS One 8:e57855. doi:10.1371/journal.pone.0057855.

Valladares, L.E., and A.H. Payne. 1979. Acute stimulation of aromatization in Leydig cells by human chorionic gonadotropin in vitro. Proc. Natl. Acad. Sci. U. S. A. 76:4460–4463. doi:10.1073/pnas.76.9.4460.

VanRaden, P.M., A.H. Sanders, M.E. Tooker, R.H. Miller, H.O. Norman, M.T. Kuhn, and G.R. Wiggans. 2004. Development of a national genetic evaluation for cow fertility. J. Dairy Sci. 87:2285–2292. doi:10.3168/jds.S0022-0302(04)70049-1.

Vernon, R.G. 1989. Endocrine control of metabolic adaptation during lactation. Proc. Nutr. Soc. 48:23–42. doi:10.1079/PNS19890006.

Wall, E., S. Brotherstone, J.A. Woolliams, G. Banos, and M.P. Coffey. 2003. Genetic evaluation of fertility using direct and correlated traits. J. Dairy Sci. 86:4093–4102. doi:10.3168/jds.S0022-0302(03)74023-5.

Wang, C., A.J.W. Hsueh, and G.F. Erickson. 1982. The role of cyclic AMP in the induction of estrogen and progestin synthesis in cultured granulosa cells. Mol. Cell. Endocrinol. 25:73–83. doi:10.1016/0303-7207(82)90170-8.

Wang, Y., T. Hu, L. Wu, X. Liu, S. Xue, and M. Lei. 2017. Identification of non-coding and coding RNAs in porcine endometrium. Genomics 109:43–50. doi:10.1016/j.ygeno.2016.11.007.

Wang, Y., S. Xue, X. Liu, H. Liu, T. Hu, X. Qiu, J. Zhang, and M. Lei. 2016. Analyses of Long Non-Coding RNA and mRNA profiling using RNA sequencing during the pre-implantation phases in pig endometrium. Sci. Rep. 6:1–11. doi:10.1038/srep20238.

Warren, B.D., S.H. Ahn, L.K. McGinnis, G. Grzesiak, R.W. Su, A.T. Fazleabas, L.K. Christenson, B.K. Petroff, and M.G. Petroff. 2019. Autoimmune Regulator is required in female mice for optimal embryonic development and implantation. Biol. Reprod. 100:1492–1504. doi:10.1093/biolre/ioz023.

Washburn, S.P., W.J. Silvia, C.H. Brown, B.T. McDaniel, and A.J. McAllister. 2002. Trends in reproductive performance in southeastern Holstein and Jersey DHI herds. J. Dairy Sci. 85:244–251. doi:10.3168/jds.S0022-0302(02)74073-3.

Wathes, D.C., Z. Cheng, W. Chowdhury, M.A. Fenwick, R. Fitzpatrick, D.G. Morris, J. Patton, and J.J. Murphy. 2009. Negative energy balance alters global gene expression and immune responses in the uterus of postpartum dairy cows. Physiol. Genomics 39:1–13. doi:10.1152/physiolgenomics.00064.2009.

Wedel, A., G. Sulski, and H.W.L. Ziegler-Heitbrock. 1996. CCAAT/enhancer binding protein is involved in the expression of the tumour necrosis factor gene in human monocytes. Cytokine 8:335–341. doi:10.1006/cyto.1996.0046.

Williams, C.Y., T.G. Harris, D.F. Battaglia, C. Viguié, and F.J. Karsch. 2001. Endotoxin inhibits pituitary responsiveness to gonadotropin-releasing hormone. Endocrinology 142:1915–1922. doi:10.1210/endo.142.5.8120.

Williams, E.J., D.P. Fischer, D.U. Pfeiffer, G.C.W. England, D.E. Noakes, H. Dobson, and I.M. Sheldon. 2005. Clinical evaluation of postpartum vaginal mucus reflects uterine bacterial infection and the immune response in cattle. Theriogenology 63:102–117. doi:10.1016/j.theriogenology.2004.03.017.

Williams, E.J., S. Herath, G.C.W. England, H. Dobson, C.E. Bryant, and I.M. Sheldon. 2008a. Effect of Escherichia coli infection of the bovine uterus from the whole animal to the cell. Animal 2:1153–1157. doi:10.1017/S1751731108002413.

Williams, E.J., K. Sibley, A.N. Miller, E.A. Lane, J. Fishwick, D.M. Nash, S. Herath, G.C.W. England, H. Dobson, and I.M. Sheldon. 2008b. The effect of Escherichia coli lipopolysaccharide and tumour necrosis factor alpha on ovarian function. Am. J. Reprod. Immunol. 60:462–73.

Wolfenson, D., B.J. Lew, W.W. Thatcher, Y. Graber, R. Meidan, B.J. Lew, R. Braw-Tal, A. Berman, and D.C. Thurley. 1997. Seasonal and acute heat stress effects on steroid production by dominant follicles in cows. Anim. Reprod. Sci. 47:9–19. doi:10.1016/S0378-4320(96)01638-7.

Wu, A., F. Liu, X. Liu, X. Feng, and H. Lin. 2019. Expression of TLR4 and its effect on Treg cells in early pregnancy decidual stromal cells after lipopolysaccharide treating. Eur. J. Obstet. Gynecol. Reprod. Biol. 237:209–214. doi:10.1016/j.ejogrb.2018.12.006.

Wu, L., J. Li, H.L. Xu, B. Xu, X.H. Tong, J. Kwak-Kim, and Y.S. Liu. 2016. IL-7/IL-7R signaling pathway might play a role in recurrent pregnancy losses by increasing inflammatory Th17 cells and decreasing Treg cells. Am. J. Reprod. Immunol. 76:454–464. doi:10.1111/aji.12588.

Wu, M.Y., H.N. Ho, S.U. Chen, K.H. Chao, C. Der Chen, and Y.S. Yang. 1999. Increase in the production of interleukin-6, interleukin-10, and interleukin-12 by lipopolysaccharide-stimulated peritoneal macrophages from women with endometriosis. Am. J. Reprod. Immunol. 41:106–111. doi:10.1111/j.1600-0897.1999.tb00082.x.

Xu, Z., H.A. Garverick, G.W. Smith, M.F. Smith, S.A. Hamiton, and R.S. Youngquist. 1995. Expression of messenger ribonucleic acid encoding cytochrome P450 side-chain cleavage, cytochrome P450 17alpha-hydroxylae, and cytochrome P450 aromatase in bovine follicles during the first follicular wave. Endocrinology 136:981–989.

Yang, S., Z. Fang, T. Suzuki, H. Sasano, J. Zhou, B. Gurates, M. Tamura, K. Ferrer, and S. Bulun. 2002. Regulation of aromatase P450 expression in endometriotic and endometrial stromal cells by CCAAT/enhancer binding proteins (C/EBPs): Decreased C/EBPβ in endometriosis is associated with overexpression of aromatase. J. Clin. Endocrinol. Metab. 87:2336–2345. doi:10.1210/jc.87.5.2336.

Yang, Y., J.Y. Zhou, L.J. Zhao, B.R. Gao, X.P. Wan, and J.L. Wang. 2016. Dual-specificity phosphatase 1 deficiency induces endometrioid adenocarcinoma progression via activation of mitogen-activated protein kinase/extracellular signal-regulated kinase pathway. Chin. Med. J. (Engl). 129:1154–1160. doi:10.4103/0366-6999.181954.

Yates, A.D., P. Achuthan, W. Akanni, J. Allen, J. Allen, J. Alvarez-Jarreta, M.R. Amode, I.M. Armean, A.G. Azov, R. Bennett, J. Bhai, K. Billis, S. Boddu, J.C. Marugán, C. Cummins, C. Davidson, K. Dodiya, R. Fatima, A. Gall, C.G. Giron, L. Gil, T. Grego, L. Haggerty, E. Haskell, T. Hourlier, O.G. Izuogu, S.H. Janacek, T. Juettemann, M. Kay, I. Lavidas, T. Le, D. Lemos, J.G. Martinez, T. Maurel, M. McDowall, A. McMahon, S. Mohanan, B. Moore, M. Nuhn, D.N. Oheh, A. Parker, A. Parton, M. Patricio, M.P. Sakthivel, A.I.A. Salam, B.M. Schmitt, H. Schuilenburg, D. Sheppard, M. Sycheva, M. Szuba, K. Taylor, A. Thormann, G. Threadgold, A. Vullo, B. Walts, A. Winterbottom, A. Zadissa, M. Chakiachvili, B. Flint, A. Frankish, S.E. Hunt, G. Iisley, M. Kostadima, N. Langridge, J.E. Loveland, F.J. Martin, J. Morales, J.M. Mudge, M. Muffato, E. Perry, M. Ruffier, S.J. Trevanion, F. Cunningham, K.L. Howe, D.R. Zerbino, and P. Flicek. 2020. Ensembl 2020. Nucleic Acids Res. 48:D682–D688. doi:10.1093/nar/gkz966.

Yenuganti, V.R., R. Ravinder, and D. Singh. 2014. Conjugated linoleic acids attenuate LPS-induced pro-inflammatory gene expression by inhibiting the NF-κB translocation through PPARγ in buffalo granulosa cells. Am. J. Reprod. Immunol. 72:296–304. doi:10.1111/aji.12261.

Yenuganti, V.R., Ravinder, and D. Singh. 2017. Endotoxin induced TLR4 signaling downregulates CYP19A1 expression through CEBPB in buffalo granulosa cells. Toxicol. Vitr. 42:93–100. doi:10.1016/j.tiv.2017.04.012.

Yoshimoto, F.K., and F.P. Guengerich. 2014. Mechanism of the third oxidative step in the conversion of androgens to estrogens by cytochrome P450 19A1 steroid aromatase. J. Am. Chem. Soc. 136:15016–15025. doi:10.1021/ja508185d.

Young, L.E., K. Fernandes, T.G. McEvoy, S.C. Butterwith, C.G. Gutierrez, C. Carolan, P.J. Broadbent, J.J. Robinson, I. Wilmut, and K.D. Sinclair. 2001. Epigenetic change in IGF2R is associated with fetal overgrowth after sheep embryo culture. Nat. Genet. 27:153–154. doi:10.1038/84769.

Yusuf, M., T. Nakao, R.B.K. Ranasinghe, G. Gautam, S.T. Long, C. Yoshida, K. Koike, and A. Hayashi. 2010. Reproductive performance of repeat breeders in dairy herds. Theriogenology 73:1220–1229. doi:10.1016/j.theriogenology.2010.01.016.

Zhang, J., X. Xu, H. Chen, P. Kang, H. Zhu, H. Ren, and Y. Liu. 2021. Construction and analysis for dys-regulated lncRNAs and mRNAs in LPS-induced porcine PBMCs. Innate Immun. 1–14. doi:10.1177/1753425920983869.

Zhang, P., N.J. Liégeois, C. Wong, M. Finegold, H. Hou, J.C. Thompson, A. Silverman, J.W. Harper, R.A. DePinho, and S.J. Elledge. 1997. Altered cell differentiation and proliferation in mice lacking p57(KIP2) indicates a role in Beckwith-Wiedemann syndrome. Nature 387:151–158. doi:10.1038/387151a0.

Zhao, S.J., Y.W. Pang, X.M. Zhao, W.H. Du, H.S. Hao, and H. Bin Zhu. 2017. Effects of lipopolysaccharide on maturation of bovine oocyte in vitro and its possible mechanisms. Oncotarget 8:4656–4667. doi:10.18632/oncotarget.13965.

Zhou, J., B. Gurates, S. Yang, S. Sebastian, and S.E. Bulun. 2001. Malignant breast epithelial cells stimulate aromatase expression via promoter II in human adipose fibroblasts: An epithelial-stromal interaction in breast tumors mediated by CCAAT/enhancer binding protein β1. Cancer Res. 61:2328–2334.

Zuckerman, S. 1951. The number of oocytes in the mature ovary. Recent Prog. Horm. Res. 6:63–109.

Zwald, N.R., K.A. Weigel, Y.M. Chang, R.D. Welper, and J.S. Clay. 2004. Genetic selection for health traits using producer-recorded data I. Incidence rates, heritability estimates, and sire breeding values. J. Dairy Sci. 87:4287–4294. doi:10.3168/jds.S0022-0302(04)73573-0.

BIOGRAPHICAL SKETCH

Mackenzie Dickson grew up in Ames, Iowa and received a Bachelor of Science degree in dairy science from Iowa State University in 2014. During her undergraduate education, she fell in love with research when working in a bacteriology laboratory and a reproductive biology laboratory. Following graduation, Mackenzie worked at Robindale Dairy in Rakaia, New Zealand for a season, feeding calves and milking cows. She came back to the United States and received a Master of Science degree in animal physiology from Iowa State University. She was co-advised by Dr. Aileen Keating and Dr. Lance Baumgard and her thesis was titled “Impact of endotoxemia on ovarian signaling and function”. After completion of her M.Sc., she moved to Gainesville in 2017 and began her doctoral studies. She focused on uterine infection in dairy cows and the impact on subsequent fertility working under the mentorship of Dr. John Bromfield. After finishing her PhD, she will take a postdoctoral scholar position at National Institute of Environmental Health Sciences in the Reproductive and Developmental Biology Laboratory working with Dr. Franco DeMayo. Her long-term career goals include continuing research and possibly leading her own laboratory one day.